UNIVERSITAT
POLITÈCNICA
DE VALÈNCIA

PhD Thesis

Modeling and Optimization of Photovoltaic Installations at Urban Scale

Author:

Enrique Fuster Palop

Supervisor:

Dr. Jorge Payá Herrero

Valencia, October 2023

Abstract

The building sector in developed countries consumes 20% to 40% of the global primary energy, contributing to 30% of the $\mathrm{CO_2}$ emissions. The population growth, particularly in urban areas, is expected to exacerbate this trend, compromising the sustainability goals outlined in international agreements and accelerating climate change. However, the increasing interest and political support in mature renewable energy sources, particularly solar photovoltaic (PV), offers improvement opportunities. The deployment of PV systems in urban areas presents advantages regarding emissions, economic, environmental, and social benefits, enhancing grid efficiency, increasing energy independence, and promoting sustainability awareness and community involvement. To increase the adoption of rooftop PV self-consumption (PVSC) systems in urban environments, studies on the PV potential can help overcome social barriers and enable public administration, utility companies, and private corporations to optimize energy planning, promote PVSC, and attract private investment in clean energy. Although most of the PV potential studies in the literature rely on geospatial physical models, the opportunities provided by Machine Learning (ML) and agile statistical approaches to reduce the high computational cost of the previous models are not fully exploited. These opportunities, especially in the economic potential assessment, remain scarce.

The present research investigates the possibilities and constraints in the massive deployment of photovoltaic self-consumption (PVSC) systems in urban areas from an urban planning perspective, considering the current technical and economic limitations. To this end, this thesis employs data-driven strategies to develop both bottom-up physical and agile regression-based models as assessment tools for the technical and economic potential of PVSC systems in urban contexts.

First, an empirical PV production submodel has been developed and validated with climate and production measurements collected from a $50\,\mathrm{MW}$ utility-scale in operation. Additionally, several improvements in modeling the performance ratio (PR) in low-irradiance environments have been investigated. In the second stage of this research, the previous submodel has been integrated into a physical 3D GIS-based techno-economic model capable of assessing the economic PVSC for a sample of residential buildings. Additionally, the model incorporates shadow modeling and hourly electric demand estimations to assess sample residential buildings. A simulation database, derived from the previous results, has allowed the development of a methodology to train a regression-based model to estimate the production and the economic

payback (PB) at a building scale with an assumable accuracy for energy planning purposes. As the last step, the demand submodel was improved by employing real aggregated time series data for multiple consumer patterns and providing realistic estimations for other building typologies. In addition to spatial restrictions, the model optimizes the sizing of the facilities according to their demand and economic constraints, maximizing the relationship between self-sufficiency (SS) and PB. Furthermore, the regression-based methodology has been extended to estimate, besides the payback, multiple key performance indicators such as internal rate of return (IRR), self-consumption rate (SC), and SS. Through an appropriate predictor identification and a training and validation methodology, these correlations allowed performance estimations with an acceptable deviation compared with the physical model. The availability of building-related data is progressively increasing in most countries, enabling widespread application and generalization of the proposed methodologies and reducing the simulation cost of these studies to cover larger urban areas.

As an application of the previous methodologies, a complete-census economic PV potential results of a Mediterranean municipality's building stock was performed under different demand and economic scenarios at a building and municipality scale. For the scenario that meets the current regulation in Spain, the municipality SS ranged between 22%-43% for the most optimistic and pessimistic scenarios, respectively. The optimal sizing of the facilities according to the load curves in the Net Billing (NB) modality is crucial to obtaining competitive economic results. Consequently, the annual PV generation represented 68% of the annual total electricity consumption of the municipality for a net billing scenario, while a net metering scenario represented 103%. Owing to economies of scale and high demand intensity, a higher profitability was found in rooftops of apartment blocks and industrial buildings, which also achieve the highest savings in emissions.

Resumen

El sector de la edificación en los países desarrollados consume entre el 20% y el 40% de la energía primaria mundial, contribuyendo al 30% de las emisiones de $\mathrm{CO_2}$. Se espera que el crecimiento demográfico, particularmente en las zonas urbanas, exacerbe esta tendencia, comprometiendo los objetivos de sostenibilidad descritos en los acuerdos internacionales y acelerando el cambio climático. Sin embargo, el creciente interés y apoyo político en las fuentes de energía renovables maduras, en particular la energía solar fotovoltaica (PV), ofrece oportunidades de mejora. El despliegue de sistemas fotovoltaicos en áreas urbanas presenta ventajas en cuanto a emisiones, beneficios económicos, ambientales y sociales, mejora la eficiencia de la red, aumenta la independencia energética y promueve la conciencia de sostenibilidad y la participación colectiva. Para aumentar la adopción de sistemas de autoconsumo fotovoltaico (PVSC) sobre tejados de entornos urbanos, los estudios sobre el potencial fotovoltaico pueden ayudar a superar las barreras sociales y permitir a la administración pública, las empresas de servicios públicos y las corporaciones privadas optimizar la planificación energética, promover los PVSC y atraer inversión privada en energías limpias. Aunque la mayoría de los estudios sobre el potencial fotovoltaico en la literatura se basan en modelos físicos geoespaciales, las oportunidades que brindan el aprendizaje automático (ML) y los enfoques estadísticos ágiles para reducir el alto coste computacional de los modelos anteriores no han sido explotados por completo. Estas oportunidades, especialmente en la evaluación del potencial económico, siguen siendo escasas.

El presente trabajo investiga las posibilidades y limitaciones en el despliegue masivo de sistemas de autoconsumo fotovoltaico (PVSC) en áreas urbanas desde una perspectiva de planificación urbana, considerando las limitaciones técnicas y económicas actuales. Con este fin, esta tesis emplea estrategias basadas en datos para desarrollar modelos físicos y modelos ágiles basados en regresiones como herramientas de evaluación del potencial técnico y económico de los sistemas PVSC en contextos urbanos.

En primer lugar, se ha desarrollado y validado un submodelo empírico de producción fotovoltaica con mediciones climáticas y de producción recopiladas de una planta fotovoltaica de $50\,\mathrm{MW}$ en funcionamiento. Además, se han investigado varias mejoras en el modelado del performance ratio (PR) en entornos de baja irradiancia. En la segunda etapa de esta investigación, el submodelo anterior se ha integrado en un modelo tecnoeconómico 3D basado en sistemas de información geográfica (GIS) capaz de evaluar el PVSC económico para una

muestra de edificios residenciales. Además, el modelo incorpora modelos de sombras y estimaciones de demanda eléctrica horaria para evaluar una muestra de edificios residenciales. Una base de datos de simulación, derivada de los resultados anteriores, ha permitido el desarrollo de una metodología para entrenar un modelo basado en regresión y con ello estimar la producción y el periodo de retorno económico (PB) a escala de edificio con una precisión asumible para fines de planificación energética. Como último paso, se mejoró el submodelo de demanda empleando datos reales agregados de series temporales para múltiples patrones de consumo y proporcionando estimaciones realistas para otras tipologías de edificios. Además de las restricciones espaciales, el modelo optimiza el tamaño de las instalaciones según su demanda y limitaciones económicas, maximizando la relación entre autosuficiencia (SS) y el PB. Además, la metodología basada en regresión se ha ampliado para estimar, además del retorno de la inversión, múltiples indicadores clave de desempeño (KPIs) como la tasa interna de retorno (IRR), la tasa de autoconsumo (SC) y SS. A través de una adecuada identificación de predictores y una metodología de entrenamiento y validación, estas correlaciones permitieron estimaciones de rendimiento con una desviación aceptable respecto al modelo físico. La disponibilidad de datos relacionados con la construcción está aumentando progresivamente en la mayoría de los países, lo que permite una amplia aplicación y generalización de las metodologías propuestas y reduce el costo de simulación de estos estudios para cubrir áreas urbanas más grandes.

Como aplicación de las metodologías anteriores, se analizaron los resultados del potencial económico fotovoltaico dedel parque inmobiliario completo de un municipio mediterráneo bajo diferentes escenarios económicos y de demanda a escala de edificio y municipal. Para el escenario que cumple con la regulación actual en España, la SS municipal oscila entre el 22%-43% para los escenarios más optimista y pesimista, respectivamente. El dimensionamiento óptimo de las instalaciones según las curvas de carga en la modalidad de Net Billing (NB) es crucial para obtener resultados económicos competitivos. En consecuencia, la generación fotovoltaica anual representó el 68% del consumo eléctrico total anual.

Resum

El sector de l'edificació als països desenvolupats consumeix entre el 20% i el 40% de l'energia primària mundial, contribuint al 30% de les emissions de CO_2. S'espera que el creixement demogràfic, particularment en les zones urbanes, exacerbe aquesta tendència, comprometent els objectius de sostenibilitat descrits en els acords internacionals i accelerant el canvi climàtic. No obstant això, el creixent interés i suport polític en les fonts d'energia renovables madures, en particular l'energia solar fotovoltaica (PV), ofereix oportunitats de millora. El desplegament de sistemes fotovoltaics en àrees urbanes presenta avantatges quant a emissions, beneficis econòmics, ambientals i socials, millora l'eficiència de la xarxa, augmenta la independència energètica i promou la consciència de sostenibilitat i la participació col·lectiva. Per a augmentar l'adopció de sistemes d'autoconsum fotovoltaic (PVSC) sobre teulades d'entorns urbans, els estudis sobre el potencial fotovoltaic poden ajudar a superar les barreres socials i permetre a l'administració pública, les empreses de serveis públics i les corporacions privades optimitzar la planificació energètica, promoure els PVSC i atraure inversió privada en energies netes. Encara que la majoria dels estudis sobre el potencial fotovoltaic en la literatura es basen en models físics geoespacials, les oportunitats que brinden l'aprenentatge automàtic (ML) i els enfocaments estadístics àgils per a reduir l'alt cost computacional dels models anteriors no han sigut explotats per complet. Aquestes oportunitats, especialment en l'avaluació del potencial econòmic, continuen sent escasses.

El present treball investiga les possibilitats i limitacions en el desplegament massiu de sistemes PVSC en àrees urbanes des d'una perspectiva de planificació urbana, considerant les limitacions tècniques i econòmiques actuals. A aquest efecte, aquesta tesi empra estratègies basades en dades per a desenvolupar models físics i models àgils basats en regressions com a eines d'avaluació del potencial tècnic i econòmic dels sistemes PVSC en contextos urbans.

En primer lloc, s'ha desenvolupat i validat un submodel empíric de producció fotovoltaica amb mesuraments climàtics i de producció recopilades d'una planta fotovoltaica de $50\,\mathrm{MW}$ en funcionament. A més, s'han investigat diverses millores en el modelatge del performance ràtio (PR) en entorns de baixa irradiància. En la segona etapa d'aquesta investigació, el submodel anterior s'ha integrat en un model tecnoeconómic 3D basat en sistemes d'informació geogràfica (GIS) capaç d'avaluar el PVSC econòmic per a una mostra d'edificis residencials. A més, el model incorpora models d'ombres i estimacions de demanda elèctrica horària per a avaluar una mostra d'edificis residencials. Una base de dades de simulació, derivada dels resultats anteriors,

ha permés el desenvolupament d'una metodologia per a entrenar un model basat en regressió i amb això estimar la producció i la període de retorn econòmic (PB) a escala d'edifici amb una precisió assumible per a fins de planificació energètica. Com a últim pas, es va millorar el submodel de demanda emprant dades reals agregats de sèries temporals per a múltiples patrons de consum i proporcionant estimacions realistes per a altres tipologies d'edificis. A més de les restriccions espacials, el model optimitza la grandària de les instal·lacions segons la seua demanda i limitacions econòmiques, maximitzant la relació entre la taxa d'autosuficiència (SS) i PB. A més, la metodologia basada en regressió s'ha ampliat per a estimar, a més del retorn de la inversió, múltiples indicadors clau d'acompliment (KPIs) com la taxa interna de retorn (IRR), la taxa d'autoconsum (SC) i la SS. A través d'una adequada identificació de predictors i una metodologia d'entrenament i validació, aquestes correlacions van permetre estimacions de rendiment amb una desviació acceptable respecte al model físic. La disponibilitat de dades relacionades amb la construcció està augmentant progressivament en la majoria dels països, la qual cosa permet una àmplia aplicació i generalització de les metodologies proposades i redueix el cost de simulació d'aquests estudis per a cobrir àrees urbanes més grans.

Com a aplicació de les metodologies anteriors, es van analitzar els resultats del potencial econòmic fotovoltaic del parc immobiliari complet d'un municipi mediterrani baix diferents escenaris econòmics i de demanda a escala d'edifici i municipal. Per a l'escenari que compleix amb la regulació actual a Espanya, la taxa d'autosuficiència municipal oscil·la entre el 22%-43% per als escenaris més optimista i pessimista, respectivament. El dimensionament òptim de les instal·lacions segons les corbes de càrrega en la modalitat de Net Billing (NB) és crucial per a obtindre resultats econòmics competitius. En conseqüència, la generació fotovoltaica anual va representar el 68% del consum elèctric total anual.

Acknowledgements

I would like to express my deep gratitude and appreciation to all those who have contributed to the completion of this doctoral thesis. I am profoundly thankful for the support and encouragement I have received along the way.

First and foremost, I would like to thank my thesis supervisor, Professor Jorgé Payá, for his support, guidance, patience, flexibility, confidence, and commitment in reviewing the articles we have published during this period, bringing out their maximum potential. His clear vision during this journey has been essential in shaping the scope of this work. Thanks also for trusting me and the potential of this thesis from the beginning. Working with you has been a pleasure.

I am profoundly grateful to the founding partners of ImpactE. Thanks to Carlos for his enthusiasm, unconditional support, trust in me, ability to ask the right questions, and all the ideas provided throughout these years. Thanks because we have learned much about self-consumption, modeling, and programming these years. His presence has dramatically facilitated this entire path. Thanks to Ximo for his support, collaboration, and enthusiasm. His business vision and contributions have been vital so that the learnings acquired in this research have a commercial sense and a real and practical application. Thanks to Joan for his positivity and teaching me almost everything I know about programming. His extensive knowledge of information sources and experience in modeling has been crucial to scaling up this research. With him, overcoming all technical obstacles has been possible.

My appreciation extends to all the members of ImpactE because with their effort, dedication, and enthusiasm, they have allowed this thesis to transcend the theoretical plane, and we have been able to apply all these models in many municipalities and projects. Furthermore, I would like to acknowledge the financial support and stability provided during these last few years. All of this has been crucial to propel my professional development and the rapid progress of this thesis.

I would like to express my gratitude to Professor Carlos Vargas for providing his availability, advice, and support, interest in my work, and positive feedback. In addition, thanks to Juan Carlos Ferri for his collaboration in providing the primary experimental data of this work. His contribution has allowed us to improve the quality of this work.

Moreover, I want to express my gratitude to all the members of the the Institute for Energy

Engineering (IIE) and the Chair of Urban Energy Transition since you were the seed with which this line of research began. Thank you for supporting it from the first moment. I am enormously grateful to all its members for their sympathy and interest in the developments performed in this thesis. Furthermore, I would like to acknowledge the financial support provided during the development of the second publication of the present thesis.

Outside of the professional field, I would also like to thank all the support and company of my friends Javi and Amadeo. Your mere presence has brought balance to my life.

Finally, none of this would have been possible without my entire family's understanding and unconditional support. Their big and small sacrifices have allowed me to culminate this research. They have my deep admiration and gratitude for everything.

I extend my heartfelt thanks to everyone who has played a part in my academic journey, whether mentioned here or not. This thesis is the culmination of our collective efforts, and I am proud to share it with you all.

Contents

Nomenclature

Abbreviations

CO_2	Carbon dioxide
3D	Three-dimensional
a-Si	Amorphous silicon
AB	Apartment block
AC	Alternating current
ANN	Artificial neural network
ANOVA	Analysis of variance
DC	Direct current
DSO	Distribution System Operator
Eq	Equation
GIS	Geographic Information System
IEC	International Electrotechnical Commission
IQR	Interquartile range
KPI	Key Performance Indicator
LiDAR	Light Detection and Ranging
LIL	Low Irradiance Losses
LoD	Level of Detail
LP	Load profile

mc-Si	Mono-crystalline silicon solar cell
MFH	Multi-family house
MLR	Multiple linear regression
ML	Machine learning
MPPT	Maximum power point tracker
NB	Net billing
NM	Net metering
O&M	Operations and maintenance
OLS	Ordinary Least Squares
pc-Si	Poly-crystalline silicon solar cell
PC	Postal code
PV	Photovoltaic
QR	Quantile regression
RD	Royal decree
REE	Red Eléctrica de España
RF	Random forest
SAM	System Advisor Model
SCADA	Supervisory control and data acquisition
SFH	Single-family house
STC	Standard test conditions
SVM	Support vector machine
TH	Terrace house
WS	Weather station

Parameters used in equations

$\bar{y}$	Mean measured value

$\beta_1, \beta_2, \beta_3$	MLR coefficients
η_{deg}	Degradation losses
η_{inv}	Inverter efficiency
η_{LIL}	Low irradiance losses efficiency
$\eta_{mismatch}$	Mismatch losses
$\eta_{PV,stc}$	PV efficiency under STC
η_{soil}	Soiling losses
η_{temp}	Temperature losses
$\eta_{wiring,DC}$	DC wiring losses
γ	Maximum power temperature coefficient
$\hat{y}_i$	Predicted value
Isc	Short-circuit current
mtry	Number of predictors selected at each split of the regression tree
ntree	Number of trees of the random forest algorithm
THD	Total harmonic distorsion
Voc	Open circuit voltage
A	Area of PV modules
a, b, c	Exponential fit coefficients
CF	Cash flow
CR	Cost ratio
CUF	Capacity Utilization Factor
d	Interest rate
D_h	Hourly demand
DL	Demand level
DSF	Demand scale factor
E_{AC}	AC PV energy production
$E_{PV,location}$	Yearly PV production per installed power in a specific location

$E_{PV,building,location}$	Yearly PV production per installed power in a specific location
$E_{PV,building,Valencia}$	Yearly PV production in a specific building of Valencia
E_{PV}	Annual photovoltaic production
$G_{0,location}$	Yearly global horizontal irradiation
G_{POA}	Global irradiance in the plane of array
G_{STC}	Reference solar irradiance at standard conditions
i	Inflation rate
I_{POA}	Global irradiance in the plane of array
IC	Installation costs
IL	Investment level
IRR	Internal rate of return
$LCOE$	Levelized cost of electricity
MAE	Mean absolute error
$n_{contracts}$	Number of contracts
N_{mod}	Number of PV modules from a PV array
$NOCT$	Normal Operating Cell Temperature
NPV	Net present value
$nRMSE$	Normalized root mean squared error
OR	Occupation rate
$P_{inv,rated}$	Rated installed power of the inverter
P_{max}	Peak power
$P_{PV,rated}$	Rated installed PV power of the system at standard test conditions
P_{PV}	PV Installed Peak Power
PB	Economic payback
PL	Price level
PR	Performance ratio
PR'	Performance ratio without considering low irradiance losses

$PR_{measured}$	Performance ratio obtained from measurements
R^2	R squared or coefficient of determination
$RMSE$	Root mean squared error
S_{PV}	Yearly PV surpluses
SC	Percentage of Self-consumption
SC_{annual}	Annual self-consumed energy
SF	Shading Factor
SL	Shadow Losses
SR	Sizing ratio or Surpluses Ratio
SR^*	Surpluses Ratio obtained with the Building Power Ratio
SS	Self-sufficiency
SVF	Sky View Factor
$T_{0,location}$	Yearly mean ambient temperature
T_a	Ambient temperature
T_{cell}	Cell temperature
VIF	Variance inflation factor
Y_F	Final yield
y_i	Measured value
Y_{R1}	Reference yield from weather station 1
Y_{R2}	Reference yield from weather station 2
Y_R	Reference yield

Units

€	Euro
°C	Degree Celsius
Hz	Hertz

kg	kilogram
m	Meter
Ω	Ohm
V	Volt
W h	Watt-hour
$\mathrm{W_p}$	Watt peak
W	Nominal Watt

List of Figures

List of Tables

Chapter 1

Introduction

1.1 Motivation

1.1.1 Climate change context

The building sector in developed countries consumes around 20% to 40% of the global primary energy [1–3], which represents 30% of the CO_2 emissions [4, 5]. With the population growth, this rate is expected to continue increasing in the following decades [6]. This phenomenon intensifies in urban areas, where two-thirds of the world are projected to live and develop their economic activities by 2050 [7].

The above-mentioned trends compromise the sustainability objectives to mitigate climate change and evolve towards low carbon economies as settled in the Paris Agreement [8] and defined by 2030 Agenda for Sustainable Development by the United Nations, especially the sustainable development goals in ensuring access to affordable, reliable, sustainable and modern energy for all and making cities inclusive, safe, resilient and sustainable [9]. Therefore, cities are potentially vulnerable to climate change, but it is also a significant improvement opportunity.

In response to previous commitments, the European Union (EU) has promoted diverse policies gathered in the "Clean Energy for All Europeans package" to increase energy efficiency, the deployment of renewable energy generation systems, and the flexibility of the electricity market to integrate new renewable systems [10]. Among these policies, the directive 2018 /2001 /EU establishes a 2030 target of 40% reduction in greenhouse gases compared with 1990 levels and at least 32% of the total energy needs of the EU covered by renewables, with a clause for a possible revision by September 2023 [11]. Additionally, in 2019, the European Commission declared with the European Green Deal [12] the aim to continue increasing the 2030 target of emissions reduction up to 55%, as well as the definition of a long-term legal framework (European Climate Law) to meet the climate neutrality in the EU by 2050 [13].

1.1.2 Contribution of PV energy

In recent years, the interest in renewable energy sources has grown worldwide as increasingly competitive technologies to replace fossil energy sources. This transition not only reduces emissions but also addresses potential national supply issues, stabilizes energy markets, and enhances reliability and resilience, among other advantages.

Alongside conventional hydropower, wind and solar PV energy present the highest installed capacity worldwide thanks to a high growth rate in the last years. Meanwhile, the other technologies, such as bioenergy, geothermal, and concentrated solar power, present lower but consistent growths despite their significant role in integrating wind and PV in grid systems [14]. Solar PV has experienced the most intensive growth in 2022, reaching 31.0% of the total renewable capacity worldwide, as shown in Figure 1.1. In the last decade (2013-2022), the worldwide PV capacity increased 7.7 times up to a total of $1{,}046$ GW in 2022, with interannual growths of up to 22.4% in the latter year [15, 16].

PV self-consumption (PVSC) facilities constitute a non-negligible fraction of the recent PV installed capacity. This segment represents approximately 48.6% of the previous interannual growth and 43.5% of the total installed capacity in 2021 (16.3% residential and 27.2% industrial) [17]. Rooftop PVSC systems constitute an effective solution for urban energy management to solve urban energy requirements and environmental issues [18].

During the late 2000s, Spain experienced a substantial PV deployment, installing world-leading utility-scale solar plants at that time, such as the power plant in Olmedilla de Alarcón, whose performance is an object of study in the present thesis. The total PV capacity in Spain increased from 0.01 GW in 2000 to 4.57 GW in 2012 [19], the year from which growth stalled due to the approval of a new regulation. As shown in Figure 1.1, the repeal of the previous regulation in 2018 led to unprecedented growth in capacity, reaching 18.21 GW in Spain by 2022 [15]. Through the Royal Decrees RDL15/2018 an RD244/2019 the PV self-consumption has been promoted increasing from 0.25 GW in 2018 to 2.74 GW in 2022 [20]. Notably, in 2022 the industrial sector accounted for approximately 61% of the installed capacity, with the remaining 39% attributed to the residential sector [21].

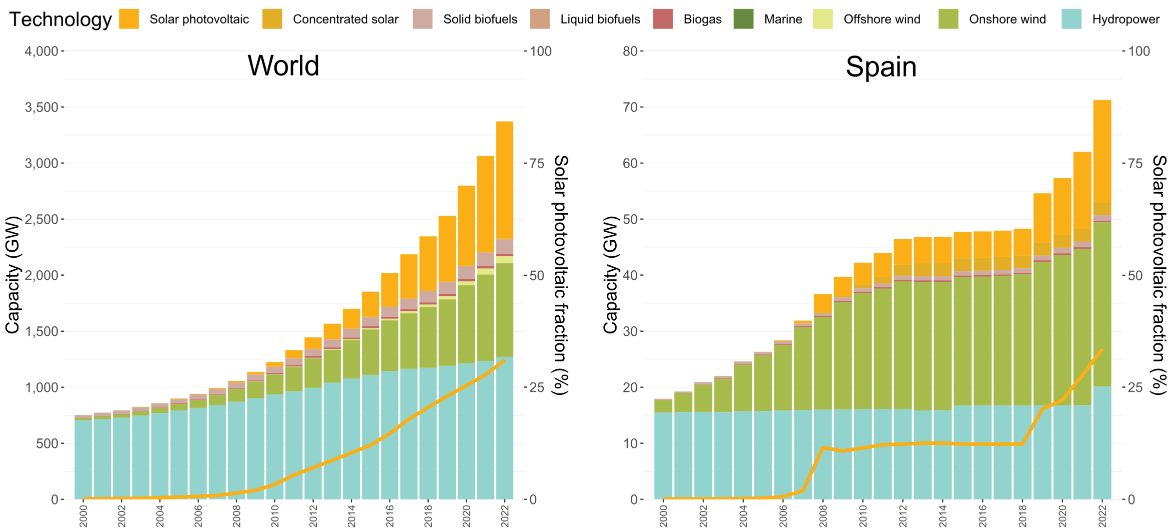

Figure 1.1: Evolution of the renewable capacity by technologies for worldwide and Spain (2000-2022) [15].

The main driver of the massive deployment of PV systems is the reach of its technological maturity. The cost reduction of PV facilities over 90% in the last decade was caused by the improvements in modules efficiency, public and private R&D, learning by doing in the manufacturing process and economies of scale [22]. For the same period, reductions of 64%, 69% and 82% in the cost of residential, commercial roof and utility-scale PV systems were registered [22]. As a result, this technology has experienced the highest drop in the Levelized Cost of Electricity ($LCOE$) compared with other renewable alternatives, reaching values below $100\,€/\mathrm{MWh}$ some EU countries [23]. This value is significantly lower than for other conventional technologies such as gas turbine, cycle gas turbines, coal, or nuclear [24].

Another technological drivers that facilitates the grid parity is the level of solar insolation of the region, such as the case of Spain both in residential [25] sector and tertiary sector [26], facilities with high economy of scale [27], and higher energy consumption levels due to the deployment of electric heat, HVAC systems or electric vehicles increase the self-consumption rates, and profitability performance of PV installations. Moreover, other external causes that improve the profitability are the electricity market fluctuations, which may result in increased electricity bills.

Together with the technological development of this technology, the political support and regulatory context have matured along with its deployment. One of the EU's objectives to mitigate climate change is to increase the PV capacity from 136 GW in 2020 to 320 GW by 2025, and 600 GW by 2030 [28]. In addition to deploying PV utility-scales, the European Solar Rooftops Initiative was proposed to deploy decentralized PV facilities in most public buildings and all new residential buildings by 2029. With this initiative, the prosumers play an active role in the energy transition. Moreover, the European Commission plans an EU Solar Industry Alliance to reduce the costs of electricity and increase the competitiveness of the European industrial sector [29].

Under this trend in Spain, a favorable legal framework was updated in 2019 to ease technically and legally the deployment of PVSC systems through the RDL 15/2018 [30] and RD 244/2019 [31]. This regulation allows a partial surplus remuneration and the possibility of connecting multiple users under the same facility, creating energy communities. Other favorable actions set by the Spanish regional and local public administrations to promote PVSC are the subsidies, whose presence is critical for a massive deployment [32], as well as tax reductions mainly in the form of reductions in the Real State Tax (IBI) and Construction, Installations and Works Tax (ICIO) [27].

1.1.3 PV systems in urban areas

The maturity of this technology, which still allows affordable costs for reduced economies of scale, and the administration's support allow the massive deployment of self-consumption in the building sector to become a reality in the short term. PV systems deployed in urban environments constitute a strategic area to mitigate the effects of climate change and provide a positive economic and social impact [33].

The reduction of local emissions is possible thanks to the abundance of unemployed rooftop areas, which range from 20% to 25% of the urban surface [34]. This provides an opportunity to leverage the solar resource, which significantly increases in low-intermediate latitudes such as Mediterranean regions. Local PV generation concurrently minimizes transportation and transmission losses, enhancing overall grid efficiency [35], deferring future grid infrastructure investments [36], and fostering the growth of decentralized smart grid systems.

The main economic benefit that the users of the facilities can perceive is the cost reduction of their electricity bill with a lower PB than the facility's lifetime, which is significantly reduced in low latitudes. Consequently, users become more independent from technical issues of the grid as well as more resilient to price volatility. These reduced electricity costs translated into increased competitiveness for consumers who conduct business activities. The massive execution of PV facilities is also associated with job creation, whose rates per PV installed power are higher than other energy sources [37].

As positive social impacts, higher penetration of PVSC systems in urban environments raises a higher citizen's awareness and responsibility for sustainability. The latter increases the number of actors sharing electricity generation's benefits. Moreover, it is possible to share the benefits among different consumers through the figure of the PV energy community, which is legally feasible in multiple countries, such as Spain [38]. This collective solution increases the penetration of rooftop PV facilities in urban environments with a high density of consumers. As a result, a higher rate of PV production is consumed by the users [39].

1.1.4 General challenges in the field

However, despite the benefits, different challenges hinder the massive implementation of the PVSC systems in urban areas.

From the technical point of view, a scenario with low electricity demand and a high concentration of PVSC facilities potentially causes the presence of reverse power flows and voltage fluctuations in a low-voltage power grid. Both lead to increased power losses, exceeding operation ratings of electrical equipment, and issues in protection equipment compromising the stability and security of the grid [36, 40].

From the economic perspective, depending on the billing regulation of each country, PVSC might lead to an unintended cost redistribution among all the consumers of the system. If grid costs are charged in the variable component of the electricity bill, consumers connected to PVSC facilities are transferring this charge to the consumers without PVSC systems [41]. Regarding the investment costs, with the current economy of scales, a complete deployment of PVSC systems with low capacity implies higher investment costs than utility-scales near the urban areas. These large PV power plants constitute an alternative to PVSC systems to increase the renewable share in the electricity mix [36].

From a social perspective, the main barriers to a massive deployment are the reduced information and social awareness [42, 43], the presence of concerns about the economic viability of PVSC systems, as well as the high initial investments and uncertainties with the PB due to the volatility of electricity prices [44]. In general, several surveys identify skepticism and a lack of confidence in the performance reliability of new unfamiliar technologies as PVSC [45]. The lack of investors' and homeowners' awareness about rooftop PV potential and the detailed information regarding rooftop spaces suitable for PV installation, especially the economic benefits [46], are significant barriers impeding the diffusion of rooftop PV systems.

Finally, legal frameworks might remain restrictive depending on the country with high organizational and planning requirements and limited institutional support [47].

In order to shorten the above-mentioned limitations and increase the penetration of rooftop PVSC systems in urban environments requires a knowledge of the energy and economic savings potential of these facilities under multiple scenarios and its further dissemination to the public. Thanks to household PV installations, awareness of the economic benefits for consumers is fundamental in promoting acceptance [48, 49]. Mass media and public administration play a significant role in motivating and disseminating the benefits of PVSC in urban areas [50]. Common solutions in this area are general studies of PV rooftop potential. Tools such as solar cadasters have become a regular tool to promote and raise public awareness of PVSC [51]. Some previous experiences in web mapping applications [52–54].

Besides shortening the social barriers, other agents can benefit from PV potential studies. These studies help the public administration define a roadmap for the city's energy transition, optimizing annual budgets or promoting self-consumption in certain buildings or neighborhoods of cities [55]. For utility companies, PV potential studies can be employed in the energy supply and infrastructure planning since peaks in distributed generation lead to strain on the electricity grid [51]. In addition, private corporations can leverage the PV potential studies to acquire potential customers, preliminary identifying the most profitable facilities on rooftops in a specific region [56]. In sum, these studies represent an incentive to mobilize private investment in this sector and move towards clean energy transition [57].

1.2 Background and research context

1.2.1 Overview of PVSC facilities on building's rooftops

One of the main PV systems configurations is grid-connected PV systems, which are PV facilities connected to the utility grid [58]. Facilities under this category range from large-scale PV power plants or PV utility-scales, which directly produce electricity to the public grid, to self-consumption facilities, whose production is partly consumed by the users, and the surpluses are injected into the grid. The latter category allows decentralized production in urban areas employing multiple solutions such as integrating solar modules in the building envelope, including roofs or façades, or using ground-mounted systems in case of unused land near the users, with the possibility to include energy storage systems to increase the on-site performance.

PV systems with batteries can present SC rates over 80% [59, 60]. However, their high cost would compromise the profitability, as shown in several studies [61, 62]. A drop in the cost of batteries of more than 50% during the thesis development period would be necessary for them to be more profitable than the sale of surpluses in the Spanish context [63]. Subsidizing storage systems is a common approach to enhance profitability [59]. Therefore, rooftop systems without storage are the most affordable solution with no financial aid and fewer requirements for already-built buildings.

A grid-connected PV facility is constituted by a solar PV array of modules, which generates DC electricity from solar irradiation. For a high performance of the facility in this stage, it is crucial to design the installation with a proper azimuth orientation and inclination to maximize the beam irradiance, which is the most energetic irradiance component. The modules are connected in series, forming strings and parallel to reach the adequate voltage and current levels, respectively, for the correct operation of the inverters. The inverter is the device that converts the direct current (DC) to alternate current (AC) electricity, adapting it for its consumption or injection of the grid. Other essential elements of PV facilities are protection systems installed in both DC and AC circuits and smart meters, employed to quantify the energy flows between the installation and the grid [64].

Three main concepts are widely employed in literature to quantify the energy balance of PVSC facilities: SC, surplus rate, and SS. On the one hand, the SC rate is the fraction of the PV production the user directly consumes, while the surplus rate is the remaining fraction of the PV production injected into the grid. The SC describes the level of sizing of a facility according to its demand. A usual range for this metric oscillates between 30% for residential users and 70% for tertiary and industrial users [65]. Higher rates in a facility mean that the production might be undersized. On the other hand, SS stands for the fraction of the electricity consumption by the user directly supplied by the production of the PV facility, which is self-consumed energy. This rate quantifies the degree of alignment of the PV production with the electricity consumption as well as the level of independence from the grid [66], and ranges typically between 20% to 40% for systems without storage [41, 60, 67].

Despite the technical performance and efficiency of the elements of the facility, which can be estimated with acceptable accuracy through their life cycle, the quality of long-term economic assessments of a facility is compromised due to internal and external fluctuating factors.

On the one hand, the main external economic factors are the evolution of inflation, interest rates, retail electricity prices, manufacturing costs of the spare parts, modifications in regulation that define the billing scheme, and political factors such as subsidies. On the other hand, internal factors depend on the facility's user. Some examples of this category are the financial attitude of the investor or homeowner, the sizing criteria, and the final installed capacity, which leads to a specific economy of scale and the habits and hours of use of consumer's electrical devices. The latter significantly influence economic performance because retail prices usually fluctuate within tariff periods, and savings might fluctuate with the alignment with sun hours depending on the billing scheme. Therefore, many particularities hinder the economic potential assessment in other contexts or regions of the world where consumption patterns, regulations, billing schemes, and the general economic conjuncture might differ.

One of the crucial elements in the economic potential assessment is the billing scheme, which depends on the current regulation of each region or country. Figure 1.2 describes the main two billing mechanisms for grid-connected PVSC facilities: net metering (NM) and NB [26, 68].

A net metering scheme enables consumers with PV production to consume their energy produced during a given period (generally monthly as the billing period) instead of only when it is produced, using the grid as storage. Therefore, the price of surpluses is equal to the retail price of the grid's energy. This mechanism has multiple variants, such as virtual NM, which enables economic benefits among other properties whose meters are not directly connected to the facility. This case is helpful for multi-tenant properties.

While NM is based on an energy exchange, NB consists of a monetary exchange for the energy injected into the grid. Under this mechanism, the surplus price is different from the retail price of the energy consumed from the grid, generally lower than the retail price.

While NM enhances facility profitability by offering higher prices for surplus energy compared to NB, it may not necessarily encourage the synchronization of production and consumption. Consequently, this fact favors the oversizing of facilities, leading to excessive intermittent surpluses in the grid. The NB approach encourages an appropriate sizing of PV systems according to their own consumption needs. As a result, surpluses are minimized, preserving the grid stability and reliability, and reducing the potential need for increased operating reserves and backup capacity [69]. Since infrastructure costs of the electricity grid are socialized through the energy tariff, another potential issue derived from a NM scheme is that consumers without PV facilities might pay higher energy bills subsidizing the grid maintenance costs derived from users with PV facilities. In this case, NB systems prevent additional costs from charging consumers without PV systems [70, 71].

In 2023 NB schemes or similar mechanisms in which surplus prices are lower than the retail price are in force with their respective peculiarities in multiple countries' regulations such as Australia, Chile, Denmark, Germany, Italy, Poland, Portugal, Spain, Sweden and Switzerland and 4 US states. The NM scheme is present in Belgium, Brazil, Finland, Israel, Mexico, Netherlands, Ontario (Canada) and 42 US states [72].

Other billing schemes are feed-in-tariff and power purchase agreements. The first one consists of a predefined price of the injected energy to the grid fixed constant during a specific period, and it is usually applied for utility-scales. The second one is based on a financial agreement between a customer and an investor who executes, operates, and maintains a PV facility on the customer's property and sells the PV electricity production to the customer at a fixed price, usually below the retail price from the grid [73].

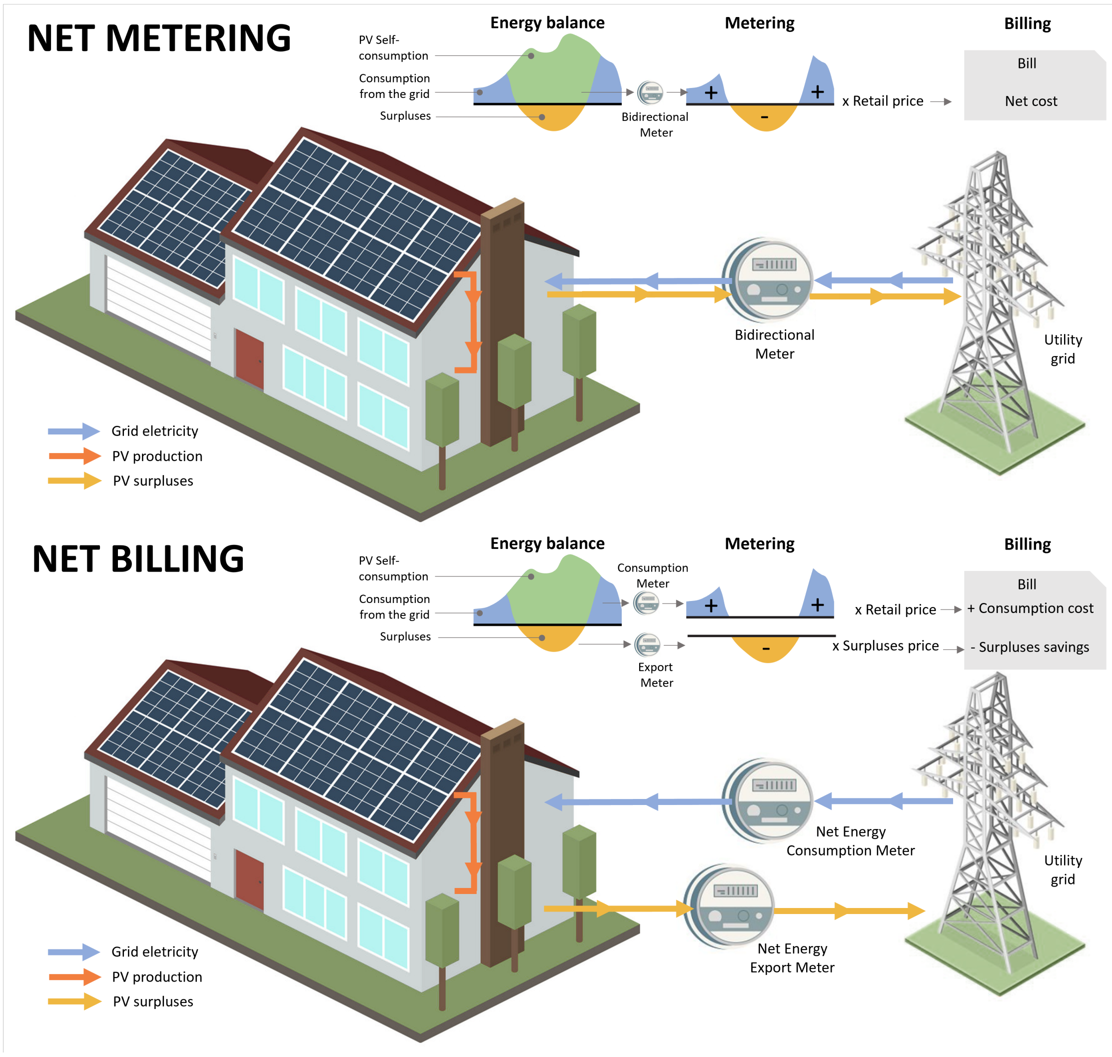

Figure 1.2: Graphical summary of the NM and NB schemes.

To finish with the regulatory trends, it is worth noting the inclusion of PV energy communities in multiple legal frameworks in different countries, such as Spain [33], implying the possibility of sharing the PV production of a PV facility among multiple consumers. This new legal figure enables the deployment in urban areas with high population density. This justifies the evaluation of photovoltaic potential as a legally feasible action in urban environments since many users are sharing one roof, especially in multistorey buildings [74], or industrial buildings that share their PV production with other residential users [75]. Thanks to the demand aggregation, these configurations tend to increase SCs, maximizing the distributed renewable generation and improving the shared facility's profitability [39, 65, 76].

A literature review published in February 2023 counted 3,931 already-constituted energy communities with 900,000 members in the EU and the United Kingdom. The energy community concept comprises several energy technologies. The most frequent are solar (PV and thermal), wind, biomass, hydro, and e-mobility. Germany leads this initiative with over 800 deployed solar energy communities, while the Netherlands and Denmark are more common wind and biomass energy communities. According to projections, energy communities could have a share of about 17% of the installed wind capacity and 21% of the solar capacity by 2030 [77]. In Spain, at the beginning of 2023 there were 73 constituted PV energy communities. The Valencian Community is the frontrunner with 85 in the process of constitution, mainly promoted by local administrations and represented by cooperatives [78].

Additional physical and geographical constraints should be considered when designing rooftop PVSC facilities in urban environments compared with the common ground-mounted power plants.

- In urban environments, the presence of shadows on the building rooftops projected by the surrounding buildings and nearby obstacles becomes relevant, especially in lower buildings [79], significantly reducing the PV production or the available space with a low level of shadows. Therefore, modeling shadows accurately is critical to provide realistic geographical potential estimations [80].
- Considering the inclination and orientation of the rooftops is crucial for adequate integration of the facilities and maximizing the installed power density per area.
- Besides assessing the technical potential, consumer demand may also be relevant in the sizing of the installations depending on the evaluated billing mechanism and the economic criteria considered in the design process. For instance, under a NB scenario, in which surpluses are remunerated at a different price than energy from the grid, the economic performance depends on the user's electricity consumption. Therefore, a good design practice for proper sizing should consider the load curve.

A wide range of sizing criteria is found in the literature to determine the PV capacity. Some of them optimize economic variables such as the net present value (NPV), the IRR, the PB [81, 82] and the Net Present Cost [83]; others optimize energy aspects such as the SS and SC [66, 84], or adjust the capacity so that the annual consumption is equal to the annual demand [85]; while others minimize the exchange of energy with the grid to guarantee the energy stability [86]. In the most recent research, multi-objective optimization of economic and energy criteria has been the object of interest, providing more balanced performances [60, 87, 88]. In summary, there is a difference between the maximum PV capacity potential limited by the rooftop characteristics and the required PV capacity according to the demand needs of the users. Therefore, considering the demand for the PV rooftop potential adds an extra complexity.

1.2.2 Main approaches to assess PVSC in urban areas

This section presents a state-of-the-art classification of the diverse approaches employed in assessing urban PV potential in the literature. The main categories are summarised in Figure 1.3.

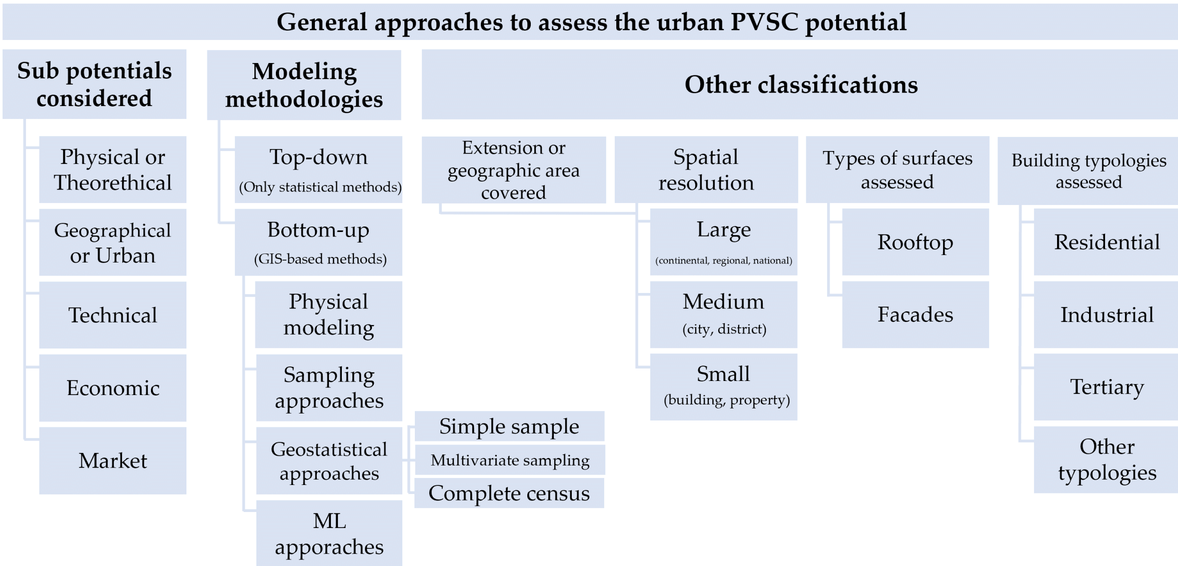

Figure 1.3: Summary of the general approaches to assess the urban PV potential.

In the literature, PV potential studies are often categorized into a series of hierarchical steps (Figure 1.4), each representing distinct **sub-potential types** described below [87, 89, 90]:

- The **physical or theoretical potential** consists of the solar irradiation on a surface in a given location, and it is defined by variables such as solar irradiation divided by its components (direct, diffuse, and reflected irradiance if no obstacles were considered). Only geographic position and climate are considered.

- The **geographical potential** reduces the theoretical potential with the spatial limitations of urban environments and architectural integration criteria. It consists of the available solar irradiation on PV modules on a rooftop surface. It is determined by the effects of shadows cast by nearby buildings and obstacles, the rooftop geometry, available roof area, orientation, and inclination of PV modules.

- The **technical potential** reduces the geographical potential considering the PV system performance and efficiency, converting the solar irradiation into AC electricity for the user. For this, it is crucial to evaluate the energy transformation efficiency of each PV facility element and the spatial constraints of the equipment, including rooftop dimensions, spacing, and the PV array configuration.

- The **economic potential** includes the economic limitations of photovoltaic installations to the technical potential such as installation costs, operation costs, potential savings in the bill, the presence of subsidies, the evolution of electricity prices, the applied billings scheme, etc. In this step, it is possible to obtain the economic feasibility of each facility according to multiple variables, such as the levelized cost of electricity, the PB, the NPV, or the IRR, among others. Nevertheless, a clear consensus about the scope or limits of this potential was not found in the literature.

- The **market potential** is the fraction of the previous potentials that finally is deployed considering other competitive alternatives, socio-cultural perception, the investors' response, policies, regulations, etc.

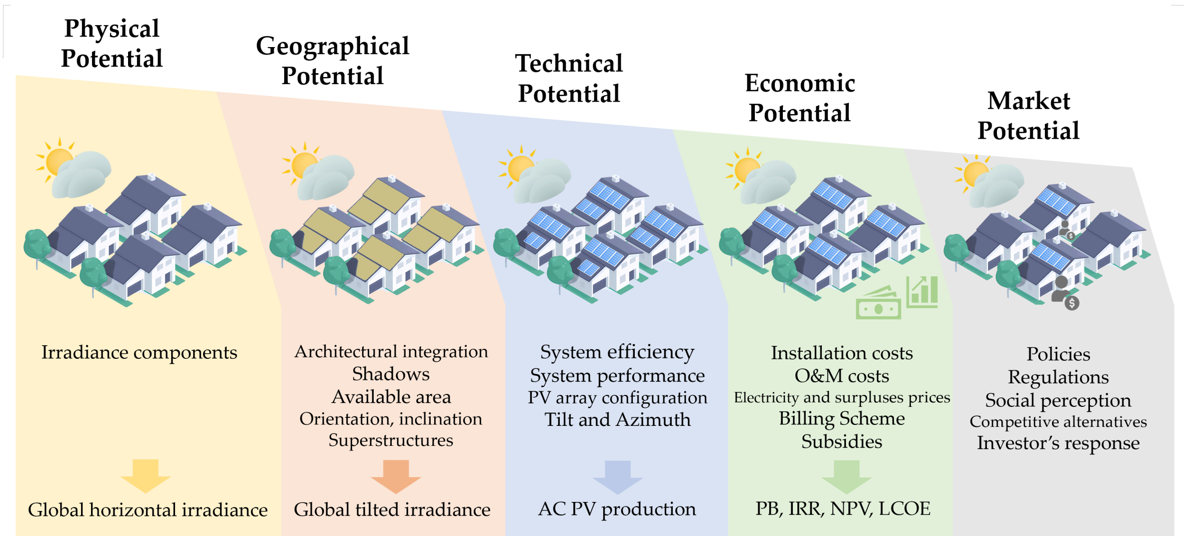

Figure 1.4: Hierarchical classification of the PV sub potentials and their main influential factors.

For each hierarchical step, the amount of required information and the number of assumptions generally increase, while the extrapolation of the results to other regions or contexts hinders. This is one of the reasons why extensive literature applied in PV urban assessment focused on the first levels of the hierarchy, namely geographical and PV potential. In contrast, the interest in economic potential remains moderated [91]. In recent years, the number of large-scale studies considering the economic constraints has increased partly thanks to the PV technological maturity [92]; however, it remains reduced compared with the technical potential [89]. For an actual deployment of PV systems, providing positive business cases is one of the crucial drivers to increase social acceptance [90].

The **methodologies** followed to estimate any of the previous sub potentials are usually conditioned by the availability of data sources in the region under study. The two most frequent methodological approaches found in literature are the following:

- The **top-down approaches**, which are based on statistical methods. Generally, these methods rely on aggregated statistical data (building census, population, density, etc.) usually applied in large geographic areas. The results provided are aggregated. Therefore it is not possible to extrapolate accurate results for smaller geographic extensions [93].
- The **bottom-up approaches**, which are based on GIS-based approaches [94], are generally applied in minor geographic extension and spatial resolution than statistical methods due to their high computational cost. There are multiple subcategories under this general approach: physical modeling, sampling, geostatistical, and ML approaches [95].
  - **Physical modeling approaches** are based on developing complex physical models involving a hierarchical methodology that concatenates multiple physical models to obtain each type of PV subpotentials. Physical models first calculate the physical potential through irradiance models, followed by geographic potential with 3D GIS models, technical potential with PV production models and technical specifications of each element of the installation, economic potential through multiple economic variables including, in some cases, load profiles, and market potential. Usually, this is the most accurate but most time-consuming approach. Therefore, its scalability is limited.
  - **Sampling approaches** are considered hybrid approaches combining bottom-up and top-down approaches. It is based on the extrapolation to a greater geographic extension of the simulation results of a sample of individuals [96]. These methods are employed when available data or calculated results are limited and allow a computational cost reduction instead of aggregated statistical estimators. The sampling approaches are classified into three categories [97, 98]:
    - The simple sampling approach is based on an estimation provided by a representative sample (i.e. buildings in this context), which is extrapolated to the entire studied area.
    - The multivariate sampling-based approach provides an extrapolated result based on the relationship between two different variables drawn from a representative sample.
    - The complete census approach consists of estimating the PV potential of each element (i.e. building) of the area studied. It is typically performed through geospatial and GIS-based methodologies.
  - **Geostatistical approaches** stand for spatial statistical analysis to obtain through interpolation results of specific locations that have not been sampled. The estimations are composed of a deterministic and a probabilistic part and are obtained through linear models. These methods are highly used to obtain physical potential or environmental data.

– **ML approaches**, which consist of algorithms that learn patterns from data to make predictions of a specific outcome. The most frequent algorithms applied in this field are multiple linear regression (MLR), Artificial Neural Networks (ANNs), Support Vector Machines (SVM), Regression Trees such as Random Forests (RFs), etc. Similar steps are followed when applying these algorithms: data collection, data preprocessing, identification of predictors, model training, model testing, and estimation of the PV potential with the validated model. The choice of an appropriate ML model depends on the structure of the problem and the available data [97, 99]. In the last decade (2010-2020), there has been a growing number of publications on the application of ML models to the detriment of traditional sampling models and physical models [89].

Another classification approach is the minimum **spatial resolution** of the potential provided, with a wide range of categories based on the studies found in the literature: large aggregation level (continental, regional, national), medium aggregation level (city, district) or small aggregation level (building, consumer). The previous categories are also applied when a classification approach based on the **geographic extension** covered by a study is addressed [94]. Additional classifications of PV potential assessments based on the **type of surfaces analyzed** (such as rooftops, façades, or both [51]) or the **building typologies** studied (residential, industrial, tertiary, etc.)

GIS-based approaches constitute one of the most used modeling approaches in this research area, allowing the development of 3D city models. The most common **data sources** for these models require multiple spatial data.

Some studies employ vectorial GIS-based data to obtain geographic extension boundaries, cadastral geometries, and the geometry footprint of the buildings. Usually, this information is available in public cadastral vectorial maps open data sources such as OpenStreetMaps [100] or CityGML [101].

Together with the vectorial data, raster data sources are crucial to obtain accurate 3D models and calculate the shading effects [102, 103]. Digital Terrain Model, also known as Digital Elevation Models, provides the elevation data of the bare-earth surface. At the same time, Digital Surface Model includes the elevation data of the urban environment, vegetation, and other built elements. Finally, Light Detection and Ranging (LiDAR) data is used to obtain the height of buildings, trees, and other obstacles.

As an alternative to the previous data sources, with orthophotos and satellite or areal images, it is possible to create 3D models through photogrammetry techniques [104]. Orthophotos are also used for rooftop segmentation and identification of obstacles undefined in vectorial data [105].

In addition to the spatial data, time series data allows the modeling of the temporal dynamics of the facilities' production and the users' consumption. For large scale, potential hourly time resolution time series are usually employed due to their high availability as well as they provide acceptable precision and a reduced computational cost compared to other lower time steps, both for the PV production [106] and the electricity demand [85]. In order to estimate the PV production, climate data time series broken down by the irradiance components usually are employed as one of the major requirements for most of the transposition models [64, 107, 108]. One of the most employed irradiance data sources in literature is PVGIS. However, typical meteorological year data or on-site measurements from weather stations (WSs) and pyranometers are also recurrent, especially for validation purposes [109]. The estimation of electricity curves is mainly present in economic potential. Common demand estimation approaches are the use of synthetic load profiles generated by software [110], or open data sources (e.g. in Spain the Distribution System Operator (DSO) provides typical demand profiles for different uses [111]). At the same time, other studies employ real consumption load curves [112]. However, this approach limits the geographic extension of the study. Other essential factors to consider are the electricity prices and surpluses remuneration fluctuations depending on the period of the day [27, 113]. Generally, this information is provided by the DSO or the electric marketer. Other structured datasets that facilitate the characterization of buildings to improve the demands estimations are the cadastral datasets, which provide the characteristics of building typologies, uses, year of construction, built area, etc [96].

Regarding the technical characterization of the elements of a PV facility, the parameters employed in the modeling process are usually obtained from literature, technical datasheets, or experimental measurements.

Finally, the economic hypothesis or assumptions for prices or costs are usually obtained from other research studies, the DSO, the electric marketer, or official institutions.

1.2.3 Detailed analysis of the modeling techniques of PVSC in urban areas studied in the present thesis

This thesis explores alternatives to computationally expensive physical modeling methods through the development of agile regression-based models within the ML category, as categorized in section 1.2.2. This section provides an extensive literature review covering both approaches and their associated challenges.

Among the **physical modeling approaches**, several limitations exist in estimating each sub potentials.

Estimating available rooftop areas for the geographic potential involves employing GIS-based 3D models for shadow estimation, representing a computationally intensive step in the simulation flow. 3D models of level of detail 1 (LOD1) and LOD2, according to the CityGML standard [101], are the most frequent. Although they provide a similar accuracy compared to more detailed models, they present limitations when datasets are not updated or when identifying other rooftop obstacles or superstructures requiring higher data precision [114]. Other specific rooftop obstacles are difficult to identify with LiDAR, or aerial images are normally modeled with reduction coefficients [115, 116].

There is a wide range of methodologies in the literature to convert the geographic potential to technical potential based on ratios from statistical data or constant values. This fact oversimplifies the diverse possibilities in the array configurations and potentially leads to high deviations when analyzing individually specific buildings. For instance, this approach is found in the conversion through a constant value of the available rooftop area and the total PV capacity installed [67, 117], or in the estimation of the previous rate through stratified sampling techniques [118]. Another area for improvement that hinders the interpretation and comparison of several research studies concerning the technical potential is the high range of criteria and constraints to arrange PV modules on rooftops. Some of the most relevant are the following:

- The definition of minimum rooftop area per installation [119].
- The optimization of tilt and azimuth angles to maximize energy or economic performance [120].
- The definition useful areas based on thresholds of total annual irradiation [55].
- The elimination of north-oriented rooftops which are not useful for PV (in the north hemisphere) [121].
- The empirical models employed for converting irradiance to electric production [108, 122].
- The modeling of the energy conversion losses of the PV systems [123].

In sum, technical potential modeling requires a high level of know-how to achieve quality and replicable results [94].

Regarding evaluating economic potential, the most significant challenges and opportunities for improvement identified are related to estimating the electricity demand. The latter are summarized in Figure 1.5.

Most economic potential assessments are based on net-metering models, which do not require a detailed demand modeling to distinguish between savings from self-consumption and savings from surpluses. Among these cases stands out the PV assessment of a $2\,\mathrm{km}^2$ area of Karlsruhe (Germany) [51], the city of Lethbridge (Canada) [124] and 11,140 rural areas in Brazil [116].

Only three bottom-up large-scale techno-economic assessments using load profiles were found in the literature, which are crucial when addressing NB scenarios, such as the case of Spain. A recent study employed 5,567 real load profiles in London (United Kingdom) [125]. Another study limited to a reduced study area of 71 buildings in the town of Grafing bei München (Germany), employed load profiles for residential, commercial, industrial, and public uses were obtained from the German DSO and scaled up employing a ratio and built area [90]. Another techno-economic study applied to old residential buildings in five districts in Nanjing (China), estimated the demand curves through aggregated statistical data, and results were provided aggregated by districts [126]. The main barriers identified for a more significant proliferation of large-scale economic studies are the computation cost of operating with thousands of load curves and the lack of data sources to estimate them accurately. Alternatively, other studies estimate the demand based on cadastral information when data is scarce. For example, in a study in Wroclaw (Poland), the aggregated demand data was divided by city sectors according to each sector's aggregated rooftop area. A correlation between demand and rooftop area was assumed [67]. Another example is found in the techno-economic assessment of the city of Valencia (Spain). By employing the sampling approach, load curves are estimated through ratios such as the relationship between the number of dwellings per floor scenarios [117]. No difference in profiles among the properties is considered, and the demand is only employed to estimate savings since retail prices vary with periods.

The optimal sizing of the capacity of facilities is a common practice in specific case studies found in the literature. However, only the study in London addressed the optimization issue maximizing the profit and the autarky [125]. In the rest of the above-mentioned large-scale studies, no sizing of PV systems according to demand was considered.

In addition, no model in this field leverages the energy community concept in which different consumers who share the same rooftop benefit from a common facility. In this matter, when analyzing the PV potential of a complete building, there is a trend to not consider different load profiles depending on the use of the properties within a building.

When addressing large-scale energy balances between production and demand, top-down approaches that quantify the SS of a large area of study are more frequent. Nevertheless, conclusions derived from demand are limited due to the approach and minimum resolution selected. For instance, disaggregated results at building level were not obtained in a study case applied in Valencia, which employed statistical data to estimate an aggregated demand for the entire municipality [127].

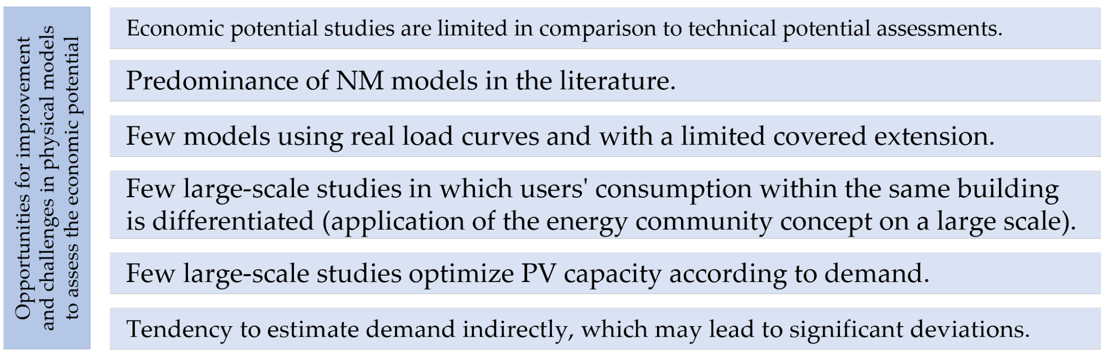

Figure 1.5: Summary of challenges and opportunities for improvement in physical models to assess the economic potential.

ML approaches have aroused high interest in recent years in the field of the integration of renewable energies in urban environments. A recent state of the art collected the most relevant works employing these approaches and identified potential gaps and future lines of research, which are the following [128]:

- 48 out of 54 papers reviewed were focused on providing theoretical, geographical, or technical potential. The most frequent are the first two potentials. Their most usual inputs are environmental or climatic data, remote sensing variables, and other parameters that characterize the physical urban landscape.

- Only one research was found addressing the economic potential to estimate the $LCOE$ using a Gaussian process regression model as inputs technical variables of equipment and real demand of a population [129].

- Systematic quantitative comparisons among methods found in literature are difficult to perform since the wide diversity of variables involved as well as data availability are conditioned by the area studied.

- There is a general trend in recent years to include data related to urban morphology and sociocultural aspects as predictors. According to recent papers, variables that provide a morphological characterization of the buildings are significantly helpful in assessing PV economic and market potential.

- Most modeling approaches are based on complex ML models with reduced interpretation, such as ANNs, Convolutional Neural Networks, RF, Gradient Boosting, Support Vector Machines (SVMs), and K-Means, while regression-based approaches are less usual.

With all the above, **regression-based approaches** applied for the economic potential remains unexplored. Regression-based models ease the interpretability, the replicability and require less computational time than the other ML models.

These approaches are suitable for predicting continuous variables and are more common in the PV urban potential context when estimating intermediate results. For instance, the horizontal irradiation and the albedo coefficient, shading, and rooftop obstacles from satellite data [130], the in-plane irradiance data from using the Sky View Factor as predictor [131], and the energy consumption predicted through urban morphological parameters [132].

Nevertheless, a few relevant experiences apply regression-based approaches to directly assess large-scale PV potential as a final output, as described below. The geographical potential estimation on each rooftop in six cities of Switzerland was calculated through MLR employing six input features: annual global horizontal irradiance, roof tilt, roof aspect, and three mean horizon heights for each roof [133]. Regression models were also applied to obtain the spatial projection of PV facilities testing of multiple linear and two spatial regression models with techno-economic and socio-demographic variables as predictors [134]. Moreover, intermediate alternatives that combine modeling and ML approaches are also present in the literature. For example, a support vectors regression model was developed to estimate technical potential at the commune level in Switzerland, the model trained with 3D-GIS model as an intermediate step [135].

As a summary of this section, the main advantages and disadvantages of the main approaches addressed in this thesis (physical and regression-based modeling) have been summarized in Table 1.1, and the most relevant modeling experiences found in the literature to assess the PV techno-economic potential have been compiled in Table 1.2.

Table 1.1: Advantages and disadvantages of the modeling approaches developed in the present thesis.

Modeling approach	**Advantages**	**Disadvantages**
GIS-based physical models	• High accuracy. • Specific details. • High customization. • Possibility of automated application in several areas.	• Computation intensive (heavy calculation). • Long simulation time. • Difficult to scale-up. • Technical experience needed. • Many data sources are required.
Agile regression-based models	• Highly scalable. • High time performance. • Ability to consider many input features. • Adaptability and flexibility.	• Large amount of data sample is required for an accurate extrapolation. • Technical experience needed. • Loss of intermediate results. • Depending on the model and complexity interpretability is compromised.

Table 1.2: Literature review of techno-economic potential studies in urban environments (2015-2023).

Author	Publication year	Potential	Methodology approach	Sampling-Extrapolation	Resolution	Geographic extension	Surfaces considered	Building typologies	Main data sources	Reference
K. Sredensek et al.	2021	Geographical, Technical and Economic	Physical modeling	Complete census	Building	Region of city of Novo Mesto (Slovenia)	Rooftops	Multiple	LiDAR, climate data from weather stations,	[87]
Karoline Fath et al.	2015	Geographical, Technical and Economic	Physical modeling	Complete census	Building	$2\,\mathrm{m}^2$ of Karlsruhe (building)	Rooftops and façades	Any	3D city model provided the Administration, Radiance software for irradiance	[51]
Fariborz Mansouri Kouhestani et al.	2018	Geographical, Technical and Economic	Physical modeling	Complete census	Building	55,877 buildings in Lethbridge (Canada)	Rooftops	Any	LiDAR data	[124]
Raul F.C. Miranda et al.	2015	Technical and Economic	Sampling approaches	Complete census	Regions of different areas	122 study groups in Brazil	Rooftops	Residential	Vectorial data for spatial boundaries, weather measurements	[116]
Jordi Olivella et al.	2021	Economic	Physical modeling	Complete census	Consumer	5567 households in London (United Kingdom)	Rooftops	Residential	climate data from WSs, dataset SmartMeter provided by UK Power Networks for load profiles	[125]
Peng Wang et al.	2022	Geographical, Technical and Economic	Physical modeling	Simple sampling	Building	Five districts in Nanjing (China)	Rooftops	Residential	ECMWF from solar irradiance, BIGEMAP software for rooftop boundaries, Nanjing City Statistical Yearbook for consumption data	[126]
Alba Torres-Rivas	2022	Geographical, Technical	Sampling approaches	Complete census	Municipality	Region of Catalonia (Spain)	Rooftop	Any	National Statistics Institute of Spain)	[136]
Sebastian Krapf et al.	2021	Technical and Economic	ML (CNN)	Simple sampling	Building	71 buildings in Grafing bei München (Germany)	Rooftop	Residential, Industrial commercial, public	Aerial images	[90]
Jakub K. Jurasz	2020	Technical	Physical modeling	Complete census	Hexagons of $1.46\,\mathrm{m}^2$	246 hexagons in Wroclaw (Poland)	Rooftop	Any	LiDAR, vector layer of buildings (BDOT10k)	[67]
Rui Zhu et al.	2022	Technical and Economic	Physical modeling	Simple sampling	Building	122 buildings	Rooftops and façades	Residential and commercial	New York City Open Data for annual demand, buildings' height, and footprint	[137]
Katalin Bódis et al.	2019	Technical and Economic	Sampling approach	Complete census	Country	EU countries	Rooftop	Any	Raster datasets for irradiance, land cover for urban areas, and human settlements, vector maps for buildings and country statistics	[97]

Author	Publication year	Potential	Methodology approach	Sampling / Extrapolation	Resolution	Geographic extension	Surfaces considered	Building typologies	Main data sources	Reference
Dan Assouline et al.	2017	Geographical, Technical	ML (SVM)	Complete census	Swiss Commune	2,477 communes (Switzerland)	Rooftop	Any	Satellite imagery solar data for irradiance, meteorological stations for other weather variables, raster Digital Elevation Model, LiDAR, Numerical 3D buildings for building roof data, areal images and vector and raster layers for land cover	[138]
Alina Walch et al.	2020	Technical	ML (RFs, Extreme Learning Machine Ensembles)	Complete census	Building	3.7 million buildings (Switzerland)	Rooftop	Any	Satellite imagery solar data for irradiance, meteorological stations for other weather, Numerical 3D buildings for buildings data, LiDAR, Numerical 3D buildings for building roof data	[130]
Jonas Müller et al.	2019	Technical	ML (Spatial Regression, MLR)	Complete census	District (average area $280\,\mathrm{m}^2$)	143 districts (Switzerland)	Rooftop	Any	Dataset with 68.341 Swiss installations, Techno-economic and socio-demographic data at district level	[134]
Lijian Sun et al.	2022	Technical	Physical model	Multivariate sampling	Area (100 m x 100 m)	Wuhan (China)	Rooftop	Any	Wuhan housing construction survey for spatial distribution of buildings, Meteosat IODC satellite for irradiance	[115]
Tomás Gómez-Navarro et al.	2021	Technical and Economic	Physical model	Multivariate sampling	Area (250 m x 250 m)	Valencia (Spain)	Rooftop	Any	PVGIS, Huellasolar, Aerial Images	[117]
Chapter 3	2021	Technical and Economic	Physical model	Simple sampling	Building	Sample of 893 (1,035) Valencia (Spain)	Rooftop	Residential	LiDAR, TMY data, cadastral data and vector maps	[139]
Chapter 3	2021	Technical and Economic	ML (MLR)	Multivariate sampling	Building	Sample of 893 (1,035) Valencia (Spain)	Rooftop	Residential	LiDAR, TMY data, cadastral data vector maps	[139]
Chapter 4	2023	Technical and Economic	Physical model	Complete census	Building	3,734 buildings Catarroja (Spain)	Rooftop	Any	LiDAR, TMY data, cadastral data and vector maps, aggregated demand by district	[140]
Chapter 4	2023	Technical and Economic	ML (MLR)	Multivariate sampling	Building	3,734 buildings Catarroja (Spain)	Rooftop	Any	LiDAR, TMY data, cadastral data and vector maps, aggregated demand by district	[140]

1.3 Identified gaps and research questions

With the previous literature review and research context presented, the following gaps were identified in this section.

First, an efficient methodology for obtaining the roof PVSC economic potential by determining suitable roofs for optimal installation of solar photovoltaics remains a challenge with physical modeling approaches [141]. For this method, there is still a scarce bibliography related to the economic constraints derived from considering the electrical demand and its influence on the feasibility of large-scale studies of PVSC potential in urban environments. For example, in NB scenarios, large-scale studies do not contemplate the optimal sizing of PV facilities conditioned by the electric demand, which leads to significant overestimations in the PV generation [103]. In addition, in this context, scarce literature was found about the inclusion of the matching with load profiles to complement the economic assessments and provide a realistic aggregated SS in urban areas in a high-resolution level (i.e. buildings scale).

Secondly, these approaches are characterized by a high computational cost, level of complexity, and detail, which depend on a large amount of information [57]. However, they are troublesome for large-scale studies, such as country-wide studies, because of the large amount of calculation required (heavy calculations) to obtain satisfying outcomes [94], and data sources may be inexistent or reduced. In contrast, ML and regression-based approaches are promising alternatives to the modeling approaches, which require less computation time to calculate all input variables leading to the rooftop solar PV potential [94]. Generally, MLRs have been used as an intermediate calculation step in physical modeling approaches, and very few regressions have been applied directly to geographic and technical potential studies. Meanwhile, no direct use of MLR models was found in the literature to assess the PV economic potential directly. The possibility of developing agile models in the economic area would reduce the cost of obtaining potential evaluations. Consequently, this improvement would facilitate the disseminating of relevant information to citizens, technicians, and poly-makers to increase the penetration of PVSC in cities.

Finally, most of the massive techno-economic potential assessments identified in the literature correspond to high-moderate latitudes and oceanic or continental climates. In this area, large-scale assessments in Mediterranean regions, which present a high solar resource, remain irrelevant in the literature.

In order to address the previous gaps, this thesis is guided along the following **two main research questions**, providing novel knowledge in this research area:

- **How can simplified (regression-based) models improve and ease the urban PV techno-economic potential estimation and facilitate their replicability?**
  - In what degree is it possible to estimate PV economic potential in urban areas employing the morphology of buildings?
  - How can regression-based models facilitate physical modeling to estimate multiple PV performance variables such as energy or economic indicators?

- **As an application of the previous models, which is the current economic PV potential in a representative Mediterranean municipality nowadays?**
  - Which energy balance with the grid because of a massive PV deployment is reached for that municipality considering economic constraints?
  - In what degree can hourly fluctuations of the electric demand affect the profitability of PV facilities and the SS of the municipality?
  - How can the adopted billing scheme affect in the municipality's PV potential?
  - In order to optimize public and private resources, which buildings typologies to deploy PVSC systems are the most interesting from an economic point of view and with greater impact on the energy transition of the municipality?

1.4 Objectives

In order to answer the above-mentioned research questions, **the global objective of this research is centered on providing data-driven methodologies to develop simplified models capable of assessing the economic PVSC potential rooftops in urban environments**. Additionally, **as an application of the previous methodologies, the research aims to offer pertinent insights and enhance comprehension regarding the possibilities and limitations of deploying PVSC systems in urban areas while considering the current technical and economic constraints**.

For its fulfillment, the following specific objectives were established:

- To develop physical GIS-based techno-economic and regression-based models for accurately estimating KPIs of PVSC systems in urban environments employing experimental data for PV production modeling, real electricity demand measurements, and other open data sources.
- To assess the performance of both modeling approaches, quantifying deviations and limitations in regression-based models to provide accurate estimations for each building.
- To quantify the economic potential of deploying PVSC systems in a Mediterranean municipality with the previous models under different economic and electric demand scenarios.
- To establish a quantitative comparison of the performance of PVSC among the multiple building typologies and determine the most strategic sectors from the urban planning perspective.
- To understand the general energy and economic impact and limitations of deploying PVSC systems on a municipality scale and provide strategic insights for fulfilling its energy transition and optimizing resources.

1.5 Scope and boundaries of the thesis

Because of obvious time constraints imposed by the framework of a thesis, a significant part of its object of study is circumscribed to a scenario with a greater probability of materializing in Spain in the current circumstances regarding legal frameworks, policies, and costs. In consequence, the following hypothesis defines the boundaries of the present research:

- This research is mainly focused on technical and economic potential, which is a gap with high interest and multiple research opportunities, as reviewed in section 1.2.2.
- The main modeling methods developed and analyzed are GIS-based physical modeling approaches and ML approaches. Most of the latter contributions are focused on MLR regressions due to their simple implementation, low computational cost, and replicability.
- The economic analysis is conducted according to the present legal framework from Spain (RD244/2019), which involves the validity of the NB mechanism. However, the NM mechanism is also studied in a theoretical scenario.
- The installation of each building supplies energy exclusively to the dwellings and premises of that building, which constitute an energy community. The remaining not self-consumed energy is injected into the grid.
- The building owners are assumed to be the investors of the PV facility, and no subsidies are considered.
- Only rooftop areas are considered suitable for PV, excluding façades.
- No energy storage systems are considered.
- Building rooftop constraints in deploying PVSC facilities due to patrimonial aspects are not considered.
- The deployment of the PVSC system on the rooftops of the building typologies residential, industrial, and tertiary, as well as their different subcategories, are the focus of this research.

1.6 Structure

The research performed to achieve the objectives of this thesis is presented in this compilation thesis following the structure described in this section. The structure contents are summarized in Figure 1.6.

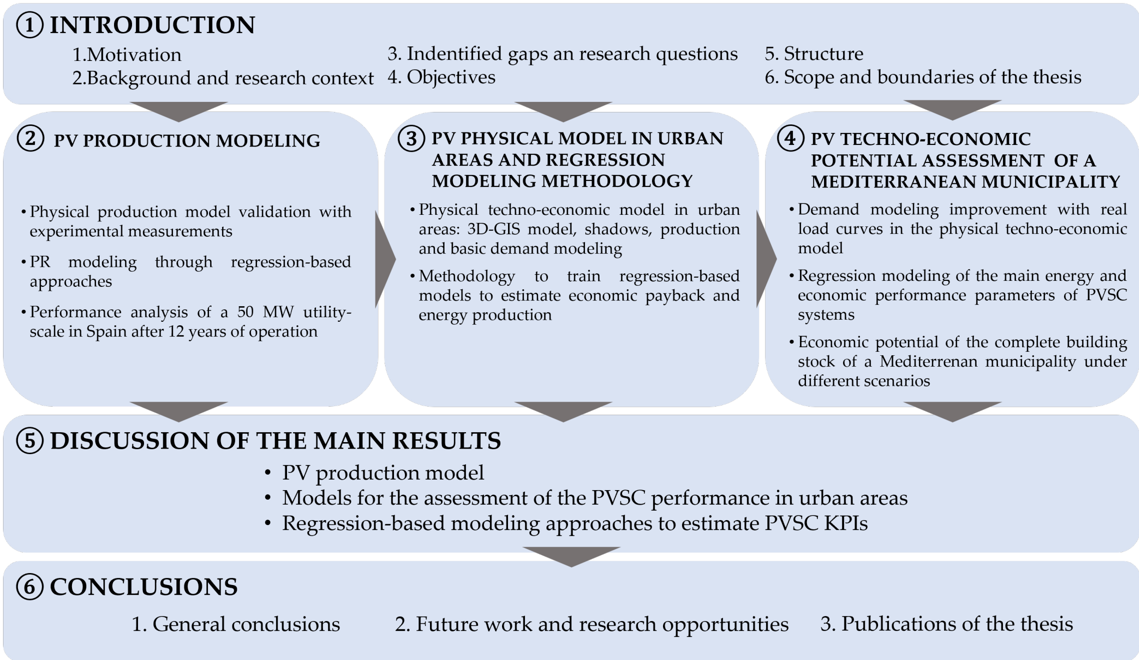

Figure 1.6: Graphical summary of the structure of the thesis.

The **present chapter** contains an **introductory presentation** of the motivation, the research context, and the scope definition of the thesis.

Chapters 2 to 4 directly correspond to each of the three peer-reviewed publications conducted during the development of the thesis. It is important to note that the structure of each of these chapters is identical to the structure of the papers included. A more detailed description and contextualization of the contents is described as follows:

- **Chapter 2: Performance analysis and modeling of a 50 MW grid-connected photovoltaic plant in Spain after 12 years of operation.** The main objective of this paper and contribution to this thesis consists of developing a PV production model and its validation through experimental irradiance and AC production measurements. Additionally, in this article, the capabilities of regression models in the PV production field are explored. For this, two contributions that improve the PV production estimations in shadowed urban environments were developed. In the first place, a methodology to estimate through regression-based models the low irradiance losses (LIL) of PV modules. In second place, multiple regression-based approaches were assessed to predict the PR using two climate predictors (temperature and irradiance). Furthermore, the performance results of the PV power plant in its half-lifetime were discussed, focusing on the effects of degradation and the quantification of the energy losses at each stage of the installation.

- **Chapter 3: Innovative regression-based methodology to assess the techno-economic performance of photovoltaic installations in urban areas.** This article aims to estimate the techno-economic potential of a representative sample of multi-storey residential buildings of a Mediterranean city through a physical model and a regression-based model. A general review of the state of the art of modeling PV facilities in urban areas is provided, and the research gap in developing simplified methodologies is identified. The production model of the previous chapter was adapted to urban environments through an isotropic irradiance model and a validated 3D GIS-based model to consider shadows on rooftops and additional technical rooftop constraints. A basic demand model based on estimated hourly load profiles was included. As a result, a physical GIS-based techno-economic model was developed to assess the technic and economic PV potential of any building that appears in the Spanish cadastre. With the results provided by the physical model for a sample of multi-story residential buildings, a regression-based methodology (based on sampling) was suggested to assess the profitability (PB) of the selected installations. Potential predictors based on constructive characteristics were defined and identified for this purpose. Additionally, a MLR model was introduced to estimate the annual PV production on rooftops in other locations with different climates to ensure the replicability of the methodology.
- **Chapter 4: Techno-economic potential of urban photovoltaics: comparison of NB and net metering in a Mediterranean municipality.** Following a better understanding of techno-economic feasibility in urban environments, this chapter focuses mainly on analyzing how load curve variations affect SC, profitability and SS. The development of the physical model from the previous article was improved by including a more detailed demand model. The latter estimates different curves for each property type from real hourly electricity consumption curves aggregated added by district. Additional improvements on the available 3D model and the sizing of facilities according to the demand were also included. As an object of study, the economic potential of a complete census of buildings of a Mediterranean municipality was assessed considering multiple constraints in the local regulation. The regression modeling of the previous chapter was expanded to estimate multiple target variables for a broader sample of buildings and multiple economic and demand scenarios. The new estimated outputs through regressions were energy (SS, SC) and economic (PB, IRR) variables. The methodology approach presented in this publication improved its versatility against multiple demand and economic scenarios through multiple predictors for higher replicability in other contexts.

Chapter 5 provides a **discussion of the results** presented in each of the previous chapters, contextualizing them under the global vision of the thesis.

Finally, **Chapter 6** summarizes this research's main **conclusions** and contributions, outlining some of the further research lines and identified challenges.

1.7 References

[1] Dougherty, T. R. and Jain, R. K. "Invisible walls: Exploration of microclimate effects on building energy consumption in New York City". In: *Sustainable Cities and Society* 90 (2023), p. 104364. DOI: 10.1016/J.SCS.2022.104364.

[2] Santamouris, M. and Vasilakopoulou, K. "Present and future energy consumption of buildings: Challenges and opportunities towards decarbonisation". In: *e-Prime - Advances in Electrical Engineering, Electronics and Energy* 1 (2021), p. 100002. DOI: 10.1016/J.PRIME.2021.100002.

[3] Molnár, G., Ürge-Vorsatz, D., and Chatterjee, S. "Estimating the global technical potential of building-integrated solar energy production using a high-resolution geospatial model". In: *Journal of Cleaner Production* 375 (2022), p. 134133. DOI: 10.1016/J.JCLEPRO.2022.134133.

[4] Costa, A., Keane, M. M., Torrens, J. I., and Corry, E. "Building operation and energy performance: Monitoring, analysis and optimisation toolkit". In: *Applied Energy* 101 (2013), pp. 310–316. DOI: 10.1016/J.APENERGY.2011.10.037.

[5] Pan, D., Bai, Y., Chang, M., Wang, X., and Wang, W. "The technical and economic potential of urban rooftop photovoltaic systems for power generation in Guangzhou, China". In: *Energy and Buildings* 277 (2022), p. 112591. DOI: 10.1016/J.ENBUILD.2022.112591.

[6] Streltsov, A., Malof, J. M., Huang, B., and Bradbury, K. "Estimating residential building energy consumption using overhead imagery". In: *Applied Energy* 280 (2020), p. 116018. DOI: 10.1016/J.APENERGY.2020.116018.

[7] United Nations (Department of Economic and Social Affairs). *World Urbanization Prospects The 2018 Revision*. New york, 2019. DOI: 10.18356/b9e995fe-en.

[8] United Nations Framework Convention on Climate Change. "The Paris Agreement". In: Paris, 2015.

[9] The General Assembly United Nations. *Resolution adopted by the General Assembly on 25 September 2015. Transforming our world: the 2030 Agenda for Sustainable Development.* Tech. rep. 2015.

[10] Strbac, G., Papadaskalopoulos, D., Chrysanthopoulos, N., Estanqueiro, A., Algarvio, H., Lopes, F., Vries, L. de, Morales-Espana, G., Sijm, J., Hernandez-Serna, R., Kiviluoma, J., and Helisto, N. "Decarbonization of Electricity Systems in Europe: Market Design Challenges". In: *IEEE Power and Energy Magazine* 19.1 (2021), pp. 53–63. DOI: 10.1109/MPE.2020.3033397.

[11] Official Journal of the European Union. *Directive (EU) 2018/2001 of the European Parliament and of the Council of 11 December 2018 on the Promotion of the Use of Energy from Renewable Sources (Recast)*. 2018.

[12] European Commission. *The European Green Deal*. Tech. rep. Brussels, 2019.

[13] Official Journal of the European Union. *Regulation (EU) 2021/1119 of the European Parliament And of The Council of 30 June 2021 establishing the framework for achieving climate neutrality and amending Regulations (EC) No 401/2009 and (EU) 2018/1999 ('European Climate Law')*. 2021.

[14] IRENA. *IRENASTAT Online Data Query Tool - Installed electricity capacity (MW) by Country/area, Technology, Grid connection and Year.*

[15] International Renewable Energy Agency. *RENEWABLE CAPACITY STATISTICS 2023.* Tech. rep. 2023.

[16] IRENA (International Renewable Energy Agency). *Capacity and Generation - Technologies.* 2023.

[17] International Energy Agency. *Renewables Data Explorer – Data Tools - IEA*. 2023.

[18] Huang, Z., Mendis, T., and Xu, S. "Urban solar utilization potential mapping via deep learning technology: A case study of Wuhan, China". In: *Applied Energy* 250 (2019), pp. 283–291. DOI: 10.1016/J.APENERGY.2019.04.113.

[19] IRENA. *IRENASTAT Online Data Query Tool.*

[20] Unión Española Fotovoltaica (UNEF). *Informe Anual UNEF - Energía Solar, apuesta segura por la recuperación económica.* Tech. rep. Madrid, 2022.

[21] APPA Renovables. *Informe Anual Autoconsumo Fotovoltaico 2022.* Tech. rep. 2022.

[22] Kavlak, G., McNerney, J., and Trancik, J. E. "Evaluating the causes of cost reduction in photovoltaic modules". In: *Energy Policy* 123 (2018), pp. 700–710. DOI: 10.1016/J.ENPOL.2018.08.015.

[23] Lobaccaro, G., Croce, S., Lindkvist, C., Munari Probst, M. C., Scognamiglio, A., Dahlberg, J., Lundgren, M., and Wall, M. "A cross-country perspective on solar energy in urban planning: Lessons learned from international case studies". In: *Renewable and Sustainable Energy Reviews* 108 (2019), pp. 209–237. DOI: 10.1016/j.rser.2019.03.041.

[24] Christoph Kost; Shivenes Shammugan; Verena Fluri; Dominik Peper; Aschkan Davoodi Nemar; Thomas Schlegl. *Levelized Cost Of Electricity Renewable Energy Technologies.* Tech. rep. Fraunhofer Institute For Solar Energy Systems ISE, 2021.

[25] Roldán Fernández, J. M., Burgos Payán, M., and Riquelme Santos, J. M. "Profitability of household photovoltaic self-consumption in Spain". In: *Journal of Cleaner Production* 279 (2021), p. 123439. DOI: 10.1016/J.JCLEPRO.2020.123439.

[26] Mendieta, Á. J. O. and Hernández, E. S. "Analysis of PV Self-Consumption in Educational and Office Buildings in Spain". In: *Sustainability 2021, Vol. 13, Page 1662* 13.4 (2021), p. 1662. DOI: 10.3390/SU13041662.

[27] Ordóñez, Á., Sánchez, E., Rozas, L., García, R., and Parra-Domínguez, J. "Net-metering and net-billing in photovoltaic self-consumption: The cases of Ecuador and Spain". In: *Sustainable Energy Technologies and Assessments* 53 (2022), p. 102434. DOI: 10.1016/J.SETA.2022.102434.

[28] European Commission. *Commission to the European Parliament; The Council; Social Commitee And The Committee of the Regions. EU solar energy strategy.* Brussels, 2022.

[29] Vezzoni, R. “Green growth for whom, how and why? The REPowerEU Plan and the inconsistencies of European Union energy policy”. In: *Energy Research & Social Science* 101 (2023), p. 103134. DOI: 10.1016/J.ERSS.2023.103134.

[30] Jefatura del Estado; Boletín Oficial del Estado (BOE). *Real Decreto-ley 15/2018, de 5 de octubre, de medidas urgentes para la transición energética y la protección de los consumidores.* Madrid, 2018.

[31] Ministerio para la Transición Ecológica (MTE); Boletín Oficial del Estado (BOE). *Real Decreto 244/2019, de 5 de abril, por el que se regulan las condiciones administrativas, técnicas y económicas del autoconsumo de energía eléctrica.* Madrid, 2019.

[32] Mundaca, L. and Samahita, M. “What drives home solar PV uptake? Subsidies, peer effects and visibility in Sweden”. In: *Energy Research & Social Science* 60 (2020), p. 101319. DOI: 10.1016/J.ERSS.2019.101319.

[33] Kurdi, Y., Alkhatatbeh, B. J., Asadi, S., and Jebelli, H. “A decision-making design framework for the integration of PV systems in the urban energy planning process”. In: *Renewable Energy* 197 (2022), pp. 288–304. DOI: 10.1016/J.RENENE.2022.07.001.

[34] Yang, J., Mohan Kumar, D. llamathy, Pyrgou, A., Chong, A., Santamouris, M., Kolokotsa, D., and Lee, S. E. “Green and cool roofs’ urban heat island mitigation potential in tropical climate”. In: *Solar Energy* 173 (2018), pp. 597–609. DOI: 10.1016/J.SOLENER.2018.08.006.

[35] Liu, Z., Liu, X., Zhang, H., and Yan, D. “Integrated physical approach to assessing urban-scale building photovoltaic potential at high spatiotemporal resolution”. In: *Journal of Cleaner Production* 388 (2023), p. 135979. DOI: 10.1016/J.JCLEPRO.2023.135979.

[36] Gallego-Castillo, C., Heleno, M., and Victoria, M. “Self-consumption for energy communities in Spain: A regional analysis under the new legal framework”. In: *Energy Policy* 150 (2021), p. 112144. DOI: 10.1016/J.ENPOL.2021.112144.

[37] Blyth, W., Speirs, J., and Gross, R. *Low carbon jobs: the evidence for net job creation from policy support for energy efficiency and renewable energy.* Tech. rep. Oxford, 2014.

[38] Dorian Frieden; Andreas Tuerk; Camilla Neumann; Stanislas d’Herbemont. *Collective self-consumption and energy communities: Trends and challenges in the transposition of the EU framework.* Tech. rep. Joanneum Research Forschungsgesellschaft mbH, 2020. DOI: 10.13140/RG.2.2.25685.04321.

[39] Reis, V., Almeida, R. H., Silva, J. A., and Brito, M. C. “Demand aggregation for photovoltaic self-consumption”. In: *Energy Reports* 5 (2019), pp. 54–61. DOI: 10.1016/J.EGYR.2018.11.002.

[40] Majeed, I. B. and Nwulu, N. I. “Reverse Power Flow Due to Solar Photovoltaic in the Low Voltage Network”. In: *IEEE Access* 11 (2023), pp. 44741–44758. DOI: 10.1109/ACCESS.2023.3273483.

[41] López Prol, J. and Steininger, K. W. "Photovoltaic self-consumption is now profitable in Spain: Effects of the new regulation on prosumers' internal rate of return". In: *Energy Policy* 146 (2020), p. 111793. DOI: 10.1016/J.ENPOL.2020.111793.

[42] Ghaleb, B., Abbasi, S. A., and Asif, M. "Application of solar PV in the building sector: Prospects and barriers in the GCC region". In: *Energy Reports* 9 (2023), pp. 3932–3942. DOI: 10.1016/J.EGYR.2023.02.085.

[43] Xue, Y., Lindkvist, C. M., and Temeljotov-Salaj, A. "Barriers and potential solutions to the diffusion of solar photovoltaics from the public-private-people partnership perspective – Case study of Norway". In: *Renewable and Sustainable Energy Reviews* 137 (2021), p. 110636. DOI: 10.1016/J.RSER.2020.110636.

[44] Thevenard, D. and Pelland, S. "Estimating the uncertainty in long-term photovoltaic yield predictions". In: *Solar Energy* 91 (2013), pp. 432–445. DOI: 10.1016/J.SOLENER.2011.05.006.

[45] Balcombe, P., Rigby, D., and Azapagic, A. "Investigating the importance of motivations and barriers related to microgeneration uptake in the UK". In: *Applied Energy* 130 (2014), pp. 403–418. DOI: 10.1016/J.APENERGY.2014.05.047.

[46] Omar, M. A. and Mahmoud, M. M. *Grid connected PV- home systems in Palestine: A review on technical performance, effects and economic feasibility.* 2018. DOI: 10.1016/j.rser.2017.09.008.

[47] Nuñez-Jimenez, A., Mehta, P., and Griego, D. "Let it grow: How community solar policy can increase PV adoption in cities". In: *Energy Policy* 175 (2023), p. 113477. DOI: 10.1016/J.ENPOL.2023.113477.

[48] Strazzera, E. and Statzu, V. "Fostering photovoltaic technologies in Mediterranean cities: Consumers' demand and social acceptance". In: *Renewable Energy* 102 (2017), pp. 361–371. DOI: 10.1016/J.RENENE.2016.10.056.

[49] Rodríguez-Segura, F. J., Osorio-Aravena, J. C., Frolova, M., Terrados-Cepeda, J., and Muñoz-Cerón, E. "Social acceptance of renewable energy development in southern Spain: Exploring tendencies, locations, criteria and situations". In: *Energy Policy* 173 (2023), p. 113356. DOI: 10.1016/J.ENPOL.2022.113356.

[50] An, Y., Chen, T., Shi, L., Heng, C. K., and Fan, J. "Solar energy potential using GIS-based urban residential environmental data: A case study of Shenzhen, China". In: *Sustainable Cities and Society* 93 (2023), p. 104547. DOI: 10.1016/J.SCS.2023.104547.

[51] Fath, K., Stengel, J., Sprenger, W., Wilson, H. R., Schultmann, F., and Kuhn, T. E. "A method for predicting the economic potential of (building-integrated) photovoltaics in urban areas based on hourly Radiance simulations". In: *Solar Energy* 116 (2015), pp. 357–370. DOI: 10.1016/J.SOLENER.2015.03.023.

[52] Dean, J., Kandt, A., Burman, K., Lisell, L., and Helm, C. "Analysis of Web-Based Solar Photovoltaic Mapping Tools". In: *Proceedings of the ASME 3rd International Conference on Energy Sustainability 2009, ES2009* 1 (2010), pp. 85–96. DOI: 10.1115/ES2009-90461.

[53] Jakubiec, J. A. and Reinhart, C. F. "A method for predicting city-wide electricity gains from photovoltaic panels based on LiDAR and GIS data combined with hourly Daysim simulations". In: *Solar Energy* 93 (2013), pp. 127–143. DOI: 10.1016/J.SOLENER.2013.03.022.

[54] Kanters, J., Wall, M., and Kjellsson, E. "The Solar Map as a Knowledge Base for Solar Energy Use". In: *Energy Procedia* 48 (2014), pp. 1597–1606. DOI: 10.1016/J.EGYPRO.2014.02.180.

[55] Pedrero, J., Hermoso, N., Hernández, P., Munoz, I., Arrizabalaga, E., Mabe, L., Prieto, I., and Izkara, J. L. "Assessment of urban-scale potential for solar PV generation and consumption". In: *IOP Conference Series: Earth and Environmental Science* 323.1 (2019), p. 012066. DOI: 10.1088/1755-1315/323/1/012066.

[56] Rodríguez-Gómez, F., Campo-Ávila, J. del, Ferrer-Cuesta, M., and Mora-López, L. "Data driven tools to assess the location of photovoltaic facilities in urban areas". In: *Expert Systems with Applications* 203 (2022), p. 117349. DOI: 10.1016/J.ESWA.2022.117349.

[57] Sánchez-Aparicio, M., Martín-Jiménez, J., Del Pozo, S., González-González, E., and Lagüela, S. "Ener3DMap-SolarWeb roofs: A geospatial web-based platform to compute photovoltaic potential". In: *Renewable and Sustainable Energy Reviews* 135 (2021), p. 110203. DOI: 10.1016/J.RSER.2020.110203.

[58] Assadeg, J., Sopian, K., and Fudholi, A. "Performance of grid-connected solar photovoltaic power plants in the Middle East and North Africa". In: *International Journal of Electrical and Computer Engineering (IJECE)* 9.5 (2019), pp. 3375–3383. DOI: 10.11591/IJECE.V9I5.PP3375-3383.

[59] Zakeri, B., Cross, S., Dodds, P. E., and Gissey, G. C. "Policy options for enhancing economic profitability of residential solar photovoltaic with battery energy storage". In: *Applied Energy* 290 (2021), p. 116697. DOI: 10.1016/J.APENERGY.2021.116697.

[60] Simoiu, M. S., Fagarasan, I., Ploix, S., and Calofir, V. "Optimising the self-consumption and self-sufficiency: A novel approach for adequately sizing a photovoltaic plant with application to a metropolitan station". In: *Journal of Cleaner Production* 327 (2021), p. 129399. DOI: 10.1016/J.JCLEPRO.2021.129399.

[61] Camilo, F. M., Castro, R., Almeida, M. E., and Pires, V. F. "Economic assessment of residential PV systems with self-consumption and storage in Portugal". In: *Solar Energy* 150 (2017), pp. 353–362. DOI: 10.1016/J.SOLENER.2017.04.062.

[62] Foles, A., Fialho, L., and Collares-Pereira, M. "Techno-economic evaluation of the Portuguese PV and energy storage residential applications". In: *Sustainable Energy Technologies and Assessments* 39 (2020), p. 100686. DOI: 10.1016/J.SETA.2020.100686.

[63] Echevarría Camarero, F., Ogando-Martínez, A., Durán Gómez, P., and Carrasco Ortega, P. "Profitability of Batteries in Photovoltaic Systems for Small Industrial Consumers in Spain under Current Regulatory Framework and Energy Prices". In: *Energies 2023, Vol. 16, Page 361* 16.1 (2022), p. 361. DOI: 10.3390/EN16010361.

[64] Perpiñán Lamigueiro, O. *Energía Solar Fotovoltaica.* 2023.

[65] Roberts, M. B., Bruce, A., and MacGill, I. "A comparison of arrangements for increasing self-consumption and maximising the value of distributed photovoltaics on apartment buildings". In: *Solar Energy* 193 (2019), pp. 372–386. DOI: 10.1016/J.SOLENER.2019.09.067.

[66] Ciocia, A., Amato, A., Leo, P. D., Fichera, S., Malgaroli, G., Spertino, F., and Tzanova, S. "Self-Consumption and Self-Sufficiency in Photovoltaic Systems: Effect of Grid Limitation and Storage Installation". In: *Energies 2021, Vol. 14, Page 1591* 14.6 (2021), p. 1591. DOI: 10.3390/EN14061591.

[67] Jurasz, J. K., Dabek, P. B., and Campana, P. E. "Can a city reach energy self-sufficiency by means of rooftop photovoltaics? Case study from Poland". In: *Journal of Cleaner Production* 245 (2020), p. 118813. DOI: 10.1016/J.JCLEPRO.2019.118813.

[68] Dufo-López, R. and Bernal-Agustín, J. L. "A comparative assessment of net metering and net billing policies. Study cases for Spain". In: *Energy* 84 (2015), pp. 684–694. DOI: 10.1016/J.ENERGY.2015.03.031.

[69] Trela, M. and Dubel, A. "Net-Metering vs. Net-Billing from the Investors Perspective—Impacts of Changes in RES Financing in Poland on the Profitability of a Joint Photovoltaic Panels and Heat Pump System". In: *Energies 2022, Vol. 15, Page 227* 15.1 (2021), p. 227. DOI: 10.3390/EN15010227.

[70] Gautier, A., Jacqmin, J., and Poudou, J. C. "The prosumers and the grid". In: *Journal of Regulatory Economics* 53.1 (2018), pp. 100–126. DOI: 10.1007/S11149-018-9350-5/METRICS.

[71] Council of European Energy Regulators. *Electricity Distribution Network Tariffs CEER Guidelines of Good Practice.* Tech. rep. Brussels, Belgium: Council of European Energy Regulators, 2017.

[72] López Prol, J. and Steininger, K. W. "Photovoltaic self-consumption regulation in Spain: Profitability analysis and alternative regulation schemes". In: *Energy Policy* 108 (2017), pp. 742–754. DOI: 10.1016/J.ENPOL.2017.06.019.

[73] Rövekamp, P., Schöpf, M., Wagon, F., Weibelzahl, M., and Fridgen, G. "Renewable electricity business models in a post feed-in tariff era". In: *Energy* 216 (2021), p. 119228. DOI: 10.1016/J.ENERGY.2020.119228.

[74] Marrone, P. and Montella, I. "An experimentation on the limits and potential of Renewable Energy Communities in the built city: buildings and proximity open spaces for energy decentralization". In: *Renewable and Sustainable Energy Transition* 2 (2022), p. 100025. DOI: 10.1016/J.RSET.2022.100025.

[75] Caballero, V., Briones, A., Coca-Ortegón, A., Pérez, A., Barrios, B., and Mano, M. de la. "Analysis and simulation of an Urban-Industrial Sustainable Energy Community: A use case in San Juan de Mozarrifar using photovoltaic energy". In: *Energy Reports* 9 (2023), pp. 1589–1605. DOI: 10.1016/J.EGYR.2022.12.059.

[76] Mehta, P. and Tiefenbeck, V. "Solar PV sharing in urban energy communities: Impact of community configurations on profitability, autonomy and the electric grid". In: *Sustainable Cities and Society* 87 (2022), p. 104178. DOI: 10.1016/J.SCS.2022.104178.

[77] Koltunov, M., Pezzutto, S., Bisello, A., Lettner, G., Hiesl, A., Sark, W. van, Louwen, A., and Wilczynski, E. "Mapping of Energy Communities in Europe: Status Quo and Review of Existing Classifications". In: *Sustainability 2023, Vol. 15, Page 8201* 15.10 (2023), p. 8201. DOI: 10.3390/SU15108201.

[78] Avaesen. *Mapa CELS - Plaza Energía.* 2023.

[79] Li, S. Y. and Han, J. Y. "The impact of shadow covering on the rooftop solar photovoltaic system for evaluating self-sufficiency rate in the concept of nearly zero energy building". In: *Sustainable Cities and Society* 80 (2022), p. 103821. DOI: 10.1016/J.SCS.2022.103821.

[80] Arias-Rosales, A. and LeDuc, P. R. "Urban solar harvesting: The importance of diffuse shadows in complex environments". In: *Renewable and Sustainable Energy Reviews* 175 (2023), p. 113155. DOI: 10.1016/J.RSER.2023.113155.

[81] Rauf, A., Al-Awami, A. T., Kassas, M., Khalid, M., Zia, F., Benbouzid, M., Elbouchikhi, E., Muyeen, S. M., and Tariq Iqbal, M. "Optimal Sizing and Cost Minimization of Solar Photovoltaic Power System Considering Economical Perspectives and Net Metering Schemes". In: *Electronics 2021, Vol. 10, Page 2713* 10.21 (2021), p. 2713. DOI: 10.3390/ELECTRONICS10212713.

[82] Domenech, B., Calleja, G., and Olivella, J. "Residential Photovoltaic Profitability with Storage under the New Spanish Regulation: A Multi-Scenario Analysis". In: *Energies 2021, Vol. 14, Page 1987* 14.7 (2021), p. 1987. DOI: 10.3390/EN14071987.

[83] Lara Monge, C., Vásquez Márquez, L., and Reyes Duke, A. M. "Case Study: Optimization of Grid-Connected Photovoltaic Self-Consumption Systems for The Commercial Sector in Honduras". In: *IOP Conference Series: Earth and Environmental Science* 801.1 (2021), p. 012025. DOI: 10.1088/1755-1315/801/1/012025.

[84] Talavera, D. L., Muñoz-Rodriguez, F. J., Jimenez-Castillo, G., and Rus-Casas, C. "A new approach to sizing the photovoltaic generator in self-consumption systems based on cost–competitiveness, maximizing direct self-consumption". In: *Renewable Energy* 130 (2019), pp. 1021–1035. DOI: 10.1016/J.RENENE.2018.06.088.

[85] Lovati, M., Dallapiccola, M., Adami, J., Bonato, P., Zhang, X., and Moser, D. "Design of a residential photovoltaic system: the impact of the demand profile and the normative framework". In: *Renewable Energy* 160 (2020), pp. 1458–1467. DOI: 10.1016/J.RENENE.2020.07.153.

[86] Thebault, M. and Gaillard, L. "Optimization of the integration of photovoltaic systems on buildings for self-consumption – Case study in France". In: *City and Environment Interactions* 10 (2021), p. 100057. DOI: 10.1016/J.CACINT.2021.100057.

[87] Sredenšek, K., Štumberger, B., Hadžiselimović, M., Mavsar, P., and Seme, S. "Physical, geographical, technical, and economic potential for the optimal configuration of photovoltaic systems using a digital surface model and optimization method". In: *Energy* 242 (2022), p. 122971. DOI: 10.1016/J.ENERGY.2021.122971.

[88] Villar, C. H., Neves, D., and Silva, C. A. "Solar PV self-consumption: An analysis of influencing indicators in the Portuguese context". In: *Energy Strategy Reviews* 18 (2017), pp. 224–234. DOI: 10.1016/J.ESR.2017.10.001.

[89] Fakhraian, E., Alier, M., Dalmau, F. V., Nameni, A., and Guerrero, J. C. "The Urban Rooftop Photovoltaic Potential Determination". In: *Sustainability 2021, Vol. 13, Page 7447* 13.13 (2021), p. 7447. DOI: 10.3390/SU13137447.

[90] Krapf, S., Kemmerzell, N., Uddin, S. K. H., Vázquez, M. H., Netzler, F., and Lienkamp, M. "Towards Scalable Economic Photovoltaic Potential Analysis Using Aerial Images and Deep Learning". In: *Energies 2021, Vol. 14, Page 3800* 14.13 (2021), p. 3800. DOI: 10.3390/EN14133800.

[91] Thebault, M., Desthieux, G., Castello, R., and Berrah, L. "Large-scale evaluation of the suitability of buildings for photovoltaic integration: Case study in Greater Geneva". In: *Applied Energy* 316 (2022), p. 119127. DOI: 10.1016/J.APENERGY.2022.119127.

[92] IRENA (International Renewable Energy Agency). *Future of Solar Photovoltaic Deployment, investment, technology, grid integration and socio-economic aspects, A Global Energy Transformation paper About IRENA*. Tech. rep. 2019.

[93] Zhou, X., Huang, Z., Scheuer, B., Lu, W., Zhou, G., and Liu, Y. "High-resolution spatial assessment of the zero energy potential of buildings with photovoltaic systems at the city level". In: *Sustainable Cities and Society* 93 (2023), p. 104526. DOI: 10.1016/J.SCS.2023.104526.

[94] Gassar, A. A. A. and Cha, S. H. "Review of geographic information systems-based rooftop solar photovoltaic potential estimation approaches at urban scales". In: *Applied Energy* 291 (2021), p. 116817. DOI: 10.1016/J.APENERGY.2021.116817.

[95] Jiang, H., Zhang, X., Yao, L., Lu, N., Qin, J., Liu, T., and Zhou, C. "High-resolution analysis of rooftop photovoltaic potential based on hourly generation simulations and load profiles". In: *Applied Energy* 348 (2023), p. 121553. DOI: 10.1016/J.APENERGY.2023.121553.

[96] Izquierdo, S., Rodrigues, M., and Fueyo, N. "A method for estimating the geographical distribution of the available roof surface area for large-scale photovoltaic energy-potential evaluations". In: *Solar Energy* 82.10 (2008), pp. 929–939. DOI: 10.1016/j.solener.2008.03.007.

[97] Bódis, K., Kougias, I., Jäger-Waldau, A., Taylor, N., and Szabó, S. "A high-resolution geospatial assessment of the rooftop solar photovoltaic potential in the European Union". In: *Renewable and Sustainable Energy Reviews* 114 (2019), p. 109309. DOI: 10.1016/j.rser.2019.109309.

[98] Koch, H., Lechner, S., Erdmann, S., and Hofmann, M. "Assessing the Potential of Rooftop Photovoltaics by Processing High-Resolution Irradiation Data, as Applied to Giessen, Germany". In: *Energies 2022, Vol. 15, Page 6991* 15.19 (2022), p. 6991. DOI: 10.3390/EN15196991.

[99] Castellanos, S., Sunter, D. A., and Kammen, D. M. "Rooftop solar photovoltaic potential in cities: How scalable are assessment approaches?" In: *Environmental Research Letters* 12.12 (2017), p. 125005. DOI: 10.1088/1748-9326/aa7857.

[100] Alhamwi, A., Medjroubi, W., Vogt, T., and Agert, C. "GIS-based urban energy systems models and tools: Introducing a model for the optimisation of flexibilisation technologies in urban areas". In: *Applied Energy* 191 (2017), pp. 1–9. DOI: 10.1016/J.APENERGY.2017.01.048.

[101] Open Geospatial Consortium. *CityGML - Open Geospatial Consortium*.

[102] Julieta, S. R., José-Julio, R. B., and Pablo, Y. R. "A methodology to estimate the photovoltaic potential on parking spaces and water deposits. The case of the Canary Islands". In: *Renewable Energy* 189 (2022), pp. 1046–1062. DOI: 10.1016/J.RENENE.2022.02.103.

[103] Fakhraian, E., Forment, M. A., Dalmau, F. V., Nameni, A., and Guerrero, M. J. C. "Determination of the urban rooftop photovoltaic potential: A state of the art". In: *Energy Reports* 7 (2021), pp. 176–185. DOI: 10.1016/J.EGYR.2021.06.031.

[104] Chen, Q., Li, X., Zhang, Z., Zhou, C., Guo, Z., Liu, Z., and Zhang, H. "Remote sensing of photovoltaic scenarios: Techniques, applications and future directions". In: *Applied Energy* 333 (2023), p. 120579. DOI: 10.1016/J.APENERGY.2022.120579.

[105] Mainzer, K., Killinger, S., McKenna, R., and Fichtner, W. "Assessment of rooftop photovoltaic potentials at the urban level using publicly available geodata and image recognition techniques". In: *Solar Energy* 155 (2017), pp. 561–573. DOI: 10.1016/J.SOLENER.2017.06.065.

[106] Mayer, M. J. "Effects of the meteorological data resolution and aggregation on the optimal design of photovoltaic power plants". In: *Energy Conversion and Management* 241 (2021), p. 114313. DOI: 10.1016/J.ENCONMAN.2021.114313.

[107] Mayer, M. J. and Gróf, G. "Extensive comparison of physical models for photovoltaic power forecasting". In: *Applied Energy* 283 (2021), p. 116239. DOI: 10.1016/J.APENERGY.2020.116239.

[108] Gilman, P., Dobos, A., Diorio, N., Freeman, J., Janzou, S., and Ryberg, D. *SAM Photovoltaic Model Technical Reference Update*. Tech. rep. National Renewable Energy Agency, 2016. DOI: NREL/TP-6A20-67399.

[109] Gueymard, C. A. "Solar Radiation Resource: Measurement, Modeling, and Methods". In: *Comprehensive Renewable Energy, Second Edition: Volume 1-9* 1 (2022), pp. 176–212. DOI: 10.1016/B978-0-12-819727-1.00101-1.

[110] Mattsson, N., Verendel, V., Hedenus, F., and Reichenberg, L. "An autopilot for energy models – Automatic generation of renewable supply curves, hourly capacity factors and hourly synthetic electricity demand for arbitrary world regions". In: *Energy Strategy Reviews* 33 (2021), p. 100606. DOI: 10.1016/J.ESR.2020.100606.

[111] Red Eléctrica de España (RRE). *Consulta los perfiles de consumo (TBD), Red Eléctrica.*

[112] Schopfer, S., Tiefenbeck, V., and Staake, T. "Economic assessment of photovoltaic battery systems based on household load profiles". In: *Applied Energy* 223 (2018), pp. 229–248. DOI: 10.1016/J.APENERGY.2018.03.185.

[113] José Gil Mena, A., Fernando Nasimba Medina, V., Bouakkaz, A., and Haddad, S. "Analysis and optimisation of collective self-consumption in residential buildings in Spain". In: *Energy and Buildings* 283 (2023), p. 112812. DOI: 10.1016/J.ENBUILD.2023.112812.

[114] Biljecki, F., Ledoux, H., and Stoter, J. "Does a finer level of detail of a 3D city model bring an improvement for estimating shadows?" In: *Lecture Notes in Geoinformation and Cartography* 9783319256894 (2017), pp. 31–47. DOI: 10.1007/978-3-319-25691-7_2.

[115] Sun, L., Chang, Y., Wu, Y., Sun, Y., and Su, D. "Potential estimation of rooftop photovoltaic with the spatialization of energy self-sufficiency in urban areas". In: *Energy Reports* 8 (2022), pp. 3982–3994. DOI: 10.1016/J.EGYR.2022.03.035.

[116] Miranda, R. F., Szklo, A., and Schaeffer, R. "Technical-economic potential of PV systems on Brazilian rooftops". In: *Renewable Energy* 75 (2015), pp. 694–713. DOI: 10.1016/J.RENENE.2014.10.037.

[117] Gómez-Navarro, T., Brazzini, T., Alfonso-Solar, D., and Vargas-Salgado, C. "Analysis of the potential for PV rooftop prosumer production: Technical, economic and environmental assessment for the city of Valencia (Spain)". In: *Renewable Energy* 174 (2021), pp. 372–381. DOI: 10.1016/j.renene.2021.04.049.

[118] Ordóñez, J., Jadraque, E., Alegre, J., and Martínez, G. "Analysis of the photovoltaic solar energy capacity of residential rooftops in Andalusia (Spain)". In: *Renewable and Sustainable Energy Reviews* 14.7 (2010), pp. 2122–2130. DOI: 10.1016/J.RSER.2010.01.001.

[119] Huang, X., Hayashi, K., Matsumoto, T., Tao, L., Huang, Y., and Tomino, Y. "Estimation of Rooftop Solar Power Potential by Comparing Solar Radiation Data and Remote Sensing Data—A Case Study in Aichi, Japan". In: *Remote Sensing 2022, Vol. 14, Page 1742* 14.7 (2022), p. 1742. DOI: 10.3390/RS14071742.

[120] Dhimish, M. and Silvestre, S. "Estimating the impact of azimuth-angle variations on photovoltaic annual energy production". In: *Clean Energy* 3.1 (2019), pp. 47–58. DOI: 10.1093/CE/ZKY022.

[121] Rinaldi, A., Soini, M. C., Patel, M. K., and Parra, D. "Optimised allocation of PV and storage capacity among different consumer types and urban settings: A prospective analysis for Switzerland". In: *Journal of Cleaner Production* 259 (2020), p. 120762. DOI: 10.1016/J.JCLEPRO.2020.120762.

[122] Wang, W., Yang, D., Huang, N., Lyu, C., Zhang, G., and Han, X. "Irradiance-to-power conversion based on physical model chain: An application on the optimal configuration of multi-energy microgrid in cold climate". In: *Renewable and Sustainable Energy Reviews* 161 (2022), p. 112356. DOI: 10.1016/J.RSER.2022.112356.

[123] Dhass, A. D., Beemkumar, N., Harikrishnan, S., and Ali, H. M. "A Review on Factors Influencing the Mismatch Losses in Solar Photovoltaic System". In: *International Journal of Photoenergy* 2022 (2022). DOI: 10.1155/2022/2986004.

[124] Mansouri Kouhestani, F., Byrne, J., Johnson, D., Spencer, L., Hazendonk, P., and Brown, B. "Evaluating solar energy technical and economic potential on rooftops in an urban setting: the city of Lethbridge, Canada". In: *International Journal of Energy and Environmental Engineering* 10.1 (2019), pp. 13–32. DOI: 10.1007/S40095-018-0289-1/TABLES/10.

[125] Olivella, J., Domenech, B., and Calleja, G. "Potential of implementation of residential photovoltaics at city level: The case of London". In: *Renewable Energy* 180 (2021), pp. 577–585. DOI: 10.1016/J.RENENE.2021.08.121.

[126] Wang, P., Yu, P., Huang, L., and Zhang, Y. "An integrated technical, economic, and environmental framework for evaluating the rooftop photovoltaic potential of old residential buildings". In: *Journal of Environmental Management* 317 (2022), p. 115296. DOI: 10.1016/J.JENVMAN.2022.115296.

[127] Cuesta-Fernández, I., Vargas-Salgado, C., Alfonso-Solar, D., and Gómez-Navarro, T. "The contribution of metropolitan areas to decarbonize the residential stock in Mediterranean cities: A GIS-based assessment of rooftop PV potential in Valencia, Spain". In: *Sustainable Cities and Society* 97 (2023), p. 104727. DOI: 10.1016/J.SCS.2023.104727.

[128] Valderrama, A., Valle, C., Allende, H., Ibarra, M., and Vásquez, C. "Machine learning applications for urban photovoltaic potential estimation: A survey". In: *Neurocomputing* 526 (2023), pp. 80–95. DOI: 10.1016/J.NEUCOM.2023.01.006.

[129] Balderrama, S., Lombardi, F., Stevanato, N., Pena, G., Colombo, E., and Quoilin, S. "Automated evaluation of levelized cost of energy of isolated micro-grids for energy planning purposes in developing countries". In: *ECOS 2019 - Proceedings of the 32nd International Conference on Efficiency, Cost, Optimization, Simulation and Environmental Impact of Energy Systems.* Institute of Thermal Technology, 2019, pp. 2999–3012.

[130] Walch, A., Castello, R., Mohajeri, N., and Scartezzini, J. L. "Big data mining for the estimation of hourly rooftop photovoltaic potential and its uncertainty". In: *Applied Energy* 262 (2020), p. 114404. DOI: 10.1016/j.apenergy.2019.114404.

[131] Calcabrini, A., Ziar, H., Isabella, O., and Zeman, M. "A simplified skyline-based method for estimating the annual solar energy potential in urban environments". In: *Nature Energy* 4.3 (2019), pp. 206–215. DOI: 10.1038/s41560-018-0318-6.

[132] Xie, M., Wang, M., Zhong, H., Li, X., Li, B., Mendis, T., and Xu, S. "The impact of urban morphology on the building energy consumption and solar energy generation potential of university dormitory blocks". In: *Sustainable Cities and Society* 96 (2023), p. 104644. DOI: 10.1016/J.SCS.2023.104644.

[133] Walch, A., Castello, R., Mohajeri, N., and Scartezzini, J.-L. "A Fast Machine Learning Model for Large-Scale Estimation of Annual Solar Irradiation on Rooftops". In: *ISES Solar World Congress 2019*. 2019. DOI: 10.18086/swc.2019.45.12.

[134] Müller, J. and Trutnevyte, E. "Spatial projections of solar PV installations at subnational level: Accuracy testing of regression models". In: *Applied Energy* 265 (2020), p. 114747. DOI: 10.1016/J.APENERGY.2020.114747.

[135] Assouline, D., Mohajeri, N., and Scartezzini, J. L. "Large-scale rooftop solar photovoltaic technical potential estimation using Random Forests". In: *Applied Energy* 217 (2018), pp. 189–211. DOI: 10.1016/J.APENERGY.2018.02.118.

[136] Torres-Rivas, A., Palumbo, M., Jiménez, L., and Boer, D. "Self-consumption possibilities by rooftop PV and building retrofit requirements for a regional building stock: The case of Catalonia". In: *Solar Energy* 238 (2022), pp. 150–161. DOI: 10.1016/J.SOLENER.2022.04.036.

[137] Zhu, R., Wong, M. S., Kwan, M. P., Chen, M., Santi, P., and Ratti, C. "An economically feasible optimization of photovoltaic provision using real electricity demand: A case study in New York city". In: *Sustainable Cities and Society* 78 (2022), p. 103614. DOI: 10.1016/J.SCS.2021.103614.

[138] Assouline, D., Mohajeri, N., and Scartezzini, J. L. "Quantifying rooftop photovoltaic solar energy potential: A machine learning approach". In: *Solar Energy* 141 (2017), pp. 278–296. DOI: 10.1016/J.SOLENER.2016.11.045.

[139] Fuster-Palop, E., Prades-Gil, C., Masip, X., Viana-Fons, J. D., and Payá, J. "Innovative regression-based methodology to assess the techno-economic performance of photovoltaic installations in urban areas". In: *Renewable and Sustainable Energy Reviews* 149 (2021), p. 111357. DOI: 10.1016/J.RSER.2021.111357.

[140] Fuster-Palop, E., Prades-Gil, C., Masip, X., Viana-Fons, J. D., and Payá, J. "Techno-Economic Potential of Urban Photovoltaics: Comparison of Net Billing and Net Metering in a Mediterranean Municipality". In: *Energies 2023, Vol. 16, Page 3564* 16.8 (2023), p. 3564. DOI: 10.3390/EN16083564.

[141] Mohajeri, N., Assouline, D., Guiboud, B., Bill, A., Gudmundsson, A., and Scartezzini, J. L. "A city-scale roof shape classification using machine learning for solar energy applications". In: *Renewable Energy* 121 (2018), pp. 81–93. DOI: 10.1016/J.RENENE.2017.12.096.

Chapter 2

Performance analysis and modelling of a 50 MW grid-connected photovoltaic plant in Spain after 12 years of operation

Chapter adapted from the paper:

Enrique Fuster-Palop[a,b], Carlos Vargas-Salgado[a], Juan Carlos Ferri-Revert[c], Jorge Payá[a]. *Performance analysis and modelling of a 50 MW grid-connected photovoltaic plant in Spain after 12 years of operation.* In: *Renewable and Sustainable Energy Reviews* (2022), Vol. 170, p. 112968.
DOI: https://doi.org/10.1016/j.rser.2022.112968.

[a] Instituto Universitario de Investigación en Ingeniería Energética, Universitat Politècnica de València, Camí de Vera s/n, Valencia, Spain.

[b] ImpactE, C/ Joan Verdeguer nº 16, Valencia, 46024, Spain.

[c] Entoria Energy, Avenida Maisonnave, 41, 7 C D, 03003, Alicante, Spain.

Abstract:

This study aims to estimate the performance and losses of a $50\,\mathrm{MW}$ photovoltaic (PV) utility-scale after 12 years of operation. The PV plant has monocrystalline and polycrystalline silicon modules and is located in the central region of Spain with an annual insolation of $1{,}976\,\mathrm{kWh/m^2}$. Monitoring data over the entire year 2020 has been analyzed and filtered to assess the performance results following the IEC 61724 standard guidelines. The annual average reference yield, final yield, performance ratio and capacity utilization factor are of 5.44 h/d, 4.28 h/d, 79.24%, and 19.77%, respectively. Besides the experimental analysis, this work improves the estimation of the daily performance ratio, especially in days with low insolation. Two different modelling approaches have been assessed and compared. In first place, a physical model has been adopted, based on the most common losses, and including an exponential expression to account for low irradiance losses. In second place, statistical models have been used, with either multiple linear regressions or random forest algorithms. In contrast with other published models which require many inputs, the best accuracy has been reached with the random forest model using only the ambient temperature and solar irradiance as predictors, obtaining a $RMSE$ of 1% for the PR and for the energy production.

Keywords: Photovoltaic; PV utility-Scale monitoring; Performance ratio; Low irradiance losses; Multiple linear regression; Random forest.

Nomenclature

a, b, c: Exponential fit coefficients.

A: Area of PV modules.

CUF: Capacity Utilization Factor.

E_{AC}: AC PV energy production.

I_{POA}: Global irradiance in the plane of array.

IRR: Internal rate of return.

Isc: Short-circuit current.

G_{STC}: Reference solar irradiance at standard conditions.

IQR: Interquartile range.

$LCOE$: Levelized cost of electricity.

MAE: Mean absolute error.

mtry: Number of predictors selected at each split of the regression tree.

N_{mod}: Number of PV modules from a PV array.

$NOCT$: Normal operating cell temperature.

NPV: Net present value.

$nRMSE$: Normalized root mean squared error.

ntree: Number of trees of the random forest algorithm.

$P_{PV,rated}$: Rated installed PV power of the system at standard test conditions.

$P_{inv,rated}$: Rated installed power of the inverter.

PR: Performance ratio.

PR': Performance ratio without considering low irradiance losses.

$PR_{measured}$: Performance ration obtained from measurements.

P_{max}: Peak power.

R^2: Coefficient of determination.

$RMSE$: Root mean squared error.

T_a: Ambient temperature.

T_{cell}: Cell temperature.

THD: Total harmonic distorsion.

VIF: Variance inflation factor.

Voc: Open circuit voltage.

$\bar{y}$: Mean measured value.

$\hat{y}_i$: Predicted value.

y_i: Measured value.

Y_F: Final yield.

Y_R: Reference yield.

Y_{R1}: Reference yield from weather station 1.

Y_{R2}: Reference yield from weather station 2.

$\beta_1, \beta_2, \beta_3$: MLR coefficients.

γ: Maximum power temperature coefficient.

$\eta_{wiring,DC}$: DC wiring losses.

η_{deg}: Degradation losses.

η_{inv}: Inverter efficiency.

η_{LIL}: Low irradiance losses efficiency.

$\eta_{mismatch}$: Mismatch losses.

$\eta_{PV,stc}$: PV efficiency under STC.

η_{soil}: Soiling losses.

η_{temp}: Temperature losses.

AC: Alternating current.

ANN: Artificial neural network.

ANOVA: Analysis of variance.

a-Si: Amorphous silicon.

DC: Direct current.

IEC: International Electrotechnical Commission.

LIL: Low Irradiance Losses.

mc-Si: Mono-crystalline silicon solar cell.

ML: Machine learning.

MLR: Multiple linear regression.

MPPT: Maximum power point tracker.

pc-Si: Poly-crystalline silicon solar cell.

O&M: Operations and maintenance.

PV: Photovoltaic.

RD: Royal decree.

RF: Random forest.

STC: Standard test conditions.

SCADA: Supervisory control and data acquisition.

SVM: Support vector machine.

WS: Weather station.

A: Ampere.

c€: Euro cent.

d: Day.

GW: Nominal Gigawatt.

GW h: Gigawatt hour.

h: Hour.

Hz: Hertz.

kV: kilovolt.

kV A: Kilovolt-ampere.

kW: Nominal kilowatt.

kW h: kilowatt hour.

$\mathrm{kW_p}$: kilowatt peak.

m: Linear meter.

m^2: Square meter.

nm: Nanometer.

MW: Nominal Megawatt.

$\mathrm{MW\,h}$: Megawatt hour.

$\mathrm{MW_p}$: Megawatt peak.

M€: Millions of Euros.

$^\circ\mathrm{C}$: Degree Celsius.

V: Volt.

W: Nominal Watt.

$\mathrm{W_p}$: Watt peak.

$\mu\mathrm{V}$: Microvolt.

Ω: Ohm.

2.1 Introduction

Photovoltaic (PV) energy systems are a key technology to increase the share of renewables in the energy mix, especially in countries with a high solar resource. In the last decade, the rapid cost reduction of up to 82% [1], together with the favorable decarbonization policies [2], has increased exponentially the global PV installed capacity from a total of 72 GW in 2011 to 707.5 GW in 2020 [3].

Literature on the operation of large photovoltaic plants is rather recent. Most of these plants are located in hot, desert, arid or semi-arid climates, such as 5 $\mathrm{MW_p}$ in Sivagangai (India) [4], 9.36 $\mathrm{MW_p}$ in Gujarat (India) [5], 10.13 $\mathrm{MW_p}$ in Soroti City (Uganda) [6], 11.15 $\mathrm{MW_p}$ in Shagaya PV plant (Kuwait) [7], 15 $\mathrm{MW_p}$ in Nouakchott (Mauritania) [8], 20.05 $\mathrm{MW_p}$ in southwestern Algeria [9], and 23.92 $\mathrm{MW_p}$ in El Bayad (Algeria) [10]. In most of the cases, these analysis were performed after only 1 to 5 years of operation, which provide limited insights on the long-term performance. To cover this gap, this paper investigates the PV production after 12 years of operation, for the largest PV power plant (50 MW) for which the performance is reported in literature.

The PV energy production potential estimation is essential to provide more accuracy in the design and monitoring stages of new PV utility-scales and to guarantee their integration to the power grid [9], and a proper performance and reliability throughout their life-cycle [11]. For this purpose, commercial modelling softwares are generally employed, with a reliability which depends on the accuracy of the irradiance and electrical submodels [12]. The latter includes parameters such as the power losses at different stages of the facility, namely, the performance ratio (PR).

In addition to the study of the performance of a power plant, this paper also investigates the modelling of the PR as one of the main points to estimate the AC energy yield (E_{AC}) in PV systems using irradiance time-series. These models are widely spread in technical specification manuals [13], open-source libraries *pvlib* [14], research literature [15], and commercial software [16]. Generally, the main inputs are the in-plane global irradiance (I_{POA}), the nominal capacity, along with the PR. The latter is introduced as a product of the different installation losses, which are strongly dependent on the technology, the system design, and the climatic conditions [17]. There is abundant literature regarding losses in which affect on the PR [18], especially when facilities operate far from the standard test conditions (STC) [19]. However, there are only a few publications which quantify the impact of low irradiance losses (LIL) [20] on the PR by adding a correction factor. Irradiances below $200\,\mathrm{W/m^2}$ to $400\,\mathrm{W/m^2}$ cause a non-negligible drop in efficiency of the modules [21], leading to an overprediction in the (E_{AC}) results when operating in such range of irradiances [22].

Generally, the modelling of LIL is addressed with logarithmic expressions to estimate either directly the PV production or the module efficiency [23] together with several empirical models with scarce peer-reviewed comparisons with other previous model proposals [24]. Another common approach to face the non-linearity of these low irradiances is by defining two or more empirical expressions by irradiance ranges [25]. The simplest model which provides a LIL correction is found in the in-house program PR-FACT [26]. Nevertheless, the employed continuous efficiency curve is not publicly reported and cannot be implemented by other researchers. More complex low irradiance models have been developed [27], but they require detailed electrical characteristics of the solar cell, which hinder the replicability when compared to simpler models. To cover this gap, this paper develops a replicable method to estimate the LIL, and hereby increase the accuracy of the global PR, using the irradiance exclusively as input.

Besides physically based models, statistical and Machine Learning (ML) models have been proposed in recent years to estimate the PV production [28]. However, literature in this field is scarce. An artificial neural network (ANN) was applied to predict the PR of the PV modules with a root mean squared error ($RMSE$) below 0.02 [29]. The PR was calculated by means of a physical expression dependent on the temperature and irradiance. S. Bandong et al. [30] developed a Support Vector Regression (SVR) and Multiple Linear Regression (MLR) using 26 climatic variables as predictors, obtaining a $RMSE$ of 1.5% compared with measured data. Behzad Hashemi et al. [31] reduced the number of inputs to 5, obtaining a $RMSE$ of 0.06 with Long Short-Term Memory networks and 8 years of recorded data from a $1.44\,\mathrm{kW_p}$ facility. The complete replicability of these models is nevertheless limited due to the large number of climatic variables that must be measured over a long period of time.

The present work explores the capability of simpler ML models to predict the global PR with only two climatic variables: I_{POA} and the ambient temperature (T_{a}). Two regression models have been employed: a MLR, which is the simplest algorithm, and Random Forest (RF), which is computationally simpler than ANN and well-suited for predicting stochastic PV generation reducing bias and variance [32]. The authors have not found any published research on its application to estimate the global PR, which is a useful alternative for prediction when there is not enough information available on the facility to develop a physical model.

To sum up, given the previous literature review, this article presents the following novelties:

- Provide relevant experimental data regarding the PV performance of a large PV system ($50\,\mathrm{MW}$) after 12 years of operation under Mediterranean climatic conditions.
- The development and assessment of a method to estimate the daily LIL, based on an empirical exponential expression and using the I_{POA} as input.
- The development and assessment of a MLR and a RF model to estimate the global PR of the utility-scale using only as inputs T_a and I_{POA}.

2.2 Materials

The grid-connected PV utility-scale of the present work is located in the east of Olmedilla de Alarcón, Spain (39.6155°N, 2.0905°W). The plant was commissioned in October 2008 with a nominal power of $50\,\mathrm{MW}$, a peak power of $60.103\,\mathrm{MW}_p$ and a total land occupation of 175.3 hectares. According to the Köppen climate classification, the climate of the power plant is classified as Csa (hot-summer Mediterranean), with daily average temperatures that vary between $0\,°\mathrm{C}$ to $31\,°\mathrm{C}$, and a horizontal irradiation of up to around $1{,}050\,\mathrm{Wh/m^2}$, according to the measured data of this study.

The solar PV power plant (Figure 2.1 and Figure 2.2) consists of 500 independent sectors, each with an inverter of $100\,\mathrm{kW}$ and an array of different PV modules whose total peak power varies per sector from $116.5\,\mathrm{MW}_p$ to $127.5\,\mathrm{MW}_p$. The peak power distribution is shown in Figure 2.3 for the different manufacturers. The PV modules have a fixed 30° tilt angle and are oriented towards the south. There are three different module manufacturers with mc-Si and pc-Si. The characteristics of the PV modules are summarized in Table 2.1, where each sector contains several models with different rated power of the same manufacturer.

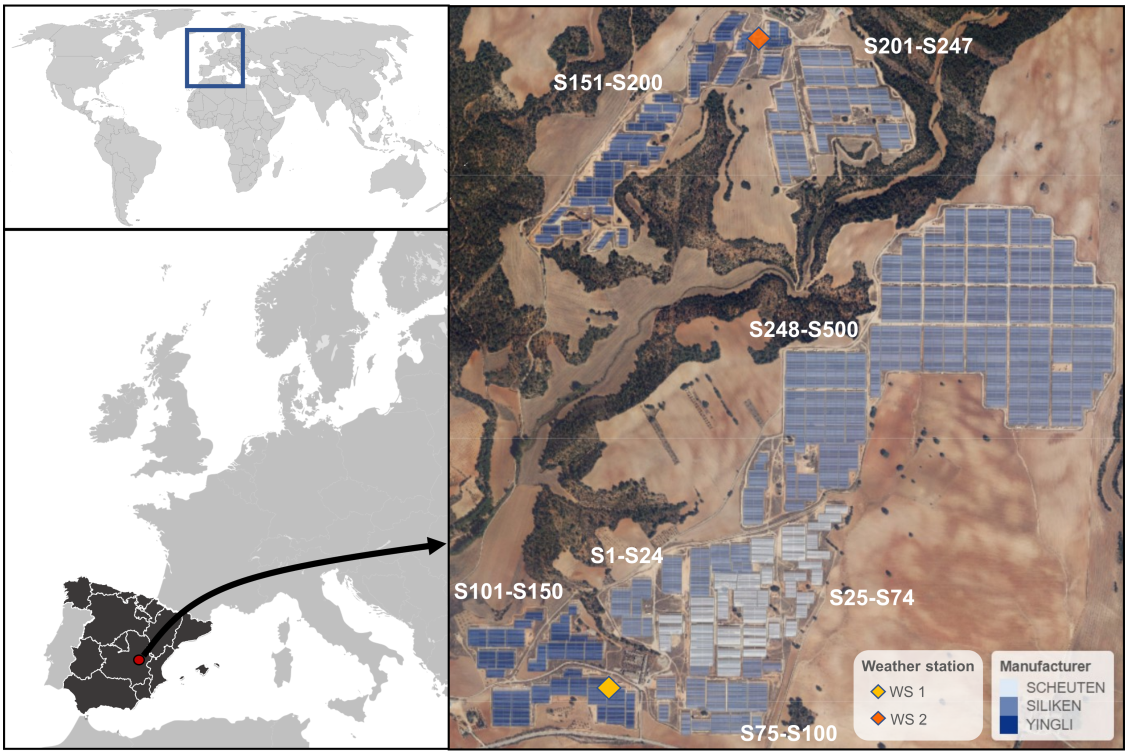

Figure 2.1: Aerial view of the PV plant (500 sectors: S1-S500).

Figure 2.2: Photograph of the PV plant.

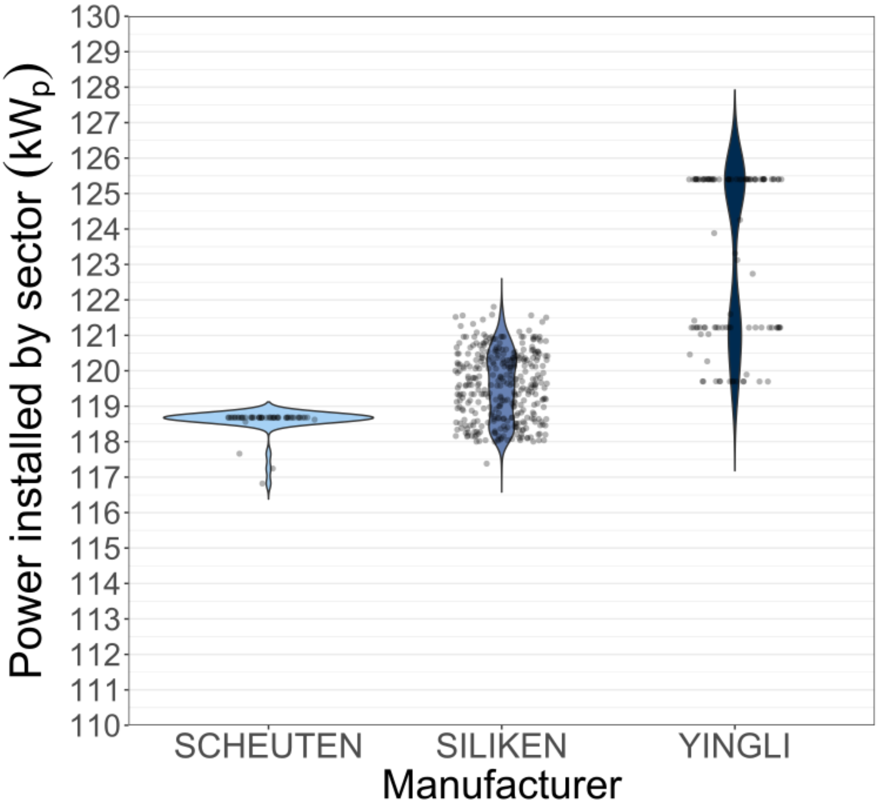

Figure 2.3: Installed peak power grouped by manufacturer.

Table 2.1: Characteristics of the PV modules.

Sectors	Manufacturer and model	Technology	Area	Peak power (Pmax)	Efficiency	Peak power voltage	Peak power current	Open-circuit voltage	Short-circuit current	Temperature coefficient of Pmax	Temperature coefficient of Isc	Temperature coefficient of Voc	Maximum system voltage	Number of cells	NOCT	Distance between PV rows
(-)	(-)	(-)	(m^2)	(SI)	(%)	(V)	(A)	(V)	(A)	(%/°C)	(%/°C)	(%/°C)	(V)	(-)	(°C)	(m)
1-24	Siliken	pc-Si	1.62	199	12.26	28.72	6.91	36.28	7.68	-0.43	0.62	-0.36	600	60	46	2.6
75-100	SLK60P6L			203	12.50	28.86	7.03	36.36	7.76							
201-500				205	12.63	28.90	7.09	36.40	7.80							
				209	12.87	28.98	7.21	36.48	7.88							
				212	13.06	29.04	7.30	36.54	7.94							
				215	13.24	29.10	7.39	36.60	8.00							
				218	13.43	29.16	7.48	36.66	8.06							
				221	13.61	29.22	7.56	36.72	8.12							
				224	13.80	29.28	7.65	36.78	8.18							
				227	13.98	29.38	7.72	36.84	8.25							
				230	14.17	29.50	7.79	36.90	8.32							
				233	14.35	29.50	7.89	36.90	8.41							
25-74	Scheuten	mc-Si	1.72	210	12.21	45.90	4.58	57.60	5.02	-0.47	0.50	-0.33	1,000	96	45	2.8
	MULTISOL 200-P5			215	12.50	46.15	4.66	57.80	5.08							
				230	13.37	46.90	4.90	58.40	5.24							
101-200	Yingli	pc-Si	1.70	210	12.40	26.60	7.90	33.60	8.45	-0.45	0.6p	-0,37	1,000	54	46	2.68
	YL210			220	12.95	26.80	8.04	33.70	8.57							

All sectors use the same inverter model INGETEAM INGECON SUN100 with a nominal power of $100\,\mathrm{kW}$ and an efficiency of 96%. The rest of the electrical parameters of the inverter are shown in Table 2.2. The energy output of the inverters is expanded to a medium voltage level of $20\,\mathrm{kV}$ by means of 500 transformers of $100\,\mathrm{kV\,A}$. The voltage is finally increased in a substation up to $132\,\mathrm{kW}$ before its injection into the grid.

Table 2.2: Summary of the characteristics of the inverters.

Parameter	**Value**	**Units**
Maximum input voltage	900	V
Maximum input current	286	A
MPPT voltage range	405 - 750	V
Number of inputs	4	-
Number of maximum power trackers	1	-
Nominal output power	100	kW
Nominal operating voltage	3x220-3x400	V
Nominal frequency range	50/60	Hz
Maximum output current	340	A
European efficiency	96	%
Power factor	1	-
THD	< 3	%

For the present study, the hourly E_{AC} has been measured by the monitoring system of the inverters. The inverter measurements are transferred to the supervisory control and data acquisition (SCADA) system, which is installed in a high-performance workstation, through an industrial RS232/RS485 to Ethernet converter and an IP-based network. The PV plant also has two weather stations (WS) located at its northern (39.6348°N, 2.0867°W) and southern (39.6151°N, 2.0938°W) ends (Table 2.1). The WS are equipped with a T_a sensor and a pyranometer which measures the I_{POA}. Both systems provide measurements every 5 minutes, and their main specifications are summarised in Table 2.3. The instrumentation of each WS is connected to an independent programmable logic controller system Omron CJ1M-CPU11 to condition the signals and send them to the SCADA system. The recorded data is stored and used for real-time monitoring, alarm management, signal processing, report generation, as well as the integration of the SCADA to the web. The measurement equipment is calibrated annually by the Spanish Centre for Energy, Environmental and Technological Research.

Table 2.3: Summary of the pyranometer specifications.

	Pyranometer		**Temperature sensor**	
Feature	Value	Units	Value	Units
Manufacturer	Delta Ohm	-	E+E Elektronik	-
Model	LP PYRA 02	-	EE21	-
Sensitivity	10	$\mu V\, W^{-1}\, m^2$	10	$mV\, ^\circ C^{-1}$
Measuring range	0 ÷ 2,000	W/m^2	-40 ÷ 60	$^\circ C$
Operating temperature range	-40 ÷ 80	$^\circ C$	-40 ÷ 60	$^\circ C$
Impedance	33 ÷ 45	Ω	-	-
Spectral range	283 ÷ 2,800	nm	-	-
Type of sensor	-	-	Pt100 (tolerance class A, DIN EN 60751)	-
Accuracy	-	$^\circ C$	0.2 ÷ 0.7	$^\circ C$

2.3 Methods

This section describes the methodology to analyze the measured data and to estimate the PR and E_{AC}.

The methodology is summarized in Figure 2.4. The aim is to perform an analysis of the 50 MW PV power plant and to propose a novel method based on climatic data that improves the PR estimations and helps reach a more accurate estimation of the E_{AC}.

The first step in the methodology (section 2.3.1) is to carry out an exploratory data analysis of the collected data. The E_{AC} data of each sector and the climatic data have been initially filtered to remove potential outliers. Afterwards, the main performance parameters of the utility-scale have been calculated, and an exploratory data analysis of these results has been performed. Additionally, the results are compared with other power plants in similar climatic regions.

As a second step, two approaches have helped to model the PR with climatic data: the first method is a physical model, considering the product of several factors that describe the energy losses in different stages of the facility. The LIL have been modelled to improve the estimated PR accuracy for low irradiances. Several regression and ML models have been assessed. This requires examining the correlations between the predictors (climatic data) and the predicted variable (PR) and obtaining one different model per manufacturer, justified by a one-way ANOVA test. Two different models have been studied: a MLR model and a RF model with their respective k-fold cross-validations with measurements.

The last step consists of predicting the total E_{AC} of the power plant through a physical model that considers the PR previously calculated from the different models, the module characteristics, and the array configuration of each sector. Finally, the production results have been compared with the measurements for the different PR models.

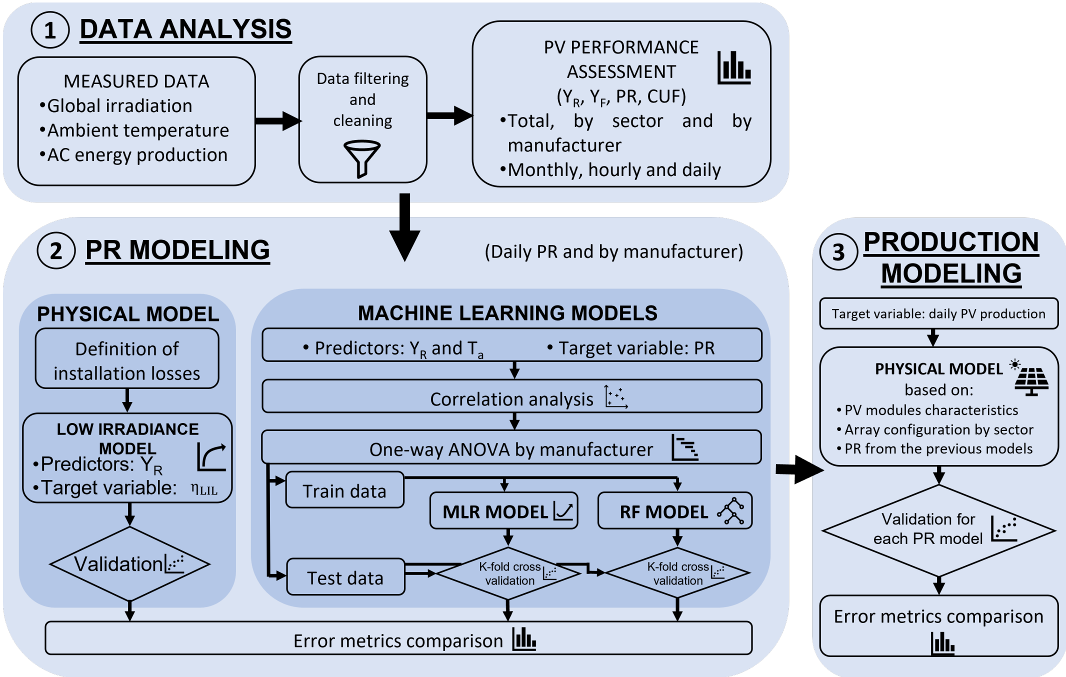

Figure 2.4: Workflow of the methodology.

2.3.1 Data pre-processing

The performance data has been analyzed on an hourly basis for year 2020. The core of the experimental data is the E_{AC} from the inverter, the T_a, and the I_{POA} for the tilt and azimuth angle of the PV arrays (30° S). To provide stable measurements and a consistent analysis without measurement errors, the data was initially filtered according to the guidelines the standard IEC 61724, as in similar PV utility-scale analysis [22]. The hourly measurements were filtered according to the ranges indicated in Table 2.4.

Table 2.4: Filtering criteria applied for the hourly measured data.

Min	Parameter	Max
$20\,\mathrm{W/m^2}$	I_{POA}	$1{,}500\,\mathrm{W/m^2}$
$-30\,°\mathrm{C}$	T_a	$50\,°\mathrm{C}$
0	E_{AC}	$1.02 \cdot P_{inv,rated}$

In Table 2.4, $P_{inv,rated}$ (upper filter threshold for the E_{AC}) can be understood as the nominal power of the inverter (in this case, $P_{inv,rated}$ = 1,500 kW).

With respect to the data filtering, some authors employ a higher threshold for the minimum I_{POA} ($200\,\mathrm{W/m^2}$) [33]. Nevertheless, to keep as much available data as possible in this work, a less restrictive threshold of $20\,\mathrm{W/m^2}$ has been considered according to the recommendation of part one of the standard IEC 61724 [34]. Keeping the irradiance values in the range $20\,\mathrm{W/m^2}$ to $200\,\mathrm{W/m^2}$ has enabled the development of a specific characterization of the system for low irradiance values.

The typical reporting periods to assess the performance of PV utility-scales are equal or longer than one day (e.g. annually, monthly, or daily) [35]. The hourly measurements were aggregated daily to avoid potential underestimations of module performances as reported in bibliography [36].

2.3.2 PV performance parameters

The performance of the present PV utility-scale has been evaluated following the IEC 61724 standard guidelines. Their definitions and expressions of the main performance parameters are described in Table 2.5.

Table 2.5: Description of the PV performance parameters.

Parameter	Description	Expression	Units
Reference Yield (Y_R)	The maximum theoretical solar energy available in a specific location is defined as the ratio between the total daily in-plane insolation ($I_{POA,d}$) and the reference solar irradiance at standard conditions (G_{STC}= 1 kW/m^2).	$Y_{\mathrm{R}} = \frac{\mathrm{G_{POA,d}}}{\mathrm{G_{STC}}}$	h/d
Final Yield (Y_F)	The ratio between the E_{AC} of the system during a certain period, in this case daily ($E_{AC,d}$), and the PV rated installed power of the system at standard test conditions ($P_{PV,rated}$)	$Y_{\mathrm{F}} = \frac{\mathrm{E_{AC,d}}}{\mathrm{P_{PV,rated}}}$	h/d
Performance Ratio (PR)	The ratio between the Y_F and the Y_R. It can be understood as an efficiency parameter that measures the energy losses between actual output of the plant with its irradiation input. PR allows comparing performance results between different PV systems regardless the geographical location and the installed peak power.	$PR = 100 \cdot \frac{\mathrm{Y_F}}{\mathrm{Y_R}}$	%
Capacity Utilization Factor (CUF)	Relationship between the Y_{F} of the plant and the maximum possible energy production, defined by its installed capacity in a given period.	$CUF = 100 \cdot \frac{\mathrm{E_{AC,d}}}{\mathrm{P_{PV,rated}} \cdot 24}$	%

2.3.3 Energy production model

The hourly E_{AC} ($E_{AC,h}$) of the entire utility-scale has been calculated using Eq. 2.1. The daily production ($E_{AC,d}$) can be obtained aggregating the hourly production as shown in Eq. 2.2.

$$E_{AC,d} = \sum_{i=1}^{500} \sum_{j=1}^{8} PR_i \cdot \eta_{PV,STC_{i,j}} \cdot A_i \cdot N_{mod_{ij}} \cdot G_{POA} \tag{2.1}$$

$$E_{AC,d} = \sum_{h=1}^{24} E_{AC,h} \tag{2.2}$$

Where:

- $A_{i,j}$ is the area of a PV panel of sector i in the array j, provided by the manufacturer in Table 2.1.
- $\eta_{PV_{i,j}}$ is the PV efficiency under STC of sector i in the array j, as provided by the manufacturer in Table 2.1.
- $N_{mod_{i,j}}$ is the total number of modules of the sector i in the array j.
- G_{POA} is the hourly measured in-plane global irradiance.
- PR_i is the performance ratio of the sector i and has been obtained either with a physical quantification of the plant losses (Section 2.3.4) or with a statistical analysis (Section 2.3.5).

2.3.4 PR physical model

The physical definition of the PR is based on the determination of the losses which occur in every energy transmission or conversion stage from I_{POA} to the E_{AC} of the inverters. The losses of the transformation stage have not been included since the measured data is before the grid injection. There are no shadow losses in the PV plant.

According to several authors [37], the PR of each sector i can be defined as the product of the losses indicated in Eq. 2.3. The term PR'_i (base PR model) refers to the PR before introducing the LIL.

$$PR'_i = \eta_{soil} \cdot \eta_{deg,i} \cdot \eta_{temp,i} \cdot \eta_{inv} \cdot \eta_{mismatch} \cdot \eta_{wiring,DC} \tag{2.3}$$

Where η is the efficiency of each stage, as indicated in Table 2.6. Whenever the efficiency data is not available, the values have been obtained from similar facilities in literature.

The temperature losses efficiency (η_{temp}) is obtained with Eq. 2.5 through the temperature coefficient of the PV modules (γ), defined in Eq. 2.1, and the PV cell temperature (T_{cell}). The latter can be estimated with Eq. 2.4 using the hourly measured T_a and I_{POA} , as well as the nominal operating cell temperature ($NOCT$ in Table 2.1), which is defined as the cell temperature obtained with T_{amb} = 20 °C and a solar irradiance of 1 kW/m^2 . This approach is widely employed in literature and provide conservative loss values compared to other cell temperature models [38].

$$T_{cell,i} = T_a \cdot G_{POA} \cdot \frac{NOCT_i - 20}{800} \tag{2.4}$$

$$\eta_{temp_i} = 1 - \gamma_i \cdot (T_{\text{cell}_i} - 25) \tag{2.5}$$

Table 2.6: Description of the losses included in the PR physical model.

Parameter		Description	Value	Reference
η_{soil}	Soiling losses	Optical losses due to dust and particles accumulated on the PV modules' surface over time. The latter fluctuate mainly with the frequency of the rainfalls, the maintenance schedule, and dust type. For this facility with a 30° tilt, 2% of soiling losses has been assumed.	0.98	[39–41]
η_{deg}	Degradation losses	Power decay over time in the output of the PV modules due to different causes of deterioration: cell cracks, corrosion, discoloration, glass breakage, etc [42]. Values extracted from the manufacturer data sheet.	0.916 0.890 0.920	Manufacturer: Siliken Scheuten Yingli
η_{temp}	Temperature losses	Drop in the PV module efficiency due to the increase of the cell operating temperature. The calculation of the hourly values is further described in this section.	$\eta_{temp_i}(T_{cell})$	[15, 37] and manufacturer
η_{LIL}	Low irradiance losses	This parameter gathers the nonlinear efficiency drop of the PV modules for low irradiance values. The calculation methodology is further explained in this section and the value depends on the I_{POA} or Y_R.	$\eta_{LIL}(Y_{\text{R}})$	Manufacturer
η_{inv}	Inverter efficiency	A constant value for inverter efficiency is provided by the manufacturer mentioned in section 2.2.	0.96	Manufacturer
$\eta_{mismatch}$	Mismatch losses	Losses due to the interconnection of solar modules of cells with different electrical properties. Following published literature, a typical loss of 2% has been assumed.	0.98	[39, 43]
$\eta_{wiring,DC}$	DC wiring losses	Direct current losses caused by the ohmnic resistance of the wiring that interconnects the PV strings with the inverter. Due to the great spatial extension of the power plant a 2% of losses has been assumed [39].	0.98	[40, 44]

Since only a single complete year with measurements is available, the absence of a cyclical component in the time series limits the use of year-on-year and statistical methods [45], which present robust results with time series of several years. As an alternative, instead of directly using the degradation losses supplied by the manufacturers (Table 2.6), the degradation losses were calculated with the daily PV production balance of Eq. 2.1, and breaking down the PR between $\eta_{deg,i}$ and another factor with the rest of the losses contemplated in Table 2.6. The $\eta_{deg,i}$ daily values were then averaged for the entire year, resulting in values of 0.9022 for Siliken, 0.8711 for Scheuten, and 0.8934 for Yingli. These coefficients represent the total loss due to degradation after 12 years of operation.

The efficiencies of Table 2.6 are typically employed to quantify the PR [18]. In the present work a new coefficient has been added, the LIL (η_{LIL}), to account for the drastic drop of the module PV production at low irradiances (below 200 $\mathrm{W/m^2}$) [20]. Additionally, this coefficient includes the drop of the inverter efficiency when the power input is low, at low irradiance values. This helps to compensate the fact that a constant inverter efficiency had been assumed in the factor η_{inv}.

η_{LIL} has been calculated in Eq. 2.6 as the ratio between the PR obtained from the measurements ($PR_{measured}$) and PR', which does not consider the impact of the LIL.

$$\eta_{LIL} = \frac{PR_{measured}}{PR'} \tag{2.6}$$

Different correlations have been developed to relate the LIL with Y_R. The best fitting has been achieved with the expressions indicated in (Eq. 2.7) and (Eq. 2.8).

$$\eta_{LIL} = 1 - \exp(b \cdot Y_R) \tag{2.7}$$

$$\eta_{LIL} = 1 - a \cdot Y_R^c \cdot \exp(b \cdot Y_R) \tag{2.8}$$

Finally, the PR employed in the production model includes η_{LIL}, as shown in Eq. 2.9.

$$PR = PR' \cdot \eta_{LIL} \tag{2.9}$$

In order to evaluate the accuracy of the developed correlations, the daily PR obtained from the measurements has been compared with the calculated PR using the error metrics described in Section 2.3.6.

2.3.5 PR Statistical and Machine Learning models

A different approach to estimate the PR is by means of statistical models (e.g. MLR) and ML models (e.g. RF). Each of the developed models employs exclusively climatic data (I_{POA} and T_a) as predictors. The data corresponds to year 2020 which is representative for the behavior at half-life of the facility.

Given the variety of equipment, a different fit is proposed for each manufacturer to provide accurate predictions of the daily PR of the PV utility-scale. A one-way ANOVA test has been employed to determine which level of aggregation is more appropriate to define the statistical models. In other words, the one-way ANOVA tests helps to determine if a single global model is better for all sectors, in comparison to a different model for each of the module manufacturers. The null hypothesis is that the manufacturer groups are equal, whereas the alternative hypothesis is that at least one of the distributions is significantly different from the others [46].

The confidence of the results rely on the degree the one-way ANOVA assumptions are met [47]. A significance value (type-I error) of 5% has been assumed for all the hypothesis tests. The choice is based on S. Vergura [48], who indicated that medium-large PV plants present a larger uncertainty due to their high complexity.

Once the PR modelling by manufacturers was justified with the one-way ANOVA test, both MLR and RF models were trained and then tested.

As shown in Eq. 2.10, the MLR model assumes a linear relationship between the predicted variable (PR) and the predictors (Y_{R1} from WS1, Y_{R2} from WS2, and T_a). The *stats* R package has been applied. The regression parameters for each manufacturer i ($\beta_{0,i}$, $\beta_{1,i}$, $\beta_{2,i}$, $\beta_{3,i}$) are estimated by ordinary least squares [49].

$$PR_i = \beta_{0,i} + \beta_{1,i} \cdot Y_{R1} + \frac{\beta_{2,i} \cdot Y_{R2}}{Y_{R1}} + \beta_{3,i} \cdot T_a \tag{2.10}$$

The confidence of the regression parameters depends on the degree of compliance of the MLR assumptions [50], which are evaluated through their respective hypothesis test in section 4.2. The multicollinearity is quantified employing the variance inflation factor (VIF) indicated in Eq. 2.11.

$$VIF_i = \frac{1}{1 - R_{i,j}^2} \tag{2.11}$$

Where $R_{i,j}$ is the correlation coefficient of the i predictor on the remaining explanatory variables. VIF values greater than 4 arise multicollinearity problems [51]. Parallel to the MLR model, a RF model has been developed. The RF algorithm is a non-linear ML model [52] that potentially explains the PR with a better accuracy for the range of low irradiances. Since the PR is a continuous variable, the suggested RF model is constituted by regression trees.

The RF model was trained using the *caret* R package [53]. In the RF algorithm, several hyperparameters need to be defined by the user. The two most relevant optimization parameters are the number of predictors at each split (mtry) and the number of trees to grow for aggregation (ntree) [54].

The mtry value is calculated by default by the algorithm as the rounded down result of the square root of the total number of predictor variables. In this case, since there are three predictors, the mtry value is 2. The ntree value was fixed once the increase of ntree improved the $RMSE$ in less than 1%. The previous criteria is commonly used by researchers [55] and employed in RF models applied to PV applications [56].

To assess the accuracy and robustness of the MLR and RF models, the validation was performed as depicted in Figure 2.5. The pre-processed dataset obtained in Section 2.3.1 was randomly split using an 80:20 ratio to create a train dataset and test dataset. This partition is done to perform an external validation of the models with unseen data from the train set [57]. Then, a k-fold cross validation was conducted with the train set formed by the 80% of the original dataset to obtain the optimized regressors coefficients of the MLR model and build the RF model. For this work a k value of 10 was considered, which is commonly used in literature [58]. Finally, external model validations with the remaining 20% of the original dataset were employed.

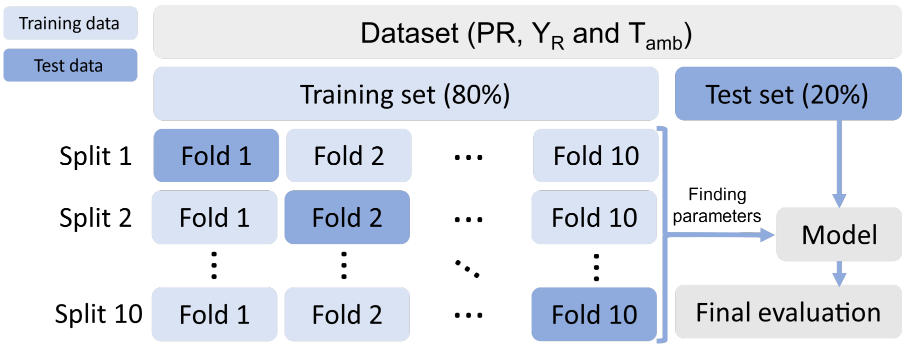

Figure 2.5: Validation methodology of the MLR and RF models.

2.3.6 Model deviation

The accuracy of the three models for the daily PR and the derived PV production has been compared. For the MLR and RF models, the trained model performance is evaluated on the test set using as error metrics the root mean squared error ($RMSE$), the normalized root mean squared error ($nRMSE$), the mean absolute error (MAE) and the coefficient of determination (R^2) as defined in equations 2.12, 2.13, 2.14, and 2.15 [59]:

$$RMSE = \sqrt{\frac{\sum_{i=1}^{N}(y_i - \hat{y}_i)^2}{N}} \tag{2.12}$$

$$nRMSE = \sqrt{\frac{1}{N}\sum_{i=1}^{N}\frac{(y_i - \hat{y}_i)^2}{(\bar{y})^2}} \tag{2.13}$$

$$MAE = \frac{1}{N}\sum_{i=1}^{N}|y_i - \hat{y}_i| \tag{2.14}$$

$$R^2 = 1 - \frac{\sum_{i=1}^{N}(y_i - \hat{y}_i)^2}{\sum_{i=1}^{N}(y_i - \bar{y})^2} \tag{2.15}$$

Where y_i, $\hat{y}_i$, and $\bar{y}$ are the measured, predicted and the mean measured values, respectively, and N the number of samples of the dataset.

2.4 Results

Following the methodology described in Figure 2.4, this section presents the performance analysis of the PV utility-scale, the results and validation of the PR models, and finally in the impact on the PV production.

2.4.1 Performance results of the PV facility

The raw measured data consists of 8,727 hourly measurements of three variables: I_{POA}, T_a and E_{AC} (in 500 sectors), during 364 days of 2020. After applying the data filtering explained in section 2.3.1, the resulting dataset was reduced by 59.33% of the original hours. The minimum irradiation threshold was the main effective filter since 49.74% of the original data was removed due to nighttime hours, and 8.30% during the sunrise and sunset hours. Additionally, there were 10 days (1.29% of the raw data) when the PV production stopped (non-productive hours in Figure 2.6. Stops on individual days are mainly due to inverter failures caused by high temperatures, blown fuses and powered surge protection devices, which need staff intervention before starting-up again. Figure 2.6 shows the hourly values of the total measured E_{AC} of the utility-scale, I_{POA}, and T_a after the data filtering.

The annual I_{POA} was $1{,}975.52\,\mathrm{kWh/m^2}$ and the E_{AC} of the complete utility-scale in 2020 was $91.32\,\mathrm{GW\,h}$, with a monthly average of $7.61\,\mathrm{GW\,h}$.

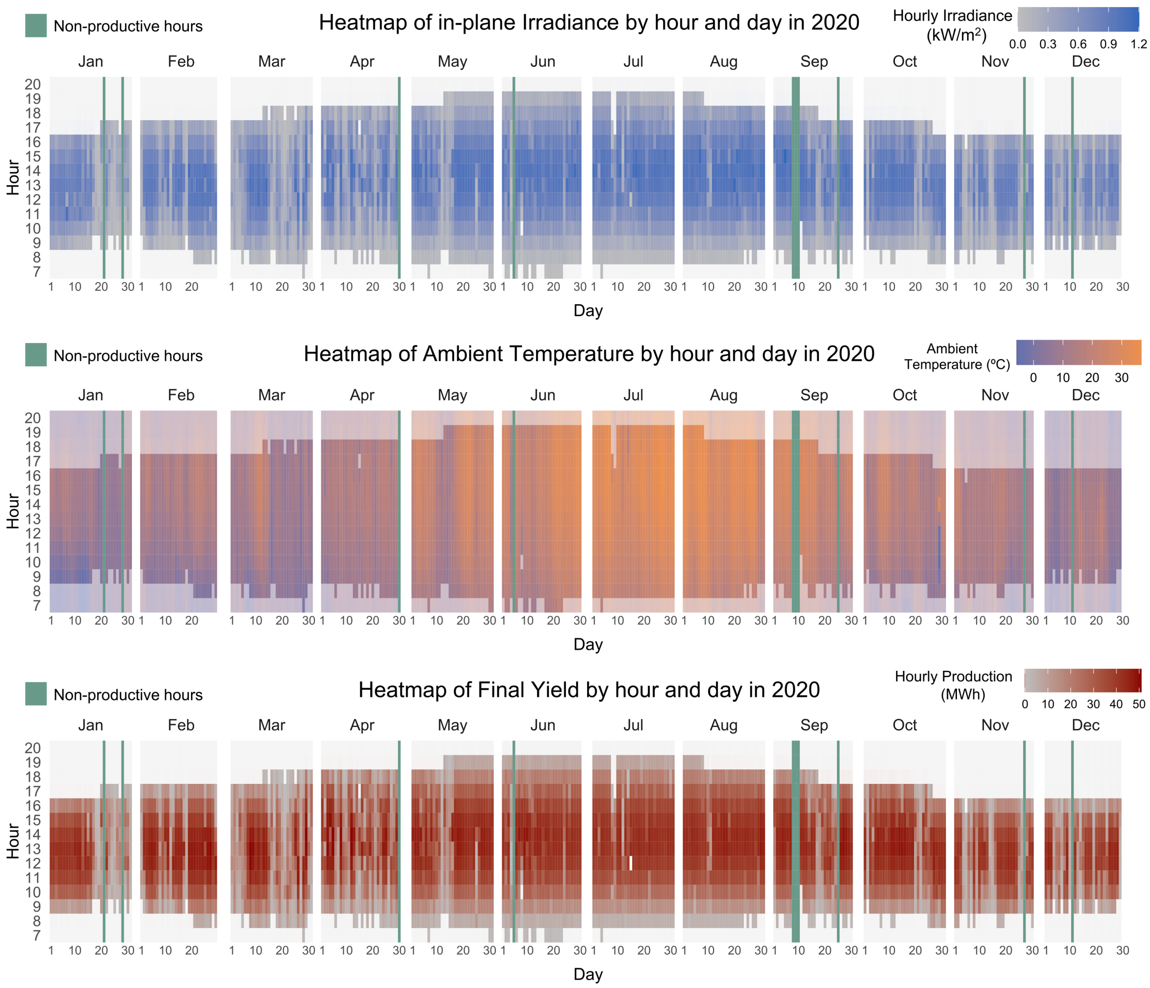

Figure 2.6: Heatmaps of hourly measured I_{POA}, T_a and E_{AC} in 2020.

At the top of Figure 2.7 the average T_a for each month is shown. The average daily T_a during the year is 16.61 °C, fluctuating from a minimum average of 7.43 °C in January, and a maximum average of 28.28 °C in July.

The monthly variation of the PV performance parameters is also presented in Figure 2.7 and Table 2.7. According to section 2.3.2, the Y_R reached its maximum in August and its minimum in December with a value of 7.35 h and of 3.63 h of irradiance equivalent to1 $\mathrm{kW/m^2}$, respectively.

Regarding the Y_F, the yearly average was 5.44 h/d. The minimum was 2.98 h/d in December and the maximum 5.49 h/d in August. However, the maximum daily values, up to 6.33 h/d (in March), were registered during the Spring season, where the lower T_a compared to summer provided a higher efficiency. There are also noticeable differences in the yearly average Y_F for the different module manufacturers. The best performance is obtained by Siliken with 4.32 h/d, followed by Yingli with 4.26 h/d and, lastly, Scheuten with 4.19 h/d. The latter also provides the lowest performances within some sectors, reaching lower values than 4 h/d, as shown in Figure 2.8.

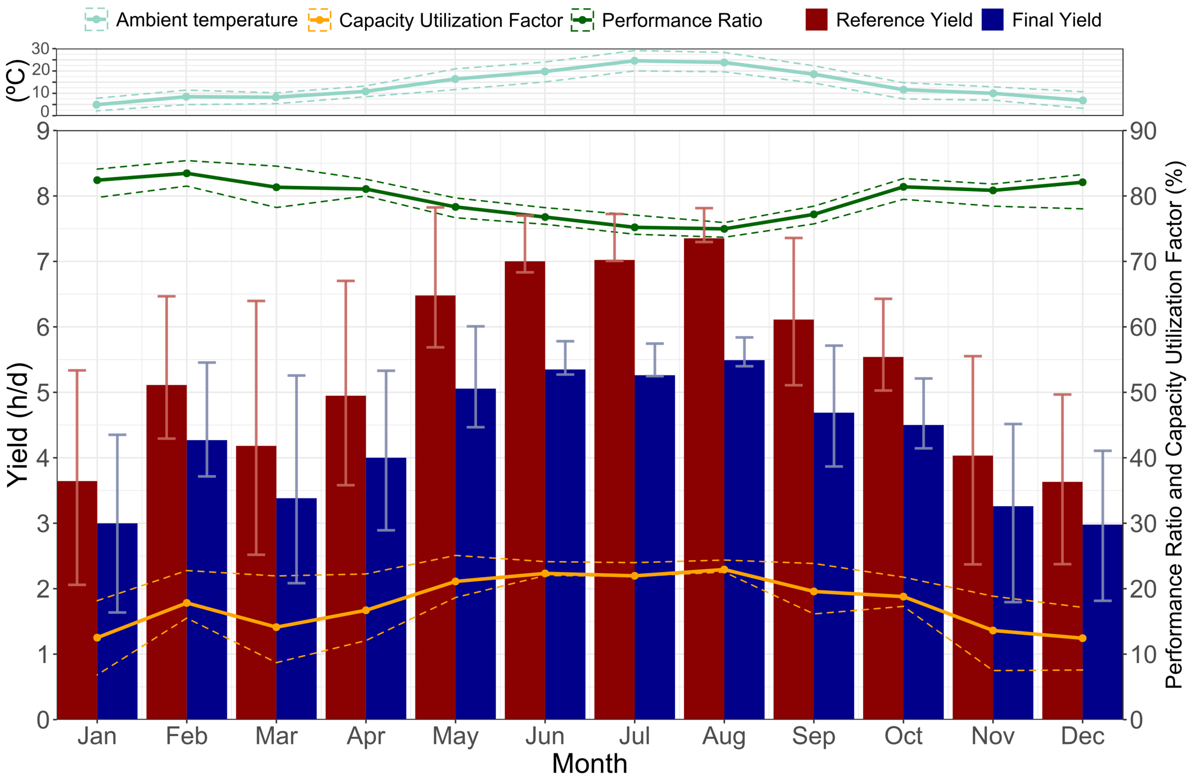

Figure 2.7: Monthly average of the T_a and PV performance parameters (Y_R, Y_F, PR and CUF) in 2020. The interquartile ranges are represented by error bars and dashed lines.

Table 2.7: Statistical results of the global daily performance parameters in 2020.

Parameter	Units	Minimum	1st Quartile	Median	Mean	3rd Quartile	Maximum	Standard deviation	Skewness[a]
Y_R	h/d	0.59	4.10	5.90	5.44	7.30	8.03	2.09	-0.68
Y_F	h/d	0.43	3.31	4.74	4.28	5.63	6.33	1.59	-0.85
PR	%	69.11%	75.93%	79.15%	79.24%	82.20%	93.44%	4.08%	0.23
CUF	%	1.81%	13.81%	19.77%	17.88%	23.52%	26.43%	6.64%	-0.85

[a] Dimensionless Value.

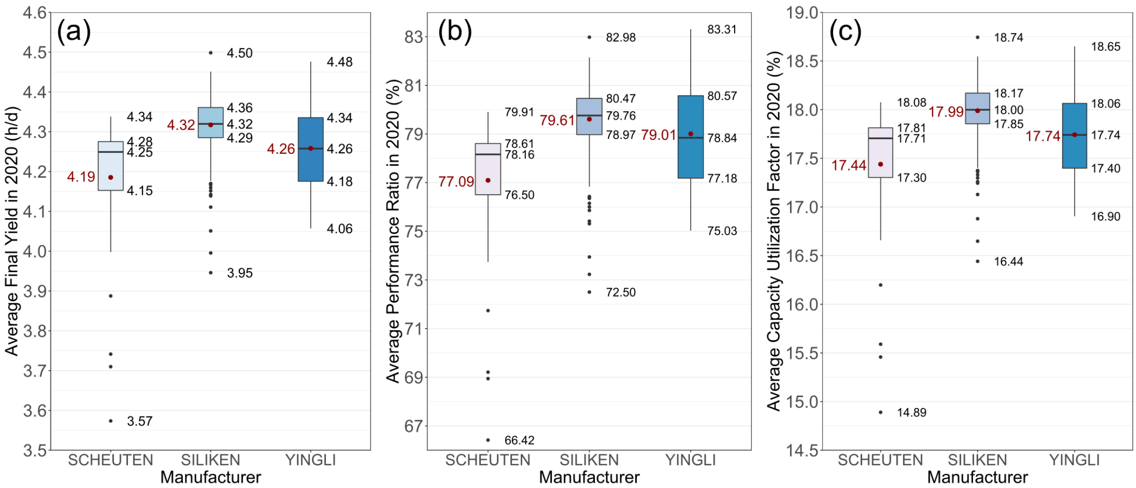

Figure 2.8: Boxplots of the average Y_F (a), PR (b) and CUF (c) of each sector and manufacturer.

The PR ranges between in 74.97% in August and 83.46% in February, with an annual average of 79.24%. The lowest PRs are obtained in summer due to the higher temperatures. There is a clear correlation with the temperature. The global PR was above 75% for 84.2% of the days with measurements, proving that the system has been working correctly in global terms. There are significant fluctuations in the PR when comparing the different manufacturers: the Siliken and Yingli (pc-Si) sectors provide an annual average of 79.61% and 79.01%, respectively, while the Scheuten (mc-Si) sectors yield 77.09%.

The PR of the mc-Si sectors is on average around 2% lower than the pc-Si sectors. Considering the similarities among manufacturer characteristics in the STC efficiencies, the performance difference is mainly caused by a greater drop in efficiency when the temperature increases. This issue can be observed in Table 2.1, since the temperature coefficient in the mc-Si modules is higher than for the pc-Si modules. The same phenomenon was also found in similar climate conditions, both in northern Algeria [60] and in Morocco [61].

The monthly average CUF ranges between 12.44% in December and 22.93% in August, with an annual average of 17.88%. The CUF dispersion decreases during the months with more sunny hours and stable weather. The annual average CUF among module manufacturers differs slightly: 17.99% for Siliken, 17.44% for Scheuten and 17.74% for Yingli, following a similar distribution scheme as the PR.

According to the assumptions described in section 2.3.4, the estimated degradation losses are generally 1-2% higher than the rates provided by the manufacturer datasheets. After 12 years of operation, the average degradation loss for Siliken modules is 9.79%, 12.89% for Scheuten, and 10.66% for Yingli, and their respective averaged yearly degradation rates are 0.816%/year, 1.074%/year, and 0.888%/year. Consequently, the averaged modules efficiency at STC drops to 12.13% for Siliken, 10.85% for Scheuten, and 11.02% for Yingli. The highest degradation is suffered by the mc-Si technology.

As indicated in Table 2.8, the performance of the present utility-scale is comparable with other PV power plants reported in scientific literature under Csa Mediterranean climate. However, due to the long operating period and consequent degradation losses, the average Y_F, PR, and CUF are slightly lower than in the other plants, where the performance was measured a few years after their commissioning. Among the registered PV utility-scales the CUF is generally greater for bigger installed powers, and mc-Si technologies on average provide better PR results.

Table 2.8: Comparison of the PV performance in different PV facilities with hot-summer Mediterranean climate (Csa).

Location	Commissioning Year	Monitoring period	Module type	Peak power (kW_p)	Y_F (h/d) min/mean/max	PR (%) min/mean/max	CUF (%) min/mean/max	Ref.
Olmedilla de Alarcón, Spain	2008	2020	mc-Si/pc-Si	60,103.4	0.43/4.28/6.33	69.11/79.24/93.44	1.81/17.83/26.43	Present study
Ar Ramtha, Jordan	-	2017-2018	pc-Si	5	2.80/4.60/5.80	74.00/80.00/90.00	11.00/18.10/23.00	[62]
Albacete, Spain	2010	2010-2013	pc-Si	4.6	2.20/-/4.37	59.46/-/78.84	9.16/-/18.22	[63]
Mugla, Turkey	-	2008	pc-Si	2.73	2.53/4.77/6.65	-/72/-	-	[64]
Albacete, Spain	2008	2012-2016	pc-Si	2.7	4.71/-/7.92	78.93/-/84.86	19.64/-/33.02	[63]
Sahinkaya, Turkey	2016	2017	pc-Si	2,130.7	2.32/4.53/6.28	73.92/81.15/91.78	9.65/18.86 /26.16	[37]
Albacete, Spain	2007	2012-2016	pc-Si	1.4	7.92/-/2.2	83.56/-/85.60	20.14/-/29.87	[63]
Albacete, Spain	2007	2010-2013	mc-Si	1.3	3.10/-/5.69	80.36/-/85.66	12.91/-/18.66	[63]
Albacete, Spain	2008	2010-2013	mc-Si	1.3	3.50/-/6.69	64.91/-/68.83	14.65/-/27.29	[63]
Monteroni, Italy	2011	2012-2015	mc-Si	960	1.70/3.80/6.20	75.00/84.4/94.00	6.90/15.60/25.60	[11]
Ciudad Real, Spain	2013	2013-2016	pc-Si	370	4.29/-/4.63	80.39/-/81.39	17.86/-/19.30	[63]
Sitia, Crete, Greece	2002	2007	pc-Si	171.36	1.96/3.66/5.07	58.00/67.36 /73.00	-/15.26/-	[15]
Manisa, Turkey	2018	1 year	mc-Si	30	1.53/4.16/6.09	81.22/83.61/86.15	6.38/17.35/25.39	[65]
Bouzareaha, Algeria	2004	2016-2018	pc-Si	9.5	-/3.37/-	-/70.00/-	-	[66]
Tangiers, Morocco	-	2015	pc-Si	5	1.96/4.45/6.42	58.00/79.00/98.00	6.55/14.84/21.42	[67]
Chania, Crete, Greece	-	2010-2012	a-Si/mc-Si	2.18	1.83/-/6.55	80.40/-/95.40	-	[68]
Tangiers, Morocco	-	2016	pc-Si	2	3.38/4.72/5.90	71.23/77.24/84.00	10.83/11.76/12.78	[69]
Los Angeles, United States	-	-	-	0	-/4.22/-	-/72.10/-	-	[70]
Casablanca, Morocco	-	-	-	0	-/4.29/-	-/71.90/-	-	[70]

Besides the energy performance assessment, an economic analysis has also been conducted. The remuneration of the facility has depended on two different Spanish legislative frameworks during its operation. The first period, from its commissioning in 2008 until July 2014, followed RD 661/2007 [71], with a fixed price. The second period, which is still in force, follows RD 413/2014 [72]. The remuneration calculations for this period are described in detail for other plants in literature [73].

The net present value (NPV), internal rate of return (IRR), payback period and the levelized cost of electricity ($LCOE$), were estimated according to N. Bansal et al. [74], considering the initial investment cost, the O&M costs, the cashflows generated by the energy selling, the annual degradation rate of the modules, the inflation rate and the discount rate summarized in Table 2.9.

Table 2.9: Parameters of the economic analysis.

Variable	**Value**	**Units**	**Reference**
Total investment cost	384	$\mathrm{M€}$	Present study
Averaged yearly E_{AC} measured for the life cycle	91,967	$\mathrm{MW\,h}$	Present study
Fixed electricity price (2008-2014)	22.976	$\mathrm{c€/kWh}$	[71]
Averaged electricity market price (2014-Present)	6.186	$\mathrm{c€/kWh}$	[75]
Specific remuneration for the operation (2014-Present)	31.754	$\mathrm{c€/kWh}$	[76]
Specific remuneration for return on the investment (2014-Present)	244,85	$\mathrm{€/MWyear}$	[76]
Average degradation rate	Siliken: 0.816 Scheuten: 1.074 Yingli: 0.888	%/year	Present study
O&M cost	11.6	$\mathrm{€/kW_p year}$	[77]
Annual Spanish inflation rate (averaged between 2008-2020)	1.062	%	[78]
Annual discount rate	7.090	%	[79]
Life cycle of the facility	25	years	Present study

The NPV, IRR and payback period are $93.02\,\mathrm{M€}$, 9.19%, and 17.61 years, and the $LCOE$ is $0.359\,\mathrm{€/kWh}$.

2.4.2 PR modelling results

Figure 2.9 shows the deviations between the modelled daily PR considering the physical losses and the measured daily PR, as calculated with Eq. 2.6 While for regular days with daily Y_F higher than 3 h/d the deviations fluctuate around 1, which means that no significant corrections are required, there is a clear drop for daily Y_R values below 2 h/d.

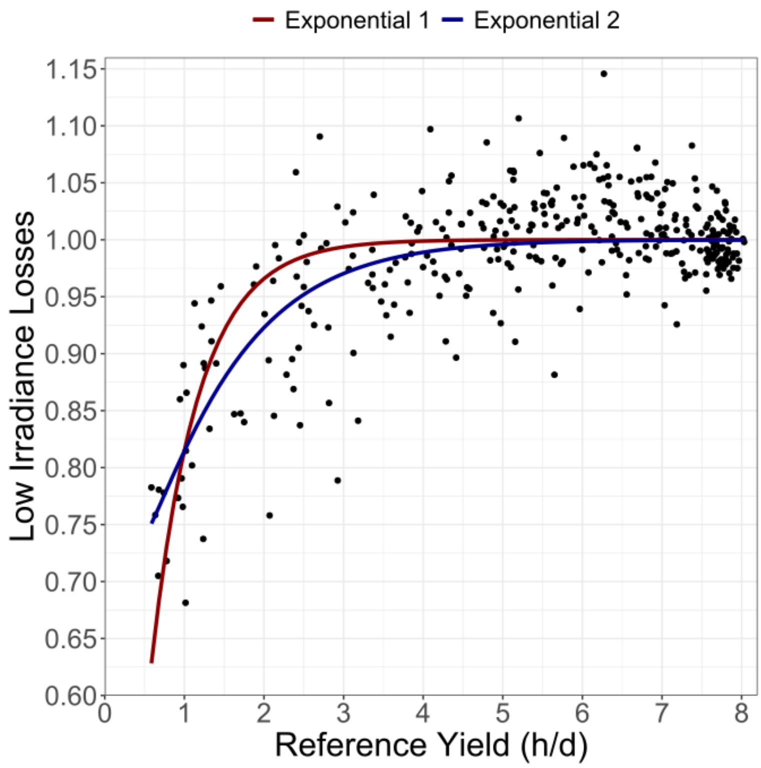

Figure 2.9: Relationship between LIL (η_{LIL}) and the Y_R.

These deviations were modelled with two nonlinear exponential fits, whose coefficients and error metrics are given in Table 2.10. The employment of an exponential fit allows reducing selectively these differences only for low Y_R values. A linear regression fit would tend to overestimate the LIL. The exponential 1 fit, despite its simplicity, tends to excessively reduce the PRs with low Y_R values s. The exponential fit 2 presents a more moderate fit and reduces the error compared with the exponential 1 for Y_R values around 2 h/d. The exponential 2 was consequently selected for the comparison with the PR models.

Table 2.10: LIL exponential model coefficients and error metrics.

Model	**Expression**	**a**	**b**	**c**	$RMSE$	MAE	R^2
Exponential 1	$\eta_{LIL} = 1 - \exp(b \cdot Y_R)$	-	-1.688	-	0.047	0.033	0.514
Exponential 2	$\eta_{LIL} = 1 - a \cdot Y_R^c \cdot \exp(b \cdot Y_R)$	0.539	-1.067	0.273	0.043	0.032	0.585

Adding the correction of the exponential fit 2 in Eq. 2.9 clearly improves the results, as may be inferred by comparing Figure 2.10a and Figure 2.10a. There are significant overpredictions with the base PR model (up to 15% of relative error) which are mitigated when η_{LIL} is introduced. With the exponential fit 2, the $nRMSE$ decreases by 48.22%.

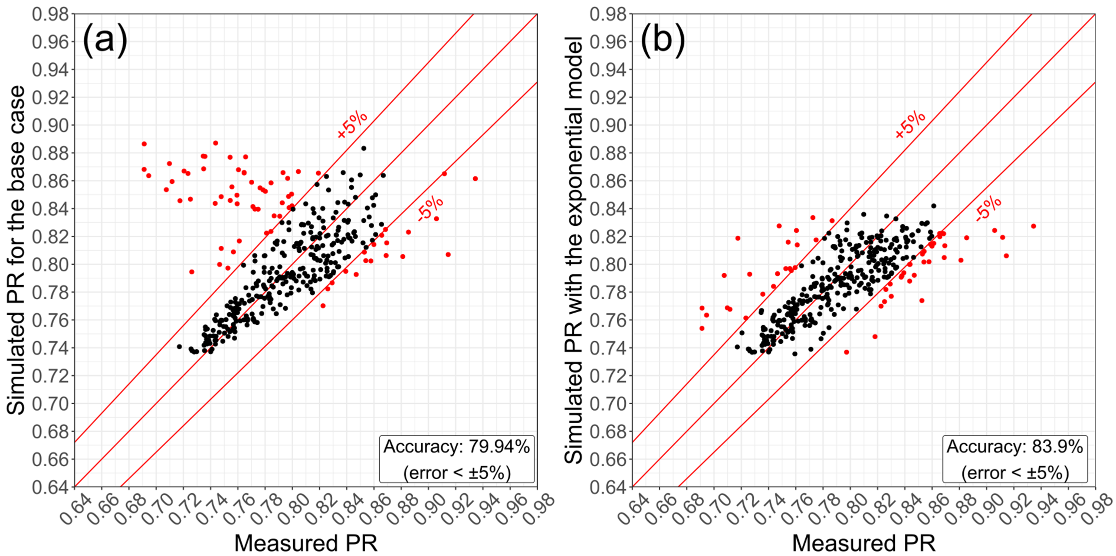

Figure 2.10: PR results validated with the base (a) and exponential (b) models

The compliance with the one-way ANOVA assumptions has been verified prior to its application. To meet the normality of the annual average PR, the inferior outliers below the limit defined by Tukey ($Q1$-1.5·IQR=0.757) were filtered applying the same method as in other PR analyses [46]. As a result, 22 facilities were omitted and the remaining PR followed a normal distribution with a mean of 0.795 and a standard deviation 0.014, as verified with the Kolmogorov-Smirnov test with a p-value of 0.239.

The normality of each PR distribution was tested with the Kolmogorov-Smirnov test for the Siliken, Scheuten and Yingli modules, providing p-values of 0.724, 0.516 and 0.0806, respectively. All the p-values are consequently higher than the type-I error threshold (0.05). A p-value of 0.239 was obtained. However, the homoscedasticity among the three PR samples was not met applying the Barlett's test. To reduce the heterogeneity of variances, the Welch's correction factor [80] was included in the one-way ANOVA test [81], which provided a p-value of 2.7e-14. Thus, the null hypothesis was rejected, which led to develop three independent PR statistical models.

For the MLR and RF model, the predictors were selected considering the global Pearson correlation coefficients between the climatic data and the global PR of the plant (Figure 2.11) and the multicollinearity among predictors measured with the VIF. There is a low negative correlation with the measured irradiance from the two WS and a moderate correlation with T_a. This reveals that the higher PR is generally reached in cold days. The VIF values between T_a and the irradiances are below 1.6, presenting reduced multicollinearity. However, there is high multicollinearity between Y_{R1} and Y_{R2} with a VIF value of 50.25. The selected predictors are T_a, Y_{R1}, and the ratio Y_{R2}/Y_{R1} to consider weather fluctuations and have both irradiance predictors uncorrelated. This ratio presents a correlation coefficient with PR and T_a of 0.51 and -0.11, respectively.

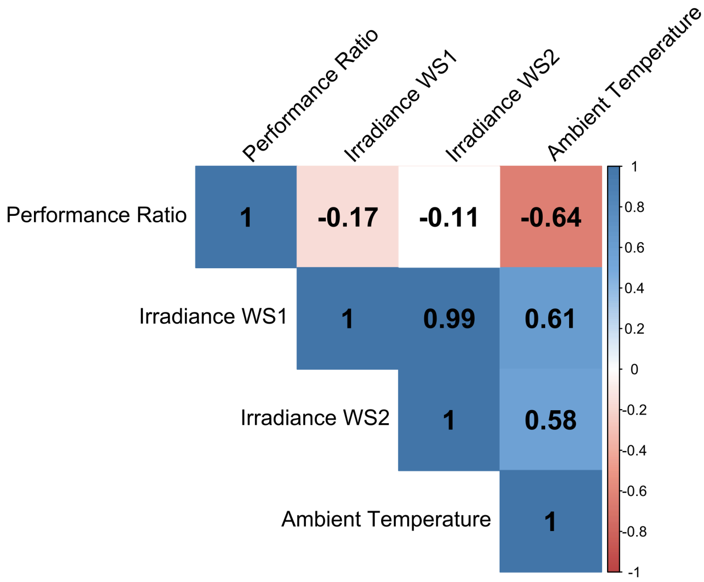

Figure 2.11: Correlation matrix of the PR and the climatic variables as predictors.

The MLR expression results from the linear combination of the variables shown in Eq. 2.10, and the fitted coefficients gathered in Table 2.11. The intercept (β_0) value is the most influential coefficient for every manufacturer, followed by the fluctuations of the measured irradiances between both WSs. The negative coefficients of β_3 explain the reduction of the PR for increasing T_a values. The regression fit provides p-values below 0.05 for all the manufacturers (see Table 2.11). This supports the null hypothesis that the independent variables do not affect significantly the dependent variable.

Another conclusion is that including nonlinear combinations of the predictors have any power in explaining the PR, as verified with the Ramsey's RESET test (p-value of 0.5671). The residuals of each regression fit follow a normal distribution according to the Kolmorov-Smirnov test with an averaged p-value of 0.0998. The residuals are uncorrelated, given the averaged Durbin-Watson D statistic of 1.839 (p-value of 0.198) [82].

Figure 2.12a compares the measured and the predicted PR of the three MLR models. There is a higher overprediction for lower PR values, as happened with the base PR model and this is not explained with linear relationships. The $nRMSE$ represents for the three regressions around 3%. Figure 2.12a, shows the global PR obtained by weighting the estimations of each regression with the number of sectors associated for each manufacturer, providing an accuracy of 87.85%. The accuracy represents the number of estimations with a relative error lower than

5%. The global $nRMSE$ is 0.0324, which is close to the value obtained for the Siliken sectors which are the most frequent sectors. The global $nRMSE$ improves by 41.54% and 15.29% compared with the base model and the exponential model, respectively. However, there is a trend to overestimate the lower PR values due to the linearity of the model similar to the base model.

Table 2.11: Coefficients and p-values of the MLR models to estimate the PR of the three manufacturers.

	MLR coefficients				p-values			
Manufaturer	β_0	β_1	β_2	β_3	β_0	β_1	β_2	β_3
Siliken	0.403	0.003	0.435	-0.004	<2e-16	1.00e-04	<2e-16	<2e-16
Scheuten	0.687	0.008	0.111	-0.005	<2e-16	2e-14	<2e-16	1.00e-04
Yingli	0.933	0.004	-0.114	-0.004	<2e-16	3.00e-07	<2e-16	8.00e-06

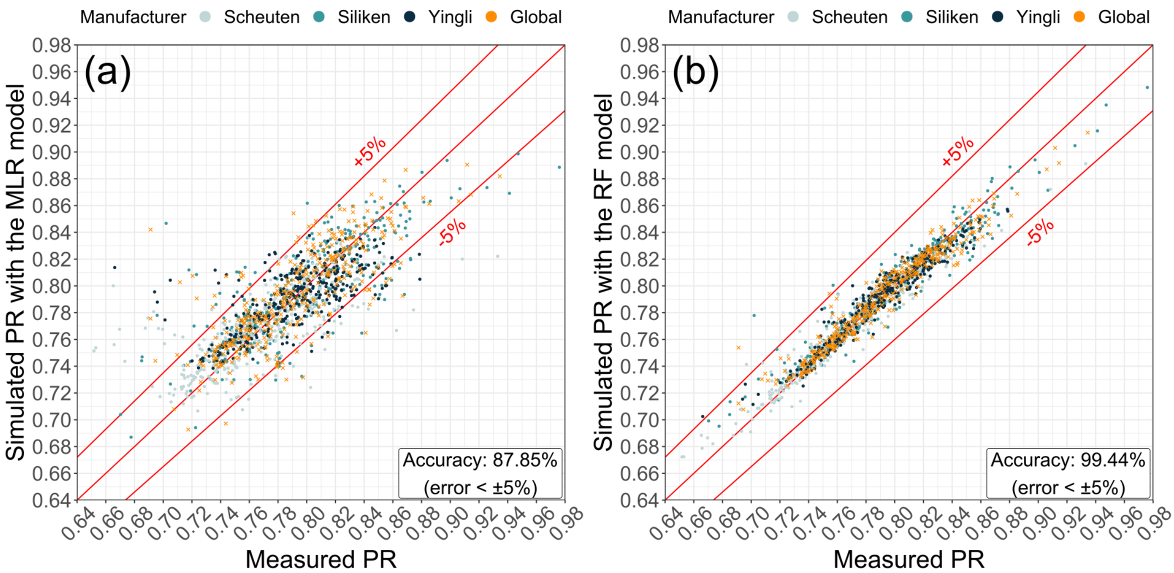

Figure 2.12: Validation of the PR results obtained with the MLR (a) and RF (b) models compared with the measured PR.

For the RF regression models, the hyperparameters were first tuned to provide the lower $RMSE$. The Siliken sectors do not require more than 50 trees, and the other manufacturers require up to 100 trees to provide stability in $RMSE$. The $nRMSE$ was below 3%. This is a major improvement compared to the MLR, as shown in Figure 2.12b, where the number of outliers has been reduced, especially for low PR values. The greater deviations are found in the extreme PR values. Nevertheless, the global accuracy rises up to 99.44%. Weighting all the sectors the global PR yields a $nRMSE$ of 0.013, shown in Table 2.13. This represents a reduction of 77.04% with respect to the base model and is similar or lower than the SVR model found in literature [30].

The manufacturer's error metrics of both MLR and RF models are shown in Table 2.12.

Table 2.12: Error metrics of the PR for the MLR and RF models.

	MLR model				RF model			
Manufacturer	$RMSE$	$nRMSE$	MAE	R^2	$RMSE$	$nRMSE$	MAE	R^2
Siliken	0.026	0.033	0.019	0.689	0.024	0.030	0.017	0.741
Scheuten	0.028	0.037	0.020	0.547	0.023	0.029	0.016	0.701
Yingli	0.025	0.031	0.018	0.497	0.019	0.024	0.014	0.683

2.4.3 PV production modelling results

The global E_{AC} of the PV power plant has been obtained for the base case, with the theoretical PR values, and compared with the production obtained with the three PR models (the exponential fit, the MLR and the RF model).

All the energy losses estimated in the energy balance are quantified in Figure 2.13 by means of a Sankey diagram. The annual in-plane global irradiance does not consider the non-productive days since they have been filtered. LIL represent 0.78% of the annual array nominal energy at STC and the degradation losses have the biggest weight due to the long operating time of the utility-scale. The estimated annual E_{AC} with the physical model differs by -0.71% compared with the measurements. The annual production would rise 2.61% (up to $93.03\,\mathrm{GW\,h}$) if the 10 non-productive days were considered.

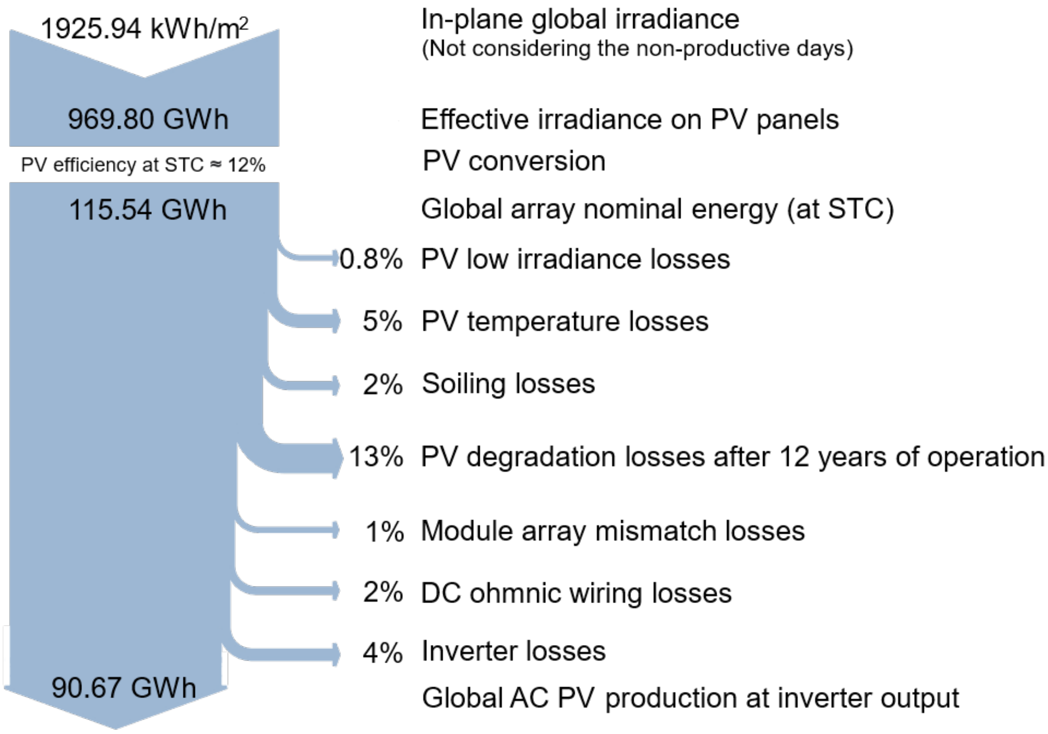

Figure 2.13: Sankey diagram of the annual losses in the PV utility-scale according to the PR physical model.

The validation results for each model are shown in Figure 2.14. The base model systematically overpredicts the production when the daily irradiance is low; however, the three PR models significantly reduce the number of outliers for low daily irradiances. Compared with the base case, the total $RMSE$ is reduced up to 68.24% with the RF, while the exponential and the MLR models provide moderate improvements in $RMSE$ of 4.16% and 23.79%, respectively. The relative error of the estimated annual production was reduced up to 0.09% with the RF model. Filtering only the days of the year in which the Y_R is below 3 h/d, an improvement in the annual production error of close to 7% is observed for the three previous models, and the RF provides the best results. Table 2.13 provides the general error metrics in the estimation of the production.

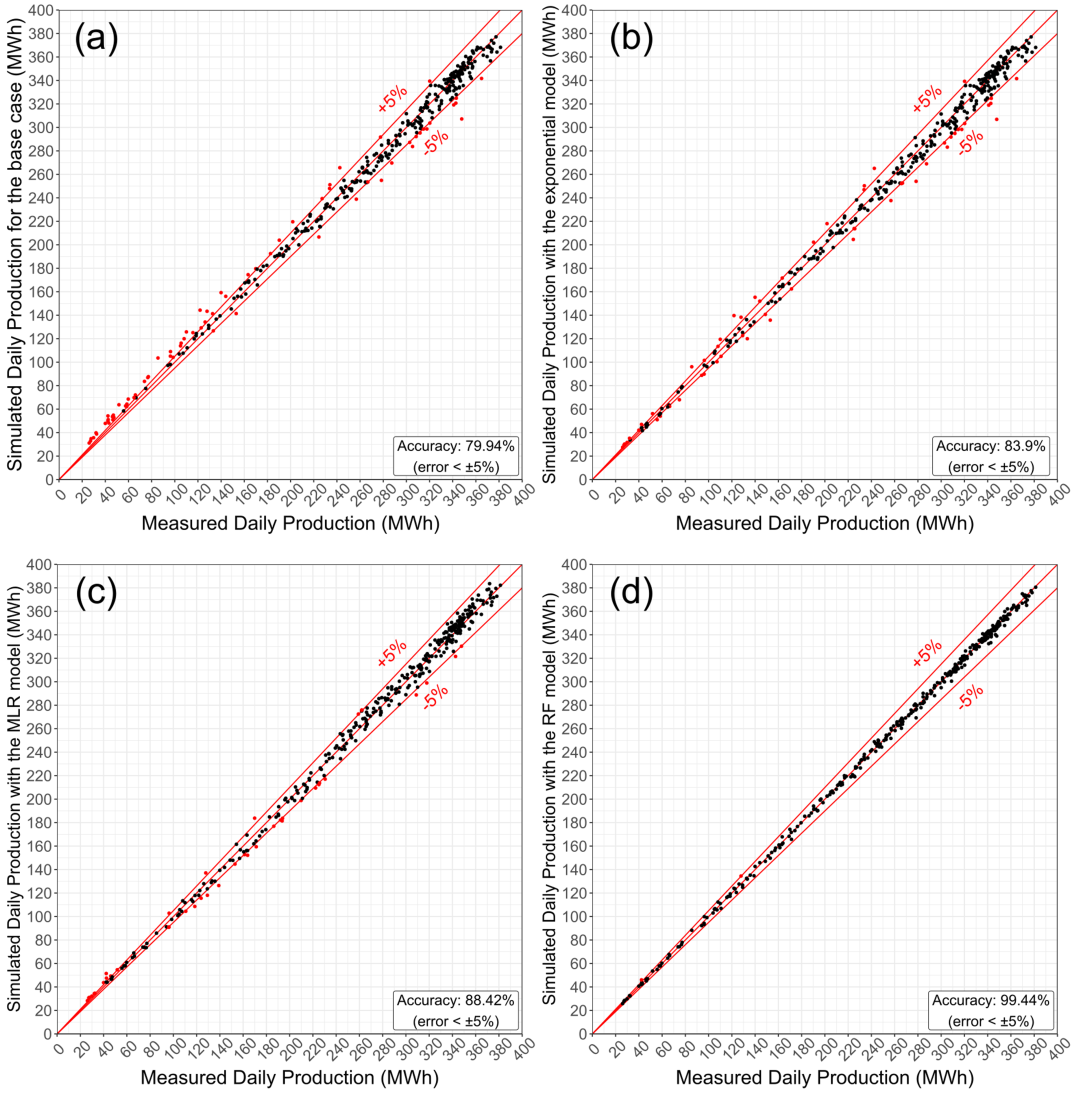

Figure 2.14: Validation of the global PV production obtained considering the PR for the base (a), exponential (b), MLR (c) and RF (d) models.

Table 2.13: General error metrics of the PR and E_{AC} models.

	$\boldsymbol{PR}$				$\boldsymbol{E_{AC}}$					
Model	$RMSE$ (-)	$nRMSE$ (-)	MAE (-)	R^2 (-)	$RMSE$ (MWh)	$nRMSE$ (-)	MAE (MWh)	R^2 (-)	Annual error (%)	Annual error (Y_R<3 h/d) (%)
Base case	0.044	0.055	0.028	0.144	8.268	0.032	6.334	0.993	1.814	7.280
Exponential 1	0.034	0.043	0.023	0.432	7.973	0.031	5.968	0.993	-1.141	-1.006
Exponential 2	0.029	0.037	0.021	0.517	7.924	0.031	5.870	0.994	-0.706	-0.474
MLR	0.026	0.032	0.018	0.617	6.301	0.024	4.978	0.996	-0.116	-0.787
RF	0.010	0.013	0.007	0.945	2.626	0.010	1.973	0.999	0.099	2,00E-04

Figure 2.15 represents the performance of each model, by means of the $nRMSE$ of the daily E_{AC}. The $nRMSE$ is clearly bigger in low irradiance days. Daily irradiation measurements lower than 2 kWh present a $nRMSE$ of 13.14%, which is significantly higher than the $nRMSE$ of 3.21% which is obtained for the full irradiance range. By incorporating the PR the LIL factor, the nRSME is reduced in the full range up to 5.87%. This value drops to 2.44% with the MLR model and 1.01% with the RF model. These three models reduce the $nRMSE$ for low irradiances by more than half compared with the base model. Nevertheless, the RF model provides the lowest fluctuations and confident production predictions for the complete range of daily irradiances.

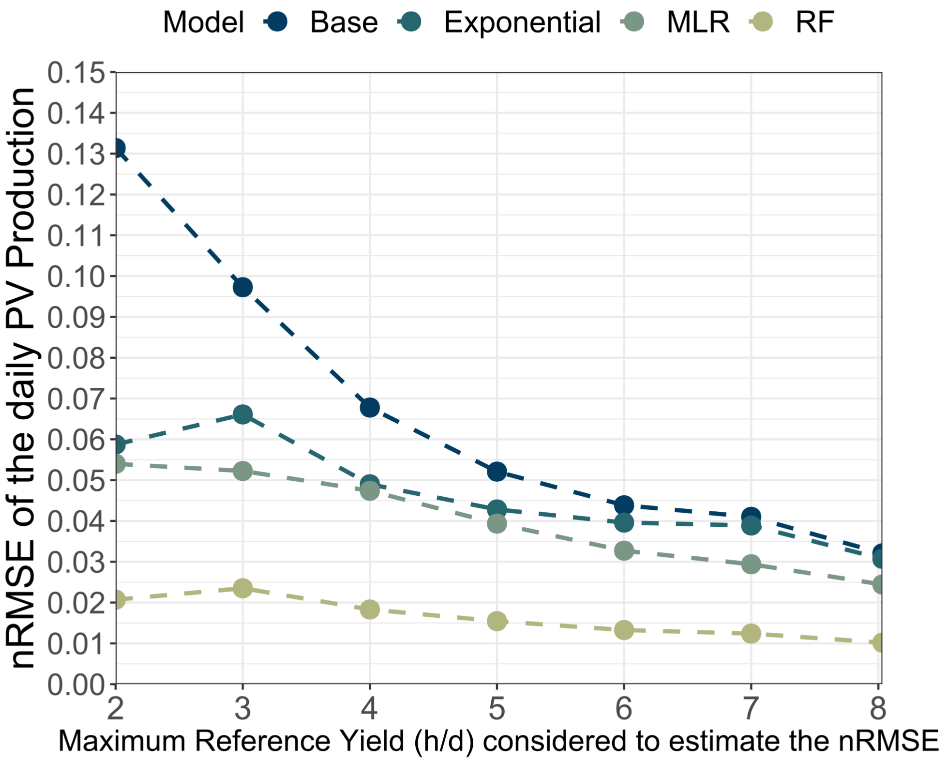

Figure 2.15: $nRMSE$ of the estimated daily production of the PV plant for days with irradiances equal or lower than the irradiance shown on the x-axis.

2.5 Conclusions

The present work involves the analysis of a 50 MW PV utility-scale plant in Olmedilla de Alarcón (Spain) after 12 years of operation under Mediterranean climatic conditions. The experimental campaign consists of a monitoring period of one year with measurements of climatic data and E_{AC} from the inverters. Using this data, the main PV performance parameters have been obtained.

The annual average and the minimum and maximum monthly average registered for the Y_R, Y_F, PR and CUF respectively are: 5.44 h/d, 4.28 h/d, 79.24%, and 19.77%. These results provided a clear seasonality, with lower system efficiencies during the summer due to the high temperatures. The performance is slightly lower than other PV power plants in the Mediterranean, although with more years of operation. Nevertheless, the PR is over 80% for almost 42% of the measured days, proving a correct performance. Furthermore, the pc-Si sectors provided PR values around 2% greater than the mc-Si sectors, mainly due to the higher PV temperature and degradation losses of the mc-Si sectors. The estimated degradation losses of the modules are approximately 2-3% higher than according to the manufacturer data. The degradation losses yield the greatest weight in the energy balance, representing a global energy loss of 13% of the global energy at STC.

After the performance analysis, a more in-depth study has been performed to reduce the outliers in the predictions in low irradiance days. A physical model was developed, as the product of the different losses of the PV system, including the LIL through irradiance measurements and an exponential fit. The results improved the $nRMSE$ by 1.9% compared with the conventional model, increasing the R^2 from 0.144 to 0.553 for low irradiances.

A second approach has been applied using two statistical methods using only Ta and YR as predictors. The RF model has provided the best performance with a $nRMSE$ of 1.27%. These results indicate a better performance than SVR models found in literature, which require significantly more predictors. In contrast, the MLR model has reduced the $nRMSE$ by 2.30% with an accuracy of 87.85%.

The inclusion of the improvements in the PR and in the PV daily production model has provided improvements in $nRMSE$ of 0.11%, 0.76%, and 2.19% for the exponential, MLR, and the RF models, respectively. These improvements are significantly greater for the low irradiance days, providing reductions in the $nRMSE$ up to 7.27%, 7.75% and 11.07% for the exponential, MLR and RF models, respectively. In any case, both statistical models provided a better PR accuracy than the physical model, and are recommended to forecast the PR whenever measured data is available. Moreover, they constitute an alternative to model and predict the PR when there is scarce technical data of the plant.

As future work, the degradation of the PV modules will be studied in more detail by analyzing the performance after more years of operation.

2.6 Acknowledgements

The authors gratefully acknowledge the operation & maintenance staff of the PV Power Plant in Olmedilla de Alarcón for providing the measured data of the solar PV power plant.

2.7 References

[1] Feldman, D., Ramasamy, V., Fu, R., Ramdas, A., Desai, J., and Margolis, R. *U.S. Solar Photovoltaic System and Energy Storage Cost Benchmark: Q1 2020*. Tech. rep. National Renewable Energy Laboratory, 2021.

[2] Mitrašinović, A. M. "Photovoltaics advancements for transition from renewable to clean energy". In: *Energy* 237 (2021), p. 121510. doi: 10.1016/J.ENERGY.2021.121510.

[3] IRENA. *Renewable Capacity Statistics 2021*. Tech. rep. 2021, pp. 1–300.

[4] Sundaram, S. and Babu, J. S. C. "Performance evaluation and validation of 5 MWp grid connected solar photovoltaic plant in South India". In: *Energy Conversion and Management* 100 (2015), pp. 429–439. doi: 10.1016/J.ENCONMAN.2015.04.069.

[5] Bansal, N., Jaiswal, S. P., and Singh, G. "Long term performance assessment and loss analysis of 9 MW grid tied PV plant in India". In: *Materials Today: Proceedings* (2022). doi: 10.1016/J.MATPR.2022.01.263.

[6] Oloya, I. T., Gutu, T. J., and Adaramola, M. S. "Techno-economic assessment of 10 MW centralised grid-tied solar photovoltaic system in Uganda". In: *Case Studies in Thermal Engineering* 25 (2021), p. 100928. doi: 10.1016/J.CSITE.2021.100928.

[7] AL-Rasheedi, M., Gueymard, C. A., Al-Khayat, M., Ismail, A., Lee, J. A., and Al-Duaj, H. "Performance evaluation of a utility-scale dual-technology photovoltaic power plant at the Shagaya Renewable Energy Park in Kuwait". In: *Renewable and Sustainable Energy Reviews* 133 (2020), p. 110139. doi: 10.1016/J.RSER.2020.110139.

[8] Elhadj Sidi, C. E. B., Ndiaye, M. L., El Bah, M., Mbodji, A., Ndiaye, A., and Ndiaye, P. A. "Performance analysis of the first large-scale (15 MWp) grid-connected photovoltaic plant in Mauritania". In: *Energy Conversion and Management* 119 (2016), pp. 411–421. doi: 10.1016/J.ENCONMAN.2016.04.070.

[9] Bentouba, S., Bourouis, M., Zioui, N., Pirashanthan, A., and Velauthapillai, D. "Performance assessment of a 20 MW photovoltaic power plant in a hot climate using real data and simulation tools". In: *Energy Reports* 7 (2021), pp. 7297–7314. doi: 10.1016/J.EGYR.2021.10.082.

[10] Dahmoun, M. E. H., Bekkouche, B., Sudhakar, K., Guezgouz, M., Chenafi, A., and Chaouch, A. "Performance evaluation and analysis of grid-tied large scale PV plant in Algeria". In: *Energy for Sustainable Development* 61 (2021), pp. 181–195. doi: 10.1016/J.ESD.2021.02.004.

[11] Malvoni, M., Leggieri, A., Maggiotto, G., Congedo, P. M., and De Giorgi, M. G. "Long term performance, losses and efficiency analysis of a 960 kWP photovoltaic system in the Mediterranean climate". In: *Energy Conversion and Management* 145 (2017), pp. 169–181. doi: 10.1016/J.ENCONMAN.2017.04.075.

[12] Copper, J. K., Sproul, A. B., and Jarnason, S. "Photovoltaic (PV) performance modelling in the absence of onsite measured plane of array irradiance (POA) and module temperature". In: *Renewable Energy* 86 (2016), pp. 760–769. doi: 10.1016/J.RENENE.2015.09.005.

[13] IDAE. *Pliego de Condiciones Técnicas de Instalaciones Conectadas a Red.* Madrid, 2011.

[14] F. Holmgren, W., W. Hansen, C., and A. Mikofski, M. "pvlib python: a python package for modeling solar energy systems". In: *Journal of Open Source Software* 3.29 (2018), p. 884. DOI: 10.21105/JOSS.00884.

[15] Kymakis, E., Kalykakis, S., and Papazoglou, T. M. "Performance analysis of a grid connected photovoltaic park on the island of Crete". In: *Energy Conversion and Management* 50.3 (2009), pp. 433–438. DOI: 10.1016/J.ENCONMAN.2008.12.009.

[16] Gilman, P., Dobos, A., Diorio, N., Freeman, J., Janzou, S., and Ryberg, D. *SAM Photovoltaic Model Technical Reference Update.* Tech. rep. National Renewable Energy Agency, 2016. DOI: NREL/TP-6A20-67399.

[17] Ozden, T. "A countrywide analysis of 27 solar power plants installed at different climates". In: *Scientific Reports 2022 12:1* 12.1 (2022), pp. 1–11. DOI: 10.1038/s41598-021-04551-7.

[18] Khalid, A. M., Mitra, I., Warmuth, W., and Schacht, V. "Performance ratio – Crucial parameter for grid connected PV plants". In: *Renewable and Sustainable Energy Reviews* 65 (2016), pp. 1139–1158. DOI: 10.1016/J.RSER.2016.07.066.

[19] Quesada, B., Sánchez, C., Cañada, J., Royo, R., and Payá, J. "Experimental results and simulation with TRNSYS of a 7.2kWp grid-connected photovoltaic system". In: *Applied Energy* 88.5 (2011), pp. 1772–1783. DOI: 10.1016/j.apenergy.2010.12.011.

[20] Mavromatakis, F., Vignola, F., and Marion, B. "Low irradiance losses of photovoltaic modules". In: *Solar Energy* 157 (2017), pp. 496–506. DOI: 10.1016/J.SOLENER.2017.08.062.

[21] Soler-Castillo, Y., Rimada, J. C., Hernández, L., and Martínez-Criado, G. "Modelling of the efficiency of the photovoltaic modules: Grid-connected plants to the Cuban national electrical system". In: *Solar Energy* 223 (2021), pp. 150–157. DOI: 10.1016/J.SOLENER.2021.05.052.

[22] Lindig, S., Louwen, A., Moser, D., and Topic, M. "Outdoor PV System Monitoring—Input Data Quality, Data Imputation and Filtering Approaches". In: *Energies 2020, Vol. 13, Page 5099* 13.19 (2020), p. 5099. DOI: 10.3390/EN13195099.

[23] Huld, T., Gottschalg, R., Beyer, H. G., and Topič, M. "Mapping the performance of PV modules, effects of module type and data averaging". In: *Solar Energy* 84.2 (2010), pp. 324–338. DOI: 10.1016/J.SOLENER.2009.12.002.

[24] Parra, I. de la, Muñoz, M., Lorenzo, E., García, M., Marcos, J., and Martínez-Moreno, F. "PV performance modelling: A review in the light of quality assurance for large PV plants". In: *Renewable and Sustainable Energy Reviews* 78 (2017), pp. 780–797. DOI: 10.1016/J.RSER.2017.04.080.

[25] Roumpakias, E. and Stamatelos, A. "Comparative performance analysis of grid-connected photovoltaic system by use of existing performance models". In: *Energy Conversion and Management* 150 (2017), pp. 14–25. DOI: 10.1016/J.ENCONMAN.2017.08.001.

[26] Busch, L., Schäfer, T., Song, W., Mack, M., and Egler, M. "PV System Energy Yield Calculation Program PR-FACT". In: *28th European Photovoltaic Solar Energy Conference and Exhibition* (2013), pp. 3699–3708. DOI: 10.4229/28THEUPVSEC2013-5CO.6.3.

[27] Parretta, A., Sarno, A., and Vicari, L. R. "Effects of solar irradiation conditions on the outdoor performance of photovoltaic modules". In: *Optics Communications* 153.1-3 (1998), pp. 153–163. DOI: 10.1016/S0030-4018(98)00192-8.

[28] Trigo-Gonzalez, M., Cortés, M., Alonso-Montesinos, J., Martínez-Durbán, M., Ferrada, P., Rabanal, J., Portillo, C., López, G., and Batlles, F. J. "Development and comparison of PV production estimation models for mc-Si technologies in Chile and Spain". In: *Journal of Cleaner Production* 281 (2021), p. 125360. DOI: 10.1016/J.JCLEPRO.2020.125360.

[29] Tossa, A. K., Soro, Y. M., Coulibaly, Y., Azoumah, Y., Migan-Dubois, A., Thiaw, L., and Lishou, C. "Artificial intelligence technique for estimating PV modules performance ratio under outdoor operating conditions". In: *Journal of Renewable and Sustainable Energy* 10.5 (2018), p. 053505. DOI: 10.1063/1.5042217.

[30] Bandong, S., Leksono, E., Purwarianti, A., and Joelianto, E. "Performance Ratio Estimation and Prediction of Solar Power Plants Using Machine Learning to Improve Energy Reliability". In: *Proceedings of the 2019 6th International Conference on Instrumentation, Control, and Automation, ICA 2019* (2019), pp. 36–41. DOI: 10.1109/ICA.2019.8916687.

[31] Hashemi, B., Taheri, S., Cretu, A. M., and Pouresmaeil, E. "Systematic photovoltaic system power losses calculation and modeling using computational intelligence techniques". In: *Applied Energy* 284 (2021). DOI: 10.1016/J.APENERGY.2020.116396.

[32] Ahmad, M. W., Mourshed, M., and Rezgui, Y. "Tree-based ensemble methods for predicting PV power generation and their comparison with support vector regression". In: *Energy* 164 (2018), pp. 465–474. DOI: 10.1016/J.ENERGY.2018.08.207.

[33] Kunaifi, K., Reinders, A., Lindig, S., Jaeger, M., and Moser, D. "Operational Performance and Degradation of PV Systems Consisting of Six Technologies in Three Climates". In: *Applied Sciences 2020, Vol. 10, Page 5412* 10.16 (2020), p. 5412. DOI: 10.3390/APP10165412.

[34] International Electrotechnical Committee. *IEC 61724 Photovoltaic System Performance Monitoring - Guidelines for Measurement, Data Exchange and Analysis*. 1998.

[35] Dhimish, M. "Thermal impact on the performance ratio of photovoltaic systems: A case study of 8000 photovoltaic installations". In: *Case Studies in Thermal Engineering* 21 (2020), p. 100693. DOI: 10.1016/J.CSITE.2020.100693.

[36] Ransome, S. and Funtan, P. "Why hourly averaged measurement data is insufficient to model PV system performance accurately". In: *20th European Photovoltaic Solar Energy Conference*. Barcelona, Spain, 2005, pp. 2752–2755.

[37] Cubukcu, M. and Gumus, H. "Performance analysis of a grid-connected photovoltaic plant in eastern Turkey". In: *Sustainable Energy Technologies and Assessments* 39 (2020), p. 100724. DOI: 10.1016/J.SETA.2020.100724.

[38] Santiago, I., Trillo-Montero, D., Moreno-Garcia, I. M., Pallarés-López, V., and Luna-Rodríguez, J. J. "Modeling of photovoltaic cell temperature losses: A review and a practice case in South Spain". In: *Renewable and Sustainable Energy Reviews* 90 (2018), pp. 70–89. DOI: 10.1016/J.RSER.2018.03.054.

[39] Roberts, J. J., Mendiburu Zevallos, A. A., and Cassula, A. M. "Assessment of photovoltaic performance models for system simulation". In: *Renewable and Sustainable Energy Reviews* 72 (2017), pp. 1104–1123. DOI: 10.1016/J.RSER.2016.10.022.

[40] Pérez, N. S., Alonso-Montesinos, J., and Batlles, F. J. "Estimation of Soiling Losses from an Experimental Photovoltaic Plant Using Artificial Intelligence Techniques". In: *Applied Sciences 2021, Vol. 11, Page 1516* 11.4 (2021), p. 1516. DOI: 10.3390/APP11041516.

[41] Polo, J., Martín-Chivelet, N., Alonso, M., Sanz, C., Batlles, F. J., López, G., Zitouni, H., Alonso-Montesinos, J., Vela, N., Bosch, J. L., and Barbero, J. "Characterization of PV Soiling Losses in Urban Mediterranean Environment". In: (2019). DOI: 10.18086/swc.2019.15.03.

[42] Kim, J., Rabelo, M., Padi, S. P., Yousuf, H., Cho, E. C., and Yi, J. "A Review of the Degradation of Photovoltaic Modules for Life Expectancy". In: *Energies 2021, Vol. 14, Page 4278* 14.14 (2021), p. 4278. DOI: 10.3390/EN14144278.

[43] Shiva Kumar, B. and Sudhakar, K. "Performance evaluation of 10 MW grid connected solar photovoltaic power plant in India". In: *Energy Reports* 1 (2015), pp. 184–192. DOI: 10.1016/J.EGYR.2015.10.001.

[44] Marion, B., Adelstein, J., Boyle, K., Hayden, H., Hammond, B., Fletcher, Canada, B., Narang, D., Kimber, A., Mitchell, L., Rich, G., and Townsend, T. "Performance parameters for grid-connected PV systems". In: *Conference Record of the IEEE Photovoltaic Specialists Conference* (2005), pp. 1601–1606. DOI: 10.1109/PVSC.2005.1488451.

[45] Malvoni, M., Kumar, N. M., Chopra, S. S., and Hatziargyriou, N. "Performance and degradation assessment of large-scale grid-connected solar photovoltaic power plant in tropical semi-arid environment of India". In: *Solar Energy* 203 (2020), pp. 101–113. DOI: 10.1016/J.SOLENER.2020.04.011.

[46] Taylor, J., Leloux, J., Hall, L. M. H., Everard, A. M., Briggs, J., and Buckley, A. "Performance of Distributed PV in the UK: A Statistical Analysis of Over 7000 Systems". In: *Conference: 31st European Photovoltaic Solar Energy Conference and Exhibition* (2015). DOI: 10.13140/RG.2.1.2019.6568.

[47] Seltman, H. J. *Experimental Design and Analysis.* Carnegie Mellon University 2012, 2018.

[48] Vergura, S. "A Statistical Tool to Detect and Locate Abnormal Operating Conditions in Photovoltaic Systems". In: *Sustainability 2018, Vol. 10, Page 608* 10.3 (2018), p. 608. DOI: 10.3390/SU10030608.

[49] Kabacoff, R. I. *R in Action SECOND EDITION Data analysis and graphics with R.* MANNING PUBLICATIONS, 2015, p. 474.

[50] Flatt, C. and Jacobs, R. L. "Principle Assumptions of Regression Analysis: Testing, Techniques, and Statistical Reporting of Imperfect Data Sets:" in: *https://doi.org/10.1177/1523422319869915* 21.4 (2019), pp. 484–502. DOI: 10.1177/1523422319869915.

[51] Fávero, L. P. and Belfiore, P. "Simple and Multiple Regression Models". In: *Data Science for Business and Decision Making* (2019), pp. 443–538. DOI: 10.1016/B978-0-12-811216-8.00013-6.

[52] Breiman, L. "Random Forests". In: *Machine Learning 2001 45:1* 45.1 (2001), pp. 5–32. DOI: 10.1023/A:1010933404324.

[53] Kuhn, M. "Building Predictive Models in R Using the caret Package". In: *Journal of Statistical Software* 28.5 (2008), pp. 1–26. DOI: 10.18637/JSS.V028.I05.

[54] Probst, P., Wright, M. N., and Boulesteix, A. L. "Hyperparameters and tuning strategies for random forest". In: *Wiley Interdisciplinary Reviews: Data Mining and Knowledge Discovery* 9.3 (2019), e1301. DOI: 10.1002/WIDM.1301.

[55] Belgiu, M. and Drăgu, L. "Random forest in remote sensing: A review of applications and future directions". In: *ISPRS Journal of Photogrammetry and Remote Sensing* 114 (2016), pp. 24–31. DOI: 10.1016/J.ISPRSJPRS.2016.01.011.

[56] Assouline, D., Mohajeri, N., and Scartezzini, J. L. "Large-scale rooftop solar photovoltaic technical potential estimation using Random Forests". In: *Applied Energy* 217 (2018), pp. 189–211. DOI: 10.1016/J.APENERGY.2018.02.118.

[57] Mathai, N., Chen, Y., and Kirchmair, J. "Validation strategies for target prediction methods". In: *Briefings in Bioinformatics* 21.3 (2020), pp. 791–802. DOI: 10.1093/BIB/BBZ026.

[58] Kuhn, M. and Johnson, K. "Applied predictive modeling". In: *Applied Predictive Modeling* (2013), pp. 1–600. DOI: 10.1007/978-1-4614-6849-3.

[59] Bounoua, Z., Ouazzani Chahidi, L., and Mechaqrane, A. "Estimation of daily global solar radiation using empirical and machine-learning methods: A case study of five Moroccan locations". In: *Sustainable Materials and Technologies* 28 (2021), e00261. DOI: 10.1016/J.SUSMAT.2021.E00261.

[60] Guenounou, A., Malek, A., and Aillerie, M. "Comparative performance of PV panels of different technologies over one year of exposure: Application to a coastal Mediterranean region of Algeria". In: *Energy Conversion and Management* 114 (2016), pp. 356–363. DOI: 10.1016/J.ENCONMAN.2016.02.044.

[61] Elamim, A., Hartiti, B., Haibaoui, A., Lfakir, A., and Thevenin, P. "Analysis and comparison of different PV technologies for determining the optimal PV panels- A case study in Mohammedia , Morocco." In: *IOSR Journal of Electrical and Electronics Engineering* 12.01 (2017), pp. 37–45. DOI: 10.9790/1676-1201013745.

[62] Alshare, A., Tashtoush, B., Altarazi, S., and El-Khalil, H. "Energy and economic analysis of a 5MW photovoltaic system in northern Jordan". In: *Case Studies in Thermal Engineering* 21 (2020), p. 100722. DOI: 10.1016/J.CSITE.2020.100722.

[63] Martín-Martínez, S., Cañas-Carretón, M., Honrubia-Escribano, A., and Gómez-Lázaro, E. “Performance evaluation of large solar photovoltaic power plants in Spain”. In: *Energy Conversion and Management* 183 (2019), pp. 515–528. DOI: 10.1016/J.ENCONMAN.2018.12.116.

[64] Eke, R. and Demircan, H. “Performance analysis of a multi crystalline Si photovoltaic module under Mugla climatic conditions in Turkey”. In: *Energy Conversion and Management* 65 (2013), pp. 580–586. DOI: 10.1016/J.ENCONMAN.2012.09.007.

[65] Murat Ates, A. and Singh, H. “Rooftop solar Photovoltaic (PV) plant – One year measured performance and simulations”. In: *Journal of King Saud University - Science* 33.3 (2021), p. 101361. DOI: 10.1016/J.JKSUS.2021.101361.

[66] Bouacha, S., Malek, A., Benkraouda, O., Arab, A. H., Razagui, A., Boulahchiche, S., and Semaoui, S. “Performance analysis of the first photovoltaic grid-connected system in Algeria”. In: *Energy for Sustainable Development* 57 (2020), pp. 1–11. DOI: 10.1016/J.ESD.2020.04.002.

[67] Attari, K., Elyaakoubi, A., and Asselman, A. “Performance analysis and investigation of a grid-connected photovoltaic installation in Morocco”. In: *Energy Reports* 2 (2016), pp. 261–266. DOI: 10.1016/J.EGYR.2016.10.004.

[68] Savvakis, N. and Tsoutsos, T. “Performance assessment of a thin film photovoltaic system under actual Mediterranean climate conditions in the island of Crete”. In: *Energy* 90 (2015), pp. 1435–1455. DOI: 10.1016/J.ENERGY.2015.06.098.

[69] Herbazi, R., Amechnoue, K., Khouya, A., Chahboun, A., Diani, M., Louzazni, M., and Addou, M. “Performance evaluation and analysis of polycrystalline photovoltaic plant located in Northern Morocco”. In: *International Journal of Ambient Energy* 43.1 (2019), pp. 1262–1268. DOI: 10.1080/01430750.2019.1694985.

[70] Merrouni, A. A., Amrani, A. I., and Mezrhab, A. “Electricity production from large scale PV plants: Benchmarking the potential of Morocco against California, US”. In: *Energy Procedia* 119 (2017), pp. 346–355. DOI: 10.1016/J.EGYPRO.2017.07.118.

[71] Government of Spain. Ministry of Industry Tourism and Trade. *Royal Decree 661/2007.* 2007.

[72] Government of Spain. Ministry of Industry Tourism and Trade. *Royal Decree 413/2014.* 2014.

[73] Blanco-Díez, P., Díez-Mediavilla, M., and Alonso-Tristán, C. “Review of the Legislative Framework for the Remuneration of Photovoltaic Production in Spain: A Case Study”. In: *Sustainability 2020, Vol. 12, Page 1214* 12.3 (2020), p. 1214. DOI: 10.3390/SU12031214.

[74] Bansal, N., Pany, P., and Singh, G. “Visual degradation and performance evaluation of utility scale solar photovoltaic power plant in hot and dry climate in western India”. In: *Case Studies in Thermal Engineering* 26 (2021), p. 101010. DOI: 10.1016/J.CSITE.2021.101010.

[75] Comisión Nacional de los Mercados y la Competencia (CNMC). *Estadísticas. Precios del Mercado de Producción de Energía Eléctrica.*

[76] Comisión Nacional de los Mercados y la Competencia (CNMC). *EVALUACIÓN DEL RÉGIMEN RETRIBUTIVO ESPECÍFICO CORRESPONDIENTE AL PERIODO 2014-2020 Expediente núm. INF/DE/037/21.* Tech. rep. 2021.

[77] Walker, A., Lockhart, E., Desai, J., Ardani, K., Klise, G., Lavrova, O., Tansy, T., Deot, J., Fox, B., and Pochiraju, A. "Model of Operation-and-Maintenance Costs for Photovoltaic Systems". In: (2020).

[78] Inflation.eu. *Historic inflation Spain – historic CPI inflation Spain.*

[79] Ministry for the Ecological Transition and the Demographic challenge. *Orden TED/171/2020.* Madrid, 2021.

[80] Wilcox, R. R. "ONE-WAY ANOVA". In: *Applying Contemporary Statistical Techniques* (2003), pp. 285–328. DOI: 10.1016/B978-012751541-0/50030-4.

[81] Liu, H. "Comparing Welch's ANOVA, a Kruskal-Wallis test and traditional ANOVA in case of Heterogeneity of Variance". In: *Theses and Dissertations* (2015). DOI: https://doi.org/10.25772/BWFP-YE95.

[82] Schreiber-Gregory, D. N., Jackson, H. M., and Bader, K. "Logistic and Linear Regression Assumptions : Violation Recognition and Control". In: (2018).

Chapter 3

Innovative regression-based methodology to assess the techno-economic performance of photovoltaic installations in urban areas

Chapter adapted from the paper:

Enrique Fuster-Palop[a], Carlos Prades-Gil[b], Ximo Masip[b], J. D. Viana-Fons[a], and Jorge Payá[a]. *Innovative regression-based methodology to assess the techno-economic performance of photovoltaic installations in urban areas.* In: *Renewable and Sustainable Energy Reviews* (2021), Vol. 149, p. 111357. DOI: https://doi.org/10.1016/J.RSER.2021.111357.

[a] Instituto Universitario de Investigación en Ingeniería Energética, Universitat Politècnica de València, Camino de Vera s/n, Edificio 8E semisótano frente acceso J, Valencia, 46022, Spain.

[b] IMPACT-E, C/ Joan Verdeguer n○16, Valencia, 46024, Spain.

Abstract:

Households present a significant contribution in the national energy consumption, and photovoltaics (PV) has become an economically feasible technology that can play an important role to lower this consumption and the associated emissions. Nevertheless, there is still a gap between too in-depth technical models for detailed studies and what urban energy planners need, which are simpler, yet reliable techno-economical tools to select which roofs of city buildings are the best candidates for PV production. In order to face this gap, a multiple linear regression (MLR) model has been developed to determine the economic payback using dimensionless parameters. The methodology has been adopted in the city of Valencia (Spain) for a large sample of multi-storey buildings, which are the most common typology. The approach has a high replicability since it can be applied for different countries. The MLR model provides a payback root mean squared error (RMSE) of 0.48 years in comparison with a complex techno-economic model which was previously developed and validated with the software System Advisor Model (SAM). The variables which have a bigger weight in the payback are the shadow losses and the power unit cost due to the economy of scale. With the current Spanish regulation, PV installations on multi-storey buildings can reach paybacks of around 7-15 years and the best option is to have large economies of scales together with a low energy surplus.

Keywords: Photovoltaics; Self-consumption; Techno-economical assessment; Economic potential; Simplified regression model; Multi-storey residential buildings.

Nomenclature

GIS: Geographic Information System.

LiDAR: Light Detection and Ranging Laser Imaging.

MLR: Multiple linear regression.

PV: Photovoltaic.

REE: Red Eléctrica de España.

SAM: System Advisor Model.

E_{PV}: Yearly PV production.

$E_{PV,location}$: Yearly PV production per power installed in a specific location.

$E_{PV,building,location}$: Yearly PV production per power installed in a specific location.

$E_{PV,building,Valencia}$: Yearly PV production in a specific building of Valencia.

$G_{0,location}$: Yearly global horizontal irradiation.

MAE: Mean Absolute Error.

$NOCT$: Normal Operating Cell Temperature.

P_{PV}: PV Installed Peak Power.

PR: Performance Ratio.

R^2: R squared or coefficient of determination.

$RMSE$: Root mean squared error.

S_{PV}: Yearly PV surpluses.

SF: Shading Factor.

SL: Shadow Losses.

SR: Surpluses Ratio.

SR^*: Surpluses Ratio obtained with the Building Power Ratio.

SVF: Sky View Factor.

$T_{0,location}$: Yearly mean ambient temperature.

CO_2: Carbon dioxide.

GW h: kilowatt-hour.

kg: kilogram.

km: kilometer.

MW: kilowatt.

$\mathrm{MW\,h}$: kilowatt-hour.

$\mathrm{MW_p}$: kilowatt peak.

m^2: Square meter.

$^\circ\mathrm{C}$: Degrees Celsius.

t: Ton.

$\mathrm{TW\,h}$: Terawatt-hour.

V: Volt.

$\mathrm{W_p}$: Watt of peak power.

3.1 Introduction

European (EU-28) households accounted in 2018 for 24% (3,299 TW h) of the total final energy consumption, and the electricity share was of 25% (811 TW h) [1, 2]. This share can be even bigger in some countries, such as in Spain, where 44% was reached (75 GW h) in 2018 [3], and the expectations are that the energy consumption will increase even further [4].

The PV sector is nowadays in a very favorable situation both technically and legally [5], particularly in Spain. The wide solar resource and the high PV penetration has led to a reduction of costs up to 90% during the last decade [6]. Self-consumption has also been promoted throughout the current Spanish regulation with the Royal Decree-Law 15/2018 cite [7] and the Royal Decree 244/2019 [8], hereby opening the possibility to install PV installations on rooftops of urban environments from which several consumers, such as community of neighbours, can benefit.

However, the scarce awareness of home-owners and investors on the cost-effectiveness of PV facilities has become an important barrier which hinders the implementation of PV facilities in cities [9]. Therefore, for a further penetration of PV in urban areas, a favorable framework is necessary, as well as the development of holistic energy plans. All the energy actors need information both on technical and on economic aspects [10].

In this context, there is a need for tools to analyze the PV economic potential [11] both accurately and with a low computational cost. These models could help energy planners, local administrations, companies, or investors to identify the urban rooftops where PV facilities would present reduced payback periods, and which are consequently more attractive for end users [12].

Literature on accurate PV models on a urban scale is abundant and includes the physical, geographic, as well as the technical PV potential. The most common approach of solar resource assessment in urban environments is based on top-down methods which require to filter the information from radiation timeseries, Laser Imaging Detection and Ranging (LiDAR) and raster or vectorial maps to obtain mainly the solar energy potential on tilted surfaces of rooftops [13] and facades [14]. Some well-known computational radiation models for this purpose are r.sun, ArcGIS Solar Analyst, SolarFlux and SORAM [15]. Additionally, many models has been proposed to estimate the technical PV potential [16], based on manufacturer data such as the module efficiency and the performance ratio (PR). A further level of detail has also been reached by including more complex electrical calculations which have achieved a very good agreement with measurement data [17]. As a result, several recent studies have helped to locate the most productive rooftops in cities such as Irun [18] or Vitoria [19]. Such studies are based on LiDAR and cadastral data and using Geographic Information System (GIS) software tools, which are widely used for this purpose. However they do not adddress cover the economic impact.

Literature regarding the economic feasibility of PV installations in urban areas is very scarce and most frequent models that calculate the energy and economic savings are complex. For instance, Michael J. Mangiante et al. [20] proposed a method that couples geospatial (with LiDAR data) and economic models to determine the size and location of PV facilities on residential rooftops. Ali Mohammad Shirazi et al. [21] carried out a 3D-based techno-economic analysis of the PV potential, and optimized the payback period with the tilt angle of panels for facades and roofs. Commercial software, such as PVsyst [22], TRNSYS [17] or SAM [23], has also been employed to simulate specific PV facilities. Nevertheless, the computational cost would be unassumable if the latter simulation tools were employed on a urban level. Furthermore, such tools do not consider systematically the available surface on rooftops nor the potential shadows cast by the urban environment. The shadowing elements have to be introduced one by one by the user.

For energy planning applications, such as the search of optimal rooftops for PV facilities with a minimum economic payback, detailed results of the PV production are not required and they imply a high computational cost. In an effort to simplify the above-mentioned methods and their high computational demand, several studies carried out bottom-up approaches based on the statistical analysis of the different input variables. Machine learning techniques have also been commonly employed for this purpose [24]. Nevertheless, most frequent machine learning models such as random forest and neural networks add a further complexity in their interpretation and hinder their replicability [25]. In this context of urban planning, one of the simplest, yet fastest, and easy-to-replicate statistical model is a linear regression. Calcabrini et al. [26] proposed a simplified MLR model to estimate the yearly energy yield of PV facilities in urban environments based on a correlation between the radiation components and the skyline profile. The results were accurately validated with measurement data from several facilities. This work is in turn based on a study carried out by Chatzipoulka et al. [27] where the PV production was highly correlated for certain latitudes with the sky view factor (SVF) as a predictor. In contrast with the previous models that require a calculation of the sky view factor, K. H. Poon et al. [28] suggested a MLR model to predict the irradiation on rooftop and facades based on predictors such as the height of the building, the slenderness and the plot ratio. Trigo-Gonzalez et al. [29] proposed a MLR model to predict the hourly PV production using minimum weather conditions and the performance ratio as predictors. With this approach, root mean squared errors ($RMSE$) lower than 16% were obtained in comparison with measured production data of different PV power plants. Other MLR models employ as predictors technoeconomic, socio-demographic and building variables. For example, the model proposed by Jonas Müller et al. [30] forecasts spatial projections of PV installations, showing the versatility and effectiveness of a multidisciplinary approach.

Nevertheless, the above-mentioned regression models focus on providing a quick estimation of the PV energy production and no additional simplified models have been found to obtain the profitability results, for instance the economic payback of any PV facility on a rooftop of a building. The latter depends on global building features that are easily known in advance, such as the amount of shadow losses or the maximum installable capacity. Consequently, there is a potential to develop simplified models based on the global building characteristics.

In order to cover this gap, the present work provides a regression model to estimate the economic payback. The proposed model is an alternative to the complex top-down models, providing clear information to the local energy planners and the rest of energy actors on the payback which can be obtained with PV installations on a large number of urban rooftops.

Given the previous literature review, the current study presents the following novelties:

- A new MLR methodology has been conceived for the simulation of PV panels in urban areas, considering both the technical and the economic performance, predicting the economic payback of PV facilities on rooftops as a function of the shadow losses, the installed capacity and unit costs.
- A MLR approach has been developed to ensure a high replicability of the methodology in different countries, with their corresponding prices and electricity tariffs.

3.2 Methods

3.2.1 Description of the methodology

The present section summarizes the methodology which has been applied to obtain the correlations. As mentioned above, the primary objective of this article is the development of a MLR economic model capable of providing the same global results as more complex and detailed models. Figure 3.1 shows the workflow which has been adopted.

In the first place, a complex techno-economic model has been built to calculate the economic payback automatically for any rooftop PV facility defined only by its coordinates. This helps to easily carry out an analysis on a urban scale without going into any further technical details. This model has been in turn validated by comparing the results with the software SAM [31]. In the second place, the predictive variables of the regression model have been identified by analyzing the results of the complex model. In the third place, the sample size has been defined through an iterative process, which starts from a reduced random sample of buildings. The minimum size to obtain a representative regression has been verified by means of an F-test. Finally, in step 4, the paybacks predicted by the MLR model have been compared against the paybacks obtained with the techno-economic model. Furthermore, alternative regressions have been developed to estimate the PV production in other regions of the world based on simple predictors such as shadow losses, installed power, annual horizontal radiation, and mean temperature. These models have been validated with the production obtained from the techno-economic model.

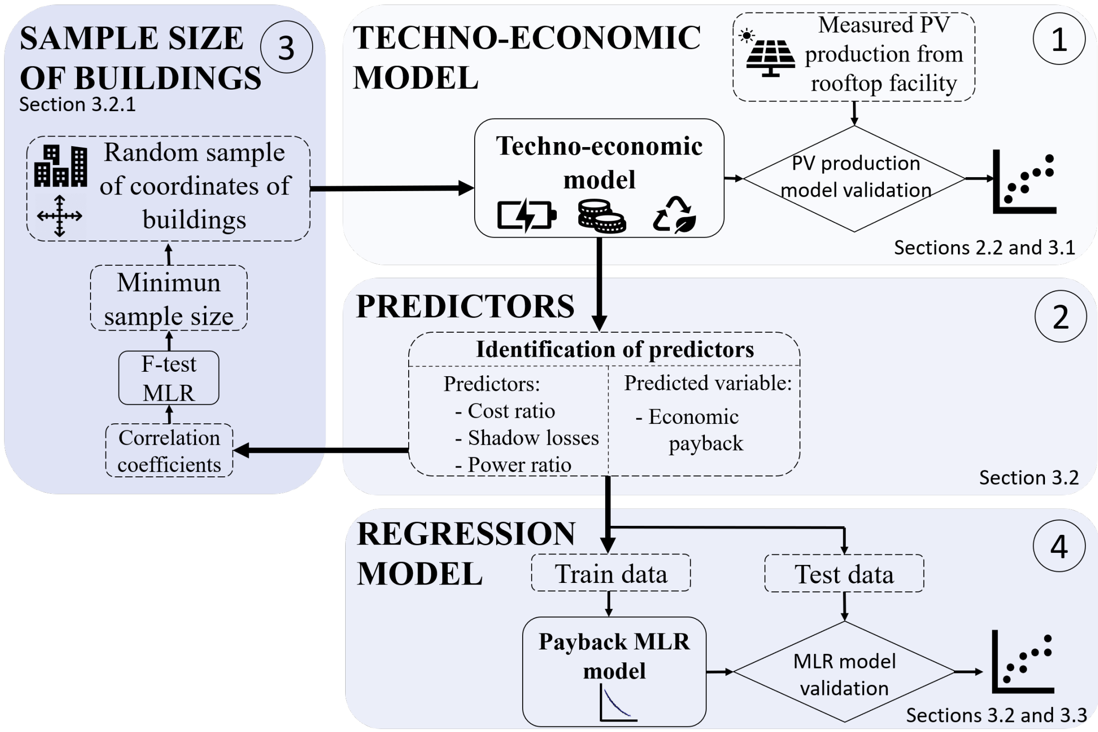

Figure 3.1: Workflow of the proposed methodology.

As stated by Campos Inês et al., multi-storey residential buildings present a high potential for electricity savings [32], and they are also the most common buildings in cities by far. Consequently, this typology (urban houses with more than two floors) has been chosen for the present study. Tillmann Lang et al. [33] also stated that large-residential multi-floor buildings provide promising combinations of key drivers of economic performance, in a study which compared the PV self-consumption of four buildings types (residential and commercial, each small and large).

3.2.2 Techno-economic model

The techno-economic model has been developed in the R programming code to estimate the PV electricity generation and to calculate the energy, economic and environmental impact. The calculations are carried out with an hourly time step. The approach only requires as main input the rooftop coordinates of the building under study.

As shown in Figure 3.2, the model is composed of several submodules. In (i) the urban spatial model helps to obtain the skyline of surrounding obstacles around the point of study using LiDAR and cadastral data. In (ii) the irradiation model enables the calculation of the irradiation on a tilted surface considering nearby shadows. In (iii) the production model is employed to calculate the electrical PV yield of the entire facility. In (iv) the electrical demand of the building is calculated and compared with the production. In (v) the economic model estimates the costs, cash flows and energy savings. Finally, in (vi) the emissions model is used to quantify the environmental impact of the facility.

The calculations are particularized to each specific building by using the LiDAR and cadastral information according to the following three variables: the skyline of the surrounding buildings, the rooftop area and the electrical demand of the building. The techno-economic model is explained in more detail in recent literature [34]. The present section describes the main assumptions and inputs which have been considered.

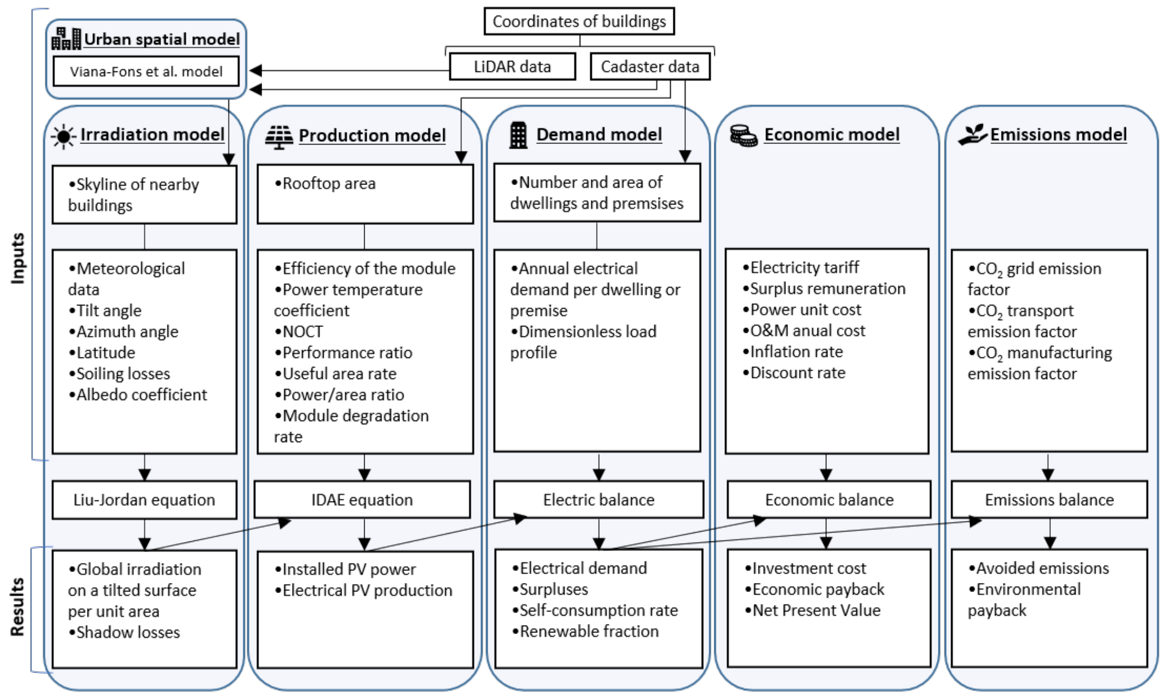

Figure 3.2: Block diagram of the PV techno-economic model.

Spatial urban model

The shadow modelling can be based on shadow profiles or based on the skyline/viewshed. The first method is computationally heavy since it requires to scan the environment for each time step. In contrast, the second method only requires a single scan to obtain the skyline of nearby buildings. The calculation of the shadow losses is performed using sun maps or knowing the sun path. As a consequence, the global irradiation is based on a single representative point selected manually for each rooftop. The latter is chosen as the area with less shadows from nearby buildings, chimneys, parapets, elevator shafts, etc.

The skyline of the surrounding buildings is calculated given the coordinates of a representative point of the rooftop. This skyline is the first step to quantify the shadow loss factors for beam and diffuse irradiation. Both factors have been obtained by means of a GIS-based model, developed by Viana-Fons et al. [35], which employs the cadaster data as inputs. The cadaster data provides the geometry of the rooftops of the buildings, and the height of the buildings is obtained from LiDAR data [36]. As a result, each polygon is assigned a determined height, hereby creating a prismatic model. The assumed error for this prismatic approach is enough to accurately estimate the shadow losses in the rooftops of Valencia [37]. Additionally, according to Filip Biljecki et al. the potential improvement on the level of detail is very small [38].

The median of the Z coordinate of the LiDAR points contained in the building footprints has been used for the calculation of the height of the buildings in the vector-based 3D city model. The median is a high robust statistic estimator for this application according to Viana-Fons et al [35]. Through geometric calculations proposed by Gál and Unger [39], the model generates a skyline profile. For each azimuthal angle step, set to $5°$, the skyline is obtained within a radius of 200 m from the calculation point on the rooftop. According to the preliminary results reported by Chen et al. [40], considering obstacles located further than 300 m do not yield more accuracy to the SVF calculation.

Irradiation model

The isotropic radiation model from Liu and Jordan [41] has been employed in the model. For a given building rooftop, the program calculates the hourly global irradiation on the PV module. The azimuth angle considers the shadows cast by the surrounding buildings and nearby obstacles. The components of the horizontal irradiation have been previously obtained from the Typical Meteorological Year data of Valencia provided by EnergyPlus [42] and the equations of J.J. Michalsky [43] for the sun path, and the ground reflectance.

The shadow losses affect the beam and the diffuse components, respectively. They have been included in the calculation of the Shading Factor (SF) and the Sky View Factor (SVF).

Moreover, the skyline must contemplate those regions of the visible sky that are blocked by a given surface of the surroundings. For this purpose, the analytical expression proposed by Arbi Gharakhani et al. [44] is used to generate a profile which associates an elevation angle for each azimuth to the sky which is blocked by the panel. This obstacle profile is combined with the skyline of the surrounding buildings, resulting in a new combined obstacle skyline on which the shadow loss factors (SF and SVF) are calculated.

Additionally, soiling losses of 5% have been applied to the global irradiation, the result is denoted as effective global irradiance.

Production model

The hourly PV energy production is calculated according to the Spanish guidelines from IDAE [45]. The latter assume typical values of PR and an efficiency of the PV module, which depends on the temperature considering a standard power's temperature coefficient and a normal operating cell temperature ($NOCT$). The production is scaled considering the effective area of panels on the rooftop area. The total area is reduced by 30% to consider other space requirements such as for Heating Ventilation Air Conditioning), chimneys, or shadows from the surrounding walls. An annual degradation of the power of the modules of 5% has also been considered.

Demand model

The PV production is compared with the electricity demand curve of the entire building. The latter is generated assuming a dimensionless hourly demand profile [29] multiplied by the annual electricity demand of the building, considering all its dwellings and premises from the cadastral information. The model assumes a same profile of the load curve for all dwellings and other premises of the building.

Economic model

The economic calculations have been developed according to the self-consumption modality with surpluses under compensation of RD 244/2019 [8]. The latter allows the energy surpluses to be sold to the grid to perceive a reduction which is as maximum the monthly electricity bill with no PV. The electricity and compensation prices are obtained from time series of 2018 provided by the corporation which operates the Spanish electric grid (Red Eléctrica de España, REE). The assumed investment costs depend on the installed power as indicated in Table 3.1. Additionally, a yearly operation and maintenance cost has been considered, as well as a yearly inflation rate and discount rate, as indicated further on in Table 3.2.

Table 3.1: Unit power costs as a function of the installed power.

Power range, P ($\mathrm{kW_p}$)	**Power unit cost** (€/$\mathrm{kW_p}$)
$P \leq 10$	1600
$10 \leq P \leq 20$	$1,800 - 20 \cdot P$
$20 \leq P \leq 50$	$1,566 - 8.33 \cdot P$
$50 \leq P \leq 500$	$1,178 - 0.556 \cdot P$
$P > 500$	900

Emissions model

The model also estimates the avoided emissions due to savings from the electricity grid considering an emission factor, as well as the environmental impact in the manufacturing of PV modules and its transportation.

The emission factors, together with all the other inputs, are listed in Table 3.2. The model is calculated in hourly terms and the simulations are run throughout the entire life cycle of the facility (25 years).

Table 3.2: Summary table of all the inputs of the simulations.

Parameter	Value	Units	Source
Default module tilt angle	30	°	-
Default azimuth tilt angle	0	°	-
Latitude	39.4697	°	-
Soiling losses	5	%	M. R. Maghami et al. [46]
Albedo coefficient	0.2	-	P. Gilman et al. [47]
Efficiency of the module	15	%	Ó. Perpiñán [48]
Power temperature coefficient of the module	-0.4	%/°C	M. C. Brito et al. [49]
NOCT	45	°C	IDAE [45]
Performance ratio	0.8	-	W.G.J.H.M. van Sark et al [50]
Useful area ratio	0.7	-	-
Area/power ratio	10	m^2/W_p	Grupotech [51]
Module degradation rate	2	%/year	D.C Jordan et al. [52]
Electrical demand per dwelling	3,500	kWh/year	IDAE [53]
Electrical demand in commerces	300	kWh/m^2year	ANPIER [54]
Electrical demand in offices	137.75	kWh/m^2year	Cámara de Madrid [55]
Electric tariff (mean)	0.12335	€/Wh	REE [56]
Surplus remuneration	0.046584	€/Wh	REE [57]
O&M costs	9.35	€/W_p	J.Chase [58]
Inflation rate	1.3	%	inflation.eu [59]
Discount rate	7	%	CNMC [60]
CO_2 grid emission factor	0.267262	kg CO_2/kWh	REE [61]
CO_2 transport emission factor	0.151	kg CO_2/tkm	PVsyst [62]
CO_2 manufacturing emission factor	932	kg CO_2/kW_p	PVsyst [63]
Module weight/power ratio	0.07047	t/kW_p	Atersa [64]
Life cycle of the facility	25	years	M. S. Chowdhury et al. [63]

3.3 Results and discussion

The correlations use as a starting point the performance of PV installations located in potential rooftops of Valencia. The performance is obtained with the techno-economic model described in section 3.2.2. In section 3.3.1., the techno-economic model is validated. In section 3.3.2, the performance results obtained with the model are employed for the development of the correlations.

3.3.1 Validation of the techno-economic model

The energy production results provided by the techno-economic model have been compared with the results provided by the software SAM. Both models have been executed for a same PV self-consumption facility, which is summarized in Table 3.3 and is located on a rooftop of a public building in Valencia (39.469072°, -0.340381°). Both models are fed with the same inputs and climate data. The Simple Module Efficiency Model was chosen in SAM and the shadow losses were introduced with the feature "solar azimuth-by-altitude beam irradiance shading losses", considering the skyline obtained with the Viana Fons et al. model [35]. Figure 3.3 compares the PV production obtained with both models. The $RMSE$ and mean absolute error (MAE) are $0.525\,\mathrm{kW\,h}$ and $0.233\,\mathrm{kW\,h}$, respectively, and the deviation is of $\pm 10\%$ except for low production levels at afternoon hours. This is probably due to the fact that the azimuth resolution allowed in SAM (20° each step) to introduce the skyline of surrounding obstacles is less accurate than the one obtained with the techno-economic model (5° each step). As a result, there are small deviations in radiation results in late hours when the sun is covered by a building in the west. Moreover, the PV production in the late afternoon may be below or above the inverter electrical thresholds defined in SAM. This aspect has not been considered in the techno-economic model to simplify the calculations.

Table 3.3: Characteristics of the PV facility located in Valencia for the model validation.

Characteristic	Value	Units
Installed power	25.94	$\mathrm{kW_p}$
Total area of panels	133.03	$\mathrm{m^2}$
Temperature coefficient	-0.36	%/°C
Maximum power voltage	33.54	Vdc
Open circuit voltage	37.38	Voc
Module efficiency	19.5	%
Inverter nominal power	25	kW
Inverter efficiency	98.3	%
Tilt angle	10	°
Azimuth angle	0	°
Modules per string in subarray	Subarray 1:22 Subarray 2:18	-
Modules parallel in subarray	Subarray 1:2 Subarray 2:2	-

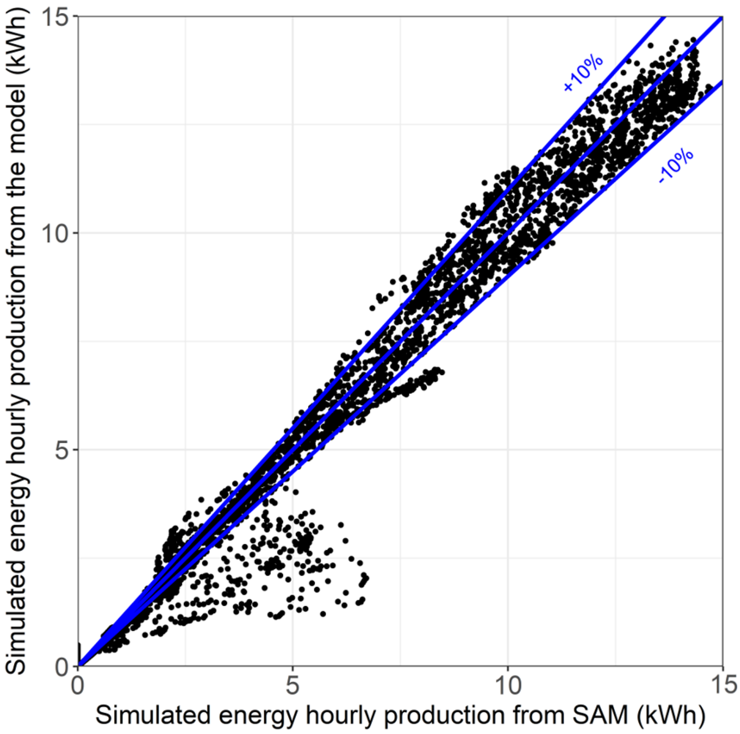

Figure 3.3: Validation of the hourly PV production from the techno-economic model compared with the energy results obtained from SAM for a same facility in Valencia.

3.3.2 Payback regression model

The payback regression model is obtained from the analysis of the simulation results provided by the techno-economic model. The first step is to define the minimum sample of buildings and to define the predictors.

Assumptions and required sample size

The payback regression model has been applied to a random sample of multi-storey buildings with flat rooftops in the urban nucleus of Valencia.

As exposed in section 3.2.2 and in Figure 3.2, PV facilities are influenced by buildings due to three different features: (i) the skyline of the surrounding buildings, which is associated with the shadow losses; (ii) the available rooftop area related with the potential economy of scale and with the energy production; and (iii) the demand profile, which defines the amount of surpluses and the self-consumption levels. Given the previous variables, four different dimensionless predictor variables were initially tested to predict the economic payback:

- The percentage of shadow losses (SL) defined as the ratio between the yearly global irradiation on the tilted surface including shadows and the yearly global irradiation on the tilted surface without shadows.

- The cost ratio (CR) defined as the relationship between the power unit cost of the facility and the maximum power unit cost (assumed as $1.6\,€/\mathrm{W_p}$ for small facilities, as shown in Table 1). This predictor indirectly considers the available rooftop area since it is related with the power unit costs and to the economy of scale.

- The building power ratio (BPR) defined as the relationship between the peak power of the demand curve and the peak PV installed power.

- The Surpluses Ratio (SR) understood as ratio between yearly energy surpluses (S_{PV}) and the production (E_{PV}). This ratio is important since surpluses in Spain are treated differently than self-consumption at an economical level.

The minimum required sample size is determined by means of an F-test performed with the software G*Power [65]. The latter carries out statistical power analyses, with the statistical F-test feature for MLR “Fixed model, R^2 deviation from zero” [66]. The F-test evaluates for a given sample size whether a continuous variable, the payback in this case, is significantly estimated by a set of predictors, in this case the SL, CR, BPR and SR. The program assumes as null hypothesis that the R^2 equals zero, and as alternative hypothesis that the R^2 is greater than zero, which means that there is a correlation between the predictors and the payback with a statistical significance.

In order to perform this test it is necessary to assign values to the type-I error, the power and the effect size index (f^2). The standard type-I and type-II errors have been fixed respectively as 5% and 20% (associated with a power of 80%, the probability of rejecting the null hypothesis). The latter values have been fixed taking as reference the five-eighty convention suggested by J. Cohen [67]. These values are also within the range proposed by other authors [68]. The effect size is set at f^2=0.29, which depends on the correlation coefficients between the four predictors and the payback. These correlation coefficients are obtained from the results of a sample of 200 buildings simulated prior to this test and yield similar values to the ones shown in Figure 3.4.

As a result of the F-test, the minimum sample of buildings is 47 with a power of 80.91%. In other words, there is a probability of 80.91% that the R^2 will significantly be greater than zero if the sample is of 47 buildings or more. Nevertheless, in order to cover all the districts of the urban nucleus, at least 50 buildings per district have been selected, hereby yielding a total of 1,035 buildings for the entire city shown in Figure 3.4. This amount has been finally reduced to 893 buildings after filtering the paybacks which are higher than the facility useful life [63]. As discussed in section 3.3.3, the sample size decision is backed by analyzing the $RMSE$ for several test and train ratios (the proportion of the dataset intended to fit the model and its complementary intended to validate the model).

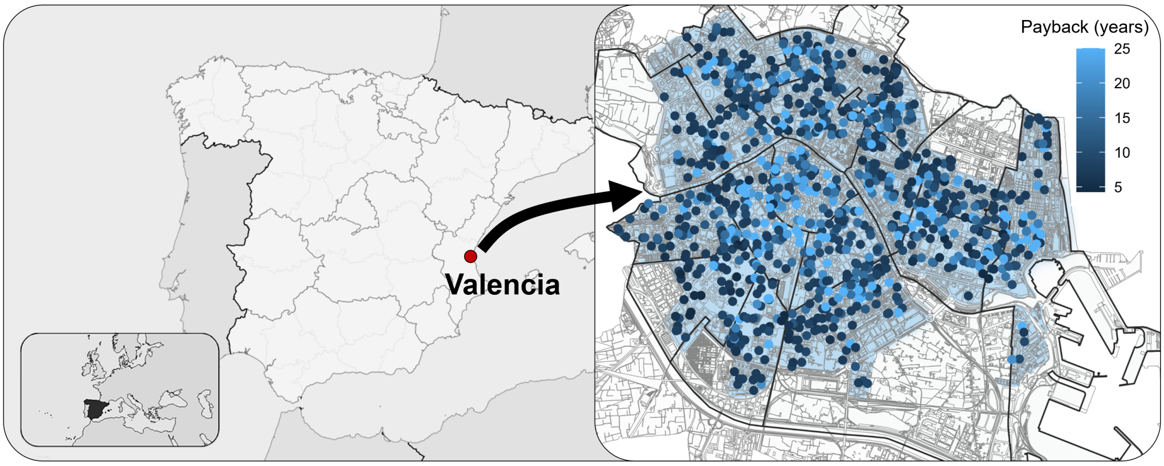

Figure 3.4: Location of the simulated buildings in the city of Valencia, Spain.

Regression model

Due to the fact that the MLR assumes that the residuals of the model are distributed normally [69] the normality of the filtered payback dataset of 893 buildings has been assessed with a Shapiro-Wilk test. The null-hypothesis is that the economic payback is distributed normally, consequently if the p-value is less than a type-I error of 5% [67], the null hypothesis is rejected. The test provides a p-value of 2.2×10^{-16}, thus the data does not meet a pure normality assuming a confidence level of 95%. Furthermore, the distribution is moderately right-skewed (skew=1.23), which indicates an asymmetric density distribution with a long tail on the right side. in order to reduce its right skewness, the payback variable has been transformed with the inverse root square (Payback$^{-0.5}$), as suggested Tabachnick et al. [70]. A normal distribution has then been obtained with a p-value of 0.18 for the Shapiro-Wilk test and a with a distribution which is practically symmetric (skew=-0.03). Finally, the payback dataset has been randomly split using a 20:80 ratio, to create the training dataset and test dataset, respectively. The first one is used to train the MLR model and the second one to assess and validate the model.

Once the minimum sample size has been obtained and the payback has been fitted properly, the correlation matrix of Figure 3.5 helps to obtain a preliminary assessment of the four predictors given their impact on the predicted variable, which is the economic payback.

As a first step it is necessary to reduce the multicollinearity among predictors. Figure 3.5 shows a strong positive correlation of 0.89 between the predictors BPR and SR, while the correlation values among the other predictors are negligible.

For this reason, a polynomial regression of degree six has been introduced to reflect the relationship between the SR and the BPR (as denoted by SR^* in Eq. 3.1). As a result, the MLR model presented in Eq. 3.2 predicts the economic payback with only three features (SL, CR and SR), as also shown in Figure 3.6. From the first row of this correlation matrix, the degree of influence of each predictor is determined. SL has the biggest impact, followed by the CR, and finally SR^* in a lower level.

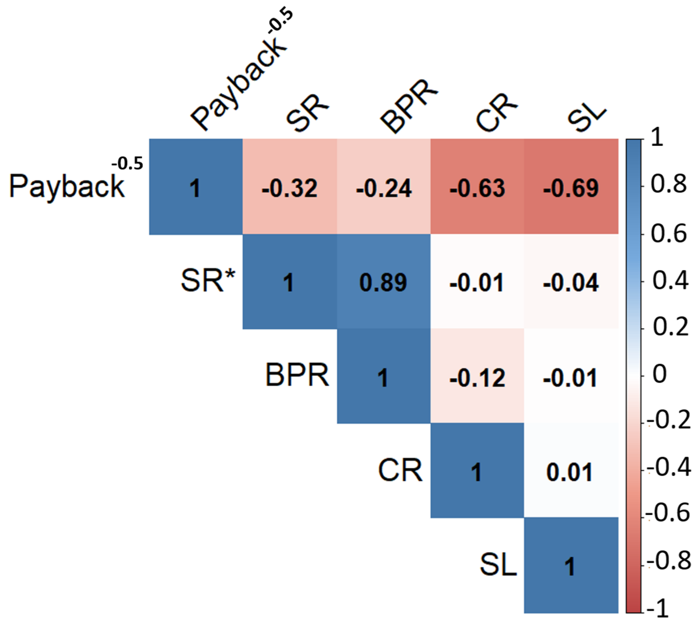

Figure 3.5: Correlation matrix with the preliminary predictors.

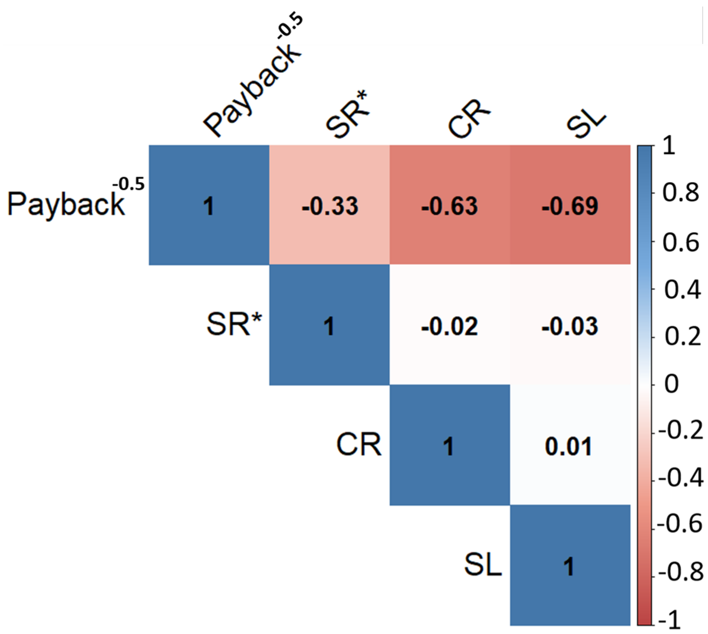

Figure 3.6: Correlation matrix with the final predictors.

$$SR^* = \frac{S_{PV}}{E_{PV}} =$$
$$= k_0 + k_1 \cdot BPR + k_2 \cdot BPR^2 + k_3 \cdot BPR^3 + k_4 \cdot BPR^4 + k_5 \cdot BPR^5 + k_6 \cdot BPR^6 \tag{3.1}$$

$$\frac{1}{\sqrt{PB}} = k_0 + k_1 \cdot SR^* + k_2 \cdot CR + k_3 \cdot SL + k_4 \cdot SL^2 \tag{3.2}$$

The coefficient results for both regressions are gathered in Table 3.4. The correlations are very good given the high R^2 values. The negative sign of the coefficients shows that an increase of any of the predictors implies an increase of the payback. Considering their absolute value and the correlation matrix, the most important predictor is CR, followed by SL and finally, to a lower extent, SR^*.

Table 3.4: Errors provided by the polynomial regression to estimate SR and the MLR to estimate the payback.

Regression	k_0	k_1	k_2	k_3	k_4	k_5	k_6	R^2
$SR^* = S_{PV}/E_{PV}$	0.036	2.107	0.822	-0.612	-0.026	0.251	-0.110	0.9975
$1/\sqrt{PB}$	0.586	-0.209	-0.279	-0.234	-0.223	-	-	0.9951

3.3.3 Validation of the regression model

The previous models have been fed with the test dataset, and the predicted values have been compared with the ones from the complex model. According to Figure 3.7, 97.97% of the predicted values present a relative error lower than 5%, and there are only three outliers in total. The MLR tends to over-predict slightly the payback in general, whereas the predictions with the greater residuals are underpredicted.

The errors shown in Table 3.5 indicate that the model provides accurate payback values, as illustrated by the $RMSE$ which is of only 0.48 years. This value is completely assumable since the purpose of this regression is to provide an order of magnitude for energy planning.

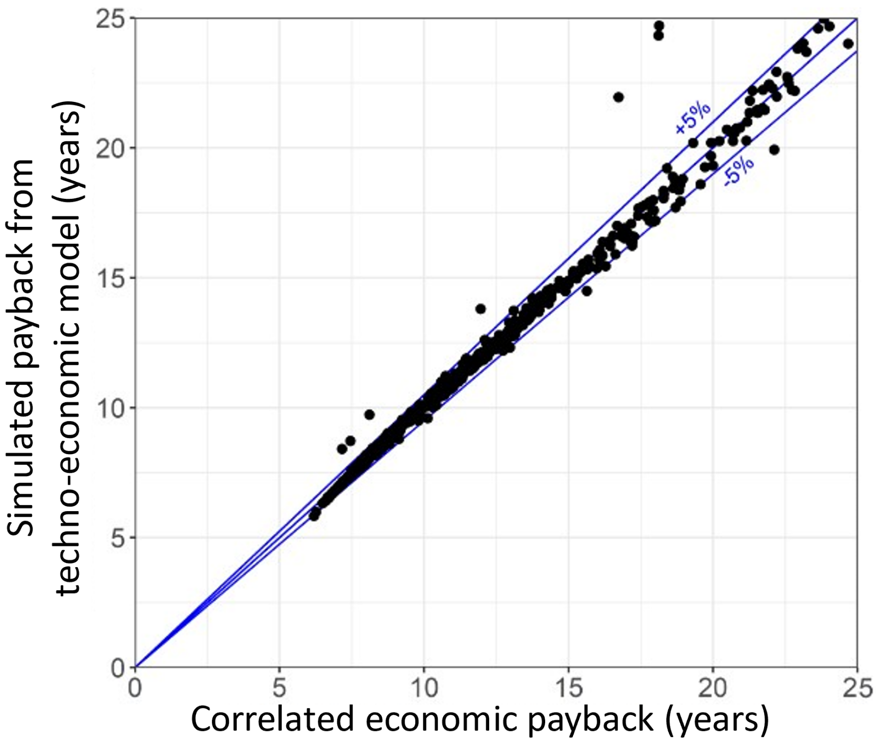

Figure 3.7: Results and validation of the MLR model to predict the payback.

Table 3.5: Errors provided by the polynomial regression to estimate SR and the MLR to estimate the PB.

Regression	$RMSE$	MAE	Units
$SR^* = S_{PV}/E_{PV}$	0.00398	0.00306	-
$1/\sqrt{PB}$	0.48242	0.19189	years

Analysis of the errors depending on the test/training data ratio

An analysis of the error dispersion depending on the training set size has been carried out to demonstrate that the chosen sample size is robust and to guarantee an accurate evaluation error score independent of the training and test data partition. For this purpose, the training dataset size is increased from 100 to 700 by steps of 100. For each step, the original dataset is split into a random training sample and its complementary for testing is taken. Finally, the $RMSE$ and MAE are calculated by repeating the process 1,000 times, resulting in a different error value in each repetition due to the randomness of the sampling. The error distributions for each training dataset size are reflected in Figure 3.8 and Figure 3.9. The mean values of the $RMSE$ and MAE register a very slight reduction, hereby confirming that a sample size of 200 buildings for train data is large enough to present an accurate regression. In both figures, there is a slight increase of the error between the 400 and 500 samples due to an overfitting of the model. The model reproduces too closely a particular dataset for samples larger than 400 buildings, consequently leading to poor generalization when predicting new testing data.

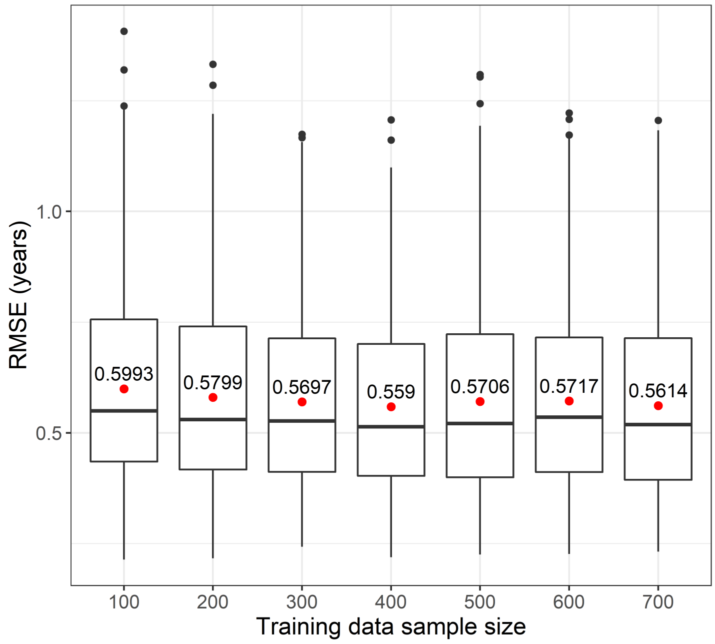

Figure 3.8: RMSE boxplots for different train/test splits.

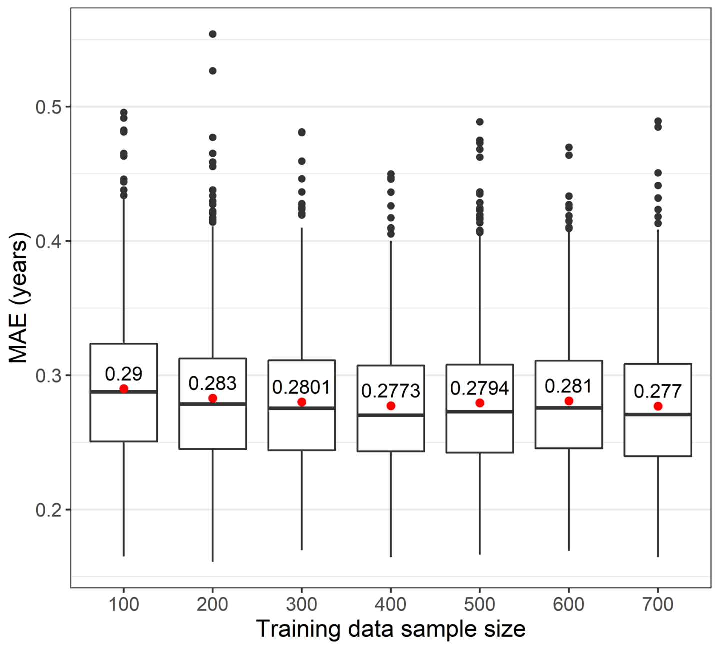

Figure 3.9: MAE for different train/test splits.

Additionally, an independent 10-fold cross-validation of the MLR model has been carried out. This is important to contrast the previous errors with a standardized methodology which is generally employed to validate regression models. The payback dataset is randomly split with a 20:80 ratio into 10 distinct subsets called folds. Afterwards, the MLR model has been fitted 10 times, choosing every evaluation step a different fold to train it and selecting the complementary folds to test it with the payback results from the complex techno-economic model. The results are similar to the previous plots in Figure 3.8 and Figure 3.9 with an average $RMSE$ of 0.59 years and a MAE of 0.28, as well as a standard deviation of 0.043 and 0.008 years, respectively.

Regression results for other locations

In order to ensure the replicability of the methodology for other locations, two regressions have been proposed, which combined estimate the yearly PV energy production, a value that can be easily converted into economic savings.

The first regression consists of a MLR model to estimate the yearly PV production in Valencia, depending on the installed peak power (P_{PV}) and SL.

$$E_{PV,building,Valencia}(P_{PV,SL}) = k_0 + k_1 \cdot P_{PV} + k_2 \cdot SL + k_3 \cdot P_{PV} \cdot SL \tag{3.3}$$

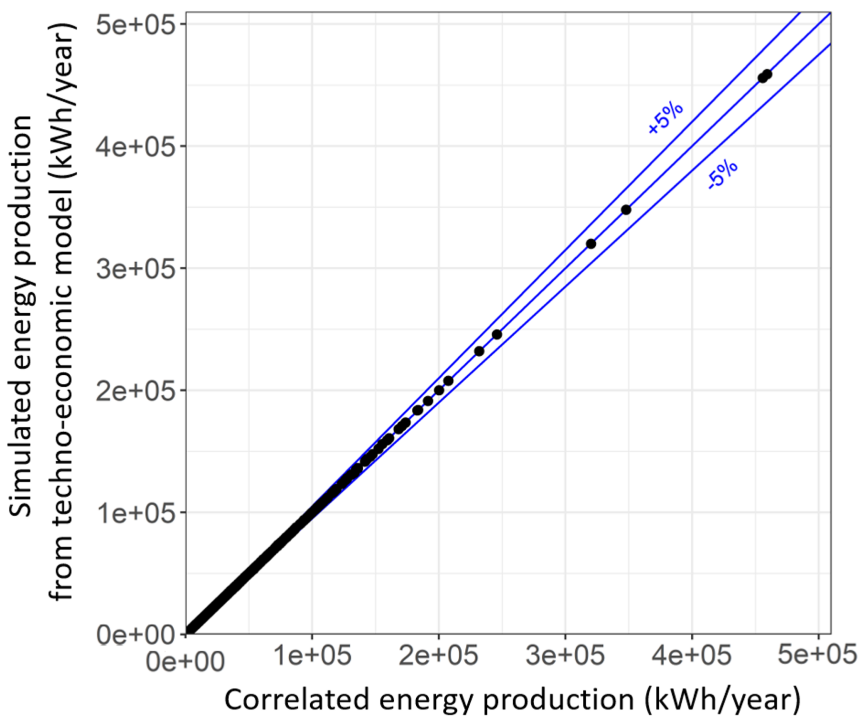

Figure 3.10: Results and validation of the MLR model to predict the energy production.

The second correlation is the simple linear regression shown in Eq. 3.4, which has been introduced to adapt the PV production (with SL=0%) from the previous MLR model to the climatic conditions of any given location. This conversion only depends on location data such as the yearly global horizontal irradiation ($G_{0,location}$) and the mean ambient temperature ($T_{location}$).

$$E_{PV,location}(G_{0,location}, T_{location}) = k_0 + k_1 \cdot G_{0,location} + k_2 \cdot T_{location} \tag{3.4}$$

The combination of both regressions enables the calculation of the yearly PV production from any given location, as indicated in Eq. 3.5. Figure 3.11 presents the validation results for several locations for facilities with null shadow losses. The deviation is below 5% for 12 of the 15 locations assessed and the regression model tends to slightly overpredict the yearly production, except for the high latitudes.

$$E_{PV,building,location} = \\ = E_{PV,building,Valencia}(P_{PV,SL}) \cdot \frac{E_{PV,location}(G_{0,location}, T_{location})}{E_{PV,location}(G_{0,Valencia}, T_{Valencia})} \tag{3.5}$$

Additionally, shadow losses in the range from 0 to 40% have been simulated in different locations to check that there is still a linear relationship between $E_{PV,location}$, $G_{0,location}$, and $T_{location}$. Figure 3.12 shows these results, revealing that most of the points are within a deviation of $\pm 10\%$. In general, there is an underprediction when the shadow losses increase for a same location. Again, as described in Figure 3.11, there is an underprediction in Brussels (the location in Figure 3.11 with a highest latitude), however for regular shadows and latitudes the regression model provides accurate results providing a $RMSE$ of 3.20 $\mathrm{kWh/kW_p}$.

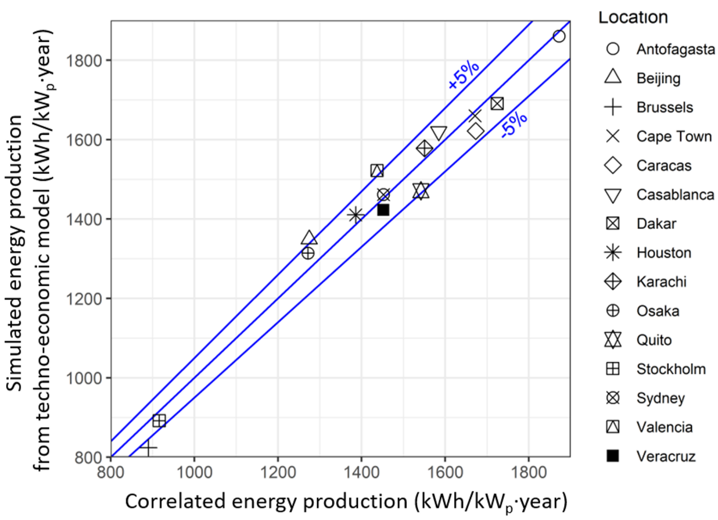

Figure 3.11: Results and validation of the polynomial regression model to predict the SR.

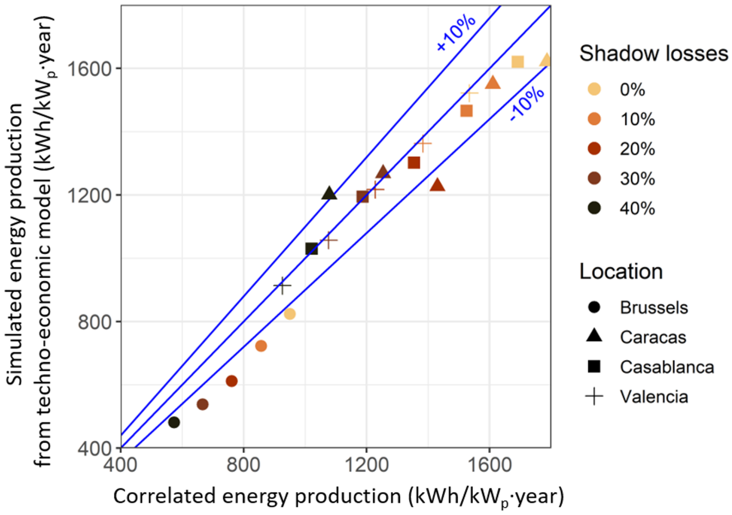

Figure 3.12: Results and validation of the MLR model to predict the payback.

Finally, the coefficients and errors of Eqs. 3.3, 3.4 and 3.5 are gathered in Table 3.6.

Table 3.6: Coefficients of the equations 3.3, 3.4 and 3.5.

Regression	$\boldsymbol{k_0}$	$\boldsymbol{k_1}$	$\boldsymbol{k_2}$	$\boldsymbol{k_3}$	$\boldsymbol{RMSE}$ (kWh/kW$_p$year)	$\boldsymbol{MBE}$ (kWh/kW$_p$year)	$\boldsymbol{R^2}$
$E_{PV,building,Valencia}(P_{PV,SL})$	-13.167	1,534.410	-85.760	-1,510.610	2.116	0.148	0.999
$E_{PV,location}(G_{0,location}, T_{location})$	185.705	0.841	-6.499	-	3.200	2.751	0.970
$E_{PV,building,location}$	-	-	-	-	3.200	2.751	0.970

The previous regressions can be employed as a starting point to make the balance with the electrical demand, to apply other costs or electricity prices and to calculate the surplus remuneration according to appropriate climate and regulation (net-metering, feed-in-tariff, and other schemes gathered by Campos Inês et al. [32]).

3.3.4 Overall analysis of the assessed multi-storey buildings

The main results obtained with the techno-economic model for the sample of 893 buildings (those whose payback is under 25 years) are showcased in the boxplots of Figure 3.13, Figure 3.14 and Table 3.7.

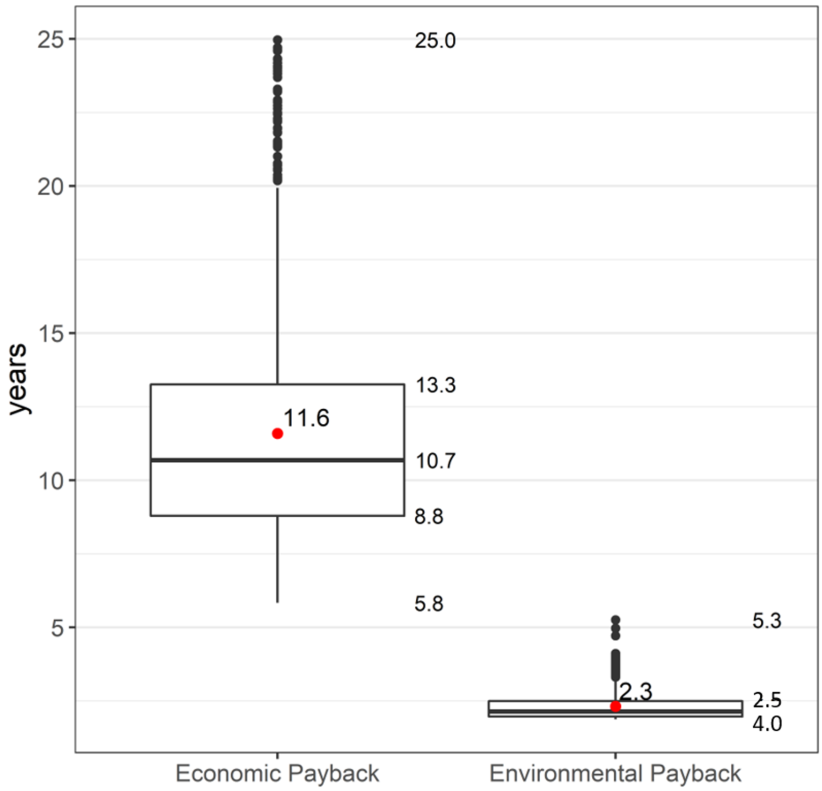

Figure 3.13: Economic and environmental payback results for the sample of buildings of Valencia.

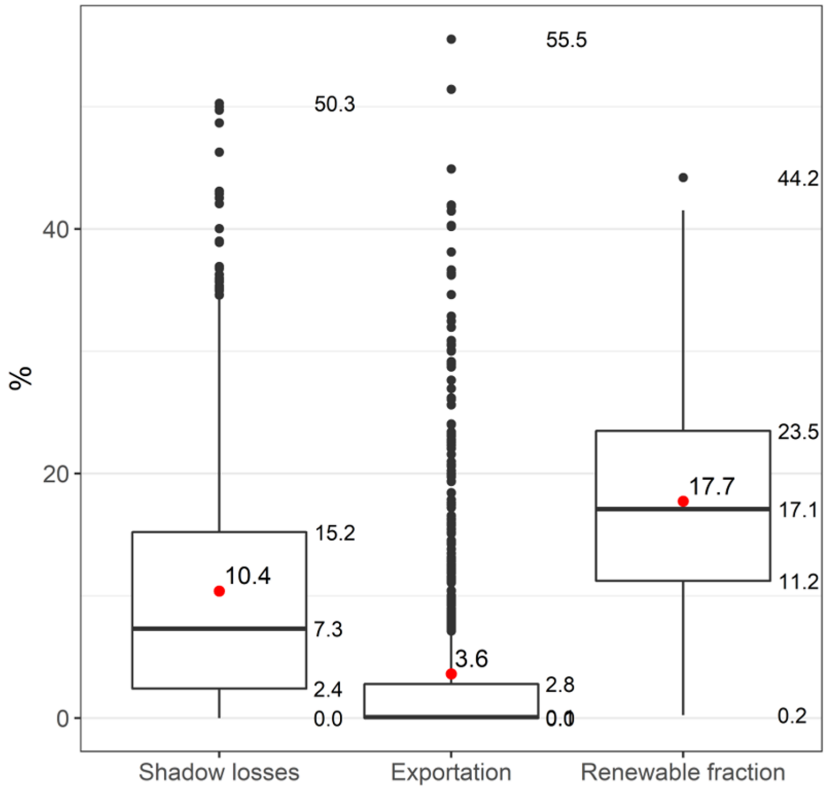

Figure 3.14: Shadow losses, exportation ratio and renewable fraction for the sample of buildings of Valencia.

Table 3.7: Statistical results for the sample of buildings in Valencia.

Variable	**Units**	**Mean**	**Standard deviation**	**Skewness**[a]	**Minimum**	**Q1**	**Median**	**Q3**	**Maximum**
Economic Payback	years	11.59	3.93	1.26	5.83	8.79	10.68	13.26	24.97
Environmental Payback	years	2.31	0.48	1.85	1.88	1.97	2.14	2.50	5.25
Shadow losses	%	10.39	10.15	1.29	0.00	2.40	7.31	15.21	50.28
Exportation	%	3.62	7.92	2.99	0.00	0.00	0.06	2.78	55.53
Renewable fraction	%	17.73	8.94	0.32	0.24	11.21	17.09	23.48	44.20

[a] Dimensionless Value.

According to Figure 3.13, the average economic payback for the sample is 11.59 years. 40.42% of the total results yield paybacks between 8 and 11 years and only 0.33% provide values under 6 years. As mentioned in section 3.3.2, the economic payback distribution is right skewed since there is a wide dispersion of cases for which the profitability is hindered by shadows and/or a low match between production and demand or high costs. In fact, this tail of the distribution would be larger if the discarded facilities with paybacks beyond the lifecycle had been represented (13.72% of the original dataset).

The environmental payback, understood as the time to recover the emissions generated during the manufacturing and transport of the panels, presents an average of 2.31 years, which shows a high positive impact on the environment even on a short term. The low standard deviation is due to the assumption of a similar emission factor for all the cases. The dispersion could increase if different manufacturers had been considered. However, this analysis provides an order of magnitude of the notorious difference between the economic and environmental paybacks.

As Figure 3.14 shows, the low levels of exports, with an average of 3.62% of the yearly production, are explained by the high level of electricity demand in comparison with the PV production, which is limited by the effective rooftop area. These small exportation values together with the low prices of surplus remuneration are the main reasons why electricity export does not play an important role to improve the economic payback for these buildings. The same conclusions were obtained with the MLR model. Given the reduced exportation, practically for half of the simulated buildings the energy generated is self-consumed on site.

Regarding the renewable fraction shown in Figure 3.14, 17.73% of the total grid electricity consumption could be supplied entirely with on-site PV production. The highest renewable fraction and exportation ratesare achieved in buildings with a yearly PV production higher than 65% of the yearly demand. In general, these installations are oversized.

The shadow losses usually have low values for this type of building due to their elevated height. An average shadow loss of 17.73% is obtained and the latter drops significantly down to 10.39% if the median is considered. These losses are generally due to shadows cast by the railings, elevator shafts and chimneys. In most modern districts, thanks to urban planning, most of the buildings have a similar height and consequently they hardly produce shadows between them. This phenomenon can be noticed with the spatial distribution of paybacks shown in Figure 3.4, where downtown buildings present higher paybacks due to abrupt skylines, whereas the modern districts on the outskirts yield lower paybacks.

At a more detailed level in the building characterization, the buildings which present the best profitability results share the following characteristics:

- Large rooftop areas, which imply lower unit costs due to the economy of scale.
- High levels of electricity consumption, since the PV generation is intended to reduce the costs of the energy term of the electricity bill, whose cost is higher than the current surplus remuneration.

- Low percentage of shadow losses to maximize the PV production.
- Coincidence of consumption hours with radiation hours to maximize the energy and bill savings and reduce surpluses, which provide a lower income.

The above-mentioned characteristics generally fit with the characteristics of industrial buildings and residential multi-storey buildings. Both typologies are consequently the most suitable for PV production. Taking the above-mentioned characteristics into account, an alternative to subsidies that could help to improve the payback consists of creating energy communities with a same PV facility, but aggregating the electrical demand from several buildings. As a result, all of the produced energy could be self-consumed and the savings in the electric bill would be higher.

According to the techno-economic model, PV facilities in single-family houses do not present as favorable economic results as multi-storey buildings, although they present a greater renewable fraction (with an average of 30% of the PV production) and exportation rates (with an average of 40% of the production), as confirmed by simulating 100 houses. The average of their shadow losses registered is 35%, which contrasts with the average of 10% for multi-storey buildings.

Likewise, with the results of the sample of buildings, Figure 3.15 shows a gradient plot representing the influence of the two main predictors (SL, and power unit costs) on the economic payback. A greater weight of the unit power cost is appreciated. For costs above $1.5\,€/\mathrm{W_p}$, the shadow losses must remain lower than 40% to guarantee a payback lower than the facility life cycle. The gradient plot has been constructed by means of a linear interpolation of the discrete points of the sample in a 200x200 grid. The presence of outliers and their consequent discontinuities in the plot for costs over $1.4\,€/\mathrm{W_p}$ are because the selected predictors do not explain entirely the payback for these specific points.

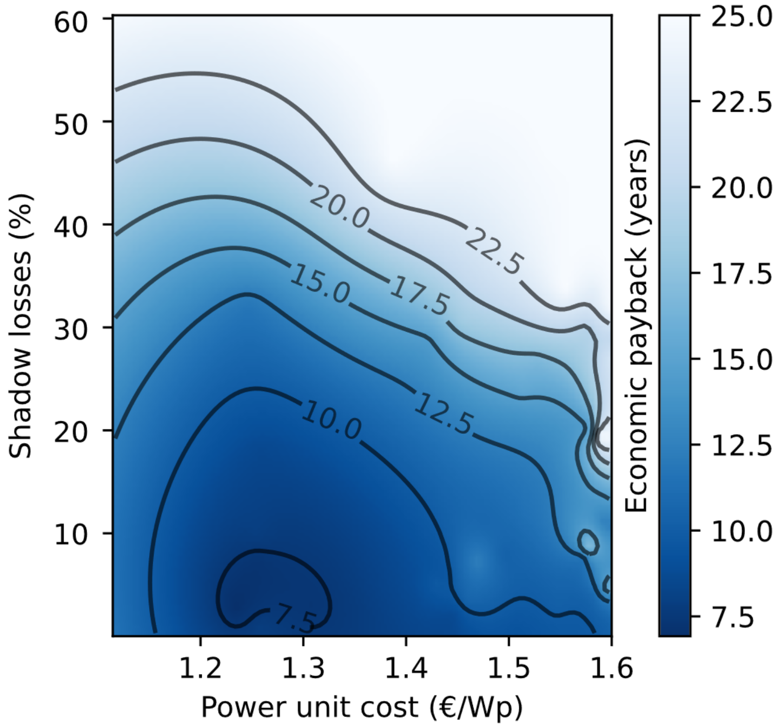

Figure 3.15: Relationship between the economic payback and the most influential predictors: shadow losses and power unit costs for the sample of buildings of Valencia.

3.4 Conclusions

The present work has been developed to shorten the gap between energy planners and detailed simulation models of PV facilities. A MLR model has been developed, in a similar approach as recent studies from literature, although including the main novelty of addressing the economic impact and ensuring a high replicability since it can be applied for other locations. As an application, the mentioned methodology has been applied for the most common buildings in the city of Valencia, which are multi-storey residential buildings.

The MLR model is based on the results given by a complex techno-economic model, which has previously been compared and validated with SAM providing a $RMSE$ of $0.53\,\mathrm{kW\,h}$ in the hourly PV production. The proposed MLR model has been validated by means of a cross-validation methodology which has provided a $RMSE$ of 0.48 years which is perfectly assumable for energy planning purposes. As a complement for other countries, a combination of regressions has been proposed to estimate the PV production on any rooftop given the capacity, shadow losses and climatic data. The relative errors for this methodology are close to 10% for the studied locations with a R^2 value of 0.97.

The following conclusions have been obtained when applying the methodology to the residential multi-storey buildings of Valencia:

- The key drivers on the payback are the shadow losses and the economy of scale. The best economic paybacks are obtained in large available rooftop areas.
- On the demand side, buildings with high levels of electricity demand tend to profit in a high percentage from on-site energy generated from self-consumption. The surpluses are very low and all the PV production is translated into energy and bill savings. In the case of low consumption levels such as buildings with very few dwellings, the savings are very limited, therefore their cashflows are low in comparison with the investment costs.
- For high electricity demands, the sale of surpluses does not represent a relevant factor to generate large savings and reduce the payback. The sale price in Spain is lower than the price of the bill. One solution to reduce the high paybacks in single-family houses and buildings with low energy demand can be the promotion of energy communities, since the results show that adding consumption and reducing exports leads to a better profitability. As future work, the authors will analyze in more detail the opportunities of PV production in energy communities.

3.5 Acknowledgements

This study was developed owing to the support provided by the Chair of Urban Energy Transition of the Universitat Politècnica de València and the foundation Las Naves.

Additionally, this work was supported by The Energy Office of Valencia and the Statistics Office of the Valencia City Council, who collaborated by providing the data of the PV facility for the validation and their recommendations on the statistical analysis.

3.6 References

[1] EUROSTAT. *Eurostat - Data Explorer. Complete energy balances.* 2021.

[2] EUROSTAT. *Eurostat - Data Explorer. Supply, transformation and consumption of electricity.*

[3] IDAE. *Estudios, informes y estadísticas | IDAE.*

[4] International Energy Agency. *Electricity – World Energy Outlook 2019.* Tech. rep. 2019.

[5] Gomez-Exposito, A., Arcos-Vargas, A., and Gutierrez-Garcia, F. "On the potential contribution of rooftop PV to a sustainable electricity mix: The case of Spain". In: *Renewable and Sustainable Energy Reviews* 132 (2020), p. 110074. DOI: 10.1016/j.rser.2020.110074.

[6] IRENA. *Solar PV Module Costs 2010-2018.* Tech. rep. 2019.

[7] Jefatura del Estado; Boletín Oficial del Estado (BOE). *Real Decreto-ley 15/2018, de 5 de octubre, de medidas urgentes para la transición energética y la protección de los consumidores.* Madrid, 2018.

[8] Ministerio para la Transición Ecológica (MTE); Boletín Oficial del Estado (BOE). *Real Decreto 244/2019, de 5 de abril, por el que se regulan las condiciones administrativas, técnicas y económicas del autoconsumo de energía eléctrica.* Madrid, 2019.

[9] Castellanos, S., Sunter, D. A., and Kammen, D. M. "Rooftop solar photovoltaic potential in cities: How scalable are assessment approaches?" In: *Environmental Research Letters* 12.12 (2017), p. 125005. DOI: 10.1088/1748-9326/aa7857.

[10] Lobaccaro, G., Croce, S., Lindkvist, C., Munari Probst, M. C., Scognamiglio, A., Dahlberg, J., Lundgren, M., and Wall, M. "A cross-country perspective on solar energy in urban planning: Lessons learned from international case studies". In: *Renewable and Sustainable Energy Reviews* 108 (2019), pp. 209–237. DOI: 10.1016/j.rser.2019.03.041.

[11] Gagnon, P., Margolis, R., Melius, J., Phillips, C., and Elmore, R. *Rooftop Solar Photovoltaic Technical Potential in the United States: A Detailed Assessment.* Tech. rep. National Renewable Energy Laboratory, 2016.

[12] Ngar-Yin Mah, D., Wang, G., Lo, K., Leung, M. K. H., Hills, P., and Lo, A. Y. "Barriers and policy enablers for solar photovoltaics (PV) in cities: Perspectives of potential adopters in Hong Kong". In: (2018). DOI: 10.1016/j.rser.2018.04.041.

[13] Ordóñez, J., Jadraque, E., Alegre, J., and Martínez, G. "Analysis of the photovoltaic solar energy capacity of residential rooftops in Andalusia (Spain)". In: *Renewable and Sustainable Energy Reviews* 14.7 (2010), pp. 2122–2130. DOI: 10.1016/J.RSER.2010.01.001.

[14] Brito, M. C., Freitas, S., Guimarães, S., Catita, C., and Redweik, P. "The importance of facades for the solar PV potential of a Mediterranean city using LiDAR data". In: *Renewable Energy* 111 (2017), pp. 85–94. DOI: 10.1016/j.renene.2017.03.085.

[15] Freitas, S., Catita, C., Redweik, P., and Brito, M. C. *Modelling solar potential in the urban environment: State-of-the-art review.* 2015. DOI: 10.1016/j.rser.2014.08.060.

[16] Schallenberg-Rodríguez, J. *Photovoltaic techno-economical potential on roofs in regions and islands: The case of the Canary Islands. Methodological review and methodology proposal.* 2013. DOI: 10.1016/j.rser.2012.11.078.

[17] Quesada, B., Sánchez, C., Cañada, J., Royo, R., and Payá, J. "Experimental results and simulation with TRNSYS of a 7.2kWp grid-connected photovoltaic system". In: *Applied Energy* 88.5 (2011), pp. 1772–1783. DOI: 10.1016/j.apenergy.2010.12.011.

[18] Pedrero, J., Hermoso, N., Hernández, P., Munoz, I., Arrizabalaga, E., Mabe, L., Prieto, I., and Izkara, J. L. "Assessment of urban-scale potential for solar PV generation and consumption". In: *IOP Conference Series: Earth and Environmental Science* 323.1 (2019), p. 012066. DOI: 10.1088/1755-1315/323/1/012066.

[19] Análisis, C. Y., Caamaño Martín, E., and Díaz-Palacios Sisternes, S. "Potencial solar fotovoltaico de las cubiertas edificatorias de la ciudad de Vitoria-Gasteiz: caracterización y análisis". 2017.

[20] Mangiante, M. J., Whung, P. Y., Zhou, L., Porter, R., Cepada, A., Campirano, E., Licon, D., Lawrence, R., and Torres, M. "Economic and technical assessment of rooftop solar photovoltaic potential in Brownsville, Texas, U.S.A". In: *Computers, Environment and Urban Systems* 80 (2020), p. 101450. DOI: 10.1016/j.compenvurbsys.2019.101450.

[21] Shirazi, A. M., Zomorodian, Z. S., and Tahsildoost, M. "Techno-economic BIPV evaluation method in urban areas". In: *Renewable Energy* 143 (2019), pp. 1235–1246. DOI: 10.1016/j.renene.2019.05.105.

[22] Omar, M. A. and Mahmoud, M. M. *Grid connected PV- home systems in Palestine: A review on technical performance, effects and economic feasibility.* 2018. DOI: 10.1016/j.rser.2017.09.008.

[23] Martín-Pomares, L., Martínez, D., Polo, J., Perez-Astudillo, D., Bachour, D., and Sanfilippo, A. *Analysis of the long-term solar potential for electricity generation in Qatar.* 2017. DOI: 10.1016/j.rser.2017.01.125.

[24] Trigo-Gonzalez, M., Cortés, M., Alonso-Montesinos, J., Martínez-Durbán, M., Ferrada, P., Rabanal, J., Portillo, C., López, G., and Batlles, F. J. "Development and comparison of PV production estimation models for mc-Si technologies in Chile and Spain". In: *Journal of Cleaner Production* 281 (2021), p. 125360. DOI: 10.1016/J.JCLEPRO.2020.125360.

[25] Antonopoulos, I., Robu, V., Couraud, B., Kirli, D., Norbu, S., Kiprakis, A., Flynn, D., Elizondo-Gonzalez, S., and Wattam, S. *Artificial intelligence and machine learning approaches to energy demand-side response: A systematic review.* 2020. DOI: 10.1016/j.rser.2020.109899.

[26] Calcabrini, A., Ziar, H., Isabella, O., and Zeman, M. "A simplified skyline-based method for estimating the annual solar energy potential in urban environments". In: *Nature Energy* 4.3 (2019), pp. 206–215. DOI: 10.1038/s41560-018-0318-6.

[27] Chatzipoulka, C., Compagnon, R., Kaempf, J., and Nikolopoulou, M. "Sky view factor as predictor of solar availability on building façades". In: *Solar Energy* 170 (2018), pp. 1026–1038. DOI: 10.1016/j.solener.2018.06.028.

[28] Poon, K. H., Kämpf, J. H., Tay, S. E., Wong, N. H., and Reindl, T. G. "Parametric study of URBAN morphology on building solar energy potential in Singapore context". In: *Urban Climate* 33 (2020), p. 100624. DOI: 10.1016/j.uclim.2020.100624.

[29] Trigo-González, M., Batlles, F. J., Alonso-Montesinos, J., Ferrada, P., Sagrado, J. del, Martínez-Durbán, M., Cortés, M., Portillo, C., and Marzo, A. "Hourly PV production estimation by means of an exportable multiple linear regression model". In: *Renewable Energy* 135 (2019), pp. 303–312. DOI: 10.1016/j.renene.2018.12.014.

[30] Müller, J. and Trutnevyte, E. "Spatial projections of solar PV installations at subnational level: Accuracy testing of regression models". In: *Applied Energy* 265 (2020), p. 114747. DOI: 10.1016/J.APENERGY.2020.114747.

[31] National Renewable Energy Laboratory. *Home - System Advisor Model (SAM).*

[32] Inês, C., Guilherme, P. L., Esther, M. G., Swantje, G., Stephen, H., and Lars, H. "Regulatory challenges and opportunities for collective renewable energy prosumers in the EU". In: *Energy Policy* 138 (2020), p. 111212. DOI: 10.1016/j.enpol.2019.111212.

[33] Lang, T., Ammann, D., and Girod, B. "Profitability in absence of subsidies: A techno-economic analysis of rooftop photovoltaic self-consumption in residential and commercial buildings". In: *Renewable Energy* 87 (2016), pp. 77–87. DOI: 10.1016/j.renene.2015.09.059.

[34] Fuster-Palop, E., Prades-Gil, C., Masip, X., Viana-Fons, J., and Paya-Herrero, J. "Evaluation of the solar photovoltaic generation potential of a district in the city of Valencia". In: *SDEWES 2020, 15th Conference of Sustainable Development of Energy, Water and Environment Systems.* Cologne, 2020, pp. 1–14.

[35] Viana-Fons, J. D., Gonzálvez-Maciá, J., and Payá, J. "Development and validation in a 2D-GIS environment of a 3D shadow cast vector-based model on arbitrarily orientated and tilted surfaces". In: *Energy and Buildings* 224 (2020), p. 110258. DOI: 10.1016/j.enbuild.2020.110258.

[36] Centro Nacional de Información Geográfica. *Centro de Descargas del CNIG.*

[37] Viana-Fons, J. D., Gonzálvez-Maciá, J., and Payá-Herrero, J. *Methodology for the calculation of the shadow factor on roofs and facades of buildings in urban areas.* 2019.

[38] Biljecki, F., Ledoux, H., and Stoter, J. "Does a finer level of detail of a 3D city model bring an improvement for estimating shadows?" In: *Lecture Notes in Geoinformation and Cartography* 9783319256894 (2017), pp. 31–47. DOI: 10.1007/978-3-319-25691-7_2.

[39] Gál, T. and Unger, J. "A new software tool for SVF calculations using building and tree-crown databases". In: *Urban Climate* 10.P3 (2014), pp. 594–606. DOI: 10.1016/j.uclim.2014.05.004.

[40] Chen, L., Ng, E., An, X., Ren, C., Lee, M., Wang, U., and He, Z. "Sky view factor analysis of street canyons and its implications for daytime intra-urban air temperature differentials in high-rise, high-density urban areas of Hong Kong: a GIS-based simulation approach". In: *International Journal of Climatology* 32.1 (2010), pp. 121–136. DOI: https://doi.org/10.1002/joc.2243.

[41] Loutzenhiser, P. G., Manz, H., Felsmann, C., Strachan, P. A., Frank, T., and Maxwell, G. M. "Empirical validation of models to compute solar irradiance on inclined surfaces for building energy simulation". In: *Solar Energy* 81.2 (2007), pp. 254–267. DOI: 10.1016/j.solener.2006.03.009.

[42] EnergyPlus. *Weather Data by Location | EnergyPlus.*

[43] Michalsky, J. J. "The Astronomical Almanac's algorithm for approximate solar position (1950-2050)". In: *Solar Energy* 40.3 (1988), pp. 227–235. DOI: 10.1016/0038-092X(88)90045-X.

[44] Rehman, N. U. and Uzair, M. "The proper interpretation of analytical sky view factors for isotropic diffuse solar irradiance on tilted planes". In: *Journal of Renewable and Sustainable Energy* 9.5 (2017). DOI: 10.1063/1.4993069.

[45] IDAE. *Pliego de Condiciones Técnicas de Instalaciones Conectadas a Red.* Madrid, 2011.

[46] Maghami, M. R., Hizam, H., Gomes, C., Radzi, M. A., Rezadad, M. I., and Hajighorbani, S. *Power loss due to soiling on solar panel: A review.* 2016. DOI: 10.1016/j.rser.2016.01.044.

[47] Gilman, P., Dobos, A., Diorio, N., Freeman, J., Janzou, S., and Ryberg, D. *SAM Photovoltaic Model Technical Reference Update.* Tech. rep. National Renewable Energy Agency, 2016. DOI: NREL/TP-6A20-67399.

[48] Perpiñán Lamigueiro, O. *Energía Solar Fotovoltaica.* 2023.

[49] Redweik, P., Catita, C., and Brito, M. "Solar energy potential on roofs and facades in an urban landscape". In: *Solar Energy* 97 (2013), pp. 332–341. DOI: 10.1016/j.solener.2013.08.036.

[50] Sark, W. van, Reich, N., Müller, B., and Armbruster, A. "Review of PV performance ratio development". In: *Conference: World Renewable Energy Forum, WREF 2012, Including World Renewable Energy Congress XII and Colorado Renewable Energy Society (CRES) Annual Conference.* Denver, 2012. DOI: 10.13140/2.1.2138.7204.

[51] Grupotech. "Posibilidades de implantacion de instalaciones fotovoltaicas en la industria valenciana". 2011.

[52] Jordan, D. C. and Kurtz, S. R. "Photovoltaic Degradation Rates – An Analytical Review: Preprint". 2012.

[53] IDAE (Institute for Diversification and Saving of Energy). *Proyecto SECH-SPAHOUSEC, Análisis del consumo energético del sector residencial en España.* Tech. rep. IDAE, 2011.

[54] ANPIER. *Anuario Fotovoltaico 2019.* Tech. rep. Asociación Nacional de Productores de Energía Renovable (ANPIER), 2019.

[55] Cámara de Madrid. *Guía sobre empresas de servicios energéticos (ESE).* Tech. rep. 2010.

[56] Red Eléctrica de España. *PVPC | ESIOS electricidad · datos · transparencia.*

[57] Red Eléctrica de España. *Análisis | ESIOS electricidad · datos · transparencia.*

[58] Chase, J. *Trends in PV O&M pricing.* Tech. rep. BloombergNEF, 2018.

[59] Inflation.eu. *Inflación histórica España – inflación histórica España IPC.*

[60] Comisión Nacional de los Mercados y la Competencia (CNMC). “Documento de consulta pública sobre la propuesta de metodología de cálculo de la tasa de retribución financiera de la actividad de producción de energía eléctrica a partir de fuentes de energía renovables, cogeneración y residuos para el siguiente periodo”. 2018.

[61] Red Eléctrica de España. *REData | Red Eléctrica de España.*

[62] PVSyst. *Project design - Carbon Balance Tool - Detailed System LCE.*

[63] Chowdhury, M. S., Rahman, K. S., Chowdhury, T., Nuthammachot, N., Techato, K., Akhtaruzzaman, M., Tiong, S. K., Sopian, K., and Amin, N. *An overview of solar photovoltaic panels’ end-of-life material recycling.* 2020. DOI: 10.1016/j.esr.2019.100431.

[64] Atersa. *Línea ULTRA - Módulos Fotovoltaicos - Productos y Servicios - Atersa.*

[65] “G * Power 3.1 manual”. 2017.

[66] Gatsonis, C. and Sampson, A. R. “Multiple Correlation: Exact Power and Sample Size Calculations”. In: *Psychological Bulletin* 106.3 (1989), pp. 516–524. DOI: 10.1037/0033-2909.106.3.516.

[67] Cohen, J. *Statistical Power Analysis for the Behavioral Sciences Second Edition.* LAWRENCE ERLBAUM ASSOCIATES, PUBLISHERS, 1988.

[68] Banerjee, A., Chitnis, U., Jadhav, S., Bhawalkar, J., and Chaudhury, S. “Hypothesis testing, type I and type II errors”. In: *Industrial Psychiatry Journal* 18.2 (2009), p. 127. DOI: 10.4103/0972-6748.62274.

[69] Aydin, G. *Modeling of energy consumption based on economic and demographic factors: The case of Turkey with projections.* 2014. DOI: 10.1016/j.rser.2014.04.004.

[70] Tabachnick, B. G. *Experimental Designs Using ANOVA Epidemiology and Neurobehaviour of FASD in South Africa View project CyGaMEs View project.* Tech. rep. 2007.

Chapter 4

Techno-Economic Potential of Urban Photovoltaics: Comparison of Net Billing and Net Metering in a Mediterranean Municipality

Chapter adapted from the paper:

Enrique Fuster-Palop[1], Carlos Prades-Gil, Ximo Masip[1], J. D. Viana-Fons[1], and Jorge Payá[2].
Techno-Economic Potential of Urban Photovoltaics: Comparison of Net Billing and Net Metering in a Mediterranean Municipality. In: *Energies* (2023), Vol. 16, p. 3564.
DOI: https://doi.org/10.3390/en16083564.

[1] Grupo ImpactE Planificación Urbana SL, Carrer Pedro Duque, Camí de Vera s/n, 46022 Valencia, Spain.

[2] Instituto Universitario de Investigación en Ingeniería Energética, Universitat Politècnica de València, Camí de Vera s/n, 46022 Valencia, Spain.

Abstract:

Solar photovoltaic self-consumption is an attractive approach to increase autarky and reduce emissions in the building sector. However, a successful deployment in urban rooftops requires both accurate and low-computational-cost methods to estimate the self-consumption potential and economic feasibility, which is especially scarce in the literature on net billing schemes. In the first part of this study, a bottom-up GIS-based techno-economic model has helped compare the self-consumption potential with net metering and net billing in a Mediterranean municipality of Spain, with 3734 buildings in total. The capacity was optimized according to load profiles obtained from aggregated real measurements. Multiple load profile scenarios were assessed, revealing that the potential self-sufficiency of the municipality ranges between 21.9% and 42.5%. In the second part of the study, simplified regression-based models were developed to estimate the self-sufficiency, self-consumption, economic payback and internal rate of return at a building scale, providing $nRMSE$ values of 3.9%, 3.1%, 10.0% and 1.5%, respectively. One of the predictors with a high correlation in the regressions is a novel coefficient that measures the alignment between the load and the hours with higher irradiance. The developed correlations can be employed for any other economic or demand scenario.

Keywords: photovoltaics; urban rooftop photovoltaic economic potential; self-consumption; self-sufficiency; net billing; regression modelling.

Nomenclature

€: Euro.

3D: Three-dimensional.

A: Area.

AB: Apartment block.

CO_2: Carbon dioxide.

CF: Cash flow.

CR: Cost ratio.

d: Interest rate.

D_h: Hourly demand.

DL: Demand level.

DSF: Demand scale factor.

E_{PV}: Annual photovoltaic production.

Eq: Equation.

GIS: Geographic Information System.

GW h: Gigawatt hour.

I: Inflation rate.

I_{POA}: Global irradiance in the plane of array.

IRR: Internal rate of return.

IC: Installation costs.

IL: Investment level.

G_{POA}: Global irradiance in the plane of array.

kg: kilogram.

MW h: kilowatt-hour.

kW_n: Nominal kilowatt.

MW_p: kilowatt peak.

LiDAR: Light Detection and Ranging.

LOD: Level of detail.

LP: Load profile.

m: Linear meter.

M€: Millions of Euros.

m^2: Square meter.

MAE: Mean absolute error.

MFH: Multi-family house.

$\mathrm{MW_p}$: Megawatt peak.

$n_{contracts}$: Number of contracts.

NB: Net billing.

NM: Net metering.

NPV: Net present value.

$nRMSE$: Normalized root mean squared error.

$^\circ\mathrm{C}$: Degrees Celsius.

OLS: Ordinary Least Squares.

OR: Occupation rate.

P_{PV}: PV peak capacity.

PB: Economic payback.

PC: Postal code.

PL: Price level.

PV: Photovoltaic.

QR: Quantile regression.

R^2: Coefficient of determination.

RD: Royal decree.

$RMSE$: Root mean squared error.

SC: Percentage of Self-consumption.

SC_{annual}: Annual self-consumed energy.

SFH: Single-family house.

SR: Sizing ratio.

SS: Self-sufficiency.

t: Tonne.

TH: Terrace house.

VIF: Variance inflation factor.

4.1 Introduction

In recent years, photovoltaic (PV) energy has experienced a massive deployment. The European Union's (EU) total PV capacity increased from $167.5\,\mathrm{GW}$ in 2021 to $208.9\,\mathrm{GW}$ in 2022 and is expected to reach $600\,\mathrm{GW}$ by 2030 [1]. This rapid growth has been fostered by the consolidation of competitive manufacturing costs [2] as well as the favorable legal frameworks, policies and funds that promote the implementation of renewable systems [3]. The latter have been promoted to reduce emissions by at least 55% by 2050 in the EU [4].

Buildings in the EU are responsible for around 40% of the energy consumption and 36% of the CO_2 emissions in the zone [5]. PV self-consumption (PVSC) is a strategic approach to reach the emissions reduction target using unexploited rooftops [6]. Moreover, PVSC reduces sensitivity towards the volatility of electricity prices [7], increases independence from the grid [8] and involves citizens and other productive agents involved in the energy transition [9]. In this context, public and private agents and researchers need tools to quantify and prioritize which potential facilities on rooftops would have more impact.

For this purpose, a wide range of PV models and methodologies have been developed to assess the PV potential in urban areas [10]. Depending on the scope of the study, PV models can be classified according to their physical, geographical, technical and economic potential [11]. Most of the literature related to the urban PV potential is circumscribed within the energy production constraints (technical potential), from the irradiance and shadow assessment to the available rooftop space or module array configurations [12, 13]. In these studies, the economic dimension of the problem is out of scope due to the complexity or uncertainty of the cost scenarios [14].

As a consequence, there is scarce literature on the economic potential [14–16]. Furthermore, the applied billing scheme has a crucial influence on the feasibility results. As a relevant study in this area, Karoline Faith et al. developed a detailed GIS-based model to assess $2\,\mathrm{km}^2$ of urban area in Karlsruhe (Germany) considering the economic feasibility of facilities on rooftops and façades under a net metering (NM) scheme [17]. Wider economic potential assessments with NM were applied to 55,887 buildings in Lethbridge (Canada) [18] and to the old residential buildings of five districts of Nanjing (China) [19]. Nevertheless, economic potential studies contemplating a net billing (NB) scheme are even scarcer and very few analyze nonresidential uses. To the authors' knowledge, only Jordi Olivella et al. provided a large-scale NB assessment. The latter studied 5567 real residential load profiles with a sensitivity analysis depending on the surplus reward price in London (United Kingdom) [20]. NB in contrast with NM requires the use of electricity demand curves to estimate accurately the economic savings and they vary depending on the assumptions taken on the demand profiles, as studied in the literature for specific study cases but not on a large urban scale [21, 22]. In this field, the present work provides a large-scale economic PV potential sensitivity analysis by fluctuating the load profiles under an NB scheme with a bottom-up technoeconomic model at a building scale. This study covers residential, industrial, and tertiary buildings, analyzing for the PV impact in a representative Mediterranean town of Spain.

In parallel, there are few proposals for agile models to reduce the computational cost in urban planning assessment. The latter would be of special interest in NB models. Simplified models based on regressions are generally employed to estimate PV production [23, 24]. Some cases require complex machine-learning models [25, 26]. In addition to an economic payback (PB) regression model proposed by the authors [27], a study case was found in which the payback and NPV model are estimated, based on installation design parameters such as power, tilt and azimuth angles, inclinations, electricity prices, among others [28]. However, both models are not very flexible to other scenarios of electricity consumption and costs. Taking advantage of the results of the PV economic potential, in the second part of this work, a methodology is proposed to develop regression-based and versatile models for different consumption and economic scenarios. For this purpose, a novel dimensionless predictor is defined to improve the correlation results. The regressions are capable of estimating energy metrics, such as self-sufficiency (SS) and self-consumption rate (SC), and economic metrics, such as PB and internal rate of return (IRR), denominated as target variables.

As a result of the previous research in the literature, the main novelties of the present work can be summarized as follows:

- NB has been compared for the first time with NM in a complete municipality. This helps to extend the impact of the results given that the regulation is different depending on the country.
- The impact of the demand profile has been studied for the first time at a municipality level under NB and NM scenarios to assess the global SS potential.
- Regressions have been developed for the first time to estimate SS, SC, PB, and IRR, including all the necessary parameters to implement them in a wide range of demand, costs, or price scenarios.
- A new dimensionless predictor has been introduced to address the alignment between the load and the hours with higher irradiance.
- A new optimization sizing criteria for NB has been included to guarantee high SS rates and low PB.

The article is structured as follows. Section 4.2 describes the techno-economic model and the scenarios, as well as the methodology to build the simplified regressions. In Section 4.3, the global potential results of the municipality are given, together with the impact of different load profiles on the global potential. Then, the simplified regression results are discussed, and their error metrics are calculated. Finally, in Section 4.4, the main conclusions are drawn.

4.2 Materials and Methods

Figure 4.1 describes the methodology that has been adopted to assess the economic potential of the municipality under an NB scheme, as well as the regressions developed to provide an agile estimation method for PV assessment in urban areas.

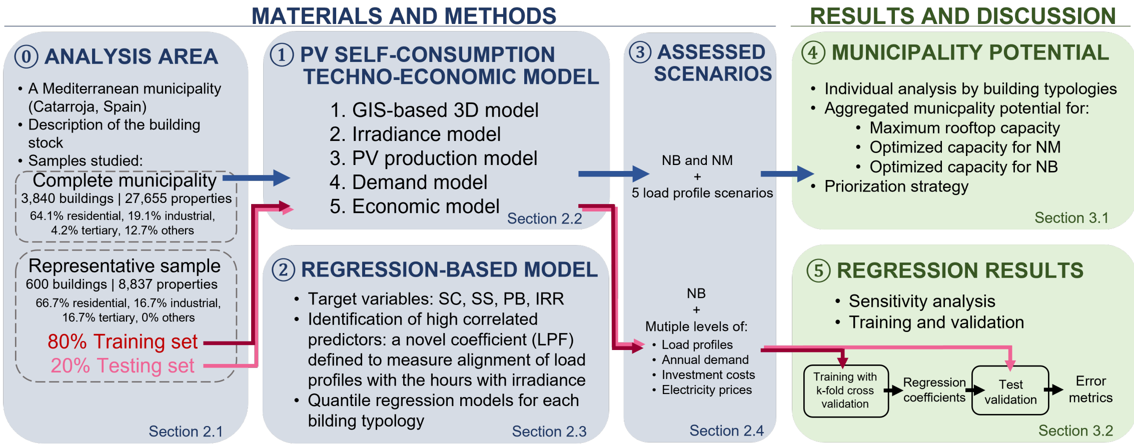

Figure 4.1: Methodology workflow.

First, the urban area as well as its building stock are described. Next, the techno-economic model is presented. In this section, the main assumptions, and inputs for the base case of each submodule are described with an emphasis on the demand model, which is based on real measurements. The third step presents the methodology to train and test the regressions as well as the novel predictors. Different scenarios are presented, regarding the demand, investment costs and electricity prices, as well as the different combinations of scenarios employed to train the regression-based model.

4.2.1 Analysis Area

The present study has been applied to the complete municipality of Catarroja, Spain (39.4028°N, 0.4044°W), which has a total extension of 13.16 km^2, and a population of 28,509 inhabitants [29]. According to the Köpen climate classification, the climate of this region is classified as Csa (hot-summer Mediterranean), with an annual global horizontal irradiation of 1,782 kWh/year and an average temperature of 17.9 °C in 2021 [30]. The weather conditions are similar to other European cities such as Rome (Italy), Nice (France), Athens (Greece), or Split (Croatia) [31]. The total building stock comprises 3,840 independent buildings [32] that are spatially distributed according to Figure 4.2. The western part is an industrial park, while the eastern part is mainly the residential town center. For a more detailed PV potential analysis among buildings, the residential sector has been classified into four typologies according to the Tabula project [33], namely, single-family houses (SFHs), terrace houses (THs), multi-family houses (MFHs) and apartment blocks (ABs).

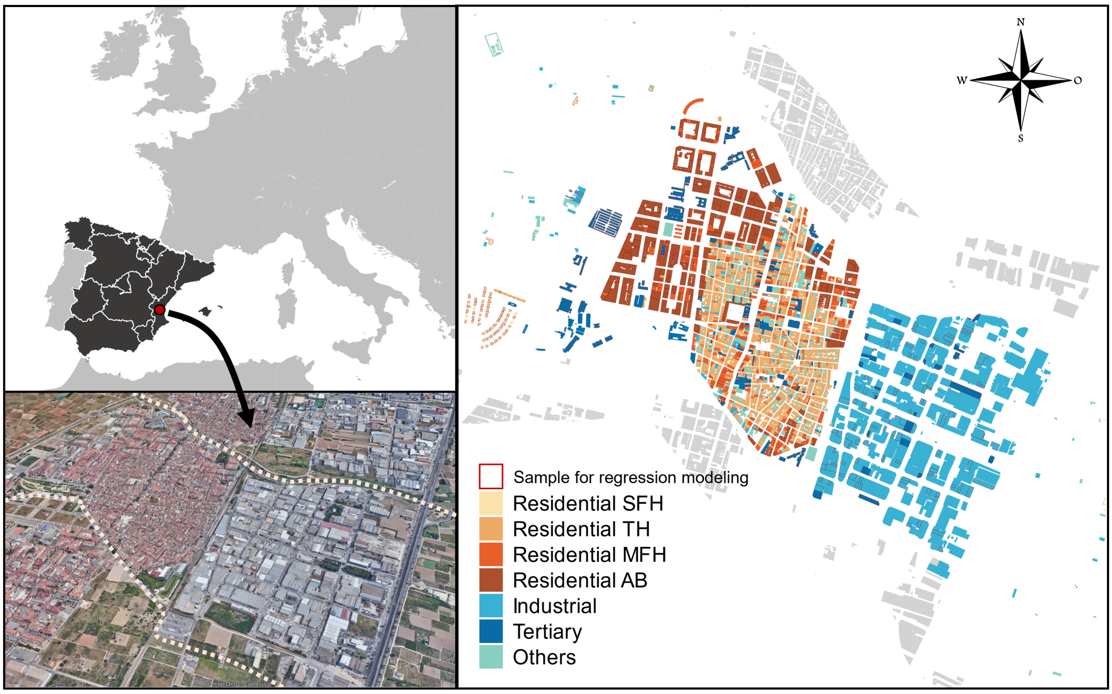

Figure 4.2: Geographical location and building typologies of Catarroja (Spain).

The most abundant typologies are THs. However, the largest cumulative rooftop areas are found in industrial, tertiary and ABs, as summarized in Table 4.1. The buildings described as others do not meet the Tabula classification criteria and are out of the scope of the present study given their wide range of patterns and uses.

Table 4.1: Building stock of the municipality of Catarroja (Spain).

Typology	**Absolute Frequency**	**Relative Frequency**	**Number of Properties**	**Built Area**	**Rooftop Area**
-	-	%	-	m^2	m^2
Residential SFH	132	3.44	578	23,904	14,091
Residential TH	1,842	48.00	6,331	451,411	206,908
Residential MFH	270	7.03	3,588	345,254	76,444
Residential AB	216	5.62	13,517	1,125,487	214,148
Industrial	734	19.10	1,283	504,124	462,607
Tertiary	160	4.17	794	348,652	17,923
Others	486	12.7	1,564	171,407	119,613
Total	3,840	100.00	27,655	2,970,239	1,273,042

For the regression modeling, a representative sample of 600 buildings Figure 4.2 was selected due to the high computational cost of simulating the complete municipality under the wide range of scenarios explained in Section 4.2.4. Six simple random samples of one hundred buildings were selected for each typology. Finally, the nonparametric Mann–Whitney U-Test [34] concluded that the difference in medians of rooftops and built areas between the samples and the total building stock is not statistically significant for each typology, providing p-values above 0.25 and 0.15, respectively.

4.2.2 Techno-Economic Model

The bottom-up techno-economic model is composed of several submodels that allow the energy and economic performance of each rooftop facility on any building of the municipality to be obtained with the specifications provided in the present section.

The 3D GIS-based, irradiance and production model foundations are detailed in previous research by the authors. The main model hypotheses are summarized below. As a first step, a 3D GIS-based model obtains a 3D model using as main inputs the vectorial geometry of the buildings from cadaster [32] and the height of the rooftops from LiDAR data with a density of $0.5\,\mathrm{points/m^2}$ [35]. The combination of GIS-based methods and LiDAR is a common and robust approach found in the literature when estimating the PV technical potential since the shadows cast by surrounding buildings reduce significantly the direct and diffuse irradiance received by the modules [10]. The model, by means of clustering techniques, helps obtain the tilt and azimuth of each surface on any rooftop, with a level of detail 2 (LOD2) in 3D models according to the CityGML standard [36]. A filter is also applied to consider a minimum rooftop area and width and to remove the small rooftop spaces [37]. For the centroid of each of the remaining surfaces, the global irradiance is applied for all combinations of azimuth and tilt using the Liu and Jordan isotropic irradiance model [38], which is widely employed in urban areas due to its accuracy and simplicity [39, 40]. The shadows cast by nearby obstacles and buildings are considered to calculate the skyline of surrounding obstacles, as detailed in a previous work [27, 41, 42]. The irradiance hourly time-series components and ambient temperatures are obtained from PVGIS for the year 2021 [30]. The PV production is obtained through time series and the module efficiency varies with the temperature through the equation defined in reference [43]. For each surface, optimization is conducted for the tilt and azimuth angles in order to maximize the annual PV production. Specific tilt and azimuth limit angles are also considered to avoid low global efficiencies, as well as a minimum distance between panel rows. The dimensions of a commercial module are also considered in this optimization of possible configurations to avoid shadows between rows. Next, specific performance ratios and other factors are considered for the conversion from DC to AC, in agreement with experimental data [43]. As a result, the maximum AC hourly time series production and installation capacity are calculated for each facility.

Parallel to the production model, a demand model was developed to estimate the hourly electricity load curves of each dwelling or property of the municipality. One of the limitations in large-scale urban PVSC studies is the availability of real load curves to provide realistic results [44]. To reduce this gap, this model is based on measured consumption data provided by the public API of Datadis [45], as also employed in other research areas [46]. Datadis supplies the aggregated hourly electricity consumption by economic sectors (residential, industrial and services) and postal code, considering all the distributor system operators in the municipality, as well as other characteristics such as the number of contracts per sector in the postal code. This study employs the aggregated load profiles of the complete postal code (PC46470) of

Catarroja. Next, the aggregated load profile of the postal code is decomposed in the following terms: (i) a dimensionless hourly time series for each economic sector normalized by its aggregated annual consumption, denominated load profile (LP). (ii) A demand scale factor (DSF) or relationship between the annual consumption and built area, calculated through Eq. 4.1. The subscript s, PC refers to the economic sector s and postal code PC for each variable.

$$DSF_{s,PC} = \frac{D_{annual,s,PC}}{n_{contracts,s,PC}} \cdot \frac{1}{OR_{s,PC}} \cdot \frac{1}{A_{s,PC}} \tag{4.1}$$

The variables in Eq. 4.1 are:

- DSF: demand scale factor.
- D_{annual}: annual demand.
- $n_{contracts}$: number of contracts. Eq. 4.1 assumes that each dwelling or property has a single electric contract.
- OR: Occupancy rate, defined as the ratio between the inhabited properties and the total number of properties. For industrial and tertiary sectors this rate was considered 1 (full occupancy), while for the residential sector, a value of 0.81 was assumed according to the 2011 building stock census [47].
- A: average built area of each building typology, as estimated from the cadaster.

Table 4.2 shows the DSF obtained with Eq. 4.1 for each economic sector in the PC studied.

Table 4.2: DSF values obtained through Eq. 4.1 for each economic sector.

Economic Sector	**Annual Demand**	$n_{contracts}$	OR	A	DSF
-	MWh/year	-	-	m^2	$\mathrm{kWh/m^2 year}$
Residential	65,839.6	24,009	0.8119	107.22	31.51
Industrial	52,247.8	760	1.0000	416.81	164.88
Tertiary	72,357.9	4,401	1.0000	246.64	66.65
Unspecified	57.1	25.1	1.0000	53.54	42.52

With both variables, and the area of each dwelling ($A_{dwelling}$), which is also provided by the cadaster together with its economic sector or use, the hourly load profile of each dwelling ($D_{h,dwelling}$) of the municipality is calculated as follows in Eq. 4.2:

$$D_{h,dwelling} = LP \cdot DSF_{s,PC} \cdot A_{dwelling} \tag{4.2}$$

The matching of the hourly load and production curves is performed at a dwelling level. In buildings with several independent properties that share the same PV installation, each user has been assigned a production curve proportional to the relationship between their annual demand and the aggregated annual demand of all the dwellings in the building. Even if the regulation contemplates the possibility of hourly dynamic coefficients per user to improve the energy and economic performance of facilities [48], they have been assumed to be constant throughout the year for this planning context with estimated load profiles.

The economic balance was implemented following an NB scheme, as established in the Spanish regulation (RD244/2019) [49]. The surpluses are remunerated with a lower price level than the average price of the energy term of the electricity tariff. A peculiarity of this billing scheme in Spain is that, in a given billing period (typically one month), the sum of the economic surplus remuneration cannot be higher than the economic value of the energy consumed from the grid. Thus, the user cannot perceive a negative energy term in the electricity bill at the end of the billing period. A three-period tariff scheme (2.0TD) was adopted in residential properties and a six-period scheme (3.0TD) for tertiary and industrial users, with hourly distributions found in the Spanish regulation [50]. The electricity prices shown in Table 4.3 are based on the average prices obtained from the operator of the Spanish electricity system [51] and an electricity supplier [52] for the 2.0TD and 3.0TD tariff, respectively, for the period between June 2021 (start of the legal application of the current tariffs schemes) and May 2022. The same period was also adopted for the price of surpluses.

Table 4.3: Electricity prices for each tariff period.

Tariff	Period 1	Period 2	Period 3	Period 4	Period 5	Period 6
2.0TD	0.2170	0.2570	0.3221	-	-	-
3.0TD	0.2900	0.2900	0.2275	0.2035	0.1867	0.1728

To estimate the investment costs of each facility, following the method of a previous study in the same region [53], a polynomial regression (Eq. 4.3) was introduced to account for the economy of scale of installation costs (IC) of 2022 according to IVACE [54], which does not consider any subsidy.

$$IC(€) = 4.816 \times 10^{3} + 1.084 \times 10^{3} \cdot P_{\mathrm{PV}} + 9.801 \times 10^{-2} \cdot P_{\mathrm{PV}}^{2} + 2.071 \times 10^{-3} \cdot P_{\mathrm{PV}}^{3} + \\ + 3.051 \times 10^{-6} \cdot P_{\mathrm{PV}}^{4} - 1.692 \times 10^{-9} \cdot P_{\mathrm{PV}}^{5} \quad (4.3)$$

Where P_{PV} is the peak installed capacity of the facility in $\mathrm{kW_p}$.

Finally, the capacity of the facility is sized according to its respective load profiles, maximizing the ratio between the global SS and the economic payback (PB) of the facility. The optimization is performed by means of the optimize function in the R package *stats* [55, 56]. The model performs multiple matching iterations for different PV capacities until convergence. The maximization of the ratio SS/PB ensures high SS values without oversizing the facilities while keeping high profitability. The optimization of this ratio, which is novel to the best of the authors' knowledge, performs similar results as the optimization of SC and SS [57]. In addition, the proposed method represents a simplified alternative to the optimization method of technical and economic potential found in the literature [11].

As a last step, the saved emissions are obtained using an average of the national grid emission factor between 2019 and 2021.

The simulations were conducted for a lifetime period of 25 years with an hourly resolution, which is the regular standard when modeling PVSC systems in urban areas [58, 59] and is sufficient to size these systems [60]. A yearly degradation in the PV modules and constant inflation and interest rates were assumed. No storage systems were considered due to their high costs [61]. The main parameters of the techno-economic model are gathered in Table 4.4.

Table 4.4: Summary of input in the base case scenario.

Parameter	Value	Units	Reference
Minimum area	5	m^2	The present study
Minimum width of the area	2	m	The present study
Minimum distance between modules	0.2	m	The present study
Maximum azimuth angle	±45	°	The present study
Maximum tilt angle	40	°	The present study
Albedo coefficient	0.2	-	[62]
Dirtiness losses	2	%	[63]
Module rated maximum power	390	kW_p	[64]
Module efficiency	20.9	%	[64]
Module width	1.052	m	[64]
Module length	1.776	m	[64]
NOCT	45	°C	[64]
Temperature coefficient of Pmax	-0.350	%/°C	[64]
Module degradation	0.816	%/year	[43]
PR	79.24	%	[43]
Surplus remuneration	0.1776	€/Wh	[51]
O&M costs	9.35	€/W_p	[65]
Inflation rate	2	%	[66]
Interest rate	5	%	[67]
VAT	21	%	[68]
Electricity tax	5.113	%	[68]
Emissions factor	0.1593	kg CO_2/kWh	[69]
Facility lifetime	25	years	[70]

4.2.3 Regression Modeling

The target variables selected (SS, SC, PB and IRR) are those that best describe the per-formance of a facility in relative terms since they can be compared with other facilities re-gardless of their PV capacity [59]. These variables are calculated as defined in Equations eqs. (4.4) to (4.7):

$$SS(\%) = \frac{100 \cdot SC_{annual}}{D_{annual}} \tag{4.4}$$

$$SC(\%) = \frac{100 \cdot SC_{annual}}{E_{PV,annual}} \tag{4.5}$$

$$PB(\text{years}) = \frac{IC}{\sum_{n=1}^{\text{lifetime}} CF_n \cdot \left(\frac{1+i}{1+d}\right)^n} \tag{4.6}$$

$$IRR \rightarrow NPV = 0 = \sum_{n=1}^{lifetime} \frac{CF_n}{(1+IRR)^n} \tag{4.7}$$

where SC_{annual} represents the annual self-consumed production, D_{annual} the annual demand, $E_{PV,annual}$ the annual PV production, i the inflation rate, d the interest rate, and CF_n the cash flows during the year n. The IRR is obtained by solving Eq. 4.7 when Net Present Value (NPV) is 0.

As one of the aims of this article is to provide a low-cost method to estimate the economic potential in buildings with scarce information available, three potential predictor variables have been introduced, based on their correlation with the target variables:

- The load profile factor (LPF) is a dimensionless coefficient between 0 and 1 that measures the alignment between the load and the sun hours with more irradiance. This novel parameter is defined in Eq. 4.8 as the cumulative sum of the product of two dimensionless time series. LPF is specific for each PV facility.

$$LPF = \sum_{1}^{8760} \frac{D_h}{\sum_1^{8760} D_h} \cdot \frac{I_{POA,h}}{\max(I_{POA,h})|_{\text{each day}}} \tag{4.8}$$

  where:

  - D_h represents the hourly demand curve result of the aggregation of all the individual load curves of all the properties that are connected to the PV facility.
  - $I_{POA,h}$ represents the hourly demand curve result of the aggregation of all the individual load curves of all the properties that are connected to the PV facility.

  The first term in Eq. 4.8 is the D_h curve normalized with respect to the annual demand and the second term is the hourly I_{POA} curve normalized with the maximum I_{POA} of each day. With this approach, the hour of maximum production in sun hours weighs the maximum (1), and the hours of consumption in which there is no radiation weigh the minimum (0). The rest of the demands in daytime hours are weighted with a normalized production between 0 and 1. The annual cumulative sum of this product is the annual fraction of total demand consumed in conditions of the hour of peak production. This concept is similar to the capacity utilization factor of a PV installation (fraction of hours per year in which energy is produced under nominal conditions) and represents the fraction of hours per year in which electricity consumption took place under maximum production conditions. This variable could partially explain the SS as well as the PB and IRR under an NB scheme.

- The sizing ratio (SR), defined as the relationship between the peak of the load curve of the building and the peak of PV installed power, quantifies the oversizing or undersizing degree of the facility compared with the demand. Low values imply a high SC and a low SS and vice versa. Quantifying this rate is crucial in an NB scheme.
- The cost ratio (CR), defined as the relationship between the installation costs and the installation capacity, implicitly measures the size and economy of scale of the facility.

Additionally, to increase the flexibility and robustness towards price and costs fluctuations and other demand scenarios, three extrinsic variables were also incorporated as predictors:

- The demand level (DL), a rate that measures the variation in the annual demand per unit area compared with the base case scenario.
- The investment level (IL), a rate that quantifies the variation in the installation unit costs compared with the base case scenario.
- The price level (PL), a rate that measures the variation in the electricity prices of each tariff period and the surplus remuneration compared with the base case scenario.

The Ordinary Least Squares (OLS) regression constitutes a typical first approach in regression modeling [71]. However, a low degree of compliance with the OLS assumptions of linearity, normality, homoscedasticity and independent residuals and an absence of multicollinearity may lead to low confidence in the intervals inferred for the regression coefficients [72]. Due to the non-parametric nature of the distributions of the target variables obtained in the preliminary global PV potential results presented in Section 3, a quantile regression (QR) approach is proposed in this paper as an alternative to train robust models and provide more simple expressions than other nonparametric approaches such as multiadaptive regression splines. QR neither assumes normality nor homoscedasticity and is robust to outliers since the estimation is based on conditional quantile functions as a linear combination of predictors instead of mean models from OLS [73, 74]. The *quantreg* R package was used to train the models [75].

Prior to the model training, the Pearson correlation coefficients are obtained to validate and select the above-defined predictors among other constructive characteristics with higher correlation with the target variables. Next, the absence of multicollinearity is checked through the variance inflation factor (VIF). As a last step in the definition of the regression formulas, multiple Box–Cox transformations [76] were applied to overcome the nonlinearity [77]. In most of the cases, the suggested exponents provided by the boxcox function of the *MASS* R package [78] were cubic and square roots. Additionally, the squared root transformation for the PB target variable was applied to reduce the skewness of the PB distribution and its linearity with the IRR. Finally, the building typology was included as a categorical predictor, according to the statistical differences in distributions among building typologies for the target variables detected in Section 4.3. As a result, six regression fits for each target variable are defined in Equations eqs. (4.9) to (4.12), where i represents a specific building typology.

$$\begin{aligned} SS_i(\%) &= f(SR, CR, LPF, DL) = \\ &= k_0 + k_{0,i} + k_{1,i} \cdot \sqrt{SR} + k_{2,i} \cdot CR + k_{3,i} \cdot LPF + k_{4,i} \cdot \sqrt{LPF} + k_{5,i} \cdot DL \end{aligned} \tag{4.9}$$

$$\begin{aligned} SC_i(\%) &= f(SR, CR, LPF, CR, DL, SS) = \\ &= k_0 + k_{0,i} + k_{1,i} \cdot SR + k_{2,i} \cdot \sqrt{SR} + k_{3,i} \cdot LPF + k_{4,i} \cdot \sqrt{LPF} + \\ &\quad + k_{5,i} \cdot \sqrt{DL} + k_{6,i} \cdot SS + k_{7,i} \cdot \sqrt{SS} \end{aligned} \tag{4.10}$$

$$\begin{aligned} IRR_i(\%) &= f(SR, CR, LPF, DL, IL, PL, SC) = \\ &= k_0 + k_{0,i} + k_{1,i} \cdot SR + k_{2,i} \cdot \sqrt{SR} + k_{3,i} \cdot CR + k_{4,i} \cdot \sqrt{CR} + k_{5,i} \cdot \sqrt[3]{CR} + \\ &\quad + k_{6,i} \cdot LPF + k_{7,i} \cdot \sqrt{LPF} + k_{8,i} \cdot \sqrt[3]{LPF} + k_{9,i} \cdot DL + k_{10,i} \cdot IL + \\ &\quad + k_{11,i} \cdot PL + k_{12,i} \cdot SC + k_{13,i} \cdot \sqrt{SC} + k_{14,i} \cdot \sqrt[3]{SC} \end{aligned} \tag{4.11}$$

$$\frac{1}{\sqrt{PB_i}}(\text{years}^{0.5}) = f(IRR) = k_{1,i} \cdot IRR + k_{2,i} \cdot IRR^2 + k_{3,i} \cdot IRR^3 \tag{4.12}$$

These novel regressions constitute an improvement in the PB regression defined by the authors in a previous work [27], since the latter only covered facilities that occupied all the rooftop area without considering their sizing according to the load profiles.

For the training process, the results dataset obtained with the techno-economic model for each scenario defined in Table 4.5 was randomly split 80% into a training set and the remaining 20% into a testing set, commonly employed in the literature [71]. With the first split, a 10-fold cross-validation [43] was conducted to model each QR for each target variable. The quantile selected to predict each target variable minimizes the $RMSE$ by performing a parametric calculation using quantiles between 0.05 and 0.95 with steps of 0.05.

Finally, the testing dataset is employed to calculate the error metrics of mean absolute error (MAE), root mean squared error ($RMSE$), normalized root mean squared error ($nRMSE$) and the coefficient of determination (R^2), through their respective Equations eqs. (4.13) to (4.16).

Table 4.5: Simulation scenarios for the development of correlations.

Variables	Municipality Global Analysis	Regression Modeling
Sample size	Complete municipality	600 buildings
Load profile	LPA, LPB, LP0*, LPC, LPD	LPA, LPB, LP0*, LPC, LPD
Demand level	1.0*	0.6, 0.8, 1.0*, 1.2, 1.4, 1.6, 1.8
Investment level	1.0*	0.5, 0.6, 0.7, 0.8, 0.9, 1.0*, 1.1, 1.2
Price level	1.0*	0.4, 0.5, 0.6, 0.7, 0.8, 0.9, 1.0*, 1.1, 1.2
Billing scheme	NB*, NM	NB*

$$RMSE = \sqrt{\frac{\sum_{i=1}^{N}(y_i - \hat{y}_i)^2}{N}} \tag{4.13}$$

$$nRMSE = \frac{\sqrt{\frac{1}{N}\sum_{i=1}^{N}(y_i - \hat{y}_i)^2}}{\bar{y}_i} \tag{4.14}$$

$$MAE = \frac{1}{N}\sum_{i=1}^{N}|y_i - \hat{y}_i| \tag{4.15}$$

$$R^2 = 1 - \frac{\sum_{i=1}^{N}(y_i - \hat{y}_i)^2}{\sum_{i=1}^{N}(y_i - \bar{y})^2} \tag{4.16}$$

Where y_i, $\hat{y}_i$, and $\bar{y}$ are the measured, predicted and mean measured values, respectively, and N is the number of samples.

4.2.4 Assessed Scenarios

The PV potential of the municipality has been performed under different values of DL, CL, PL, load profiles and billing schemes. In addition to the base load profile obtained from Datadis for each economic sector (named henceforth as LP0), four different hourly profiles were considered for each sector (LPA, LPB, LPC and LPD), using measured profiles from several consumers in the municipality, as shown in Figure 4.3. The choice is based on finding different consumption patterns with the help of the values obtained for the load profile factor (LPF) for the global horizontal irradiance of the municipality. As a result, and according to the LPF values, two scenarios (LPA and LPB) have demands more aligned with high irradiance hours compared with LP0, while the other two (LPC, LPD) present more consumption during the extreme hours of the day.

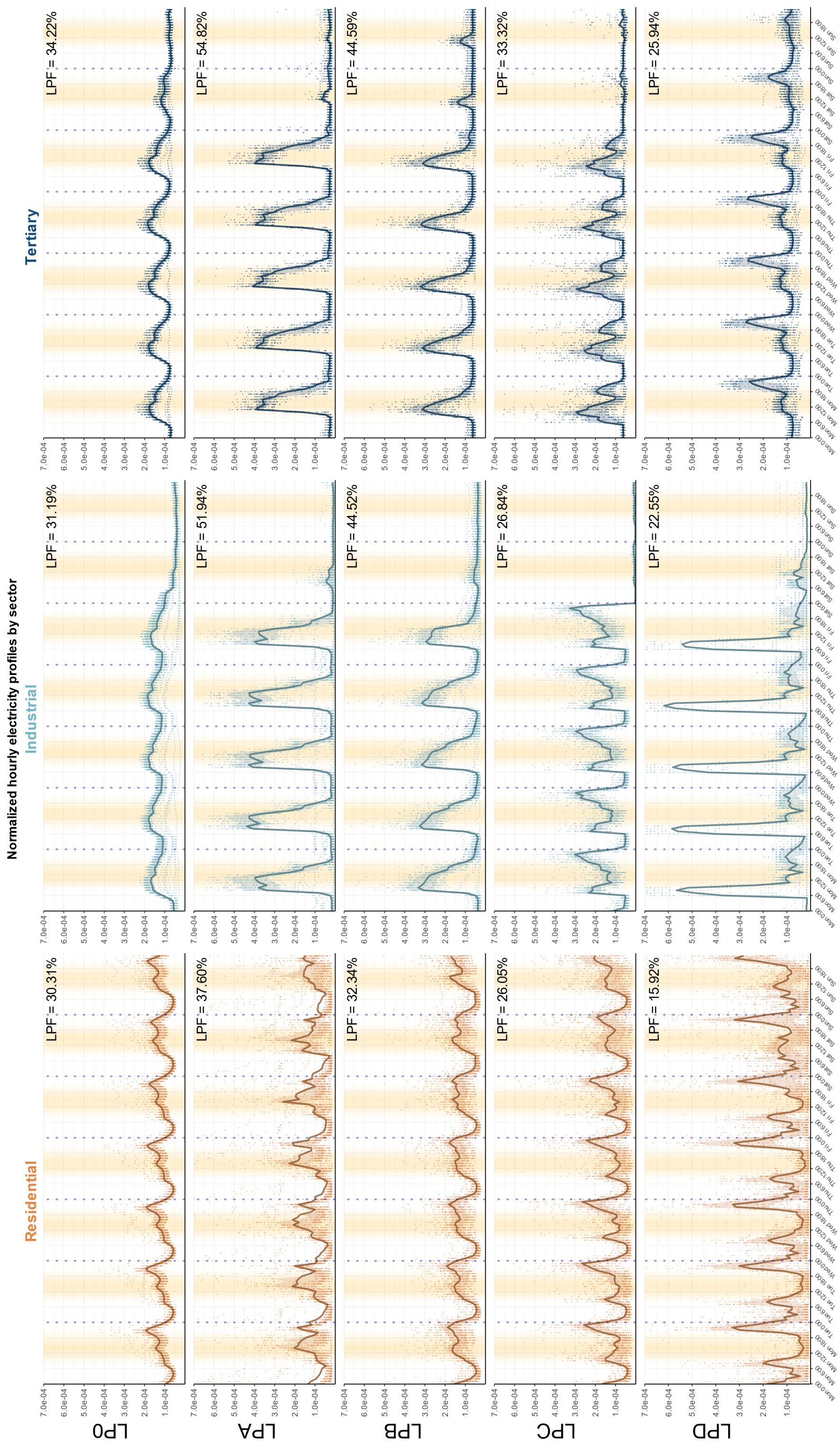

Figure 4.3: Normalized hourly load profiles of the assessed scenarios and their respective load profile factor.

In sum, five load profile scenarios have been studied for NB and NM schemes, respectively, as summarized in Table 4.5.

For the regression modeling to predict the target variables, in addition to including the above-mentioned load profiles scenarios, the variables of DL, IL and PL were modulated with the multiplication factors shown in Table 4.5. When modulating a variable, the other variables remain constant in the base scenario values.

4.3 Results and Discussion

This section is structured in two parts. The first part, Section 4.3.1, presents the results of the individual PVSC of the different building typologies, and also on an overall scale for the entire municipality. The second part, Section 4.3.2, shows the regression modeling results of SS, SC, PB and IRR for a representative sample of buildings in the municipality.

4.3.1 Municipality Self-Consumption Potential

Individual Results for the Different Building Typologies

For the NB base scenario, which meets the current regulatory framework in Spain, Figure 4.4 shows the spatial distribution of the optimized PV capacity and PB of each building of the municipality. While the buildings in the town center, mostly THs, require low PV capacities with higher PB, the opposite trend is detected in the buildings on the outskirts, which are generally industrial and MFHs. This is reflected in the bimodality of the histograms. A total of 358 buildings were not suitable for installing PV systems due to a lack of rooftop space without shadows.

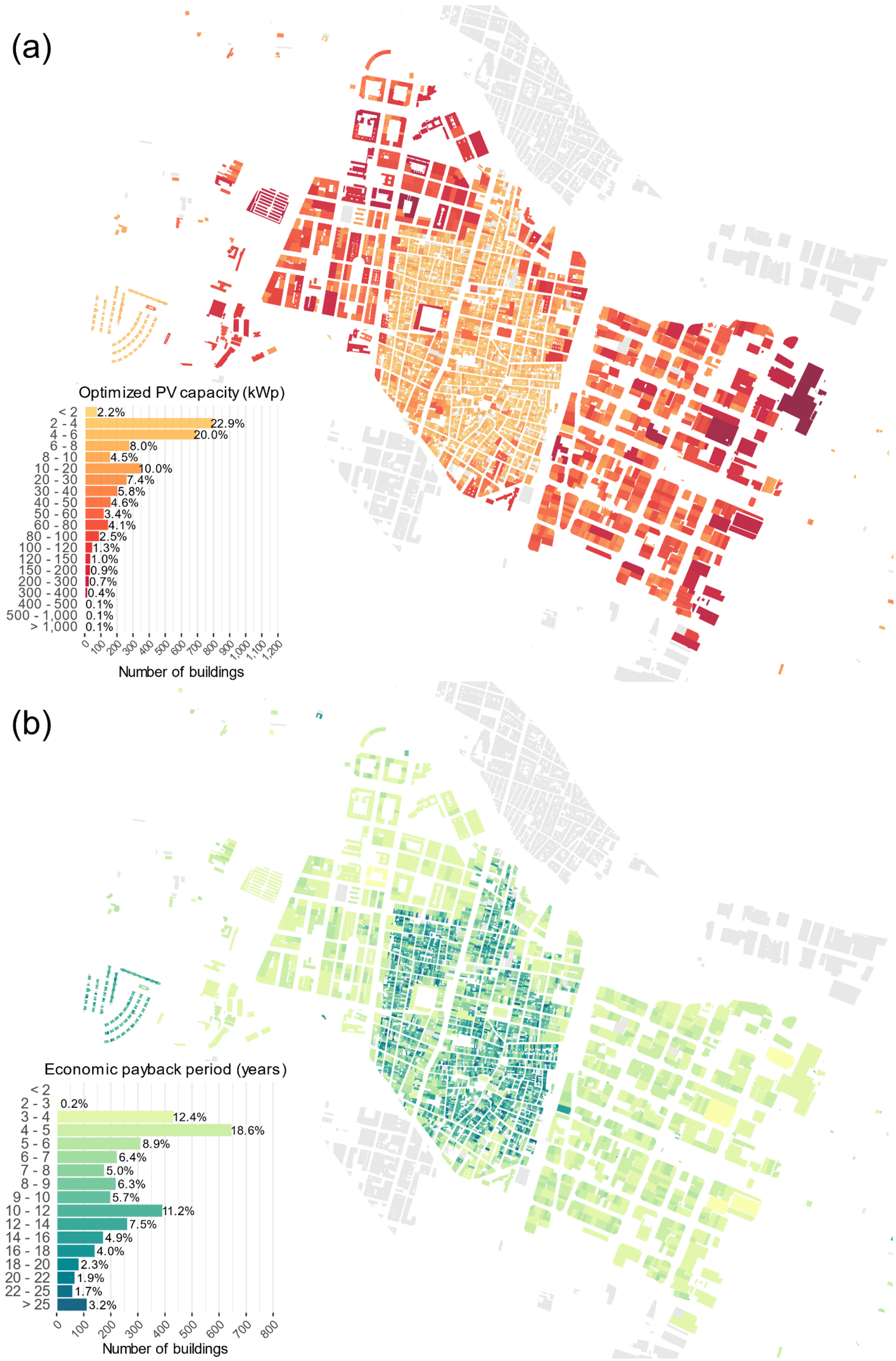

Figure 4.4: Spatial distribution in the municipality and histograms of (a) optimal capacity and (b) economic payback of the facilities for the base scenario.

Figure 4.5a and Table 4.6 show the impact of the billing scheme on the optimal sizing of PV facilities. Since surplus remuneration in NB represents approximately one-third of the regular price in the electricity tariff, the sizing optimization tends to minimize the surpluses to guarantee the profitability of each facility. In an NM scheme, the sizing tends to maximize the PV production, reaching peak powers near the maximum available on the rooftops. Despite this increase, SS and SC remain similar to the values obtained with the NB scheme. However, SS and SC of facilities with a smaller number of consumers, normally located in residential SFH and TH, are more sensitive to an increase in PV capacity, experiencing increments of $5.0\,\%/\mathrm{kW_p}$ for SS and $3.1\,\%/\mathrm{kW_p}$ for SC in contrast with the $0.9\,\%/\mathrm{kW_p}$ for SC and $1.0\,\%/\mathrm{kW_p}$ for SS of the residential AB according to their median values.

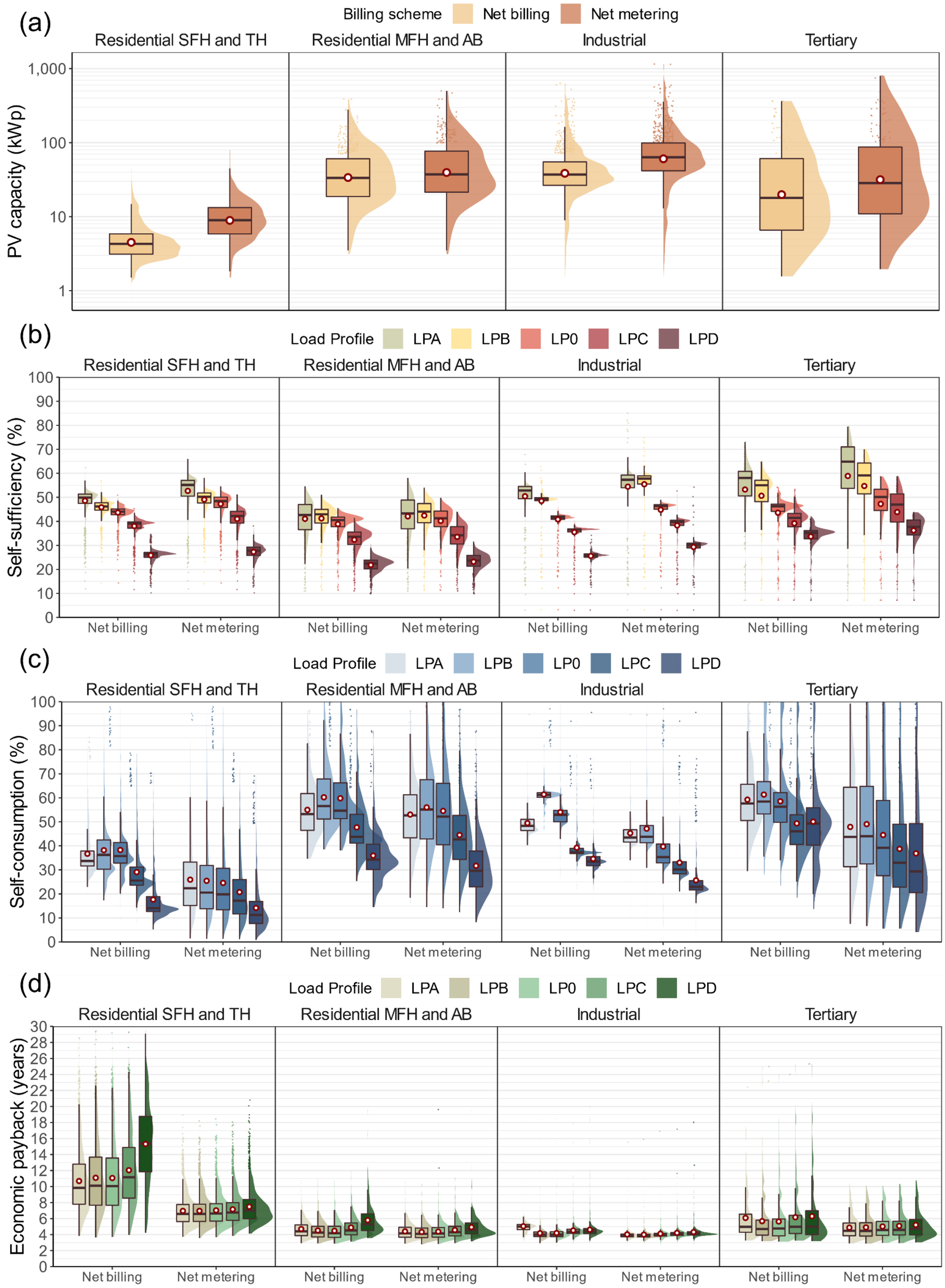

Figure 4.5: Boxplots of (a) optimal capacity of the facilities for the base scenario, and (b) SS, (c) SC and (d) PB for the different building typologies and load profiles scenarios.

Table 4.6: Main statistical values of PV capacity, SS, SC and PB by building typologies and billing scheme for the base load profile scenario.

Billing Scheme	**Building Typology**	**Capacity**[a]	$\boldsymbol{SS}$[a]	$\boldsymbol{SC}$[a]	$\boldsymbol{PB}$[a]
-	-	kW_p	%	%	years
NB	Residential SFH	4.68/9.20	42.77/43.34	41.75/40.43	6.75/9.07
	Residential TH	4.29/5.23	44.06/43.66	35.71/38.24	9.96/10.77
	Residential MFH	20.70/23.30	40.58/38.66	54.69/59.58	4.77/5.02
	Residential AB	66.50/78.60	40.48/39.12	54.58/60.05	3.69/3.80
	Industrial	37.10/54.90	41.57/40.82	52.94/54.01	4.01/4.18
	Tertiary	17.90/48.80	46.27/43.60	56.32/58.79	4.60/5.45
NM	Residential SFH	16.80/28.60	50.36/48.83	12.24/19.31	5.31/5.85
	Residential TH	8.97/10.30	48.42/47.23	19.87/24.65	6.65/7.05
	Residential MFH	23.80/28.00	41.15/39.88	54.18/54.76	4.62/4.85
	Residential AB	77.60/95.70	41.49/40.57	51.61/54.26	3.72/3.79
	Industrial	63.60/88.60	46.39/44.83	35.30/39.70	3.96/4.11
	Tertiary	28.50/76.90	50.14/47.26	39.29/44.86	4.57/5.02

[a] Median/Mean.

For the base case scenario, SS are similar among building typologies, presenting the SFHs and THs average values over 43% since the optimization tends to oversize facilities to reduce power unit costs and maximize SS, as seen in their low SC levels. This rate is similar in tertiary buildings thanks to the high LPF of the load profile, and higher consumers present SS values below 40%, mainly because of their high demand density.

The SC results for small residential consumers, such as TH, present an average value of 28.2%, which contrasts with the 60.1% from the residential AB. The aggregation of consumers and the rooftop space limitation allow higher SC rates to be obtained.

The most significant differences between NB and NM schemes are identified in the PB values. The highest drop in paybacks adopting an NM scenario is perceived by SFH and TH consumers. Their PB is reduced from 9.1 years to 5.9 and from 10.8 years to 7.1 years, respectively. The high payback values in the NB scheme are caused by higher power unit costs and a greater surpluses rate, with lower remuneration than the electricity tariff. In contrast, installations on ABs and industrial buildings, with greater economies of scale and SC, present average PBs of 3.8 and 4.2 years, respectively.

The effect of the load profile alignment with the sun hours is also gathered in Figure 4.5b–d and Table 4.7. As defined in the methodology section, the lowest SS rates match with the profiles with the lowest LPF, in this case, residential AB. In residential MFH and TH, with few dwellings and electricity consumption in the central sun hours, SS rates above 50% can be obtained in some cases. In MFH and AB buildings with multiple uses, the load profile aggregation tends to flatten the global demand resulting in an asymptotic growth of up to 44.2% for average SS with higher LPF. The highest SS rates are found in the tertiary and industrial sectors with averages of 52.5% and 56.8%, respectively. Regarding the lower limits, the average SS is over 20% for all the load profiles assessed.

Table 4.7: Main statistical values of LPA, LPB, LPC and LPD by building typologies and billing scheme for the base load profile scenario.

Variable	**Building Typology**	**LPA***	**LPB***	**LP0***	**LPC***	**LPD***
SS (%)	Residential SFH	48.65/48.51	52.18/51.94	46.56/46.48	40.62/40.87	27.35/27.73
	Residential TH	51.65/51.40	48.16/48.05	46.00/46.02	40.22/40.12	27.04/27.01
	Residential MFH	44.00/42.15	43.91/42.42	41.28/40.11	34.59/33.58	23.69/23.18
	Residential AB	44.00/42.15	43.91/42.42	41.06/40.42	34.59/33.58	23.69/23.18
	Industrial	54.50/52.52	51.17/52.06	42.64/42.98	37.09/36.98	27.08/27.53
	Tertiary	60.31/56.84	56.23/53.52	47.13/46.14	43.01/42.13	36.08/35.42
PB (years)	Residential SFH	5.62/5.78	5.66/5.79	5.69/5.82	5.72/5.89	5.81/6.07
	Residential TH	6.64/6.93	6.65/6.93	6.70/6.99	6.82/7.12	7.05/7.41
	Residential MFH	4.78/4.95	4.67/4.87	4.76/4.94	4.95/5.14	5.30/5.53
	Residential AB	3.76/3.85	3.73/3.81	3.79/3.86	3.92/4.02	4.20/4.32
	Industrial	3.86/4.02	3.85/3.99	3.97/4.12	4.04/4.21	4.12/4.32
	Tertiary	4.49/4.91	4.51/4.93	4.60/5.05	4.64/5.11	4.73/5.24

For the NB scenario, the average profitability of PV facilities in all building typologies is not sensitive to the studied load profiles, especially in scenarios with equal or higher LPF than the base scenario. Nevertheless, residential buildings with few consumers are more sensitive to load profiles with low LPF. The load in these cases is mostly during the early morning, evening hours and at midnight, increasing the PB 38.4% for SFH (from 11.2 to 15.5 years) and 48.9% for TH (from 9.4 to 14.0 years). The other building typologies experience averaged increases in PBs and IRR below 0.5 years and -3.0%, respectively, mainly due to the concentration of consumption in the daytime hours. The fluctuations detected in the NM are mainly caused by fluctuations in the optimal PV sizing capacity compared to the NB scenario and by the different tariff periods defined in Section 4.2.2.

Aggregated Results by Building Typologies

The aggregated results for each building typology and the complete municipality and for each billing scheme are gathered in Table 4.8.

Table 4.8: Overall PV potential of the municipality.

Billing Scheme	Building Typology	PV Peak Capacity	Annual PV Production	Self-consumption	Surpluses	Self-sufficiency	Production-Demand ratio	Investment Costs	Economic Savings	Emission Savings
		MW_p	GW h	%	%	%	%	M€	M€/year	$t\ CO_2$/year
NB	SFH	0.25	0.34	48.53	51.47	42.02	86.58	0.43	0.08	54.11
	TH	9.96	13.45	41.32	58.68	42.01	101.66	22.41	2.99	2,141.88
	MFH	6.29	8.48	57.73	42.27	37.82	65.50	9.77	2.30	1,350.99
	AB	16.98	22.97	58.39	41.61	39.04	66.86	21.32	6.30	3,658.92
	Industrial	40.97	56.52	53.96	46.04	40.60	75.24	49.00	13.94	9,001.71
	Tertiary	7.86	10.62	67.85	32.15	23.58	34.75	9.95	2.77	1,691.49
	Others	2.52	3.43	56.46	43.54	39.88	70.63	3.60	0.82	546.27
	All	84.83	115.82	54.98	45.02	37.14	67.54	116.49	29.20	18,445.36
NM	SFH	0.77	1.05	17.18	82.82	46.16	268.65	1.08	0.24	167.90
	TH	19.58	26.44	22.38	77.62	44.74	199.85	36.15	6.34	4,210.84
	MFH	7.57	10.20	49.29	50.71	38.83	78.78	11.35	2.75	1,624.75
	AB	20.68	27.97	49.64	50.36	40.42	81.41	25.38	7.52	4,455.11
	Industrial	66.09	89.30	37.52	62.48	44.60	118.88	76.11	21.62	14,221.83
	Tertiary	12.38	16.75	45.53	54.47	24.96	54.82	14.80	4.16	2,668.27
	Others	4.47	6.06	33.38	66.62	41.66	124.80	6.12	1.47	965.26
	All	131.54	177.78	38.35	61.65	39.76	103.68	171.00	44.10	28,313.97

In an ideal scenario considering all the rooftop areas of the municipality occupied by PV facilities, the maximum PV peak power installed is $145.98\,\mathrm{MW_p}$, providing an annual production of $196.48\,\mathrm{GW\,h}$, which represents 114.59% of the annual demand of the municipality. The potential annual emissions savings are $31{,}292\,\mathrm{t\,CO_2}$. However, only 35.38% of the production is self-consumed and the global SS reaches 40.54%.

The NM scenario provides slightly lower installed capacities than the maximum power scenario. The maximum is $131.54\,\mathrm{MW_p}$ and the main results are shown in Table 4.8. The main difference is that the economic savings in this scenario yield an increase of 26.97% owing to higher surplus remuneration.

The above-mentioned values contrast significantly when considering the technical and economical limitations of an NB scenario, which is the most feasible with the current regulation. For this billing scheme, the aggregated optimal peak capacity reaches $84.33\,\mathrm{MW_p}$ and an annual production that represents 67.54% of the total annual demand. Despite a reduction in the maximum capacity of 57.08%, the SS rate only decreases an 8.38% and the SC rises to 54.98%, thereby increasing the economic profitability. With these higher rates of on-site production use, the annual economic savings would only decrease by 16.92% compared with the maximum power scenario.

Figure 4.6 shows the aggregated monthly municipality demand and PV production, in which the limitation of non-remunerated surpluses established by Spanish regulation is appreciated during the months with high insolation. The latter represent up to 34.3% of the total surpluses in August for the base scenario and 72.2% for the maximum power scenario. The most affected typologies by this limitation are SFHs and THs, in which up to 32.2% and 40.7% of the annual surpluses are non-remunerated, respectively. In industrial and tertiary buildings, this rate is below 10%, and for facilities shared by several consumers, the latter could be minimized with more variable sharing coefficients.

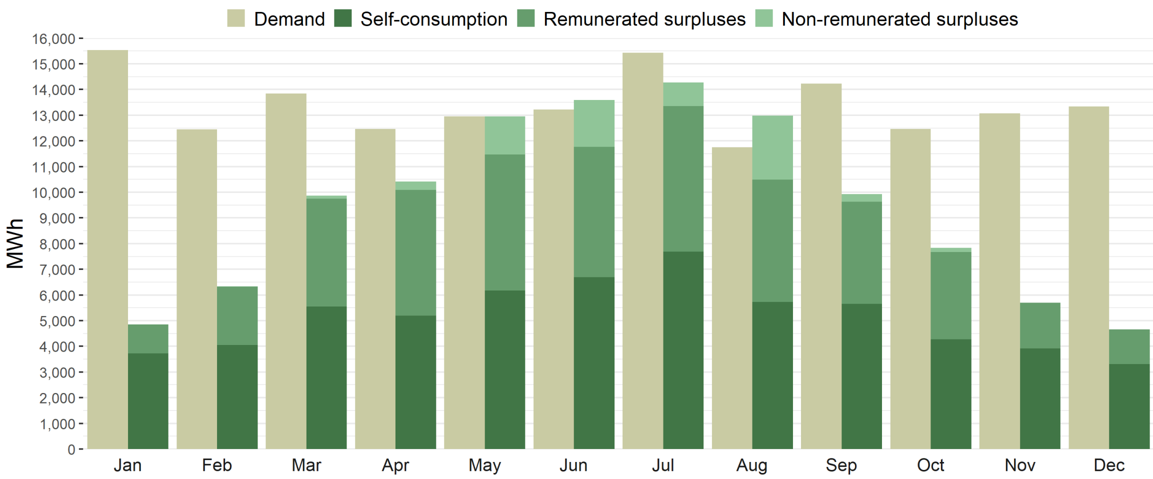

Figure 4.6: Monthly electricity demand and PV production for the base scenario.

Another regulatory limiting factor to increase the production potential is the maximum allowed capacity for each facility, which is up to 100 $\mathrm{MW_n}$ under the regime for domestic prosumers. This is the most feasible scenario since the administrative and technical procedures are simplified. Applying this limitation and assuming a scale factor of 1.2 [63], the total capacity, SS and SC drop to 73.63 $\mathrm{MW_p}$, 32.90% and 57.17%, respectively. Industrial and tertiary buildings are most affected by this limitation, with cumulative capacities falling to 34.60 $\mathrm{MW_p}$, and 5.90 $\mathrm{MW_p}$, respectively.

If the non-profitable facilities ($IRR < 0$) for the later scenario were not installed, the final potential would drop to 73.39 $\mathrm{MW_p}$. The facilities with paybacks higher than their lifetime are 24.1% of the SFHs and 21.3%.

Figure 4.7 reveals that high-capacity scenarios provide higher annual production than the annual demand, thereby contributing to the reduction in the emission factor from the grid. However, the global self-sufficiency barely increases compared with the NB scenarios, which require approximately half the maximum capacity.

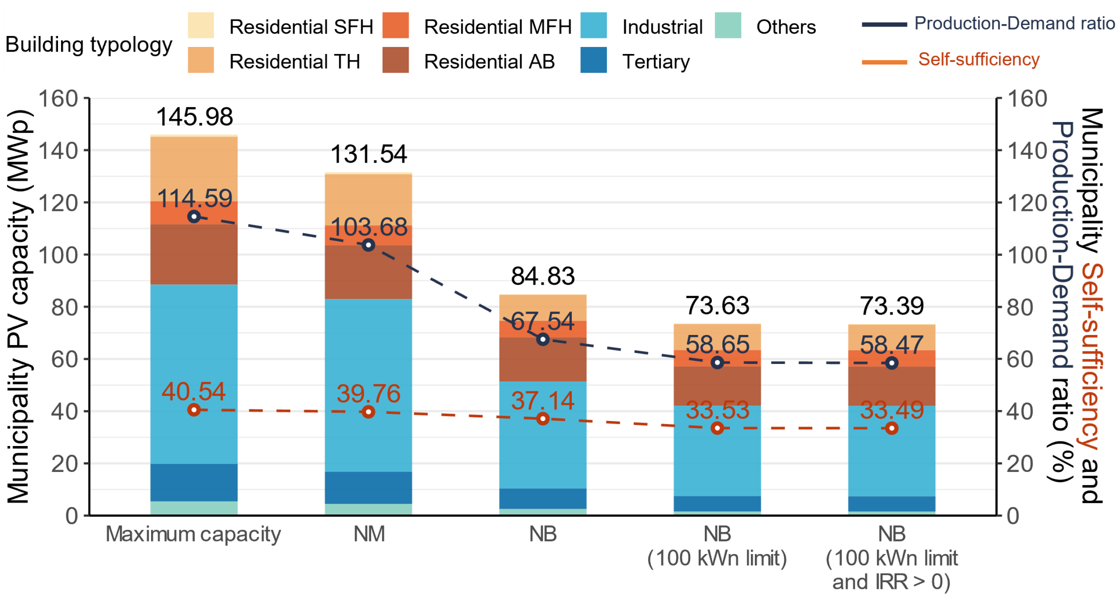

Figure 4.7: Comparison of aggregated capacities, self-sufficiencies and production-demand ratio for the complete municipality.

From the strategic point of view of reducing emissions, industrial building typologies provide the highest impact, followed by ABs. Both can reduce the potential emissions by 46.36%. Figure 4.8 (top) shows the cumulative potential emission savings if PV facilities were installed according to different prioritization criteria. The first actions should be focused on buildings with greater demands and rooftop areas such as ABs, and industrial and tertiary buildings. Similar to the Pareto rule, by acting on 1,067 buildings (90.74% AB, 87.83% industrial, 0.39% tertiary, 28.6% of the building stock municipality), 80% of the potential emission savings are reached.

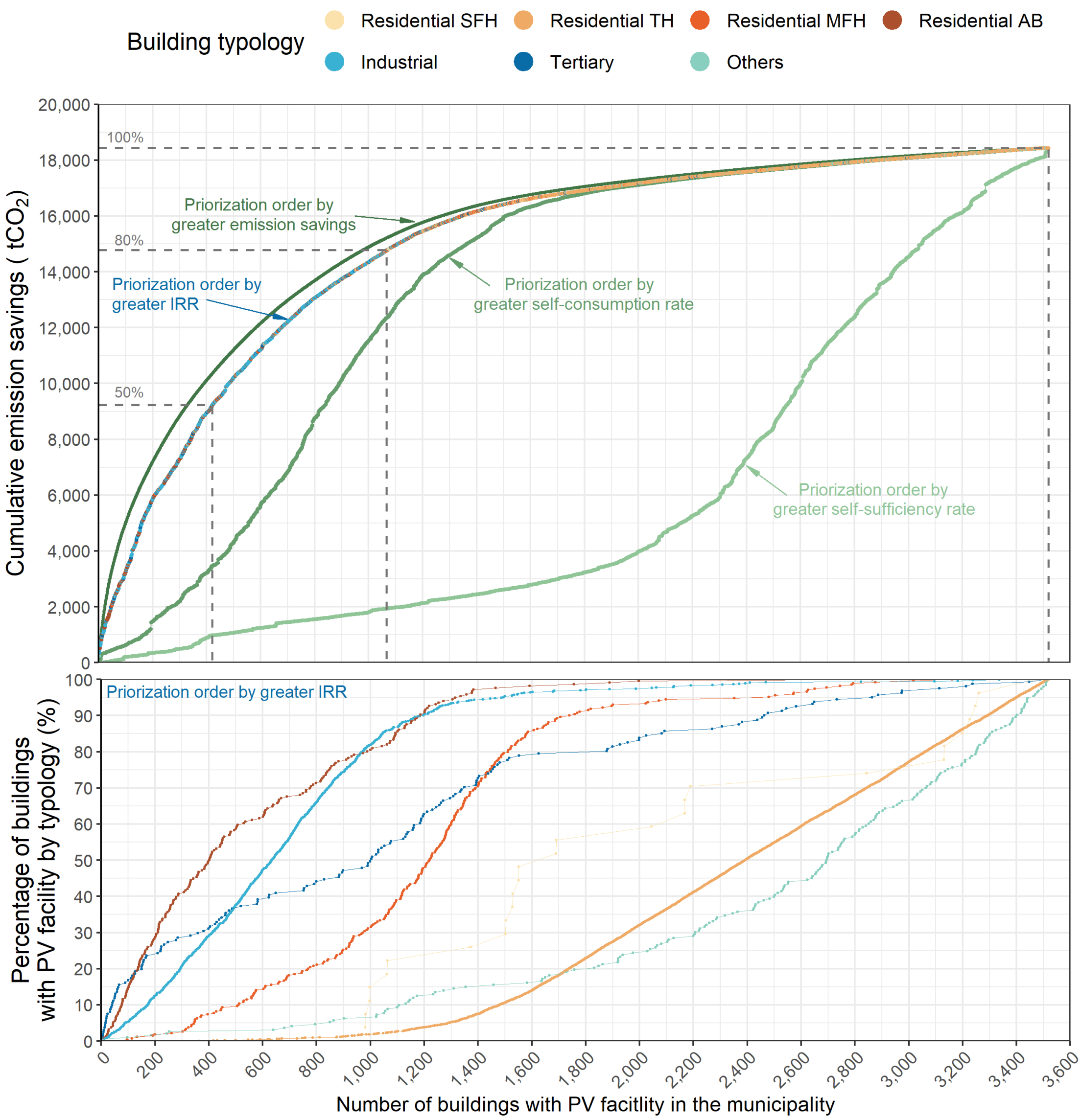

Figure 4.8: Cumulative potential emission savings prioritizing installations on buildings by greater IRR, SC and SS.

Regarding the global SS of the municipality, the scenarios evaluated with the different demand profiles show an asymptotic growth for the best scenario of up to 42.49%, as shown in Figure 4.9. This limitation is mainly caused by the presence of nighttime consumptions in all the assessed hourly profiles. Figure 4.9 provides a magnitude order of the error that may exist when using a given consumption profile. For the LPD scenario, which presents more nighttime consumption than the others, the SS is 21.93%.

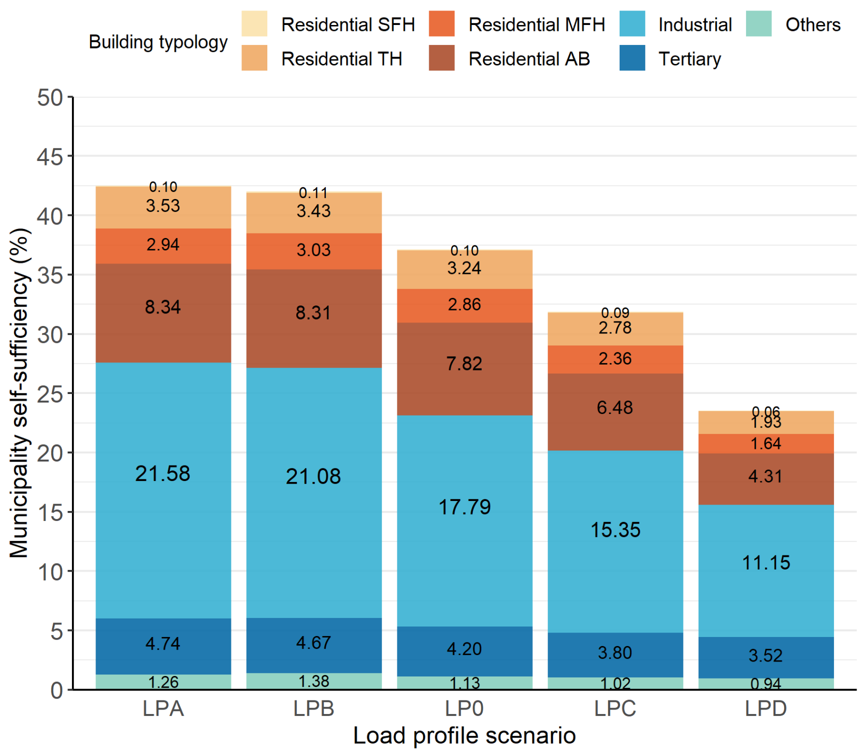

Figure 4.9: Contribution to the SS of the municipality of the aggregated PV production by building typology.

4.3.2 Regression Results

In addition to the variations assessed with the demand profiles, the global results are also conditioned by the situation of electricity prices, installation costs, and the demand level. A sensitivity analysis was performed to quantify these variations in relation to the NB base scenario and to provide a broader view of the economic feasibility of the deployment of PV systems in the municipality.

According to Figure 4.10 an increase in the buildings' electrification would especially benefit SFHs and THs, increasing their SC up to 45% and a PB reduction of 2.5 years with respect to the base scenario. The profitability of installations of several users of high annual demands remains practically insensitive towards these fluctuations since their SC rates remain high for any scenario.

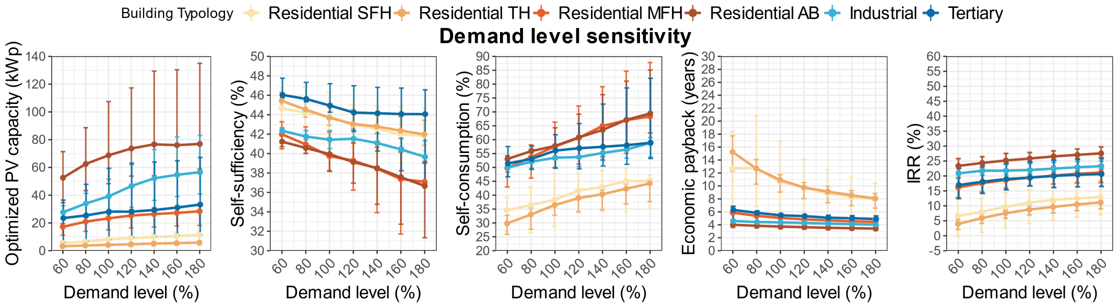

Figure 4.10: Sensitivity of the main PVSC variables as a function of DL with respect to the NB base scenario for the selected sample of buildings.

The variations in the results in the economic scenarios mainly affect the profitability of the facilities, as shown in Figure 4.11. Investment cost variations are practically linear with PB, with increments for the payback for each percentual cost variation of 0.117 years for SFH and TH reaching some cases up to 20 years, while industrial or tertiary present rates around 0.05 years. Unlike investment costs, electricity price fluctuations cause similar variations in PB. A price scenario of 0.4 times lower than the base case scenario, which is representative of the first half of 2021 in Spain, would increase the average PBs up to 26.5 years for SFHs, 12.0 years for ABs and 14.4 years for industrial buildings.

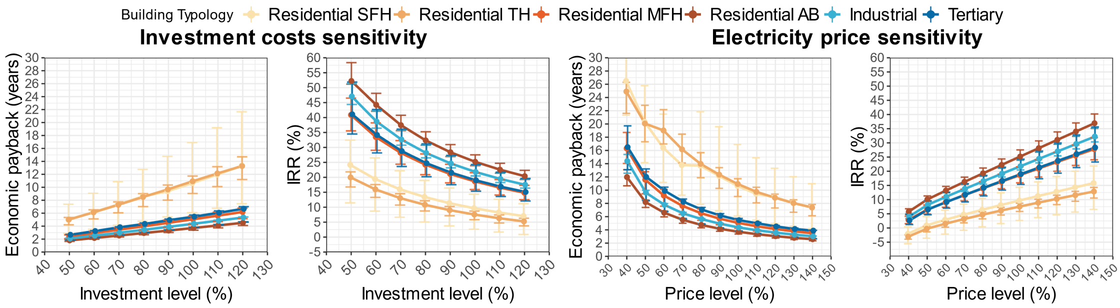

Figure 4.11: Sensitivity of the main PVSC variables as a function of investment CL and PL with respect to the NB base scenario for the selected sample of buildings.

With the results of the sample of buildings, the Pearson correlation matrix in Figure 4.12 helps identify the most explanatory variables to predict the SS, SC, PB and IRR using QR models. Among the preliminary predictors, the constructive characteristics of buildings such as height, rooftop area and dwellings area were discarded due to their low correlation values with the target variables. Furthermore, their information is partially included in the other predictors. As mentioned in Section 4.2.3, the predictors selected for the final models are the following: SR, CR, LPF, DL, IL and PL.

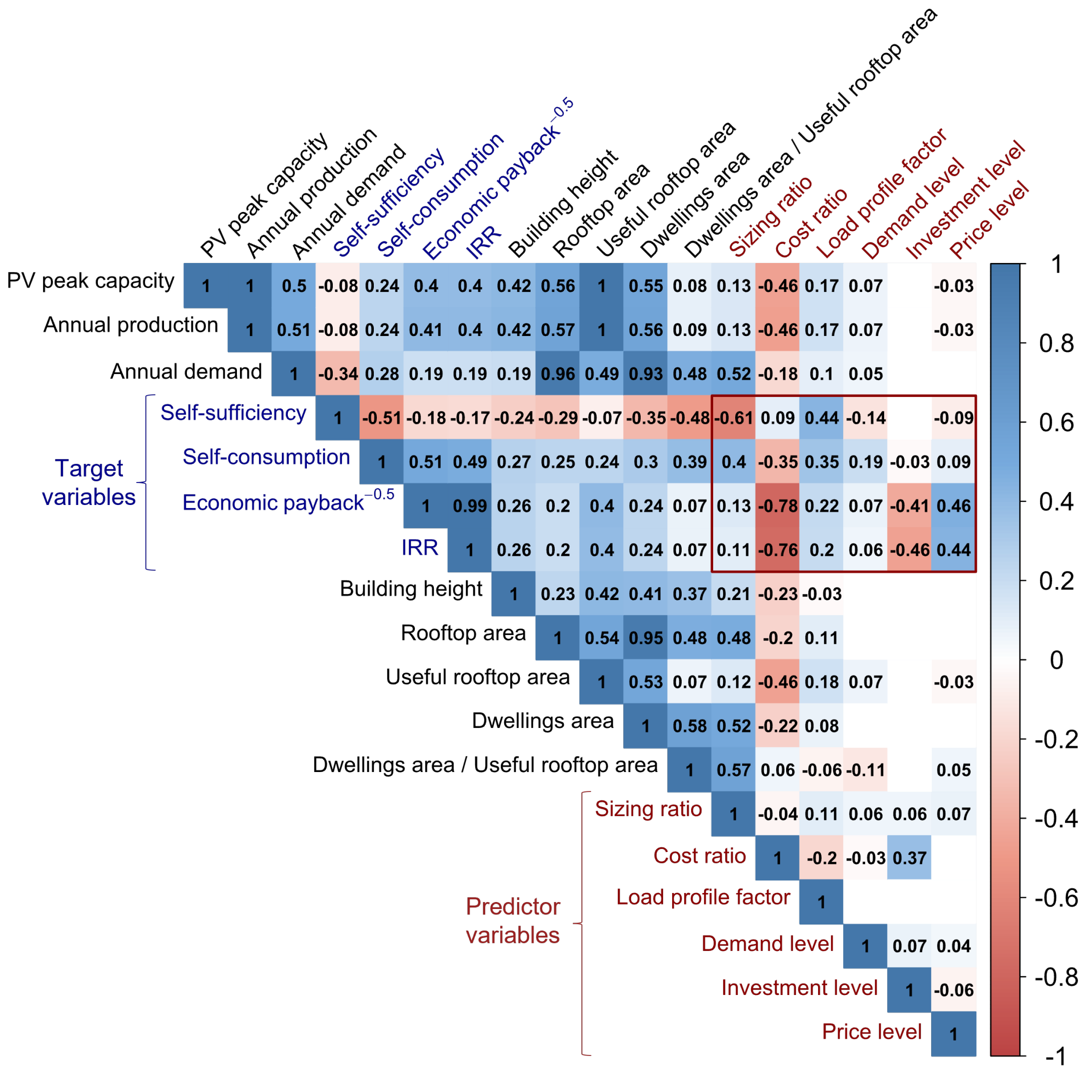

Figure 4.12: Correlation matrix of the main PVSC variables, physical characteristics of the buildings and assessed techno-economic scenarios.

The correlation matrix values provide an intuitive idea about the workflow proposed in the training of the regressions. As a first step, SS is predicted thanks to the high correlation with the SR and the LPF, which are less correlated with the other target variables. Next, the predicted SS is used as a reinforcement predictor of SC. Lastly, the economic target variables (PB and IRR) present a low correlation with the two intrinsic predictors (SR and LPF), which potentially leads to mispredictions due to scarce differentiation among individuals. To reduce the errors in the economic regressions, the SC variable is also employed as a predictor with a moderate correlation. The multicollinearity, measured with the VIF, is lower than 2 for all of them, except for a VIF of 7.1 between cost ratio and investment level to predict the IRR.

The relationship between the two main predictors for SS is shown in Figure 4.13. Each point represents a result for a specific building. The LPF provides a clear positive correlation with SS, however, this variable only considers the alignment of consumption with sun hours and no other effects such as how a facility is undersized compared with its load. The latter aspect is expressed with the sizing factor (relationship between the peak demand and peak PV capacity).

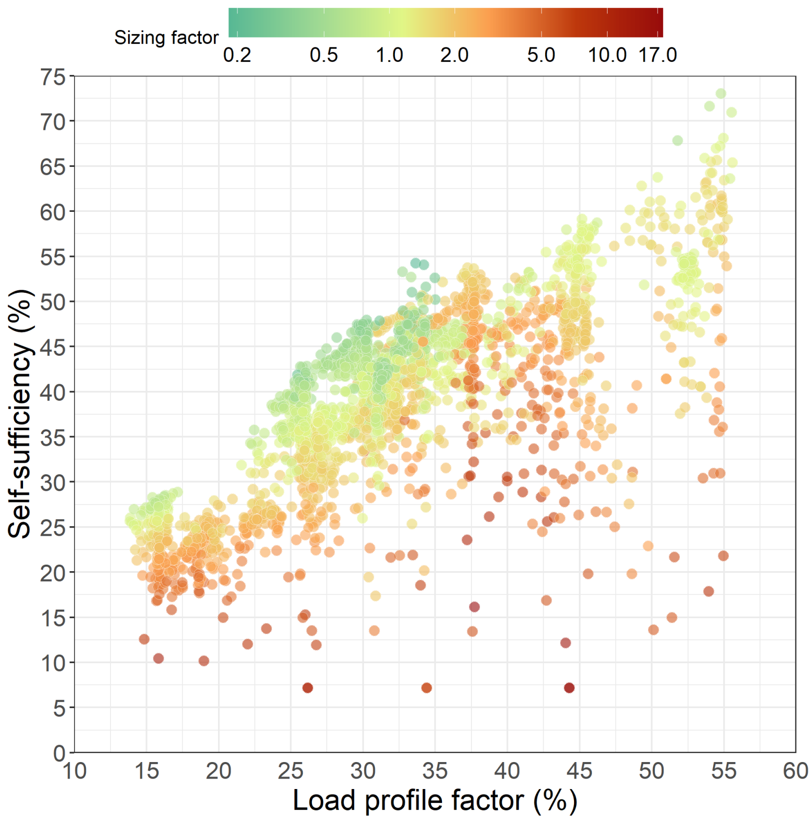

Figure 4.13: Scatter plot of SS and its main predictor variables (load profile factor and sizing factor).

The QR expressions are defined in Section 4.2.3 and the values of the fitted coefficients for each variable and building typology are described in Appendix A.

Figure 4.14 compares the calculated target variables through the techno-economic model and the prediction from each regression model. The greater relative errors are found in the overpredictions in the economic variables with less profitable facilities. This is partially caused by an overprediction of the SS regression model for big consumers, for which the optimal capacity is limited by the available rooftop space. This non-linearity, for instance, causes differences in accuracy between ABs (84.00%) or Tertiary (90.53%) and SFHs (98.44%) or THs (96.83%).

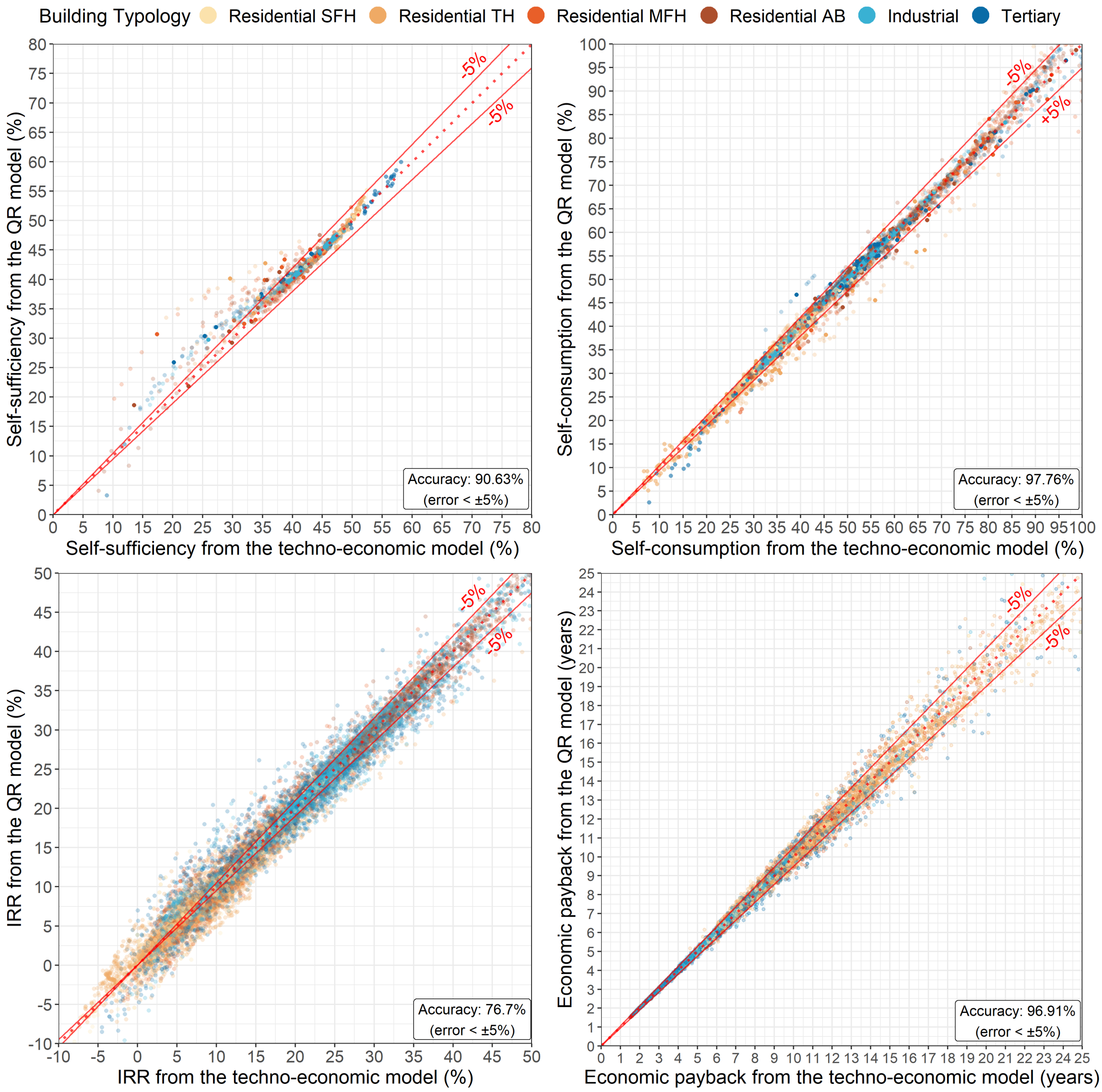

Figure 4.14: Validation of the predicted values SS, SC, IRR and PB by the QR models.

Finally, the main error metrics of each model are gathered in Table 4.9. The $nRMSE$s of SS and SC are below 4%, and of PB is below 2%, which are reasonable for planning purposes.

Table 4.9: Error metrics of the predicted SS, SC, IRR and PB by the QR models.

Target Variable	MAE	$RMSE$	$nRMSE$	R^2
SC	0.805%	1.627%	3.866%	0.911
SS	0.831%	1.536%	3.097%	0.992
IRR	0.012%	0.018%	10.020%	0.974
PB	0.015 years	0.023 years	1.479%	0.997

4.4 Conclusions

Currently, there are few studies in the literature on the economic assessment of PVSC facilities on an urban scale for NB schemes. In the present work, a bottom-up techno-economic model was developed to estimate hourly load profiles at a property level. In the first part of this paper, the techno-economic potential was evaluated for the complete building stock of 3,840 buildings in the Mediterranean municipality of Catarroja, Spain. Different hourly load profiles were analyzed and compared within the NM scenario.

According to the electricity prices between 2021 and 2022, and based on the present legal framework in Spain, the average payback is 9–10 years for SFHs and THs, while MFHs, Industrial and Tertiary building typologies yield paybacks of 4–5 years. The most feasible facilities are placed on ABs owing to their high number of consumers and scarce surpluses. Except for SFHs and THs, the other building typologies yield nevertheless very similar paybacks with the NM scheme.

Regarding the variation in load profiles, for the scenarios with the lowest LPF, the PB of facilities on SFHs and THs experiences on average an increase of around 5 years, while buildings with higher demands are not sensitive to these fluctuations. The highest SS are found in facilities on Tertiary buildings for the highest LPF, reaching on average up to 67.6%, while residential typologies barely surpass the SS values of 50%.

For the aggregated balance of the municipality, there is a wide difference between the total capacity under NM and NB schemes, with $131.54\,\mathrm{MW_p}$ and $84.83\,\mathrm{MW_p}$, respectively. This reduction shows the importance of considering the economic constraints when estimating the urban PV potential of any city under the NB regulation. Under the NB scheme, the total SS of the municipality fluctuates between 42.5% for the highest LPF scenario and 21.9% for the lowest. However, the total PV energy produced would represent 67.5% of the total electricity consumption of the municipality. This rate could rise to 103.7% with an NM scheme. For the municipality energy strategy, prioritizing PV facilities on 28.6% of the most economically feasible rooftops would deliver 80% of the potential emission savings due to electricity consumption. The most relevant typologies in this process are those with high consumption and high rooftops such as ABs and industrial buildings.

As a second part of this work, four QR models were developed to predict SS, SC, PB and IRR through the intrinsic characteristics of the installations as well as other conjunctural characteristics such as demand, prices, or cost variations. One of the predictors defined is the LPF, a novel coefficient that addresses the alignment of the building consumption and the PV production, which is one of the main explanatory variables to predict the SS. The cost ratio, which measures the economy of scale of the facility, is a significant predictor to estimate the economic target variables. The models provide estimations for the above-mentioned variables with $nRMSE$ values of 3.9%, 3.1%, 10.0% and 1.5%, respectively, compared with the techno-economic model.

The most relevant outcomes are:

- The sizing of the facilities according to the load curves in the NB modality, optimizing SS and profitability, is crucial to obtain competitive economic returns while maintaining similar levels of SS with those obtained in NM.
- SFHs and THs are the most sensitive to the shape of the hourly load profile. More detailed approaches are required in residential areas to estimate load profiles of SFHs and THs.
- Considering the profitability constraints under the current NB scheme, the total neutrality of emissions of municipal electricity consumption would not be achieved by the deployment of rooftop PVSC systems, in contrast to the NM scheme.
- The best economic and environmental results are achieved with ABs, industrial and tertiary buildings.
- The LPF is a crucial predictor to estimate SS and SC through regression-based models for the NB in which there is not a direct relationship between these variables and other constructive aspects of the building.

4.5 Acknowledgments

The authors would like to thank the City Council of Catarroja and Grupo ImpactE Planificación Urbana S.L. for supporting this project.

4.6 Appendix A

Table 4.10: QR coefficients to estimate SS for each building typology.

Building Typology	Coefficient	Value	95% CI	p-Value
-	k_0 $(Intercept)$	-13.46	-246.1; 219.2	>0.910
Residential SFH	k_0 $(Intercept)$	-	-	-
	k_1 $(SR^{0.5})$	-17.69	-19.01; -16.37	0.000
	k_2 (LPF)	-114.11	-877.9; 649.7	0.770
	k_3 $(LPF^{0.5})$	194.00	-648.2; 1036	0.652
	k_4 $(DL^{0.5})$	-0.41	-0.809; -0.004	0.048
Residential TH	k_0 $(Intercept)$	-280.88	-513.9; -47.84	0.018
	k_1 $(SR^{0.5})$	-19.15	-19.18; -19.12	<0.001
	k_2 (LPF)	-1,092.27	-1,139; -1,046	<0.001
	k_3 $(LPF^{0.5})$	1,243.85	1,193; 1,294	<0.001
	k_4 $(DL^{0.5})$	-0.06	-0.149; 0.021	0.139
Residential MFH	k_0 $(Intercept)$	-930.61	-1,271; -590.6	<0.001
	k_1 $(SR^{0.5})$	-23.24	-23.57; -22.91	<0.001
	k_2 (LPF)	-3,391.60	-4,198; -2586	<0.001
	k_3 $(LPF^{0.5})$	3,696.59	2,802; 4591	<0.001
	k_4 $(DL^{0.5})$	-0.22	-0.652; 0.203	0.304
Residential AB	k_0 $(Intercept)$	2,540.30	2,235; 2,846	<0.001
	k_1 $(SR^{0.5})$	-21.47	-21.79; -21.15	<0.001
	k_2 (LPF)	7,839.67	7,204; 8,476	<0.001
	k_3 $(LPF^{0.5})$	-8,793.75	-9,504; -8,084	<0.001
	k_4 $(DL^{0.5})$	-0.51	-0.822; -0.197	0.001
Industrial	k_0 $(Intercept)$	198.66	-182.0; 579.3	0.306
	k_1 $(SR^{0.5})$	-28.85	-28.99; -28.72	<0.001
	k_2 (LPF)	563.56	-416.1; 1543	0.260
	k_3 $(LPF^{0.5})$	-533.48	-1,620; 553.1	0.336
	k_4 $(DL^{0.5})$	-0.66	-0.732; -0.580	<0.001
Tertiary	k_0 $(Intercept)$	-7.95	-525.0; 509.1	0.976
	k_1 $(SR^{0.5})$	-28.75	-29.30; -28.20	<0.001
	k_2 (LPF)	-16.96	-1,389; 1,355	0.981
	k_3 $(LPF^{0.5})$	162.53	-1,430; 1,755	0.841
	k_4 $(DL^{0.5})$	-0.37	-0.628; -0.119	0.004

Table 4.11: QR coefficients to estimate SC for each building typology.

Building Typology	Coefficient	Value	95% CI	p-Value
-	$k_0\ (Intercept)$	-564.71	-1,599.58; 470.15	0.285
Residential SFH	$k_0\ (Intercept)$	-	-	-
	$k_0\ (SR)$	39.68	14.08; 65.27	0.002
	$k_2\ (SR^{0.5})$	-3.87	-35.46; 27.71	0.810
	$k_3\ (LPF)$	860.61	-3,992.07; 5,713.29	0.728
	$k_4\ (LPF^{0.5})$	-842.09	-6,153.69; 4,469.51	0.756
	$k_5\ (DL^{0.5})$	0.02	-0.39; 0.43	0.925
	$k_6\ (SS)$	-19.25	-37.08; -1.41	0.034
	$k_7\ (SS^{0.5})$	245.64	2.63; 488.65	0.048
Residential TH	$k_0\ (Intercept)$	2,490.66	1,441.75; 3,539.57	<0.001
	$k_0\ (SR)$	4.58	0.02; 9.14	0.049
	$k_2\ (SR^{0.5})$	22.39	14.59; 30.18	<0.001
	$k_3\ (LPF)$	6,521.00	6,046.98; 6,995.01	<0.001
	$k_4\ (LPF^{0.5})$	-6,832.29	-7,343.48; -6,321.11	<0.001
	$k_5\ (DL^{0.5})$	0.12	0.03; 0.21	0.012
	$k_6\ (SS)$	-1.72	-4.36; 0.91	0.200
	$k_7\ (SS^{0.5})$	-7.29	-41.59; 27	0.677
Residential MFH	$k_0\ (Intercept)$	3,593.36	2,551.86; 4634.86	<0.001
	$k_0\ (SR)$	10.71	9.5; 11.92	<0.001
	$k_2\ (SR^{0.5})$	-7.80	-10.39; -5.21	<0.001
	$k_3\ (LPF)$	11,761.48	11,367.87; 12,155.1	<0.001
	$k_4\ (LPF^{0.5})$	-12,320.11	-12,749.3; -11,890.93	<0.001
	$k_5\ (DL^{0.5})$	-0.25	-0.35; -0.14	<0.001
	$k_6\ (SS)$	-12.35	-12.57; -12.13	<0.001
	$k_7\ (SS^{0.5})$	116.26	113.61; 118.9	<0.001
Residential AB	$k_0\ (Intercept)$	6,224.83	4,405.08; 8,044.57	<0.001
	$k_0\ (SR)$	8.18	5.07; 11.28	<0.001
	$k_2\ (SR^{0.5})$	-3.81	-9.61; 2	0.198
	$k_3\ (LPF)$	20,214.43	15,382.25; 25,046.61	<0.001
	$k_4\ (LPF^{0.5})$	-21,747.05	-27,132.16; -16,361.93	<0.001
	$k_5\ (DL^{0.5})$	-0.27	-0.35; -0.18	<0.001
	$k_6\ (SS)$	-12.40	-13.15; -11.65	<0.001
	$k_7\ (SS^{0.5})$	115.80	106.5; 125.1	<0.001
Industrial	$k_0\ (Intercept)$	3,008.01	1,956.49; 4,059.53	<0.001
	$k_0\ (SR)$	-8.29	-10.44; -6.14	<0.001
	$k_2\ (SR^{0.5})$	48.38	45.11; 51.65	<0.001
	$k_3\ (LPF)$	9,127.51	8,520.73; 9,734.29	<0.001
	$k_4\ (LPF^{0.5})$	-9,758.73	-10,442.43; -9,075.04	<0.001
	$k_5\ (DL^{0.5})$	0.15	0.1; 0.2	<0.001
	$k_6\ (SS)$	-8.76	-8.99; -8.52	<0.001

Building Typology	Coefficient	Value	95% CI	p-Value
	$k_7\ (SS^{0.5})$	84.59	81.63; 87.56	<0.001
Tertiary	$k_0\ (Intercept)$	-2,930.08	-4,111.86; -1,748.29	<0.001
	$k_1\ (SR)$	5.75	-5.55; 17.05	0.319
	$k_2\ (SR^{0.5})$	45.51	34.17; 56.84	<0.001
	$k_3\ (LPF)$	-8,977.73	-10,751.11; -7,204.36	<0.001
	$k_4\ (LPF^{0.5})$	10,741.19	8,664.91; 12,817.48	<0.001
	$k_5\ (DL^{0.5})$	-0.06	-0.19; 0.08	0.396
	$k_6\ (SS)$	-10.24	-11.31; -9.17	<0.001
	$k_7\ (SS^{0.5})$	114.37	97.94; 130.8	<0.001

Table 4.12: QR coefficients to estimate IRR for each building typology.

Building Typology	Coefficient	Value	95% CI	p-Value
-	k_0 $(Intercept)$	-2.94	-16.14; 10.27	0.663
Residential SFH	k_0 $(Intercept)$	0.01	-0.16; 0.19	0.891
	k_1 (SR)	0.00	-0.38; 0.37	0.981
	k_2 $(SR^{0.5})$	0.00	0; 0	<0.001
	k_3 (CR)	0.34	0.19; 0.49	<0.001
	k_4 $(CR^{0.5})$	-1.50	-2.12; -0.88	<0.001
	k_5 $(CR^{1/3})$	11.62	-15.78; 39.03	0.406
	k_6 (LPF)	-57.63	-165.6; 50.34	0.295
	k_7 $(LPF^{0.5})$	54.73	-40.9; 150.37	0.262
	k_8 $(LPF^{1/3})$	0.00	-0.01; 0	0.889
	k_9 (DL)	0.02	0.01; 0.04	0.001
	k_{10} (IL)	0.17	0.16; 0.17	<0.001
	k_{11} (PL)	-0.01	-0.02; 0	0.135
	k_{12} (SC)	0.43	0.09; 0.77	0.012
	k_{13} $(SC^{0.5})$	-0.87	-1.45; -0.28	0.004
	k_{14} $(SC^{1/3})$	0.01	-0.16; 0.19	0.891
Residential TH	k_0 $(Intercept)$	15.71	0.49; 30.93	0.043
	k_1 (SR)	-0.01	-0.02; -0.01	0.001
	k_2 $(SR^{0.5})$	0.05	0.03; 0.07	<0.001
	k_3 (CR)	0.00	0; 0	<0.001
	k_4 $(CR^{0.5})$	0.24	0.19; 0.29	<0.001
	k_5 $(CR^{1/3})$	-1.08	-1.29; -0.87	<0.001
	k_6 (LPF)	-19.43	-35.27; -3.59	0.016
	k_7 $(LPF^{0.5})$	72.46	10.33; 134.58	0.022
	k_8 $(LPF^{1/3})$	-62.69	-117.65; -7.73	0.025
	k_9 (DL)	0.00	0; 0.01	0.008
	k_{10} (IL)	0.04	0.03; 0.05	<0.001
	k_{11} (PL)	0.14	0.14; 0.14	<0.001
	k_{12} (SC)	-0.01	-0.01; -0.01	<0.001
	k_{13} $(SC^{0.5})$	0.59	0.46; 0.73	<0.001
	k_{14} $(SC^{1/3})$	-1.21	-1.49; -0.94	<0.001
Residential MFH	k_0 $(Intercept)$	4.67	-8.7; 18.04	0.494
	k_1 (SR)	0.01	0.01; 0.01	<0.001
	k_2 $(SR^{0.5})$	-0.03	-0.04; -0.02	<0.001
	k_3 (CR)	0.00	0; 0	<0.001
	k_4 $(CR^{0.5})$	0.45	0.39; 0.51	<0.001
	k_5 $(CR^{1/3})$	-1.91	-2.12; -1.7	<0.001
	k_6 (LPF)	10.36	6.75; 13.97	<0.001
	k_7 $(LPF^{0.5})$	-46.98	-62.27; -31.7	<0.001
	k_8 $(LPF^{1/3})$	43.57	29.69; 57.45	<0.001

Building Typology	Coefficient	Value	95% CI	p-Value
	$k_9\ (DL)$	0.00	0; 0	<0.001
	$k_{10}\ (IL)$	0.01	0; 0.01	0.028
	$k_{11}\ (PL)$	0.23	0.23; 0.24	<0.001
	$k_{12}\ (SC)$	-0.03	-0.03; -0.02	<0.001
	$k_{13}\ (SC^{0.5})$	1.43	1.29; 1.57	<0.001
	$k_{14}\ (SC^{1/3})$	-2.99	-3.28; -2.71	<0.001
	$k_0\ (Intercept)$	10.68	-2.72; 24.08	0.118
	$k_1\ (SR)$	0.01	0; 0.02	0.035
	$k_2\ (SR^{0.5})$	-0.03	-0.05; -0.01	0.011
	$k_3\ (CR)$	0.00	0; 0	<0.001
	$k_4\ (CR^{0.5})$	0.61	0.54; 0.68	<0.001
	$k_5\ (CR^{1/3})$	-2.50	-2.75; -2.24	<0.001
	$k_6\ (LPF)$	4.81	0.56; 9.05	0.027
Residential AB	$k_7\ (LPF^{0.5})$	-23.85	-41.75; -5.96	0.009
	$k_8\ (LPF^{1/3})$	22.74	6.51; 38.96	0.006
	$k_9\ (DL)$	0.00	0; 0	0.106
	$k_{10}\ (IL)$	0.00	-0.01; 0	0.164
	$k_{11}\ (PL)$	0.30	0.3; 0.3	<0.001
	$k_{12}\ (SC)$	-0.04	-0.04; -0.03	<0.001
	$k_{13}\ (SC^{0.5})$	2.24	1.88; 2.6	<0.001
	$k_{14}\ (SC^{1/3})$	-4.88	-5.67; -4.09	<0.001
	$k_0\ (Intercept)$	17.96	4.47; 31.46	0.009
	$k_1\ (SR)$	0.03	0.02; 0.05	<0.001
	$k_2\ (SR^{0.5})$	-0.06	-0.09; -0.03	<0.001
	$k_3\ (CR)$	0.00	0; 0	<0.001
	$k_4\ (CR^{0.5})$	0.51	0.45; 0.58	<0.001
	$k_5\ (CR^{1/3})$	-2.12	-2.38; -1.87	<0.001
	$k_6\ (LPF)$	-15.37	-19.02; -11.73	<0.001
Industrial	$k_7\ (LPF^{0.5})$	66.58	48.73; 84.44	<0.001
	$k_8\ (LPF^{1/3})$	-60.91	-77.94; -43.87	<0.001
	$k_9\ (DL)$	-0.01	-0.01; -0.01	<0.001
	$k_{10}\ (IL)$	-0.01	-0.02; 0	0.010
	$k_{11}\ (PL)$	0.27	0.27; 0.27	<0.001
	$k_{12}\ (SC)$	0.01	0.01; 0.01	<0.001
	$k_{13}\ (SC^{0.5})$	-0.31	-0.39; -0.24	<0.001
	$k_{14}\ (SC^{1/3})$	0.54	0.4; 0.67	<0.001
	$k_0\ (Intercept)$	3.37	-10.24; 16.97	0.628
	$k_1\ (SR)$	0.00	0; 0	0.737
	$k_2\ (SR^{0.5})$	0.00	-0.01; 0.01	0.935
	$k_3\ (CR)$	0.00	0; 0	<0.001
	$k_4\ (CR^{0.5})$	0.42	0.38; 0.46	<0.001
	$k_5\ (CR^{1/3})$	-1.78	-1.94; -1.62	<0.001

Tertiary

Building Typology	Coefficient	Value	95% CI	p-Value
	k_6 (LPF)	7.28	2.73; 11.82	0.002
	k_7 $(LPF^{0.5})$	-37.45	-59.16; -15.75	0.001
	k_8 $(LPF^{1/3})$	36.17	15.63; 56.71	0.001
	k_9 (DL)	0.00	0; 0	0.261
	k_{10} (IL)	-0.02	-0.03; -0.02	<0.001
	k_{11} (PL)	0.25	0.25; 0.25	<0.001
	k_{12} (SC)	-0.01	-0.01; -0.01	<0.001
	k_{13} $(SC^{0.5})$	0.45	0.34; 0.57	<0.001
	k_{14} $(SC^{1/3})$	-0.96	-1.21; -0.71	<0.001

Table 4.13: QR coefficients to estimate PB for each building typology.

Building Typology	Coefficient	Value	95% CI	p-Value
-	k_0 $(Intercept)$	0.22	0.21; 0.22	<0.001
Residential SFH	k_1 (IRR)	1.60	1.49; 1.7	<0.001
	k_2 (IRR^2)	-1.80	-2.74; -0.86	<0.001
	k_3 (IRR^3)	1.46	-0.63; 3.54	0.171
Residential TH	k_1 (IRR)	1.56	1.54; 1.59	<0.001
	k_2 (IRR^2)	-1.40	-1.57; -1.23	<0.001
	k_3 (IRR^3)	0.74	0.43; 1.06	<0.001
Residential MFH	k_1 (IRR)	1.55	1.53; 1.57	<0.001
	k_2 (IRR^2)	-1.47	-1.57; -1.37	<0.001
	k_3 (IRR^3)	0.90	0.74; 1.06	<0.001
Residential AB	k_1 (IRR)	1.55	1.53; 1.57	<0.001
	k_2 (IRR^2)	-1.49	-1.58; -1.39	<0.001
	k_3 (IRR^3)	0.88	0.75; 1	<0.001
Industrial	k_1 (IRR)	1.54	1.53; 1.56	<0.001
	k_2 (IRR^2)	-1.40	-1.47; -1.34	<0.001
	k_3 (IRR^3)	0.76	0.67; 0.85	<0.001
Tertiary	k_1 (IRR)	1.56	1.55; 1.58	<0.001
	k_2 (IRR^2)	-1.48	-1.54; -1.43	<0.001
	k_3 (IRR^3)	0.84	0.77; 0.91	<0.001

4.7 References

[1] SolarPower Europe. *EU Market Outlook For Solar Power 2022-2026*. 2022.

[2] IRENA. *Renewable Power Generation Costs in 2020*. Tech. rep. 2020.

[3] Bórawski, P., Holden, L., and Bełdycka-Bórawska, A. "Perspectives of photovoltaic energy market development in the european union". In: *Energy* 270 (2023), p. 126804. DOI: 10.1016/J.ENERGY.2023.126804.

[4] European Commission. *'Fit for 55': delivering the EU's 2030 climate target on the way to climate neutrality*. Tech. rep. 2021.

[5] European Climate Foundation. *Building Europe's Net-Zero Future Why the Transition to Energy Efficient and Electrified Buildings Strengthens Europe's Economy*. Tech. rep. The Hague: European Climate Foundation, 2022.

[6] Sun, L., Chang, Y., Wu, Y., Sun, Y., and Su, D. "Potential estimation of rooftop photovoltaic with the spatialization of energy self-sufficiency in urban areas". In: *Energy Reports* 8 (2022), pp. 3982–3994. DOI: 10.1016/J.EGYR.2022.03.035.

[7] Matute, G., Yusta, J. M., Beyza, J., and Monteiro, C. "Optimal dispatch model for PV-electrolysis plants in self-consumption regime to produce green hydrogen: A Spanish case study". In: *International Journal of Hydrogen Energy* 47.60 (2022), pp. 25202–25213. DOI: 10.1016/J.IJHYDENE.2022.05.270.

[8] Talavera, D. L., Muñoz-Rodriguez, F. J., Jimenez-Castillo, G., and Rus-Casas, C. "A new approach to sizing the photovoltaic generator in self-consumption systems based on cost–competitiveness, maximizing direct self-consumption". In: *Renewable Energy* 130 (2019), pp. 1021–1035. DOI: 10.1016/J.RENENE.2018.06.088.

[9] Hamann, K. R., Bertel, M. P., Ryszawska, B., Lurger, B., Szymański, P., Rozwadowska, M., Goedkoop, F., Jans, L., Perlaviciute, G., Masson, T., Fritsche, I., Favaro, T., Hofer, A., Eisenberger, I., Gutschi, C., Grosche, C., Held, J., Athenstaedt, U., and Corcoran, K. "An interdisciplinary understanding of energy citizenship: Integrating psychological, legal, and economic perspectives on a citizen-centred sustainable energy transition". In: *Energy Research & Social Science* 97 (2023), p. 102959. DOI: 10.1016/J.ERSS.2023.102959.

[10] Gassar, A. A. A. and Cha, S. H. "Review of geographic information systems-based rooftop solar photovoltaic potential estimation approaches at urban scales". In: *Applied Energy* 291 (2021), p. 116817. DOI: 10.1016/J.APENERGY.2021.116817.

[11] Sredenšek, K., Štumberger, B., Hadžiselimović, M., Mavsar, P., and Seme, S. "Physical, geographical, technical, and economic potential for the optimal configuration of photovoltaic systems using a digital surface model and optimization method". In: *Energy* 242 (2022), p. 122971. DOI: 10.1016/J.ENERGY.2021.122971.

[12] Gómez-Navarro, T., Brazzini, T., Alfonso-Solar, D., and Vargas-Salgado, C. "Analysis of the potential for PV rooftop prosumer production: Technical, economic and environmental assessment for the city of Valencia (Spain)". In: *Renewable Energy* 174 (2021), pp. 372–381. DOI: 10.1016/j.renene.2021.04.049.

[13] Han, J. Y., Chen, Y. C., and Li, S. Y. "Utilising high-fidelity 3D building model for analysing the rooftop solar photovoltaic potential in urban areas". In: *Solar Energy* 235 (2022), pp. 187–199. DOI: 10.1016/J.SOLENER.2022.02.041.

[14] Fakhraian, E., Alier, M., Dalmau, F. V., Nameni, A., and Guerrero, J. C. "The Urban Rooftop Photovoltaic Potential Determination". In: *Sustainability 2021, Vol. 13, Page 7447* 13.13 (2021), p. 7447. DOI: 10.3390/SU13137447.

[15] Fakhraian, E., Forment, M. A., Dalmau, F. V., Nameni, A., and Guerrero, M. J. C. "Determination of the urban rooftop photovoltaic potential: A state of the art". In: *Energy Reports* 7 (2021), pp. 176–185. DOI: 10.1016/J.EGYR.2021.06.031.

[16] Krapf, S., Kemmerzell, N., Uddin, S. K. H., Vázquez, M. H., Netzler, F., and Lienkamp, M. "Towards Scalable Economic Photovoltaic Potential Analysis Using Aerial Images and Deep Learning". In: *Energies 2021, Vol. 14, Page 3800* 14.13 (2021), p. 3800. DOI: 10.3390/EN14133800.

[17] Fath, K., Stengel, J., Sprenger, W., Wilson, H. R., Schultmann, F., and Kuhn, T. E. "A method for predicting the economic potential of (building-integrated) photovoltaics in urban areas based on hourly Radiance simulations". In: *Solar Energy* 116 (2015), pp. 357–370. DOI: 10.1016/J.SOLENER.2015.03.023.

[18] Mansouri Kouhestani, F., Byrne, J., Johnson, D., Spencer, L., Hazendonk, P., and Brown, B. "Evaluating solar energy technical and economic potential on rooftops in an urban setting: the city of Lethbridge, Canada". In: *International Journal of Energy and Environmental Engineering* 10.1 (2019), pp. 13–32. DOI: 10.1007/S40095-018-0289-1/TABLES/10.

[19] Wang, P., Yu, P., Huang, L., and Zhang, Y. "An integrated technical, economic, and environmental framework for evaluating the rooftop photovoltaic potential of old residential buildings". In: *Journal of Environmental Management* 317 (2022), p. 115296. DOI: 10.1016/J.JENVMAN.2022.115296.

[20] Olivella, J., Domenech, B., and Calleja, G. "Potential of implementation of residential photovoltaics at city level: The case of London". In: *Renewable Energy* 180 (2021), pp. 577–585. DOI: 10.1016/J.RENENE.2021.08.121.

[21] Ordóñez, Á., Sánchez, E., Rozas, L., García, R., and Parra-Domínguez, J. "Net-metering and net-billing in photovoltaic self-consumption: The cases of Ecuador and Spain". In: *Sustainable Energy Technologies and Assessments* 53 (2022), p. 102434. DOI: 10.1016/J.SETA.2022.102434.

[22] Vargas-Salgado, C., Aparisi-Cerdá, I., Alfonso-Solar, D., and Gómez-Navarro, T. "Can photovoltaic systems be profitable in urban areas? Analysis of regulation scenarios for four cases in Valencia city (Spain)". In: *Solar Energy* 233 (2022), pp. 461–477. DOI: 10.1016/J.SOLENER.2022.01.057.

[23] Calcabrini, A., Ziar, H., Isabella, O., and Zeman, M. "A simplified skyline-based method for estimating the annual solar energy potential in urban environments". In: *Nature Energy* 4.3 (2019), pp. 206–215. DOI: 10.1038/s41560-018-0318-6.

[24] Poon, K. H., Kämpf, J. H., Tay, S. E., Wong, N. H., and Reindl, T. G. "Parametric study of URBAN morphology on building solar energy potential in Singapore context". In: *Urban Climate* 33 (2020), p. 100624. DOI: 10.1016/j.uclim.2020.100624.

[25] Assouline, D., Mohajeri, N., and Scartezzini, J. L. "Large-scale rooftop solar photovoltaic technical potential estimation using Random Forests". In: *Applied Energy* 217 (2018), pp. 189–211. DOI: 10.1016/J.APENERGY.2018.02.118.

[26] Mora-López, L. and Sidrach-De-Cardona, M. "Models for the optimization and evaluation of photovoltaic self-consumption facilities". In: *Proceedings of the ISES Solar World Congress 2019 and IEA SHC International Conference on Solar Heating and Cooling for Buildings and Industry 2019* (2020), pp. 1555–1562. DOI: 10.18086/SWC.2019.30.01.

[27] Fuster-Palop, E., Prades-Gil, C., Masip, X., Viana-Fons, J. D., and Payá, J. "Innovative regression-based methodology to assess the techno-economic performance of photovoltaic installations in urban areas". In: *Renewable and Sustainable Energy Reviews* 149 (2021), p. 111357. DOI: 10.1016/J.RSER.2021.111357.

[28] Varo-martínez, M., Fernández-ahumada, L. M., López-luque, R., and Ramírez-faz, J. "Simulation of Self-Consumption Photovoltaic Installations: Profitability Thresholds". In: *Applied Sciences 2021, Vol. 11, Page 6517* 11.14 (2021), p. 6517. DOI: 10.3390/APP11146517.

[29] Generalitat Valenciana. *Fichas municipal Catarroja - Portal Estadístico de la Generalitat Valenciana - Generalitat Valenciana.*

[30] European Commission. *JRC Photovoltaic Geographical Information System (PVGIS).*

[31] *Weather Similarity.*

[32] Dirección General del Catastro. *Sede Electrónica del Catastro - Difusión de datos catastrales.*

[33] Tobias Loga, Nikolaus Diefenbach, Britta Stein, Elena Dascalaki, Constantinos A. Balaras, Kalliopi Droutsa, Simon Kontoyiannidis, Marjana Šijanec Zavrl, Andraž Rakuščček, Vincenzo Corrado, Stefano Corgnati, Ilaria Ballarini, Charles Roarty, Michael Hanratty, Bill Sheldrick, Marlies Van Holm, Nele Renders, Małgorzata Popiołek, Jerzy Kwiatkowski, Maria Amtmann, Tomáš Vimmr, Otto Villatoro, Kim B. Wittchen, Jesper Kragh, Hubert Despretz, Zdravko Georgiev, Karin Spets, Leticia Ortega, Begoña Serrano Lanzarote, Milica Jovanovic Popovic, and Dusan Ignjatovic. *Typology Approach for Building Stock Energy Assessment. Main Results of the TABULA project.* Tech. rep. 2012.

[34] Neuhäuser, M. "Wilcoxon–Mann–Whitney Test". In: *International Encyclopedia of Statistical Science* (2011), pp. 1656–1658. DOI: 10.1007/978-3-642-04898-2_615.

[35] Centro Nacional de Información Geográfica. *Centro de Descargas del CNIG.*

[36] Biljecki, F., Ledoux, H., and Stoter, J. "An improved LOD specification for 3D building models". In: *Computers, Environment and Urban Systems* 59 (2016), pp. 25–37. DOI: 10.1016/J.COMPENVURBSYS.2016.04.005.

[37] Masip, X., Fuster-Palop, E., Prades-Gil, C., Viana-Fons, J. D., Payá, J., and Navarro-Peris, E. "Case study of electric and DHW energy communities in a Mediterranean district". In: *Renewable and Sustainable Energy Reviews* 178 (2023), p. 113234. DOI: 10.1016/J.RSER.2023.113234.

[38] Liu, B. Y. and Jordan, R. C. "The interrelationship and characteristic distribution of direct, diffuse and total solar radiation". In: *Solar Energy* 4.3 (1960), pp. 1–19. DOI: 10.1016/0038-092X(60)90062-1.

[39] Memme, S. and Fossa, M. "Maximum energy yield of PV surfaces in France and Italy from climate based equations for optimum tilt at different azimuth angles". In: *Renewable Energy* 200 (2022), pp. 845–866. DOI: 10.1016/J.RENENE.2022.10.019.

[40] Liu, Z., Liu, X., Zhang, H., and Yan, D. "Integrated physical approach to assessing urban-scale building photovoltaic potential at high spatiotemporal resolution". In: *Journal of Cleaner Production* 388 (2023), p. 135979. DOI: 10.1016/J.JCLEPRO.2023.135979.

[41] Viana-Fons, J. D., Gonzálvez-Maciá, J., and Payá-Herrero, J. *Methodology for the calculation of the shadow factor on roofs and facades of buildings in urban areas.* 2019.

[42] Viana-Fons, J. D., Gonzálvez-Maciá, J., and Payá, J. "Development and validation in a 2D-GIS environment of a 3D shadow cast vector-based model on arbitrarily orientated and tilted surfaces". In: *Energy and Buildings* 224 (2020), p. 110258. DOI: 10.1016/j.enbuild.2020.110258.

[43] Fuster-Palop, E., Vargas-Salgado, C., Ferri-Revert, J. C., and Payá, J. "Performance analysis and modelling of a 50 MW grid-connected photovoltaic plant in Spain after 12 years of operation". In: *Renewable and Sustainable Energy Reviews* 170 (2022), p. 112968. DOI: 10.1016/J.RSER.2022.112968.

[44] Mehta, P. and Tiefenbeck, V. "Solar PV sharing in urban energy communities: Impact of community configurations on profitability, autonomy and the electric grid". In: *Sustainable Cities and Society* 87 (2022), p. 104178. DOI: 10.1016/J.SCS.2022.104178.

[45] Datadis. *Datadis.*

[46] Mor, G., Cipriano, J., Martirano, G., Pignatelli, F., Lodi, C., Lazzari, F., Grillone, B., and Chemisana, D. "A data-driven method for unsupervised electricity consumption characterisation at the district level and beyond". In: *Energy Reports* 7 (2021), pp. 5667–5684. DOI: 10.1016/J.EGYR.2021.08.195.

[47] Instituto Nacional de Estadística. *INEbase / Demografía y población / Cifras de población y censos demográficos / Censos de Población y Viviendas 2011.*

[48] Manso-Burgos, Ribó-Pérez, D., Gómez-Navarro, T., and Alcázar-Ortega, M. "Local energy communities modelling and optimisation considering storage, demand configuration and sharing strategies: A case study in Valencia (Spain)". In: *Energy Reports* 8 (2022), pp. 10395–10408. DOI: 10.1016/J.EGYR.2022.08.181.

[49] Ministerio para la Transición Ecológica (MTE); Boletín Oficial del Estado (BOE). *Real Decreto 244/2019, de 5 de abril, por el que se regulan las condiciones administrativas, técnicas y económicas del autoconsumo de energía eléctrica.* Madrid, 2019.

[50] Comisión Nacional de los Mercados y la Competencia. *Circular 3/2020, de 15 de enero, de la Comisión Nacional de los Mercados y la Competencia, por la que se establece la metodología para el cálculo de los peajes de transporte y distribución de electricidad.* Tech. rep. 2020.

[51] Red Eléctrica de España. *Analysis - ESIOS electricity.*

[52] Som Energia. *Histórico de Tarifas de Electricidad.*

[53] Manso-Burgos, Á., Ribó-Pérez, D., Alcázar-Ortega, M., and Gómez-Navarro, T. "Local Energy Communities in Spain: Economic Implications of the New Tariff and Variable Coefficients". In: *Sustainability 2021, Vol. 13, Page 10555* 13.19 (2021), p. 10555. DOI: 10.3390/SU131910555.

[54] Instituto Valenciano de Competitividad Empresarial. *Resolución de 24 de marzo de 2022, del presidente del Instituto Valenciano de Competitividad Empresarial (IVACE), por la que se convocan ayudas destinadas al fomento de instalaciones de autoconsumo de energía eléctrica en los municipios de la Comunitat Va.* Tech. rep. 2022.

[55] *optimize function - RDocumentation.*

[56] Brent, R. P. (P. "Algorithms for minimization without derivatives". In: (2002), p. 195.

[57] Simoiu, M. S., Fagarasan, I., Ploix, S., and Calofir, V. "Optimising the self-consumption and self-sufficiency: A novel approach for adequately sizing a photovoltaic plant with application to a metropolitan station". In: *Journal of Cleaner Production* 327 (2021), p. 129399. DOI: 10.1016/J.JCLEPRO.2021.129399.

[58] Mansó Borràs, I., Neves, D., and Gomes, R. "Using urban building energy modeling data to assess energy communities' potential". In: *Energy and Buildings* 282 (2023), p. 112791. DOI: 10.1016/J.ENBUILD.2023.112791.

[59] Ciocia, A., Amato, A., Leo, P. D., Fichera, S., Malgaroli, G., Spertino, F., and Tzanova, S. "Self-Consumption and Self-Sufficiency in Photovoltaic Systems: Effect of Grid Limitation and Storage Installation". In: *Energies 2021, Vol. 14, Page 1591* 14.6 (2021), p. 1591. DOI: 10.3390/EN14061591.

[60] Beck, T., Kondziella, H., Huard, G., and Bruckner, T. "Assessing the influence of the temporal resolution of electrical load and PV generation profiles on self-consumption and sizing of PV-battery systems". In: *Applied Energy* 173 (2016), pp. 331–342. DOI: 10.1016/J.APENERGY.2016.04.050.

[61] Gallego-Castillo, C., Heleno, M., and Victoria, M. "Self-consumption for energy communities in Spain: A regional analysis under the new legal framework". In: *Energy Policy* 150 (2021), p. 112144. DOI: 10.1016/J.ENPOL.2021.112144.

[62] Gilman, P., Dobos, A., Diorio, N., Freeman, J., Janzou, S., and Ryberg, D. *SAM Photovoltaic Model Technical Reference Update.* Tech. rep. National Renewable Energy Agency, 2016. DOI: NREL/TP-6A20-67399.

[63] Perpiñán Lamigueiro, O. *Energía Solar Fotovoltaica.* 2023.

[64] JA SOLAR. *JAM60S20 365-390 Datasheet.*

[65] Feldman, D., Ramasamy, V., Fu, R., Ramdas, A., Desai, J., and Margolis, R. *U.S. Solar Photovoltaic System and Energy Storage Cost Benchmark: Q1 2020*. Tech. rep. National Renewable Energy Laboratory, 2021.

[66] Eurostat. *HICP - annual data (average index and rate of change)*.

[67] Domenech, B., Calleja, G., and Olivella, J. "Residential Photovoltaic Profitability with Storage under the New Spanish Regulation: A Multi-Scenario Analysis". In: *Energies 2021, Vol. 14, Page 1987* 14.7 (2021), p. 1987. DOI: 10.3390/EN14071987.

[68] Agencia Tributaria. *Tax Agency: VAT tax rates*.

[69] Red Eléctrica de España. *REData - Non renewable detail CO2 emissions | Red Eléctrica*.

[70] López Prol, J. and Steininger, K. W. "Photovoltaic self-consumption is now profitable in Spain: Effects of the new regulation on prosumers' internal rate of return". In: *Energy Policy* 146 (2020), p. 111793. DOI: 10.1016/J.ENPOL.2020.111793.

[71] Talayero, A. P., Melero, J. J., Llombart, A., and Yürüşen, N. Y. "Machine Learning models for the estimation of the production of large utility-scale photovoltaic plants". In: *Solar Energy* 254 (2023), pp. 88–101. DOI: 10.1016/J.SOLENER.2023.03.007.

[72] Huang, S. "Linear regression analysis". In: *International Encyclopedia of Education(Fourth Edition)* (2023), pp. 548–557. DOI: 10.1016/B978-0-12-818630-5.10067-3.

[73] Koenker, R. "Quantile regression". In: *Quantile Regression* (2005), pp. 1–349. DOI: 10.1017/CBO9780511754098.

[74] Hao, L. and Naiman, D. Q. *Quantile regression*. Vol. 149. SAGE Publications, 2007.

[75] Koenker, R. *CRAN - Package quantreg*.

[76] Box, G. E. P. and Cox, D. R. "An Analysis of Transformations". In: *Journal of the Royal Statistical Society: Series B (Methodological)* 26.2 (1964), pp. 211–243. DOI: 10.1111/J.2517-6161.1964.TB00553.X.

[77] Sheather, S. J. "Diagnostics and Transformations for Multiple Linear Regression". In: (2009), pp. 151–225. DOI: 10.1007/978-0-387-09608-7_6.

[78] Ripley, B. "Support Functions and Datasets for Venables and Ripley's MASS [R package MASS version 7.3-58.2]". In: (2023).

Chapter 5

Discussion of the main results

This chapter offers a comprehensive overview of the findings and insights derived from this research. The discussion of the results is organized into three sections: the first addresses the findings of the PV production modeling, the second relates to the analysis of PVSC results in the evaluated buildings, and the third to the regression-based approaches.

5.1 PV production model

In Chapter 2, **the analysis focused on a 50 MW PV utility-scale in a Mediterranean climate, yielding main performance results such as a Y_R of 5.44 h/d, Y_F of 4.28 h/d, PR of 79.24%, and CUF of 19.77%**. Despite reaching lower PR values than in other similar plants, the Y_F and CUF remain higher due to the region's high annual insolation. The abundant solar resource in Mediterranean countries significantly enhances the production performance within these latitudes. The greatest PR values are typically found during the Spring season, when the irradiance is high enough compared with the Summer's levels and the temperatures are not high enough to reduce the facility's performance drastically.

Degradation constituted 13% of annual energy losses, with annual degradation rates 2-3% higher than manufacturer specifications. These values underscore the significance of incorporating degradation into long-term PV potential assessments and avoiding overestimations.

A daily production model was developed using the measured I_{POA} and E_{AC} timeseries from the inverters. This allowed the validation of the physical model to convert the geographic potential into technical potential and was integrated into the model for the other publications.

By employing one of the most common PV production models found in literature, as shown in section 2.3.3 (Eq. 2.1), **the more significant deviations in the estimated PV production were found during days with low irradiance levels. The deviation becomes more significant when the plant operates during low irradiance days. For instance, on days with 3 peak sun hours (Y_R = 3 h/d), the annual error obtained with the base model rises 7.3%, which is a non-negligible amount. This finding motivated an exploration of different approaches to reduce these errors, which can also be applied in the context of urban PVSC**. In these facilities, the PV modules are more exposed to shadows. Therefore, there are more working hours with diffuse irradiance. In this scenario, an accurate prediction in all the irradiance ranges is essential to optimize the performance of these facilities.

Multiple approaches were introduced to improve the modeling of the global PR of the utility-scale, and the estimated energy production was validated with real measurements:

- As the first alternative, **an exponential regression** model based on the available measurements was defined to **selectively reduce the global PR for low irradiance measurements. This approach reduced the $nRMSE$ of PR from 0.13 to 0.06 for days with low irradiances**. In addition, this approach reduced by 0.71% the annual AC production error.

- As a second alternative, **two regression-based approaches were investigated**. The errors were slightly improved by training an MLR model with only two predictors: the T_a and the I_{POA}. Nevertheless, **the best performance was found by training a RF model, which reduced to 0.02 the $nRMSE$ of PR in days with low irradiances**. As a disadvantage, despite improving the prediction accuracy, this method requires a higher computational time than the MLR model when trained with large databases.

As an advantage of using general predictors such as I_{POA} and T_a, it is possible to obtain this information by means of remote sensing techniques and georeferenced databases, which would ease the replicability of the previous models for general PV potential assessments in urban areas. These regression-based approaches can be integrated as part of the physical modeling for the urban PV assessment. Regardless of the replicability of these models, the results are conditioned by the operating year in which the models were trained. Thus, models trained with measurements obtained during the early lifetime of the facility would provide overestimations in PR, while models trained in the late operating lifetime would provide underestimations. **Training the models with representative operating periods throughout the facility's lifetime is recommended, such as halfway of the installation's lifetime** as performed in the present research.

If possible, another aspect that improves the accuracy of predictions of large-scale utilities is modeling by manufacturers' technical characteristics. This approach can obtain disaggregated results for any installation or sector with acceptable accuracies.

Although straightforward, **another important element that helps in the modeling process is to have more than one WS to combine the measurements as new predictors in the regression fits**. This method is helpful in large installations in which irradiance may fluctuate significantly in different installation areas, for example, during days with cloudy intervals.

5.2 Models for the assessment of the of the PVSC performance in urban areas

5.2.1 Physical modeling approach

The PV production model was included in Chapter 3 as a submodule of a global physical model to assess the techno-economic potential of PVSC facilities from a representative sample of 893 residential multistorey buildings in a Mediterranean municipality.

An isotropic irradiance model proceeded by a 3D-GIS model based on LiDAR and cadastral data, allowing obtaining the SL at a representative point of each building. In order to validate the complete effect of shadows and other production losses when obtaining the technical potential, the hourly AC energy production estimated by the physical model was compared with the results provided by the software System Advisor Model for the same irradiance TMY time series and skyline of buildings in a specific building within the urban fabric. As a result, an $RMSE$ of $0.525\,\mathrm{kW\,h}$ for the hourly measurements was obtained.

Chapter 4 addresses the multiple possibilities that offer the regression-based approaches to estimate the most significant PVSC performance parameters, as well as the study of the impact of several demand scenarios on the PV potential assessment.

In addition, several improvements in the physical modeling with respect to the previous research were implemented. The improved 3D GIS model provided a LOD2 in 3D modeling of the buildings, allowing the identification of tilted rooftops and segmenting the multiple rooftop sectors to install PV modules. The demand modeling in this chapter was based on real aggregated data from the municipality, and load profiles assessed were selected from aggregated real measurements by postal code and socio-economic sector. **Installations were sized according to the demand of the building through the optimization of the relationship between SS and PB**. This novel ratio constitutes a trade-off between economic feasibility and guaranteeing a minimum amount of grid independence. **This criterion ensures that the installation is optimally sized to balance energy efficiency and economic viability**. Exclusively minimizing PB often leads to undersized systems, covering only partial daytime consumption. This approach minimizes surplus production, which is compensated at lower prices than grid energy. Incorporating SS into the ratio increases installed capacity, extending the coverage of the load curves for more hours.

5.2.2 Analysis of the PVSC performance per category of buildings

The following findings were obtained regarding the results provided in **Chapter 3** by the physical model for a sample of 1,035 residential buildings, installing the maximum capacity available on each rooftop:

- On the one hand, **SFHs presented PBs above 25 years mainly from the production point of view due to high costs per unit of installed power and high shadow losses**. Because of their low height, the average shadow losses in energy terms of single-family houses were 35%, which contrasts with 10% of multistorey buildings. Additionally, regarding the demand side, this building typology presents limited potential savings in the electricity bill since surpluses are more usual due to higher fluctuations of the load profile compared with the aggregated demand curves of buildings with several consumers.

- On the other hand, **PVSC on multistorey residential buildings presented an average PB of 11.6 years**. The average yearly surpluses represented 3.6% of the annual production, and the average SS was 17.73%. In general, for this building typology, **the shadow losses are below 20% and do not significantly alter economic performance**. In contrast with the SFHs, the aggregation of multiple users sharing a facility increases the amount of self-consumed PV production, which is higher remunerated than surpluses, and therefore reduced economic PBs are obtained. Energy communities represent an alternative to increasing the SC so that the users of these buildings can have PVSC facilities with a lower PB. The average environmental PB is 2.3 years, which is significantly reduced compared with the economic PB. This shows the low environmental impact of these facilities during their lifetime. As in SFHs, low SC values in a significant part of the assessed buildings warn of oversized facilities' presence according to their consumption. These rates imply a potential overestimation of the PV production in urban areas when PV potential is assessed without considering the electricity consumption, especially under the NB scheme.

Under a NB scheme, this research highlighted the importance of considering the load curve, besides rooftop production assessment, to enhance the economic performance of PVSC systems for small consumers. This aspect was addressed in Chapter 4. With the improvements to the physical model by sizing according to optimizing the SS/PB ratio. In this chapter, a complete census simulation of a Mediterranean municipality of 3,734 buildings was assessed.

Concerning the aggregated energy results at the municipal level, in the NM scenario, the total installed capacity accounted for 90.1% of the maximum potential capacity, resulting in an annual energy production exceeding the municipality's cumulative demand by 103.7%. Conversely, in the NB scenario, it represented 50.3% of the capacity potential and met 67.5% of the annual energy demand. Although these ratios fluctuate according to the sizing criteria and the cost of surpluses, this study case provided a realistic order of magnitude for the economic background in 2022. Regarding the production-demand energy balance, under a NB scheme only with rooftop PVSC facilities, a null electricity balance in the district is not reached, but if sectored by building typologies, the PV energy produced on THs is enough to achieve a positive energy balance in this sector. According to these trends, municipalities with few AB buildings, such as rural areas, present more possibilities of achieving a higher annual production injected into the grid than their electricity needs. **Municipalities with many ABs would require other solutions to achieve a neutral balance with only on-site PV energy**, such as storage or façade integrated PV modules. As a particularity in this municipality studied, the industries are less energy intensive than in other municipalities of Spain. This aspect explains the tendency to achieve similar climate neutrality in buildings with large roofs compared with their consumption.

In relation to the **energy results per building typologies**, the SS rates slightly differ between the NM and NB scenario, which shows that PVSC systems without storage would not guarantee complete independence from the grid for most of the cases, understood as not requiring electricity from the grid in any hour of the year. **The greatest SS rates** under a NB scheme for the base case (using LP0) **are found in tertiary buildings** with an average of 46.1% and THs with an average of 46.0%, while lower averaged values are found in ABs with 40.4%. Regarding the most extreme SS values found in this study, in the scenario in which more consumption is aligned with sun hours, the SS for tertiary buildings would rise to 56.8%, whereas in the scenario in which most of the consumption takes place during night hours the SS in ABs decreases up to 23.2%. In this matter, **the regular range of SS is between 30-50% for most buildings**.

For the most optimistic scenario assessed, the global municipality SS obtained through an hourly balance reached 42.5%. Higher rates would require significant efforts to shift night consumption to the hours with insolation or assess the inclusion of storage in PV systems. Both alternatives would impact the capacity installed due to economic constraints. The capacity for the first solution would be higher, whereas it would presumably be lower in the second one.

Installations in buildings with few consumers, such as SFHs and THs (few aggregated load curves) are the most sensitive to greater fluctuations in profitability when patterns in demand vary. Robust predictions in the global energy performance of PV facilities are found when aggregating load profiles. In buildings with consumers, users SS and SC rates could be improved by using the hourly dynamic sharing coefficients contemplated by the Spanish law. Nevertheless, this approach is beyond energy planning purposes since it requires each user's real load curves to provide useful and applicable results.

Regarding the **economic results per building typologies**, the non-remunerated surplus of the current Spanish regulation hinders a higher profitability performance of PV facilities, especially during the months with higher insolation. Nevertheless, it is not as determinant as the difference between the retail and surplus prices, which is the main cause of the difference in optimal installed capacity between the NM and NB scenarios. The average PBs remain similar for each billing scheme since the sizing optimization of the PV facility maximizes the ratio between SS and PB. Under a NB scheme, **the lower PBs are found in ABs and industrial buildings** with averages of 3.8 and 4.2 years, respectively, while **the greatest PBs were found in small consumers such as SHFs and THs** whose average PBs are 9.1 and 10.7 years. Except for buildings with few users (SFHs and THs), the building typologies averaged PBs below 5.5 years. 24.1% of the SFHs and 21.3% of the THs presented PBs greater than the lifecycle of the facilities. The results are highly sensitive to economies of scale and the shape of their load profile.

There are two main reasons why this low value contrasts with the averaged PB of 11.6 years obtained for PVSC systems on residential multi-storey buildings in Chapter 3 and illustrate how PVSC results are highly conditioned by the hypothesis employed:

- First, the optimization of the PV facility considering the ratio SS/PB was not included in the latter. Hence, some installations were oversized according to their energy needs.
- Second, the electricity and surpluses prices of the most recent study, developed in 2022, were around 2-2.5 times higher than the prices of the first assessment, based on prices between 2018 and 2019. In this case, a price increase due to an economic situation of increased inflation or scarcity of energy resources allows more significant savings in the PVSC performance.

In any case, the study provided the averaged PBs for other scenarios for electricity prices. If prices were similar to the levels found in 2018-2019 (around 0.4 times lower than in 2022), the average PBs of the building typologies MFHs, ABs, and industrial tertiary would range between 10 to 15 years. Nevertheless, for SFHs and THs, the PBs would exceed 20 years, aligning with the findings in Chapter 3.

This high volatility of prices was addressed in the regression approaches by introducing multiple situational factors, such as coefficients that model the increase of prices and the increase of costs. With this research, a realistic quantification for all electricity price ranges was provided, showing that in most cases, the investment would be recovered around half of the useful life of the installation, except for SFs and THs, which would require a particular analysis with their consumption load curves. These results are limited to a conservative scenario in which the facilities are not subsidized.

Comparing the previous results with the economic performance of the utility-scale analyzed in Chapter 2, commissioned in 2008, a notable reduction in installation costs was present during the last decade. The investment costs of 2008 (estimated in $6.4\,€/\mathrm{W_p}$) contrast with the assumed costs for the recent studies for large facilities (<$1\,€/\mathrm{W_p}$), this fact mainly explains the high PB of 17.6 years obtained for the utility-scale.

In terms of defining a **general strategy for the municipality** in deploying PVSC systems, similar impacts were identified by employing economic and environmental optimizations. For example, an economic prioritization that arranges the buildings with facilities according to the greatest IRR would provide a similar prioritization order as arranging the buildings by potential emission savings from the grid. The latter approach is aligned with the EU's sustainability policies to reduce the environmental impact. Following the latter strategy, tertiary, ABs, and industrial buildings are the typologies with more significant potential emission savings and **only acting on the 28.6% of the building stock of the municipality (mainly formed by these typologies) would reduce up to 80% of the emissions of the entire municipality due to electricity consumption** of the grid. Thus, concentrating efforts on industrial areas and large residential buildings would generate the greater environmental impact with the smallest number of installations possible.

5.3 Regression-based modeling approaches to estimate PVSC KPIs

Based on the techno-economic results derived from the physical model for the representative sample of buildings from **Chapter 2, two production regressions were provided in the technical potential field**.

Firstly, a methodology was developed to build a MLR model to estimate the yearly PV production in a specific building using the installed capacity and the potential shadow losses. This model facilitates the technical potential assessment of any other building with similar climate conditions. Validation results provided an $RMSE$ of $2.1\,\mathrm{kWh/kW_p year}$.

Secondly, **the previous production regression model included an extrapolation of the yearly energy production for other climates**. The latter allows the PV production potential assessment if the user modifies the irradiance and temperature hypothesis, which helps to use the model in other geographic regions or countries. The estimations provided by this novel correlation compared with the simulation of the techno-economic model for other four climates **provided an $RMSE$ of** $3.2\,\mathrm{kWh/kW_p year}$. The simplicity of this contribution allows an easy implementation into user-friendly tools.

In the economic potential field, four independent dimensionless parameters highly based on the building morphology were defined to quantify the PB through a MLR model. However, only **the cost ratio**, which measured the economy of scale of the facility, **and the percentage of shadows provided higher correlations** (>0.6). The first one was highly dependent on the total rooftop area suitable for PV, facilitating its estimation in other regions and replicability. The non-dimensionality of the above-mentioned parameters improves the regression fit and, thus, the prediction performance. **The $RMSE$ provided by the PB regression for the selected sample was 0.48 years, which is an acceptable deviation in this context**. This method provides technicians a "rule of thumb" when assessing urban rooftops and can be implemented in user-friendly web tools such as solar cadasters.

Concerning the regression modeling addressed in Chapter 4, four main PVSC KPIs were identified: SS, SC, IRR, and PB. As a consequence of optimizing the size of PV capacity, Pearson's correlation coefficients between the PB and predictors such as SL or SR decrease. Nevertheless, the CR, which considers the economy of scale, remains highly correlated. This scarce correlation and the need to quantify other PVSC performance parameters motivated the research of novel dimensionless parameters, among them:

- The surplus ratio, which is the relation between surpluses and energy production, was redefined as the sizing ratio, which compares the peak power production and the peak power demand. This new ratio is easier to estimate than the previous one since it does not require calculating the results of the match between production and load curves.
- **The LPF provides a quantitative definition of how much the demand curves are aligned with PV production rating with higher values when consumption occurs during the high insolation hours of the day**. This novel definition would provide researchers with a quantitative alternative to characterize any load profile assessed with

PV production. Its definition is similar to the capacity utilization factor of PV plants but applied in the demand context.

- Three independent ratios to improve the robustness of predictions under different scenarios of demand, cost, and price levels were included. This approach provides flexibility when training regression models for multiple scenarios.

In Chapter 4, the sequential estimation through QR models allowed obtaining, firstly, energy variables and, secondly, profitability variables. **The sizing ratio complemented with the LPF significantly explains the SS values obtained with accuracy with an $RMSE$ of 1.53%**. The latter result and the two initially defined predictors allowed the estimation of SCs with a $RMSE$ of 1.63%. The IRR was moderately correlated with SC. Including SS and the initial predictors into the regression fit, the estimations provided a $nRMSE$ of 10%, with the most significant deviations for low IRR values. The PB required the estimation of all the above-mentioned predictors with multiple transformations to increase the linearity among predictors with the PB. **The results provided a $RMSE$ of 0.02 year for PB**.

The obtained correlations hinder the direct interpretation of the results, compared with the regressions obtained in the Chapter 3, which, in most cases, highly correlated with the rooftop area. Nevertheless, it is shown that it is possible to estimate the performance results of the installation with some morphological and intermediate parameters without the need for hourly matching.

The three publications addressed multiple regression modeling strategies to obtain a simplified MLR model and ease its replicability in other contexts. **The main learnings in the regression modeling applied in this context are the following**:

- The definition of dimensionless and normalized predictors based on the relationship of multiple PVSC performance parameters or building characteristics allowed a similar scale on the features of the datasets, reducing the range of possible values of the predictors. This aspect allows obtaining models more robust to outliers. In addition, it guarantees similar weights on each feature in the model, limiting the possibility that the features with larger scales might dominate the model, and it would be challenging to compare their contributions accurately. No standardization process was performed in this research since the predictors were within acceptable ranges, without greater outliers. However, this technique can be potentially useful in other applications.
- The reduction of multicollinearity among predictors through the study of their Pearson correlation coefficients allows the identification of redundant variables whose effects on the target variable are already explained by other more relevant predictors.
- Box-cox transformations are helpful to address the linearity assumption as well as the homoscedasticity in residuals in linear regression. In this research, this technique helped model PB and increased the linearity of multiple predictors for the QR models defined in Chapter 4. However, this approach leads to a reduction in the direct interpretation of the models.

- The determination of a minimum sample size is relevant to obtain representative results for a greater urban area. In this matter, Chapter 3 performed a parametric study quantifying the $RMSE$ of PB for several sample sizes. Results provided similar errors ($RMSE$ and MAE) from about a sample size of 200 buildings, which is an admissible quantity to replicate in other contexts as long as the building typologies studied remained similar. Another alternative approach is using spatial stratified sampling by regions or districts in this context, selecting a representative sample of buildings for each city district.

- In Chapter 4, the sizing of PV facilities considering the demand generally reduces the correlation between the predictors and the target variables assessed. In this case, when the general parametric regression assumptions are not fully met with the available data so that a probability distribution cannot be assumed, nonparametric regression approaches constitute a robust alternative due to their reliance on fewer assumptions. Nonparametric models are highly flexible and can capture complex and nonlinear relationships. Among them, QR models were employed, motivated by non-normal and heteroscedasticity residuals. In contrast to Chapter 3 regressions, which rely heavily on available roof space, reduced predictor-objective correlations suggest a need for additional variables. However, in line with our aim to explore simplified models, nonparametric models abstain from introducing new predictors.

- The model evaluation is always performed employing data that was not employed in the model's training. This approach assists in evaluating how effectively the model generalizes from the training data to unfamiliar, unseen data, offering valuable insights into its overall performance quality. Additionally, employing k-fold cross-validation, which is mainly detailed in Chapter 2, helps address the variability in model performance that can arise from a single train-test split. It provides a more stable assessment of a model's generalization performance and can help identify potential issues like overfitting or underfitting.

Chapter 6

Conclusions

In section 6.1 of this chapter, the conclusions of the present research work are discussed, summarizing the main contributions and comparing them with the research questions stated in Chapter 1.

As the object of study is very extensive, there are still multiple possibilities and modeling improvements to evaluate and open new lines of research. The latter have been compiled in section 6.2.

Finally, the research publications for the present thesis are listed in section 6.3.

6.1 General conclusions

This research involves a comprehensive investigation of strategies for developing bottom-up physical and agile regression-based models to evaluate the PV potential in urban areas. As an application, these approaches were implemented to assess the PV economic potential of a representative sample of buildings within a Mediterranean urban setting. **The major conclusions are presented below**:

One-year measurements were collected from 500 installations of $100\,\mathrm{kW_n}$ from a $50\,\mathrm{MW_n}$ PV utility-scale under Mediterranean conditions after operating half of its projected lifetime. The main conclusions of PV performance of the utility-scale for the measurements collected in 2020 are the following:

- Regarding PR and CUF, the performance was slightly lower than other PV power plants under Mediterranean climate conditions found in the literature. Nevertheless, the studied utility-scale approximately doubles the average age of other published assessed facilities. **The PR is over 80% for almost 42% of the measured days, proving a correct performance**.
- The **degradation losses** yield the greatest weight in the energy balance, representing a **global energy loss of 13%** of the global energy at STC.

A PV production model that converts in-plane irradiance into AC PV production was validated with one-year measurements of the previous utility-scale. With the climate measurements collected for this facility, three different modeling approaches were developed to reduce the accuracy when estimating the low irradiance losses. The model uses measured irradiance and ambient temperature as predictors. The assessed models include an exponential fit that decreases the global PR for the days with low irradiance, a MLR model and a RF model. The following conclusions were drawn:

- The RF model, based on regression trees, reduced the $nRMSE$ of PR to 0.013 and a relative error of the PV production for days with low insolation to 0.002%.
- In any case, **the assessed regression-based models provided a better PR accuracy than the physical model and are recommended to forecast the PR whenever measured data is available**. These approaches constitute an alternative to model and predict the PR when the plant has scarce technical data.
- The regression-based models developed provided higher performance than other ML approaches found in literature, which required more measurements.

The **simulation results of the physical models** applied to 893 residential multi-storey buildings and the complete building stock (3,734 buildings) in a Mediterranean municipality yielded the following conclusions:

- SFHs and THs are the most sensitive to the shape and fluctuations of the hourly load profile.
- **Under the constraints of the current NB scheme, rooftop PVSC systems do not attain annual emissions neutrality for municipal electricity consumption**. In contrast, this objective becomes attainable by adopting a NM approach.
- **The best economic and environmental results are achieved with ABs, industrial and tertiary buildings**.
- Optimizing the sizing of facilities combining economic and energy criteria and using load curves in the NB modality is crucial for achieving competitive PB and comparable SS levels to NM. **Maximizing the ratio PB/SS has proven an effective and practical criterion for sizing installations**.
- One solution to reduce the high PB values in SFHs and buildings with low energy demand is the aggregation of load curves under shared PV facilities by promoting energy communities. The results show that adding consumption and reducing surpluses increases the profitability in NB cases.

Based on the previous simulation results. **A bottom-up methodology to train MLR models to assess the performance of potential PVSC systems on rooftops was developed**. The following conclusions were drawn:

- **To estimate the PB of facilities that occupy all the available rooftop area**, a **MLR model** was performed based on a generated dataset obtained through physical modeling. After studying a sample of 893 residential multi-storey buildings, which is the most frequent typology, it was concluded that **three dimensionless parameters were enough to provide accurate PB estimations**: the cost ratio (economy of scale), the percentage of shadow losses and in a lower degree the percentage of surpluses compared with PV production. Validation results provided an assumable error for urban energy planning purposes.
- For the same sample of buildings, another MLR model was developed to estimate annual PV production and extrapolate these results in other climates and shadow circumstances. Annual horizontal irradiation, mean ambient temperature, the percentage of shadow losses, and the peak power installed on the rooftop were the inputs of this model.
- **The second MLR modeling approach was developed for other PVSC KPIs when facilities are sized according to a combined energy and economic criterion. SC, SS, PB, and IRR** were estimated through more predictors than the previous regression for PB since the sizing of PV capacities does not present a direct relationship with the available rooftop areas for all the cases.
- The main predictors defined are the following: the SR, the CR (economy of scale), and **the LPF, a new parameter that is crucial to estimate SS and SC** and measures

the alignment between the load and the sun hours with more irradiance. This coefficient provides an objective quantitative characterization of load profiles in the PVSC context, which is encouraged to be used by other research works as a benchmarking value when describing load profiles.

- **The validation results of the MLR models for SC, SS, PB, and IRR provided $nRMSE$ values below 10%**, which are acceptable as first estimation in urban planning.

6.2 Future work and research opportunities

The research development and findings have revealed several limitations, presenting **opportunities for future research**. The more significant areas for improvement fall under three categories: physical modeling, regression modeling, and PV potential assessment insights (the focal point of this study).

The accuracy of **physical modeling approaches** is closely linked to the data availability. Investigating new data sources and exploring alternative databases would improve the accuracy of the estimations. The main areas of improvement are the following:

- **Validation challenges**: Despite the possibility of conducting theoretical assessments using practical, measured data from executed PV facilities (e.g., the $50\,\mathrm{MW_n}$ utility-scale assessed), massive validation of already existing facilities remains challenging due to limited data availability. The low penetration of PV systems in urban areas hinders the validation of the estimation of the technical potential through real-case experiences, and the sizing criteria in deployed installations depend on the installer. Thus, they may not align with the assumptions followed in this research. Moreover, validating the real economic PV potential requires consumption measurements of all users, which are scarce and not publicly available.
- **Cadastral data availability**: Building characterization and demand estimations in this thesis heavily rely on cadastral information, making replication in other countries challenging because of the data availability and structuring. Exploring alternatives using open data is essential to improve replicability.
- **Considering rooftops obstacles in detail**: Incorporating alternative sources of information, such as satellite images, would provide a more detailed view of roof areas occupied by obstacles or utilized for other purposes, enabling better identification of suitable locations for photovoltaic installations.
- **Challenges in inferring load curves from open data**: Scarce open data solutions provide limited real measurements for specific locations in other countries or regions. As this data is often aggregated to preserve user privacy, inferring specific load curves for each consumer in the municipality remains challenging.
- **Addressing seasonal occupancy in buildings**: Dealing with the heterogeneous occupancy of dwellings and premises poses another challenge, hindering the accurate estimation of consumption levels for each property. Factors such as buildings not occupied year-round or with solid seasonality, which is common in Mediterranean areas, could significantly reduce the estimated electricity consumption and economic potential.
- **Computational intensity in sizing optimization**: The optimization of PV facility sizing based on demand poses one of the most computationally intensive steps. Multiple iterations are required to match load profiles and production time series, especially in buildings with numerous independent consumers. Implementing agile methods for sizing according to demand would enhance model scalability.

The following potential improvements have been detected regarding **regression-based models**:

- **Estimation of novel target variables**: The proposed methodology could be extended to estimate various techno-economic variables not covered in this paper. By identifying new predictors and acknowledging their limitations, a broader view of regression models' capacity in this research field emerges.
- **Diversifying data sources**: Regression models rely partly on cadastral information, which may vary in availability across different countries. Enhancing replicability involves studying alternative and widespread data sources, such as satellite data, to obtain relevant information.
- **Reducing predictor variables**: The challenge of reducing the number of predictors when assessing the economic results of PV facilities is acknowledged. Exploring alternative machine learning approaches beyond multiple linear regressions may help reduce the number of predictors while maintaining similar accuracy.
- **Handling large datasets**: The need to train these models with large datasets has driven the development of high-computation demanding physical models in this thesis, whose replicability is difficult. Finding efficient ways to generate large datasets of PV performance results in urban areas is essential for broader applicability.

Finally, given the techno-economic constraints of this research, potential future lines of investigation for the topic of **PV potential assessment in urban areas** include:

- **Comparing the global municipality PV potential across different urban morphologies** (e.g., rural towns and high-population density cities) enhances the knowledge for policy and decision-making, enabling targeted resource allocation in specific regions. Evaluating a municipality's economic potential and its global self-sufficiency level is crucial in identifying which municipalities benefit the most from PV systems.
- Quantifying potential improvements in energy and economic PV performance parameters when **optimizing the sharing coefficients** of facilities with several consumers.
- **Comparing multiple sizing criteria** found in the literature for a large sample of facilities and users and identifying their limitations or trends when assessing large areas under a NB scheme.
- The **assessment of the current market potential** considering legal, economic, and social barriers to provide the most realistic scenario of PV penetration in urban areas.
- The **study of strategies to increase the on-site SS rate** and their impact on the global techno-economic PV potential. Among them, the assessment of façade integrated PV systems in large buildings, such as multi-storey buildings, and the inclusion of storage energy systems in buildings with scarce envelope space.

6.3 Publications and research activities

6.3.1 Journal publications

The research findings in the present PhD thesis has led to the following publications:

- Enrique Fuster-Palop, Carlos Prades-Gil, Ximo Masip, J. D. Viana-Fons, and Jorge Payá. *Innovative regression-based methodology to assess the techno-economic performance of photovoltaic installations in urban areas.* In: *Renewable and Sustainable Energy Reviews* (2021), Vol. 149, p. 111357. DOI: https://doi.org/10.1016/J.RSER.2021.111357. Impact factor: 16.8 (2021).
- Enrique Fuster-Palop, Carlos Vargas-Salgado, Juan Carlos Ferri-Revert, and Jorge Payá. *Performance analysis and modelling of a 50 MW grid-connected photovoltaic plant in Spain after 12 years of operation.* In: *Renewable and Sustainable Energy Reviews* (2022), Vol. 170, p. 112968. DOI: https://doi.org/10.1016/j.rser.2022.112968. Impact factor: 15.9 (2022).
- Enrique Fuster-Palop, Carlos Prades-Gil, Ximo Masip, J. D. Viana-Fons, and Jorge Payá. *Techno-Economic Potential of Urban Photovoltaics: Comparison of Net Billing and Net Metering in a Mediterranean Municipality.* In: *Energies* (2023), Vol. 16, p. 3564. DOI: https://doi.org/10.3390/en16083564. Impact factor: 3.2 (2022).

Outside the scope of this thesis, the author contributed to the following research publication during the development of his PhD:

- Ximo Masip, Enrique Fuster-Palop, Carlos Prades-Gil, Ximo Masip, J. D. Viana-Fons, Jorge Payá, and Emilio Navarro-Peris. *Case study of electric and DHW energy communities in a Mediterranean district.* In: *Renewable and Sustainable Energy Reviews* (2023), Vol. 178, p. 113234. DOI: https://doi.org/10.1016/j.rser.2023.113234. Impact factor: 15.9 (2022).

6.3.2 Conferences

The author contributed to the following conferences:

- Enrique Fuster-Palop, Carlos Prades-Gil, Ximo Masip, J. D. Viana-Fons, and Jorge Payá. *Profitability of PV generators in urban environments considering the new Spanish regulation.* In: *X Congreso Ibérico y VIII Congreso Iberoamericano de Ciencias y Técnicas del Frío (CYTEF 2020)* (2020). ISBN: 978-2-36215-043-2.
- Enrique Fuster-Palop, Carlos Prades-Gil, Ximo Masip, J. D. Viana-Fons, and Jorge Payá. *Evaluation of the Solar Photovoltaic Generation Potential of a sample of residential buildings in the City of Valencia.* In: *15th Conference on Sustainable Development of Energy, Water and Environment Systems* (2020). (pp. 288-299). ISSN: 1847-7178 978-84-09-46920-8.

- Elisa Gimeno Gómez, Enrique Fuster-Palop, Ximo Masip, Carlos Prades-Gil, and J. D. Viana-Fons. *Comunidades Energéticas como el modelo perfecto para la Transición Energética de las ciudades y la democratización de la energía. Caso práctico de la ciudad de Catarroja.* In: *XVI Congreso Nacional del Medio Ambiente (CONAMA 2022)* (2022). ISBN: 978-84-09-46920-8.

Global Bibliography

Agencia Tributaria. *Tax Agency: VAT tax rates* (cited on page 135).

Ahmad, M. W., Mourshed, M., and Rezgui, Y. "Tree-based ensemble methods for predicting PV power generation and their comparison with support vector regression". In: *Energy* 164 (2018), pp. 465–474. DOI: 10.1016/J.ENERGY.2018.08.207 (cited on page 46).

Alhamwi, A., Medjroubi, W., Vogt, T., and Agert, C. "GIS-based urban energy systems models and tools: Introducing a model for the optimisation of flexibilisation technologies in urban areas". In: *Applied Energy* 191 (2017), pp. 1–9. DOI: 10.1016/J.APENERGY.2017.01.048 (cited on page 13).

Alshare, A., Tashtoush, B., Altarazi, S., and El-Khalil, H. "Energy and economic analysis of a 5MW photovoltaic system in northern Jordan". In: *Case Studies in Thermal Engineering* 21 (2020), p. 100722. DOI: 10.1016/J.CSITE.2020.100722 (cited on page 65).

An, Y., Chen, T., Shi, L., Heng, C. K., and Fan, J. "Solar energy potential using GIS-based urban residential environmental data: A case study of Shenzhen, China". In: *Sustainable Cities and Society* 93 (2023), p. 104547. DOI: 10.1016/J.SCS.2023.104547 (cited on page 5).

Análisis, C. Y., Caamaño Martín, E., and Díaz-Palacios Sisternes, S. "Potencial solar fotovoltaico de las cubiertas edificatorias de la ciudad de Vitoria-Gasteiz: caracterización y análisis". 2017 (cited on page 89).

ANPIER. *Anuario Fotovoltaico 2019*. Tech. rep. Asociación Nacional de Productores de Energía Renovable (ANPIER), 2019 (cited on page 97).

Antonopoulos, I., Robu, V., Couraud, B., Kirli, D., Norbu, S., Kiprakis, A., Flynn, D., Elizondo-Gonzalez, S., and Wattam, S. *Artificial intelligence and machine learning approaches to energy demand-side response: A systematic review*. 2020. DOI: 10.1016/j.rser.2020.109899 (cited on page 90).

APPA Renovables. *Informe Anual Autoconsumo Fotovoltaico 2022*. Tech. rep. 2022 (cited on page 2).

Arias-Rosales, A. and LeDuc, P. R. "Urban solar harvesting: The importance of diffuse shadows in complex environments". In: *Renewable and Sustainable Energy Reviews* 175 (2023), p. 113155. DOI: 10.1016/J.RSER.2023.113155 (cited on page 9).

Assadeg, J., Sopian, K., and Fudholi, A. “Performance of grid-connected solar photovoltaic power plants in the Middle East and North Africa”. In: *International Journal of Electrical and Computer Engineering (IJECE)* 9.5 (2019), pp. 3375–3383. DOI: 10.11591/IJECE.V9I5.PP3375-3383 (cited on page 6).

Assouline, D., Mohajeri, N., and Scartezzini, J. L. “Quantifying rooftop photovoltaic solar energy potential: A machine learning approach”. In: *Solar Energy* 141 (2017), pp. 278–296. DOI: 10.1016/J.SOLENER.2016.11.045 (cited on page 20).

Assouline, D., Mohajeri, N., and Scartezzini, J. L. “Large-scale rooftop solar photovoltaic technical potential estimation using Random Forests”. In: *Applied Energy* 217 (2018), pp. 189–211. DOI: 10.1016/J.APENERGY.2018.02.118 (cited on pages 17, 58, 129).

Atersa. *Línea ULTRA - Módulos Fotovoltaicos - Productos y Servicios - Atersa* (cited on page 97).

Attari, K., Elyaakoubi, A., and Asselman, A. “Performance analysis and investigation of a grid-connected photovoltaic installation in Morocco”. In: *Energy Reports* 2 (2016), pp. 261–266. DOI: 10.1016/J.EGYR.2016.10.004 (cited on page 65).

Avaesen. *Mapa CELS - Plaza Energía.* 2023 (cited on page 9).

Aydin, G. *Modeling of energy consumption based on economic and demographic factors: The case of Turkey with projections.* 2014. DOI: 10.1016/j.rser.2014.04.004 (cited on page 101).

Balcombe, P., Rigby, D., and Azapagic, A. “Investigating the importance of motivations and barriers related to microgeneration uptake in the UK”. In: *Applied Energy* 130 (2014), pp. 403–418. DOI: 10.1016/J.APENERGY.2014.05.047 (cited on page 5).

Balderrama, S., Lombardi, F., Stevanato, N., Pena, G., Colombo, E., and Quoilin, S. “Automated evaluation of levelized cost of energy of isolated micro-grids for energy planning purposes in developing countries”. In: *ECOS 2019 - Proceedings of the 32nd International Conference on Efficiency, Cost, Optimization, Simulation and Environmental Impact of Energy Systems.* Institute of Thermal Technology, 2019, pp. 2999–3012 (cited on page 17).

Bandong, S., Leksono, E., Purwarianti, A., and Joelianto, E. “Performance Ratio Estimation and Prediction of Solar Power Plants Using Machine Learning to Improve Energy Reliability”. In: *Proceedings of the 2019 6th International Conference on Instrumentation, Control, and Automation, ICA 2019* (2019), pp. 36–41. DOI: 10.1109/ICA.2019.8916687 (cited on pages 46, 70).

Banerjee, A., Chitnis, U., Jadhav, S., Bhawalkar, J., and Chaudhury, S. “Hypothesis testing, type I and type II errors”. In: *Industrial Psychiatry Journal* 18.2 (2009), p. 127. DOI: 10.4103/0972-6748.62274 (cited on page 100).

Bansal, N., Jaiswal, S. P., and Singh, G. “Long term performance assessment and loss analysis of 9 MW grid tied PV plant in India”. In: *Materials Today: Proceedings* (2022). DOI: 10.1016/J.MATPR.2022.01.263 (cited on page 45).

Bansal, N., Pany, P., and Singh, G. “Visual degradation and performance evaluation of utility scale solar photovoltaic power plant in hot and dry climate in western India”. In: *Case Studies in Thermal Engineering* 26 (2021), p. 101010. DOI: 10.1016/J.CSITE.2021.101010 (cited on page 66).

Beck, T., Kondziella, H., Huard, G., and Bruckner, T. “Assessing the influence of the temporal resolution of electrical load and PV generation profiles on self-consumption and sizing of PV-battery systems”. In: *Applied Energy* 173 (2016), pp. 331–342. DOI: 10.1016/J.APENERGY.2016.04.050 (cited on page 135).

Belgiu, M. and Drăgu, L. “Random forest in remote sensing: A review of applications and future directions”. In: *ISPRS Journal of Photogrammetry and Remote Sensing* 114 (2016), pp. 24–31. DOI: 10.1016/J.ISPRSJPRS.2016.01.011 (cited on page 58).

Bentouba, S., Bourouis, M., Zioui, N., Pirashanthan, A., and Velauthapillai, D. “Performance assessment of a 20 MW photovoltaic power plant in a hot climate using real data and simulation tools”. In: *Energy Reports* 7 (2021), pp. 7297–7314. DOI: 10.1016/J.EGYR.2021.10.082 (cited on page 45).

Biljecki, F., Ledoux, H., and Stoter, J. “An improved LOD specification for 3D building models”. In: *Computers, Environment and Urban Systems* 59 (2016), pp. 25–37. DOI: 10.1016/J.COMPENVURBSYS.2016.04.005 (cited on page 132).

Biljecki, F., Ledoux, H., and Stoter, J. “Does a finer level of detail of a 3D city model bring an improvement for estimating shadows?” In: *Lecture Notes in Geoinformation and Cartography* 9783319256894 (2017), pp. 31–47. DOI: 10.1007/978-3-319-25691-7_2 (cited on pages 14, 95).

Blanco-Díez, P., Díez-Mediavilla, M., and Alonso-Tristán, C. “Review of the Legislative Framework for the Remuneration of Photovoltaic Production in Spain: A Case Study”. In: *Sustainability 2020, Vol. 12, Page 1214* 12.3 (2020), p. 1214. DOI: 10.3390/SU12031214 (cited on page 66).

Blyth, W., Speirs, J., and Gross, R. *Low carbon jobs: the evidence for net job creation from policy support for energy efficiency and renewable energy.* Tech. rep. Oxford, 2014 (cited on page 4).

Bódis, K., Kougias, I., Jäger-Waldau, A., Taylor, N., and Szabó, S. “A high-resolution geospatial assessment of the rooftop solar photovoltaic potential in the European Union”. In: *Renewable and Sustainable Energy Reviews* 114 (2019), p. 109309. DOI: 10.1016/j.rser.2019.109309 (cited on pages 12, 13, 19).

Bórawski, P., Holden, L., and Bełdycka-Bórawska, A. “Perspectives of photovoltaic energy market development in the european union”. In: *Energy* 270 (2023), p. 126804. DOI: 10.1016/J.ENERGY.2023.126804 (cited on page 128).

Bouacha, S., Malek, A., Benkraouda, O., Arab, A. H., Razagui, A., Boulahchiche, S., and Semaoui, S. “Performance analysis of the first photovoltaic grid-connected system in Algeria”. In: *Energy for Sustainable Development* 57 (2020), pp. 1–11. DOI: 10.1016/J.ESD.2020.04.002 (cited on page 65).

Bounoua, Z., Ouazzani Chahidi, L., and Mechaqrane, A. “Estimation of daily global solar radiation using empirical and machine-learning methods: A case study of five Moroccan locations”. In: *Sustainable Materials and Technologies* 28 (2021), e00261. DOI: 10.1016/J.SUSMAT.2021.E00261 (cited on page 59).

Box, G. E. P. and Cox, D. R. “An Analysis of Transformations”. In: *Journal of the Royal Statistical Society: Series B (Methodological)* 26.2 (1964), pp. 211–243. DOI: 10.1111/J.2517-6161.1964.TB00553.X (cited on page 137).

Breiman, L. “Random Forests”. In: *Machine Learning 2001 45:1* 45.1 (2001), pp. 5–32. DOI: 10.1023/A:1010933404324 (cited on page 58).

Brent, R. P. (P. “Algorithms for minimization without derivatives”. In: (2002), p. 195 (cited on page 134).

Brito, M. C., Freitas, S., Guimarães, S., Catita, C., and Redweik, P. “The importance of facades for the solar PV potential of a Mediterranean city using LiDAR data”. In: *Renewable Energy* 111 (2017), pp. 85–94. DOI: 10.1016/j.renene.2017.03.085 (cited on page 89).

Busch, L., Schäfer, T., Song, W., Mack, M., and Egler, M. “PV System Energy Yield Calculation Program PR-FACT”. In: *28th European Photovoltaic Solar Energy Conference and Exhibition* (2013), pp. 3699–3708. DOI: 10.4229/28THEUPVSEC2013-5CO.6.3 (cited on page 45).

Caballero, V., Briones, A., Coca-Ortegón, A., Pérez, A., Barrios, B., and Mano, M. de la. “Analysis and simulation of an Urban-Industrial Sustainable Energy Community: A use case in San Juan de Mozarrifar using photovoltaic energy”. In: *Energy Reports* 9 (2023), pp. 1589–1605. DOI: 10.1016/J.EGYR.2022.12.059 (cited on page 9).

Calcabrini, A., Ziar, H., Isabella, O., and Zeman, M. “A simplified skyline-based method for estimating the annual solar energy potential in urban environments”. In: *Nature Energy* 4.3 (2019), pp. 206–215. DOI: 10.1038/s41560-018-0318-6 (cited on pages 17, 90, 129).

Cámara de Madrid. *Guía sobre empresas de servicios energéticos (ESE)*. Tech. rep. 2010 (cited on page 97).

Camilo, F. M., Castro, R., Almeida, M. E., and Pires, V. F. “Economic assessment of residential PV systems with self-consumption and storage in Portugal”. In: *Solar Energy* 150 (2017), pp. 353–362. DOI: 10.1016/J.SOLENER.2017.04.062 (cited on page 6).

Castellanos, S., Sunter, D. A., and Kammen, D. M. “Rooftop solar photovoltaic potential in cities: How scalable are assessment approaches?” In: *Environmental Research Letters* 12.12 (2017), p. 125005. DOI: 10.1088/1748-9326/aa7857 (cited on pages 13, 89).

Centro Nacional de Información Geográfica. *Centro de Descargas del CNIG* (cited on pages 95, 132).

Chase, J. *Trends in PV O&M pricing*. Tech. rep. BloombergNEF, 2018 (cited on page 97).

Chatzipoulka, C., Compagnon, R., Kaempf, J., and Nikolopoulou, M. “Sky view factor as predictor of solar availability on building façades”. In: *Solar Energy* 170 (2018), pp. 1026–1038. DOI: 10.1016/j.solener.2018.06.028 (cited on page 90).

Chen, L., Ng, E., An, X., Ren, C., Lee, M., Wang, U., and He, Z. “Sky view factor analysis of street canyons and its implications for daytime intra-urban air temperature differentials in high-rise, high-density urban areas of Hong Kong: a GIS-based simulation approach”. In: *International Journal of Climatology* 32.1 (2010), pp. 121–136. DOI: https://doi.org/10.1002/joc.2243 (cited on page 95).

Chen, Q., Li, X., Zhang, Z., Zhou, C., Guo, Z., Liu, Z., and Zhang, H. “Remote sensing of photovoltaic scenarios: Techniques, applications and future directions”. In: *Applied Energy* 333 (2023), p. 120579. DOI: 10.1016/J.APENERGY.2022.120579 (cited on page 13).

Chowdhury, M. S., Rahman, K. S., Chowdhury, T., Nuthammachot, N., Techato, K., Akhtaruzzaman, M., Tiong, S. K., Sopian, K., and Amin, N. *An overview of solar photovoltaic panels' end-of-life material recycling*. 2020. DOI: 10.1016/j.esr.2019.100431 (cited on pages 97, 100).

Christoph Kost; Shivenes Shammugan; Verena Fluri; Dominik Peper; Aschkan Davoodi Nemar; Thomas Schlegl. *Levelized Cost Of Electricity Renewable Energy Technologies*. Tech. rep. Fraunhofer Institute For Solar Energy Systems ISE, 2021 (cited on page 3).

Ciocia, A., Amato, A., Leo, P. D., Fichera, S., Malgaroli, G., Spertino, F., and Tzanova, S. “Self-Consumption and Self-Sufficiency in Photovoltaic Systems: Effect of Grid Limitation and Storage Installation”. In: *Energies 2021, Vol. 14, Page 1591* 14.6 (2021), p. 1591. DOI: 10.3390/EN14061591 (cited on pages 6, 9, 135).

Cohen, J. *Statistical Power Analysis for the Behavioral Sciences Second Edition*. LAWRENCE ERLBAUM ASSOCIATES, PUBLISHERS, 1988 (cited on pages 100, 101).

Comisión Nacional de los Mercados y la Competencia. *Circular 3/2020, de 15 de enero, de la Comisión Nacional de los Mercados y la Competencia, por la que se establece la metodología para el cálculo de los peajes de transporte y distribución de electricidad*. Tech. rep. 2020 (cited on page 134).

Comisión Nacional de los Mercados y la Competencia (CNMC). “Documento de consulta pública sobre la propuesta de metodología de cálculo de la tasa de retribución financiera de la actividad de producción de energía eléctrica a partir de fuentes de energía renovables, cogeneración y residuos para el siguiente periodo”. 2018 (cited on page 97).

Comisión Nacional de los Mercados y la Competencia (CNMC). *EVALUACIÓN DEL RÉGIMEN RETRIBUTIVO ESPECÍFICO CORRESPONDIENTE AL PERIODO 2014-2020 Expediente núm. INF/DE/037/21*. Tech. rep. 2021 (cited on page 66).

Comisión Nacional de los Mercados y la Competencia (CNMC). *Estadísticas. Precios del Mercado de Producción de Energía Eléctrica* (cited on page 66).

Copper, J. K., Sproul, A. B., and Jarnason, S. “Photovoltaic (PV) performance modelling in the absence of onsite measured plane of array irradiance (POA) and module temperature”. In: *Renewable Energy* 86 (2016), pp. 760–769. DOI: 10.1016/J.RENENE.2015.09.005 (cited on page 45).

Costa, A., Keane, M. M., Torrens, J. I., and Corry, E. “Building operation and energy performance: Monitoring, analysis and optimisation toolkit”. In: *Applied Energy* 101 (2013), pp. 310–316. DOI: 10.1016/J.APENERGY.2011.10.037 (cited on page 1).

Council of European Energy Regulators. *Electricity Distribution Network Tariffs CEER Guidelines of Good Practice*. Tech. rep. Brussels, Belgium: Council of European Energy Regulators, 2017 (cited on page 7).

Cubukcu, M. and Gumus, H. “Performance analysis of a grid-connected photovoltaic plant in eastern Turkey”. In: *Sustainable Energy Technologies and Assessments* 39 (2020), p. 100724. DOI: 10.1016/J.SETA.2020.100724 (cited on pages 55, 56, 65).

Cuesta-Fernández, I., Vargas-Salgado, C., Alfonso-Solar, D., and Gómez-Navarro, T. “The contribution of metropolitan areas to decarbonize the residential stock in Mediterranean cities: A GIS-based assessment of rooftop PV potential in Valencia, Spain”. In: *Sustainable Cities and Society* 97 (2023), p. 104727. DOI: 10.1016/J.SCS.2023.104727 (cited on page 16).

Dahmoun, M. E. H., Bekkouche, B., Sudhakar, K., Guezgouz, M., Chenafi, A., and Chaouch, A. “Performance evaluation and analysis of grid-tied large scale PV plant in Algeria”. In: *Energy for Sustainable Development* 61 (2021), pp. 181–195. DOI: 10.1016/J.ESD.2021.02.004 (cited on page 45).

Datadis. *Datadis* (cited on page 132).

Dean, J., Kandt, A., Burman, K., Lisell, L., and Helm, C. “Analysis of Web-Based Solar Photovoltaic Mapping Tools”. In: *Proceedings of the ASME 3rd International Conference on Energy Sustainability 2009, ES2009* 1 (2010), pp. 85–96. DOI: 10.1115/ES2009-90461 (cited on page 5).

Dhass, A. D., Beemkumar, N., Harikrishnan, S., and Ali, H. M. “A Review on Factors Influencing the Mismatch Losses in Solar Photovoltaic System”. In: *International Journal of Photoenergy* 2022 (2022). DOI: 10.1155/2022/2986004 (cited on page 15).

Dhimish, M. “Thermal impact on the performance ratio of photovoltaic systems: A case study of 8000 photovoltaic installations”. In: *Case Studies in Thermal Engineering* 21 (2020), p. 100693. DOI: 10.1016/J.CSITE.2020.100693 (cited on page 54).

Dhimish, M. and Silvestre, S. “Estimating the impact of azimuth-angle variations on photovoltaic annual energy production”. In: *Clean Energy* 3.1 (2019), pp. 47–58. DOI: 10.1093/CE/ZKY022 (cited on page 15).

Dirección General del Catastro. *Sede Electrónica del Catastro - Difusión de datos catastrales* (cited on pages 130, 132).

Domenech, B., Calleja, G., and Olivella, J. “Residential Photovoltaic Profitability with Storage under the New Spanish Regulation: A Multi-Scenario Analysis”. In: *Energies 2021, Vol. 14, Page 1987* 14.7 (2021), p. 1987. DOI: 10.3390/EN14071987 (cited on pages 9, 135).

Dorian Frieden; Andreas Tuerk; Camilla Neumann; Stanislas d’Herbemont. *Collective self-consumption and energy communities: Trends and challenges in the transposition of the EU framework.* Tech. rep. Joanneum Research Forschungsgesellschaft mbH, 2020. DOI: 10.13140/RG.2.2.25685.04321 (cited on page 4).

Dougherty, T. R. and Jain, R. K. “Invisible walls: Exploration of microclimate effects on building energy consumption in New York City”. In: *Sustainable Cities and Society* 90 (2023), p. 104364. DOI: 10.1016/J.SCS.2022.104364 (cited on page 1).

Dufo-López, R. and Bernal-Agustín, J. L. “A comparative assessment of net metering and net billing policies. Study cases for Spain”. In: *Energy* 84 (2015), pp. 684–694. DOI: 10.1016/J.ENERGY.2015.03.031 (cited on page 7).

Echevarría Camarero, F., Ogando-Martínez, A., Durán Gómez, P., and Carrasco Ortega, P. “Profitability of Batteries in Photovoltaic Systems for Small Industrial Consumers in Spain under Current Regulatory Framework and Energy Prices”. In: *Energies 2023, Vol. 16, Page 361* 16.1 (2022), p. 361. DOI: 10.3390/EN16010361 (cited on page 6).

Eke, R. and Demircan, H. “Performance analysis of a multi crystalline Si photovoltaic module under Mugla climatic conditions in Turkey”. In: *Energy Conversion and Management* 65 (2013), pp. 580–586. DOI: 10.1016/J.ENCONMAN.2012.09.007 (cited on page 65).

Elamim, A., Hartiti, B., Haibaoui, A., Lfakir, A., and Thevenin, P. “Analysis and comparison of different PV technologies for determining the optimal PV panels- A case study in Mohammedia , Morocco.” In: *IOSR Journal of Electrical and Electronics Engineering* 12.01 (2017), pp. 37–45. DOI: 10.9790/1676-1201013745 (cited on page 63).

Elhadj Sidi, C. E. B., Ndiaye, M. L., El Bah, M., Mbodji, A., Ndiaye, A., and Ndiaye, P. A. “Performance analysis of the first large-scale (15 MWp) grid-connected photovoltaic plant in Mauritania”. In: *Energy Conversion and Management* 119 (2016), pp. 411–421. DOI: 10.1016/J.ENCONMAN.2016.04.070 (cited on page 45).

EnergyPlus. *Weather Data by Location | EnergyPlus* (cited on page 95).

European Climate Foundation. *Building Europe’s Net-Zero Future Why the Transition to Energy Efficient and Electrified Buildings Strengthens Europe’s Economy.* Tech. rep. The Hague: European Climate Foundation, 2022 (cited on page 128).

European Commission. *The European Green Deal.* Tech. rep. Brussels, 2019 (cited on page 1).

European Commission. *’Fit for 55’: delivering the EU’s 2030 climate target on the way to climate neutrality.* Tech. rep. 2021 (cited on page 128).

European Commission. *Commission to the European Parliament; The Council; Social Commitee And The Committee of the Regions. EU solar energy strategy.* Brussels, 2022 (cited on page 3).

European Commission. *JRC Photovoltaic Geographical Information System (PVGIS)* (cited on pages 130, 132).

EUROSTAT. *Eurostat - Data Explorer. Complete energy balances.* 2021 (cited on page 89).

EUROSTAT. *Eurostat - Data Explorer. Supply, transformation and consumption of electricity* (cited on page 89).

Eurostat. *HICP - annual data (average index and rate of change)* (cited on page 135).

F. Holmgren, W., W. Hansen, C., and A. Mikofski, M. “pvlib python: a python package for modeling solar energy systems”. In: *Journal of Open Source Software* 3.29 (2018), p. 884. DOI: 10.21105/JOSS.00884 (cited on page 45).

Fakhraian, E., Alier, M., Dalmau, F. V., Nameni, A., and Guerrero, J. C. “The Urban Rooftop Photovoltaic Potential Determination”. In: *Sustainability 2021, Vol. 13, Page 7447* 13.13 (2021), p. 7447. DOI: 10.3390/SU13137447 (cited on pages 10, 11, 13, 128).

Fakhraian, E., Forment, M. A., Dalmau, F. V., Nameni, A., and Guerrero, M. J. C. “Determination of the urban rooftop photovoltaic potential: A state of the art”. In: *Energy Reports* 7 (2021), pp. 176–185. DOI: 10.1016/J.EGYR.2021.06.031 (cited on pages 13, 21, 128).

Fath, K., Stengel, J., Sprenger, W., Wilson, H. R., Schultmann, F., and Kuhn, T. E. "A method for predicting the economic potential of (building-integrated) photovoltaics in urban areas based on hourly Radiance simulations". In: *Solar Energy* 116 (2015), pp. 357–370. DOI: 10.1016/J.SOLENER.2015.03.023 (cited on pages 5, 13, 15, 19, 128).

Fávero, L. P. and Belfiore, P. "Simple and Multiple Regression Models". In: *Data Science for Business and Decision Making* (2019), pp. 443–538. DOI: 10.1016/B978-0-12-811216-8.00013-6 (cited on page 58).

Feldman, D., Ramasamy, V., Fu, R., Ramdas, A., Desai, J., and Margolis, R. *U.S. Solar Photovoltaic System and Energy Storage Cost Benchmark: Q1 2020.* Tech. rep. National Renewable Energy Laboratory, 2021 (cited on pages 45, 135).

Flatt, C. and Jacobs, R. L. "Principle Assumptions of Regression Analysis: Testing, Techniques, and Statistical Reporting of Imperfect Data Sets:" in: *https://doi.org/10.1177/1523422319869915* 21.4 (2019), pp. 484–502. DOI: 10.1177/1523422319869915 (cited on page 58).

Foles, A., Fialho, L., and Collares-Pereira, M. "Techno-economic evaluation of the Portuguese PV and energy storage residential applications". In: *Sustainable Energy Technologies and Assessments* 39 (2020), p. 100686. DOI: 10.1016/J.SETA.2020.100686 (cited on page 6).

Freitas, S., Catita, C., Redweik, P., and Brito, M. C. *Modelling solar potential in the urban environment: State-of-the-art review.* 2015. DOI: 10.1016/j.rser.2014.08.060 (cited on page 89).

Fuster-Palop, E., Prades-Gil, C., Masip, X., Viana-Fons, J. D., and Payá, J. "Innovative regression-based methodology to assess the techno-economic performance of photovoltaic installations in urban areas". In: *Renewable and Sustainable Energy Reviews* 149 (2021), p. 111357. DOI: 10.1016/J.RSER.2021.111357 (cited on pages 20, 129, 132, 138).

Fuster-Palop, E., Prades-Gil, C., Masip, X., Viana-Fons, J. D., and Payá, J. "Techno-Economic Potential of Urban Photovoltaics: Comparison of Net Billing and Net Metering in a Mediterranean Municipality". In: *Energies 2023, Vol. 16, Page 3564* 16.8 (2023), p. 3564. DOI: 10.3390/EN16083564 (cited on page 20).

Fuster-Palop, E., Prades-Gil, C., Masip, X., Viana-Fons, J., and Paya-Herrero, J. "Evaluation of the solar photovoltaic generation potential of a district in the city of Valencia". In: *SDEWES 2020, 15th Conference of Sustainable Development of Energy, Water and Environment Systems.* Cologne, 2020, pp. 1–14 (cited on page 94).

Fuster-Palop, E., Vargas-Salgado, C., Ferri-Revert, J. C., and Payá, J. "Performance analysis and modelling of a 50 MW grid-connected photovoltaic plant in Spain after 12 years of operation". In: *Renewable and Sustainable Energy Reviews* 170 (2022), p. 112968. DOI: 10.1016/J.RSER.2022.112968 (cited on pages 132, 135, 138).

"G * Power 3.1 manual". 2017 (cited on page 100).

Gagnon, P., Margolis, R., Melius, J., Phillips, C., and Elmore, R. *Rooftop Solar Photovoltaic Technical Potential in the United States: A Detailed Assessment.* Tech. rep. National Renewable Energy Laboratory, 2016 (cited on page 89).

Gál, T. and Unger, J. "A new software tool for SVF calculations using building and tree-crown databases". In: *Urban Climate* 10.P3 (2014), pp. 594–606. DOI: 10.1016/j.uclim.2014.05.004 (cited on page 95).

Gallego-Castillo, C., Heleno, M., and Victoria, M. "Self-consumption for energy communities in Spain: A regional analysis under the new legal framework". In: *Energy Policy* 150 (2021), p. 112144. DOI: 10.1016/J.ENPOL.2021.112144 (cited on pages 4, 5, 135).

Gassar, A. A. A. and Cha, S. H. "Review of geographic information systems-based rooftop solar photovoltaic potential estimation approaches at urban scales". In: *Applied Energy* 291 (2021), p. 116817. DOI: 10.1016/J.APENERGY.2021.116817 (cited on pages 12, 13, 15, 21, 128, 132).

Gatsonis, C. and Sampson, A. R. "Multiple Correlation: Exact Power and Sample Size Calculations". In: *Psychological Bulletin* 106.3 (1989), pp. 516–524. DOI: 10.1037/0033-2909.106.3.516 (cited on page 100).

Gautier, A., Jacqmin, J., and Poudou, J. C. "The prosumers and the grid". In: *Journal of Regulatory Economics* 53.1 (2018), pp. 100–126. DOI: 10.1007/S11149-018-9350-5/METRICS (cited on page 7).

Generalitat Valenciana. *Fichas municipal Catarroja - Portal Estadístico de la Generalitat Valenciana - Generalitat Valenciana* (cited on page 130).

Ghaleb, B., Abbasi, S. A., and Asif, M. "Application of solar PV in the building sector: Prospects and barriers in the GCC region". In: *Energy Reports* 9 (2023), pp. 3932–3942. DOI: 10.1016/J.EGYR.2023.02.085 (cited on page 5).

Gilman, P., Dobos, A., Diorio, N., Freeman, J., Janzou, S., and Ryberg, D. *SAM Photovoltaic Model Technical Reference Update*. Tech. rep. National Renewable Energy Agency, 2016. DOI: NREL/TP-6A20-67399 (cited on pages 14, 15, 45, 97, 135).

Gomez-Exposito, A., Arcos-Vargas, A., and Gutierrez-Garcia, F. "On the potential contribution of rooftop PV to a sustainable electricity mix: The case of Spain". In: *Renewable and Sustainable Energy Reviews* 132 (2020), p. 110074. DOI: 10.1016/j.rser.2020.110074 (cited on page 89).

Gómez-Navarro, T., Brazzini, T., Alfonso-Solar, D., and Vargas-Salgado, C. "Analysis of the potential for PV rooftop prosumer production: Technical, economic and environmental assessment for the city of Valencia (Spain)". In: *Renewable Energy* 174 (2021), pp. 372–381. DOI: 10.1016/j.renene.2021.04.049 (cited on pages 15, 16, 20, 128).

Government of Spain. Ministry of Industry Tourism and Trade. *Royal Decree 661/2007*. 2007 (cited on page 66).

Government of Spain. Ministry of Industry Tourism and Trade. *Royal Decree 413/2014*. 2014 (cited on page 66).

Grupotech. "Posibilidades de implantacion de instalaciones fotovoltaicas en la industria valenciana". 2011 (cited on page 97).

Guenounou, A., Malek, A., and Aillerie, M. “Comparative performance of PV panels of different technologies over one year of exposure: Application to a coastal Mediterranean region of Algeria”. In: *Energy Conversion and Management* 114 (2016), pp. 356–363. DOI: 10.1016/J.ENCONMAN.2016.02.044 (cited on page 63).

Gueymard, C. A. “Solar Radiation Resource: Measurement, Modeling, and Methods”. In: *Comprehensive Renewable Energy, Second Edition: Volume 1-9* 1 (2022), pp. 176–212. DOI: 10.1016/B978-0-12-819727-1.00101-1 (cited on page 14).

Hamann, K. R., Bertel, M. P., Ryszawska, B., Lurger, B., Szymański, P., Rozwadowska, M., Goedkoop, F., Jans, L., Perlaviciute, G., Masson, T., Fritsche, I., Favaro, T., Hofer, A., Eisenberger, I., Gutschi, C., Grosche, C., Held, J., Athenstaedt, U., and Corcoran, K. “An interdisciplinary understanding of energy citizenship: Integrating psychological, legal, and economic perspectives on a citizen-centred sustainable energy transition”. In: *Energy Research & Social Science* 97 (2023), p. 102959. DOI: 10.1016/J.ERSS.2023.102959 (cited on page 128).

Han, J. Y., Chen, Y. C., and Li, S. Y. “Utilising high-fidelity 3D building model for analysing the rooftop solar photovoltaic potential in urban areas”. In: *Solar Energy* 235 (2022), pp. 187–199. DOI: 10.1016/J.SOLENER.2022.02.041 (cited on page 128).

Hao, L. and Naiman, D. Q. *Quantile regression.* Vol. 149. SAGE Publications, 2007 (cited on page 137).

Hashemi, B., Taheri, S., Cretu, A. M., and Pouresmaeil, E. “Systematic photovoltaic system power losses calculation and modeling using computational intelligence techniques”. In: *Applied Energy* 284 (2021). DOI: 10.1016/J.APENERGY.2020.116396 (cited on page 46).

Herbazi, R., Amechnoue, K., Khouya, A., Chahboun, A., Diani, M., Louzazni, M., and Addou, M. “Performance evaluation and analysis of polycrystalline photovoltaic plant located in Northern Morocco”. In: *International Journal of Ambient Energy* 43.1 (2019), pp. 1262–1268. DOI: 10.1080/01430750.2019.1694985 (cited on page 65).

Huang, S. “Linear regression analysis”. In: *International Encyclopedia of Education(Fourth Edition)* (2023), pp. 548–557. DOI: 10.1016/B978-0-12-818630-5.10067-3 (cited on page 137).

Huang, X., Hayashi, K., Matsumoto, T., Tao, L., Huang, Y., and Tomino, Y. “Estimation of Rooftop Solar Power Potential by Comparing Solar Radiation Data and Remote Sensing Data—A Case Study in Aichi, Japan”. In: *Remote Sensing 2022, Vol. 14, Page 1742* 14.7 (2022), p. 1742. DOI: 10.3390/RS14071742 (cited on page 15).

Huang, Z., Mendis, T., and Xu, S. “Urban solar utilization potential mapping via deep learning technology: A case study of Wuhan, China”. In: *Applied Energy* 250 (2019), pp. 283–291. DOI: 10.1016/J.APENERGY.2019.04.113 (cited on page 2).

Huld, T., Gottschalg, R., Beyer, H. G., and Topič, M. “Mapping the performance of PV modules, effects of module type and data averaging”. In: *Solar Energy* 84.2 (2010), pp. 324–338. DOI: 10.1016/J.SOLENER.2009.12.002 (cited on page 45).

IDAE. *Pliego de Condiciones Técnicas de Instalaciones Conectadas a Red.* Madrid, 2011 (cited on pages 45, 95, 97).

IDAE. *Estudios, informes y estadísticas | IDAE* (cited on page 89).

IDAE (Institute for Diversification and Saving of Energy). *Proyecto SECH-SPAHOUSEC, Análisis del consumo energético del sector residencial en España.* Tech. rep. IDAE, 2011 (cited on page 97).

Inês, C., Guilherme, P. L., Esther, M. G., Swantje, G., Stephen, H., and Lars, H. "Regulatory challenges and opportunities for collective renewable energy prosumers in the EU". In: *Energy Policy* 138 (2020), p. 111212. DOI: 10.1016/j.enpol.2019.111212 (cited on pages 93, 110).

Inflation.eu. *Historic inflation Spain – historic CPI inflation Spain* (cited on page 66).

Inflation.eu. *Inflación histórica España – inflación histórica España IPC* (cited on page 97).

Instituto Nacional de Estadística. *INEbase / Demografía y población / Cifras de población y censos demográficos / Censos de Población y Viviendas 2011* (cited on page 133).

Instituto Valenciano de Competitividad Empresarial. *Resolución de 24 de marzo de 2022, del presidente del Instituto Valenciano de Competitividad Empresarial (IVACE), por la que se convocan ayudas destinadas al fomento de instalaciones de autoconsumo de energía eléctrica en los municipios de la Comunitat Va.* Tech. rep. 2022 (cited on page 134).

International Electrotechnical Committee. *IEC 61724 Photovoltaic System Performance Monitoring - Guidelines for Measurement, Data Exchange and Analysis.* 1998 (cited on page 53).

International Energy Agency. *Electricity – World Energy Outlook 2019.* Tech. rep. 2019 (cited on page 89).

International Energy Agency. *Renewables Data Explorer – Data Tools - IEA.* 2023 (cited on page 2).

International Renewable Energy Agency. *RENEWABLE CAPACITY STATISTICS 2023.* Tech. rep. 2023 (cited on pages 2, 3).

IRENA. *Solar PV Module Costs 2010-2018.* Tech. rep. 2019 (cited on page 89).

IRENA. *Renewable Power Generation Costs in 2020.* Tech. rep. 2020 (cited on page 128).

IRENA. *Renewable Capacity Statistics 2021.* Tech. rep. 2021, pp. 1–300 (cited on page 45).

IRENA. *IRENASTAT Online Data Query Tool* (cited on page 2).

IRENA. *IRENASTAT Online Data Query Tool - Installed electricity capacity (MW) by Country/area, Technology, Grid connection and Year* (cited on page 2).

IRENA (International Renewable Energy Agency). *Future of Solar Photovoltaic Deployment, investment, technology, grid integration and socio-economic aspects, A Global Energy Transformation paper About IRENA.* Tech. rep. 2019 (cited on page 11).

IRENA (International Renewable Energy Agency). *Capacity and Generation - Technologies.* 2023 (cited on page 2).

Izquierdo, S., Rodrigues, M., and Fueyo, N. "A method for estimating the geographical distribution of the available roof surface area for large-scale photovoltaic energy-potential evaluations". In: *Solar Energy* 82.10 (2008), pp. 929–939. DOI: 10.1016/j.solener.2008.03.007 (cited on pages 12, 14).

JA SOLAR. *JAM60S20 365-390 Datasheet* (cited on page 135).

Jakubiec, J. A. and Reinhart, C. F. "A method for predicting city-wide electricity gains from photovoltaic panels based on LiDAR and GIS data combined with hourly Daysim simulations". In: *Solar Energy* 93 (2013), pp. 127–143. DOI: 10.1016/J.SOLENER.2013.03.022 (cited on page 5).

Jefatura del Estado; Boletín Oficial del Estado (BOE). *Real Decreto-ley 15/2018, de 5 de octubre, de medidas urgentes para la transición energética y la protección de los consumidores.* Madrid, 2018 (cited on pages 4, 89).

Jiang, H., Zhang, X., Yao, L., Lu, N., Qin, J., Liu, T., and Zhou, C. "High-resolution analysis of rooftop photovoltaic potential based on hourly generation simulations and load profiles". In: *Applied Energy* 348 (2023), p. 121553. DOI: 10.1016/J.APENERGY.2023.121553 (cited on page 12).

Jordan, D. C. and Kurtz, S. R. "Photovoltaic Degradation Rates – An Analytical Review: Preprint". 2012 (cited on page 97).

José Gil Mena, A., Fernando Nasimba Medina, V., Bouakkaz, A., and Haddad, S. "Analysis and optimisation of collective self-consumption in residential buildings in Spain". In: *Energy and Buildings* 283 (2023), p. 112812. DOI: 10.1016/J.ENBUILD.2023.112812 (cited on page 14).

Julieta, S. R., José-Julio, R. B., and Pablo, Y. R. "A methodology to estimate the photovoltaic potential on parking spaces and water deposits. The case of the Canary Islands". In: *Renewable Energy* 189 (2022), pp. 1046–1062. DOI: 10.1016/J.RENENE.2022.02.103 (cited on page 13).

Jurasz, J. K., Dabek, P. B., and Campana, P. E. "Can a city reach energy self-sufficiency by means of rooftop photovoltaics? Case study from Poland". In: *Journal of Cleaner Production* 245 (2020), p. 118813. DOI: 10.1016/J.JCLEPRO.2019.118813 (cited on pages 6, 15, 16, 19).

Kabacoff, R. I. *R in Action SECOND EDITION Data analysis and graphics with R.* MANNING PUBLICATIONS, 2015, p. 474 (cited on page 58).

Kanters, J., Wall, M., and Kjellsson, E. "The Solar Map as a Knowledge Base for Solar Energy Use". In: *Energy Procedia* 48 (2014), pp. 1597–1606. DOI: 10.1016/J.EGYPRO.2014.02.180 (cited on page 5).

Kavlak, G., McNerney, J., and Trancik, J. E. "Evaluating the causes of cost reduction in photovoltaic modules". In: *Energy Policy* 123 (2018), pp. 700–710. DOI: 10.1016/J.ENPOL.2018.08.015 (cited on page 3).

Khalid, A. M., Mitra, I., Warmuth, W., and Schacht, V. "Performance ratio – Crucial parameter for grid connected PV plants". In: *Renewable and Sustainable Energy Reviews* 65 (2016), pp. 1139–1158. DOI: 10.1016/J.RSER.2016.07.066 (cited on pages 45, 56).

Kim, J., Rabelo, M., Padi, S. P., Yousuf, H., Cho, E. C., and Yi, J. "A Review of the Degradation of Photovoltaic Modules for Life Expectancy". In: *Energies 2021, Vol. 14, Page 4278* 14.14 (2021), p. 4278. DOI: 10.3390/EN14144278 (cited on page 56).

Koch, H., Lechner, S., Erdmann, S., and Hofmann, M. “Assessing the Potential of Rooftop Photovoltaics by Processing High-Resolution Irradiation Data, as Applied to Giessen, Germany”. In: *Energies 2022, Vol. 15, Page 6991* 15.19 (2022), p. 6991. DOI: 10.3390/EN15196991 (cited on page 12).

Koenker, R. “Quantile regression”. In: *Quantile Regression* (2005), pp. 1–349. DOI: 10.1017/CBO9780511754098 (cited on page 137).

Koenker, R. *CRAN - Package quantreg* (cited on page 137).

Koltunov, M., Pezzutto, S., Bisello, A., Lettner, G., Hiesl, A., Sark, W. van, Louwen, A., and Wilczynski, E. “Mapping of Energy Communities in Europe: Status Quo and Review of Existing Classifications”. In: *Sustainability 2023, Vol. 15, Page 8201* 15.10 (2023), p. 8201. DOI: 10.3390/SU15108201 (cited on page 9).

Krapf, S., Kemmerzell, N., Uddin, S. K. H., Vázquez, M. H., Netzler, F., and Lienkamp, M. “Towards Scalable Economic Photovoltaic Potential Analysis Using Aerial Images and Deep Learning”. In: *Energies 2021, Vol. 14, Page 3800* 14.13 (2021), p. 3800. DOI: 10.3390/EN14133800 (cited on pages 10, 11, 15, 19, 128).

Kuhn, M. “Building Predictive Models in R Using the caret Package”. In: *Journal of Statistical Software* 28.5 (2008), pp. 1–26. DOI: 10.18637/JSS.V028.I05 (cited on page 58).

Kuhn, M. and Johnson, K. “Applied predictive modeling”. In: *Applied Predictive Modeling* (2013), pp. 1–600. DOI: 10.1007/978-1-4614-6849-3 (cited on page 58).

Kunaifi, K., Reinders, A., Lindig, S., Jaeger, M., and Moser, D. “Operational Performance and Degradation of PV Systems Consisting of Six Technologies in Three Climates”. In: *Applied Sciences 2020, Vol. 10, Page 5412* 10.16 (2020), p. 5412. DOI: 10.3390/APP10165412 (cited on page 53).

Kurdi, Y., Alkhatatbeh, B. J., Asadi, S., and Jebelli, H. “A decision-making design framework for the integration of PV systems in the urban energy planning process”. In: *Renewable Energy* 197 (2022), pp. 288–304. DOI: 10.1016/J.RENENE.2022.07.001 (cited on pages 4, 8).

Kymakis, E., Kalykakis, S., and Papazoglou, T. M. “Performance analysis of a grid connected photovoltaic park on the island of Crete”. In: *Energy Conversion and Management* 50.3 (2009), pp. 433–438. DOI: 10.1016/J.ENCONMAN.2008.12.009 (cited on pages 45, 56, 65).

Lang, T., Ammann, D., and Girod, B. “Profitability in absence of subsidies: A techno-economic analysis of rooftop photovoltaic self-consumption in residential and commercial buildings”. In: *Renewable Energy* 87 (2016), pp. 77–87. DOI: 10.1016/j.renene.2015.09.059 (cited on page 93).

Lara Monge, C., Vásquez Márquez, L., and Reyes Duke, A. M. “Case Study: Optimization of Grid-Connected Photovoltaic Self-Consumption Systems for The Commercial Sector in Honduras”. In: *IOP Conference Series: Earth and Environmental Science* 801.1 (2021), p. 012025. DOI: 10.1088/1755-1315/801/1/012025 (cited on page 9).

Li, S. Y. and Han, J. Y. "The impact of shadow covering on the rooftop solar photovoltaic system for evaluating self-sufficiency rate in the concept of nearly zero energy building". In: *Sustainable Cities and Society* 80 (2022), p. 103821. DOI: 10.1016/J.SCS.2022.103821 (cited on page 9).

Lindig, S., Louwen, A., Moser, D., and Topic, M. "Outdoor PV System Monitoring—Input Data Quality, Data Imputation and Filtering Approaches". In: *Energies 2020, Vol. 13, Page 5099* 13.19 (2020), p. 5099. DOI: 10.3390/EN13195099 (cited on pages 45, 53).

Liu, B. Y. and Jordan, R. C. "The interrelationship and characteristic distribution of direct, diffuse and total solar radiation". In: *Solar Energy* 4.3 (1960), pp. 1–19. DOI: 10.1016/0038-092X(60)90062-1 (cited on page 132).

Liu, H. "Comparing Welch's ANOVA, a Kruskal-Wallis test and traditional ANOVA in case of Heterogeneity of Variance". In: *Theses and Dissertations* (2015). DOI: https://doi.org/10.25772/BWFP-YE95 (cited on page 68).

Liu, Z., Liu, X., Zhang, H., and Yan, D. "Integrated physical approach to assessing urban-scale building photovoltaic potential at high spatiotemporal resolution". In: *Journal of Cleaner Production* 388 (2023), p. 135979. DOI: 10.1016/J.JCLEPRO.2023.135979 (cited on pages 4, 132).

Lobaccaro, G., Croce, S., Lindkvist, C., Munari Probst, M. C., Scognamiglio, A., Dahlberg, J., Lundgren, M., and Wall, M. "A cross-country perspective on solar energy in urban planning: Lessons learned from international case studies". In: *Renewable and Sustainable Energy Reviews* 108 (2019), pp. 209–237. DOI: 10.1016/j.rser.2019.03.041 (cited on pages 3, 89).

López Prol, J. and Steininger, K. W. "Photovoltaic self-consumption regulation in Spain: Profitability analysis and alternative regulation schemes". In: *Energy Policy* 108 (2017), pp. 742–754. DOI: 10.1016/J.ENPOL.2017.06.019 (cited on page 8).

López Prol, J. and Steininger, K. W. "Photovoltaic self-consumption is now profitable in Spain: Effects of the new regulation on prosumers' internal rate of return". In: *Energy Policy* 146 (2020), p. 111793. DOI: 10.1016/J.ENPOL.2020.111793 (cited on pages 5, 6, 135).

Loutzenhiser, P. G., Manz, H., Felsmann, C., Strachan, P. A., Frank, T., and Maxwell, G. M. "Empirical validation of models to compute solar irradiance on inclined surfaces for building energy simulation". In: *Solar Energy* 81.2 (2007), pp. 254–267. DOI: 10.1016/j.solener.2006.03.009 (cited on page 95).

Lovati, M., Dallapiccola, M., Adami, J., Bonato, P., Zhang, X., and Moser, D. "Design of a residential photovoltaic system: the impact of the demand profile and the normative framework". In: *Renewable Energy* 160 (2020), pp. 1458–1467. DOI: 10.1016/J.RENENE.2020.07.153 (cited on pages 9, 14).

Maghami, M. R., Hizam, H., Gomes, C., Radzi, M. A., Rezadad, M. I., and Hajighorbani, S. *Power loss due to soiling on solar panel: A review.* 2016. DOI: 10.1016/j.rser.2016.01.044 (cited on page 97).

Mainzer, K., Killinger, S., McKenna, R., and Fichtner, W. "Assessment of rooftop photovoltaic potentials at the urban level using publicly available geodata and image recognition techniques". In: *Solar Energy* 155 (2017), pp. 561–573. DOI: 10.1016/J.SOLENER.2017.06.065 (cited on page 13).

Majeed, I. B. and Nwulu, N. I. "Reverse Power Flow Due to Solar Photovoltaic in the Low Voltage Network". In: *IEEE Access* 11 (2023), pp. 44741–44758. DOI: 10.1109/ACCESS.2023.3273483 (cited on page 5).

Malvoni, M., Leggieri, A., Maggiotto, G., Congedo, P. M., and De Giorgi, M. G. "Long term performance, losses and efficiency analysis of a 960 kWP photovoltaic system in the Mediterranean climate". In: *Energy Conversion and Management* 145 (2017), pp. 169–181. DOI: 10.1016/J.ENCONMAN.2017.04.075 (cited on pages 45, 65).

Malvoni, M., Kumar, N. M., Chopra, S. S., and Hatziargyriou, N. "Performance and degradation assessment of large-scale grid-connected solar photovoltaic power plant in tropical semi-arid environment of India". In: *Solar Energy* 203 (2020), pp. 101–113. DOI: 10.1016/J.SOLENER.2020.04.011 (cited on page 56).

Mangiante, M. J., Whung, P. Y., Zhou, L., Porter, R., Cepada, A., Campirano, E., Licon, D., Lawrence, R., and Torres, M. "Economic and technical assessment of rooftop solar photovoltaic potential in Brownsville, Texas, U.S.A". In: *Computers, Environment and Urban Systems* 80 (2020), p. 101450. DOI: 10.1016/j.compenvurbsys.2019.101450 (cited on page 89).

Mansó Borràs, I., Neves, D., and Gomes, R. "Using urban building energy modeling data to assess energy communities' potential". In: *Energy and Buildings* 282 (2023), p. 112791. DOI: 10.1016/J.ENBUILD.2023.112791 (cited on page 135).

Manso-Burgos, Á., Ribó-Pérez, D., Alcázar-Ortega, M., and Gómez-Navarro, T. "Local Energy Communities in Spain: Economic Implications of the New Tariff and Variable Coefficients". In: *Sustainability 2021, Vol. 13, Page 10555* 13.19 (2021), p. 10555. DOI: 10.3390/SU131910555 (cited on page 134).

Manso-Burgos, Ribó-Pérez, D., Gómez-Navarro, T., and Alcázar-Ortega, M. "Local energy communities modelling and optimisation considering storage, demand configuration and sharing strategies: A case study in Valencia (Spain)". In: *Energy Reports* 8 (2022), pp. 10395–10408. DOI: 10.1016/J.EGYR.2022.08.181 (cited on page 134).

Mansouri Kouhestani, F., Byrne, J., Johnson, D., Spencer, L., Hazendonk, P., and Brown, B. "Evaluating solar energy technical and economic potential on rooftops in an urban setting: the city of Lethbridge, Canada". In: *International Journal of Energy and Environmental Engineering* 10.1 (2019), pp. 13–32. DOI: 10.1007/S40095-018-0289-1/TABLES/10 (cited on pages 15, 19, 128).

Marion, B., Adelstein, J., Boyle, K., Hayden, H., Hammond, B., Fletcher, Canada, B., Narang, D., Kimber, A., Mitchell, L., Rich, G., and Townsend, T. "Performance parameters for grid-connected PV systems". In: *Conference Record of the IEEE Photovoltaic Specialists Conference* (2005), pp. 1601–1606. DOI: 10.1109/PVSC.2005.1488451 (cited on page 56).

Marrone, P. and Montella, I. “An experimentation on the limits and potential of Renewable Energy Communities in the built city: buildings and proximity open spaces for energy decentralization”. In: *Renewable and Sustainable Energy Transition* 2 (2022), p. 100025. DOI: 10.1016/J.RSET.2022.100025 (cited on page 9).

Martín-Martínez, S., Cañas-Carretón, M., Honrubia-Escribano, A., and Gómez-Lázaro, E. “Performance evaluation of large solar photovoltaic power plants in Spain”. In: *Energy Conversion and Management* 183 (2019), pp. 515–528. DOI: 10.1016/J.ENCONMAN.2018.12.116 (cited on page 65).

Martín-Pomares, L., Martínez, D., Polo, J., Perez-Astudillo, D., Bachour, D., and Sanfilippo, A. *Analysis of the long-term solar potential for electricity generation in Qatar*. 2017. DOI: 10.1016/j.rser.2017.01.125 (cited on page 90).

Masip, X., Fuster-Palop, E., Prades-Gil, C., Viana-Fons, J. D., Payá, J., and Navarro-Peris, E. “Case study of electric and DHW energy communities in a Mediterranean district”. In: *Renewable and Sustainable Energy Reviews* 178 (2023), p. 113234. DOI: 10.1016/J.RSER.2023.113234 (cited on page 132).

Mathai, N., Chen, Y., and Kirchmair, J. “Validation strategies for target prediction methods”. In: *Briefings in Bioinformatics* 21.3 (2020), pp. 791–802. DOI: 10.1093/BIB/BBZ026 (cited on page 58).

Mattsson, N., Verendel, V., Hedenus, F., and Reichenberg, L. “An autopilot for energy models – Automatic generation of renewable supply curves, hourly capacity factors and hourly synthetic electricity demand for arbitrary world regions”. In: *Energy Strategy Reviews* 33 (2021), p. 100606. DOI: 10.1016/J.ESR.2020.100606 (cited on page 14).

Matute, G., Yusta, J. M., Beyza, J., and Monteiro, C. “Optimal dispatch model for PV-electrolysis plants in self-consumption regime to produce green hydrogen: A Spanish case study”. In: *International Journal of Hydrogen Energy* 47.60 (2022), pp. 25202–25213. DOI: 10.1016/J.IJHYDENE.2022.05.270 (cited on page 128).

Mavromatakis, F., Vignola, F., and Marion, B. “Low irradiance losses of photovoltaic modules”. In: *Solar Energy* 157 (2017), pp. 496–506. DOI: 10.1016/J.SOLENER.2017.08.062 (cited on pages 45, 56).

Mayer, M. J. “Effects of the meteorological data resolution and aggregation on the optimal design of photovoltaic power plants”. In: *Energy Conversion and Management* 241 (2021), p. 114313. DOI: 10.1016/J.ENCONMAN.2021.114313 (cited on page 14).

Mayer, M. J. and Gróf, G. “Extensive comparison of physical models for photovoltaic power forecasting”. In: *Applied Energy* 283 (2021), p. 116239. DOI: 10.1016/J.APENERGY.2020.116239 (cited on page 14).

Mehta, P. and Tiefenbeck, V. “Solar PV sharing in urban energy communities: Impact of community configurations on profitability, autonomy and the electric grid”. In: *Sustainable Cities and Society* 87 (2022), p. 104178. DOI: 10.1016/J.SCS.2022.104178 (cited on pages 9, 132).

Memme, S. and Fossa, M. "Maximum energy yield of PV surfaces in France and Italy from climate based equations for optimum tilt at different azimuth angles". In: *Renewable Energy* 200 (2022), pp. 845–866. DOI: 10.1016/J.RENENE.2022.10.019 (cited on page 132).

Mendieta, Á. J. O. and Hernández, E. S. "Analysis of PV Self-Consumption in Educational and Office Buildings in Spain". In: *Sustainability 2021, Vol. 13, Page 1662* 13.4 (2021), p. 1662. DOI: 10.3390/SU13041662 (cited on pages 3, 7).

Merrouni, A. A., Amrani, A. I., and Mezrhab, A. "Electricity production from large scale PV plants: Benchmarking the potential of Morocco against California, US". In: *Energy Procedia* 119 (2017), pp. 346–355. DOI: 10.1016/J.EGYPRO.2017.07.118 (cited on page 65).

Michalsky, J. J. "The Astronomical Almanac's algorithm for approximate solar position (1950-2050)". In: *Solar Energy* 40.3 (1988), pp. 227–235. DOI: 10.1016/0038-092X(88)90045-X (cited on page 95).

Ministerio para la Transición Ecológica (MTE); Boletín Oficial del Estado (BOE). *Real Decreto 244/2019, de 5 de abril, por el que se regulan las condiciones administrativas, técnicas y económicas del autoconsumo de energía eléctrica.* Madrid, 2019 (cited on pages 4, 89, 96, 134).

Ministry for the Ecological Transition and the Demographic challenge. *Orden TED/171/2020.* Madrid, 2021 (cited on page 66).

Miranda, R. F., Szklo, A., and Schaeffer, R. "Technical-economic potential of PV systems on Brazilian rooftops". In: *Renewable Energy* 75 (2015), pp. 694–713. DOI: 10.1016/J.RENENE.2014.10.037 (cited on pages 14, 15, 19).

Mitrašinović, A. M. "Photovoltaics advancements for transition from renewable to clean energy". In: *Energy* 237 (2021), p. 121510. DOI: 10.1016/J.ENERGY.2021.121510 (cited on page 45).

Mohajeri, N., Assouline, D., Guiboud, B., Bill, A., Gudmundsson, A., and Scartezzini, J. L. "A city-scale roof shape classification using machine learning for solar energy applications". In: *Renewable Energy* 121 (2018), pp. 81–93. DOI: 10.1016/J.RENENE.2017.12.096 (cited on page 21).

Molnár, G., Ürge-Vorsatz, D., and Chatterjee, S. "Estimating the global technical potential of building-integrated solar energy production using a high-resolution geospatial model". In: *Journal of Cleaner Production* 375 (2022), p. 134133. DOI: 10.1016/J.JCLEPRO.2022.134133 (cited on page 1).

Mor, G., Cipriano, J., Martirano, G., Pignatelli, F., Lodi, C., Lazzari, F., Grillone, B., and Chemisana, D. "A data-driven method for unsupervised electricity consumption characterisation at the district level and beyond". In: *Energy Reports* 7 (2021), pp. 5667–5684. DOI: 10.1016/J.EGYR.2021.08.195 (cited on page 132).

Mora-López, L. and Sidrach-De-Cardona, M. "Models for the optimization and evaluation of photovoltaic self-consumption facilities". In: *Proceedings of the ISES Solar World Congress 2019 and IEA SHC International Conference on Solar Heating and Cooling for Buildings and Industry 2019* (2020), pp. 1555–1562. DOI: 10.18086/SWC.2019.30.01 (cited on page 129).

Müller, J. and Trutnevyte, E. “Spatial projections of solar PV installations at subnational level: Accuracy testing of regression models”. In: *Applied Energy* 265 (2020), p. 114747. DOI: 10.1016/J.APENERGY.2020.114747 (cited on pages 17, 20, 90).

Mundaca, L. and Samahita, M. “What drives home solar PV uptake? Subsidies, peer effects and visibility in Sweden”. In: *Energy Research & Social Science* 60 (2020), p. 101319. DOI: 10.1016/J.ERSS.2019.101319 (cited on page 4).

Murat Ates, A. and Singh, H. “Rooftop solar Photovoltaic (PV) plant – One year measured performance and simulations”. In: *Journal of King Saud University - Science* 33.3 (2021), p. 101361. DOI: 10.1016/J.JKSUS.2021.101361 (cited on page 65).

National Renewable Energy Laboratory. *Home - System Advisor Model (SAM)* (cited on page 92).

Neuhäuser, M. “Wilcoxon–Mann–Whitney Test”. In: *International Encyclopedia of Statistical Science* (2011), pp. 1656–1658. DOI: 10.1007/978-3-642-04898-2_615 (cited on page 131).

Ngar-Yin Mah, D., Wang, G., Lo, K., Leung, M. K. H., Hills, P., and Lo, A. Y. “Barriers and policy enablers for solar photovoltaics (PV) in cities: Perspectives of potential adopters in Hong Kong”. In: (2018). DOI: 10.1016/j.rser.2018.04.041 (cited on page 89).

Nuñez-Jimenez, A., Mehta, P., and Griego, D. “Let it grow: How community solar policy can increase PV adoption in cities”. In: *Energy Policy* 175 (2023), p. 113477. DOI: 10.1016/J.ENPOL.2023.113477 (cited on page 5).

Official Journal of the European Union. *Directive (EU) 2018/2001 of the European Parliament and of the Council of 11 December 2018 on the Promotion of the Use of Energy from Renewable Sources (Recast)*. 2018 (cited on page 1).

Official Journal of the European Union. *Regulation (EU) 2021/1119 of the European Parliament And of The Council of 30 June 2021 establishing the framework for achieving climate neutrality and amending Regulations (EC) No 401/2009 and (EU) 2018/1999 (‘European Climate Law’)*. 2021 (cited on page 1).

Olivella, J., Domenech, B., and Calleja, G. “Potential of implementation of residential photovoltaics at city level: The case of London”. In: *Renewable Energy* 180 (2021), pp. 577–585. DOI: 10.1016/J.RENENE.2021.08.121 (cited on pages 15, 16, 19, 128).

Oloya, I. T., Gutu, T. J., and Adaramola, M. S. “Techno-economic assessment of 10 MW centralised grid-tied solar photovoltaic system in Uganda”. In: *Case Studies in Thermal Engineering* 25 (2021), p. 100928. DOI: 10.1016/J.CSITE.2021.100928 (cited on page 45).

Omar, M. A. and Mahmoud, M. M. *Grid connected PV- home systems in Palestine: A review on technical performance, effects and economic feasibility*. 2018. DOI: 10.1016/j.rser.2017.09.008 (cited on pages 5, 90).

Open Geospatial Consortium. *CityGML - Open Geospatial Consortium* (cited on pages 13, 14).

optimize function - RDocumentation (cited on page 134).

Ordóñez, Á., Sánchez, E., Rozas, L., García, R., and Parra-Domínguez, J. “Net-metering and net-billing in photovoltaic self-consumption: The cases of Ecuador and Spain”. In: *Sustainable Energy Technologies and Assessments* 53 (2022), p. 102434. DOI: 10.1016/J.SETA.2022.102434 (cited on pages 3, 4, 14, 128).

Ordóñez, J., Jadraque, E., Alegre, J., and Martínez, G. "Analysis of the photovoltaic solar energy capacity of residential rooftops in Andalusia (Spain)". In: *Renewable and Sustainable Energy Reviews* 14.7 (2010), pp. 2122–2130. DOI: 10.1016/J.RSER.2010.01.001 (cited on pages 15, 89).

Ozden, T. "A countrywide analysis of 27 solar power plants installed at different climates". In: *Scientific Reports 2022 12:1* 12.1 (2022), pp. 1–11. DOI: 10.1038/s41598-021-04551-7 (cited on page 45).

Pan, D., Bai, Y., Chang, M., Wang, X., and Wang, W. "The technical and economic potential of urban rooftop photovoltaic systems for power generation in Guangzhou, China". In: *Energy and Buildings* 277 (2022), p. 112591. DOI: 10.1016/J.ENBUILD.2022.112591 (cited on page 1).

Parra, I. de la, Muñoz, M., Lorenzo, E., García, M., Marcos, J., and Martínez-Moreno, F. "PV performance modelling: A review in the light of quality assurance for large PV plants". In: *Renewable and Sustainable Energy Reviews* 78 (2017), pp. 780–797. DOI: 10.1016/J.RSER.2017.04.080 (cited on page 45).

Parretta, A., Sarno, A., and Vicari, L. R. "Effects of solar irradiation conditions on the outdoor performance of photovoltaic modules". In: *Optics Communications* 153.1-3 (1998), pp. 153–163. DOI: 10.1016/S0030-4018(98)00192-8 (cited on page 46).

Pedrero, J., Hermoso, N., Hernández, P., Munoz, I., Arrizabalaga, E., Mabe, L., Prieto, I., and Izkara, J. L. "Assessment of urban-scale potential for solar PV generation and consumption". In: *IOP Conference Series: Earth and Environmental Science* 323.1 (2019), p. 012066. DOI: 10.1088/1755-1315/323/1/012066 (cited on page 89).

Pedrero, J., Hermoso, N., Hernández, P., Munoz, I., Arrizabalaga, E., Mabe, L., Prieto, I., and Izkara, J. L. "Assessment of urban-scale potential for solar PV generation and consumption". In: *IOP Conference Series: Earth and Environmental Science* 323.1 (2019), p. 012066. DOI: 10.1088/1755-1315/323/1/012066 (cited on pages 5, 15).

Pérez, N. S., Alonso-Montesinos, J., and Batlles, F. J. "Estimation of Soiling Losses from an Experimental Photovoltaic Plant Using Artificial Intelligence Techniques". In: *Applied Sciences 2021, Vol. 11, Page 1516* 11.4 (2021), p. 1516. DOI: 10.3390/APP11041516 (cited on page 56).

Perpiñán Lamigueiro, O. *Energía Solar Fotovoltaica.* 2023 (cited on pages 6, 14, 97, 135, 152).

Polo, J., Martín-Chivelet, N., Alonso, M., Sanz, C., Batlles, F. J., López, G., Zitouni, H., Alonso-Montesinos, J., Vela, N., Bosch, J. L., and Barbero, J. "Characterization of PV Soiling Losses in Urban Mediterranean Environment". In: (2019). DOI: 10.18086/swc.2019.15.03 (cited on page 56).

Poon, K. H., Kämpf, J. H., Tay, S. E., Wong, N. H., and Reindl, T. G. "Parametric study of URBAN morphology on building solar energy potential in Singapore context". In: *Urban Climate* 33 (2020), p. 100624. DOI: 10.1016/j.uclim.2020.100624 (cited on pages 90, 129).

Probst, P., Wright, M. N., and Boulesteix, A. L. "Hyperparameters and tuning strategies for random forest". In: *Wiley Interdisciplinary Reviews: Data Mining and Knowledge Discovery* 9.3 (2019), e1301. DOI: 10.1002/WIDM.1301 (cited on page 58).

PVSyst. *Project design - Carbon Balance Tool - Detailed System LCE* (cited on page 97).

Quesada, B., Sánchez, C., Cañada, J., Royo, R., and Payá, J. "Experimental results and simulation with TRNSYS of a 7.2kWp grid-connected photovoltaic system". In: *Applied Energy* 88.5 (2011), pp. 1772–1783. DOI: 10.1016/j.apenergy.2010.12.011 (cited on pages 45, 89, 90).

Ransome, S. and Funtan, P. "Why hourly averaged measurement data is insufficient to model PV system performance accurately". In: *20th European Photovoltaic Solar Energy Conference*. Barcelona, Spain, 2005, pp. 2752–2755 (cited on page 54).

AL-Rasheedi, M., Gueymard, C. A., Al-Khayat, M., Ismail, A., Lee, J. A., and Al-Duaj, H. "Performance evaluation of a utility-scale dual-technology photovoltaic power plant at the Shagaya Renewable Energy Park in Kuwait". In: *Renewable and Sustainable Energy Reviews* 133 (2020), p. 110139. DOI: 10.1016/J.RSER.2020.110139 (cited on page 45).

Rauf, A., Al-Awami, A. T., Kassas, M., Khalid, M., Zia, F., Benbouzid, M., Elbouchikhi, E., Muyeen, S. M., and Tariq Iqbal, M. "Optimal Sizing and Cost Minimization of Solar Photovoltaic Power System Considering Economical Perspectives and Net Metering Schemes". In: *Electronics 2021, Vol. 10, Page 2713* 10.21 (2021), p. 2713. DOI: 10.3390/ELECTRONICS10212713 (cited on page 9).

Red Eléctrica de España. *Análisis | ESIOS electricidad · datos · transparencia* (cited on page 97).

Red Eléctrica de España. *Analysis - ESIOS electricity* (cited on pages 134, 135).

Red Eléctrica de España. *PVPC | ESIOS electricidad · datos · transparencia* (cited on page 97).

Red Eléctrica de España. *REData - Non renewable detail CO2 emissions | Red Eléctrica* (cited on page 135).

Red Eléctrica de España. *REData | Red Eléctrica de España* (cited on page 97).

Red Eléctrica de España (RRE). *Consulta los perfiles de consumo (TBD), Red Eléctrica* (cited on page 14).

Redweik, P., Catita, C., and Brito, M. "Solar energy potential on roofs and facades in an urban landscape". In: *Solar Energy* 97 (2013), pp. 332–341. DOI: 10.1016/j.solener.2013.08.036 (cited on page 97).

Rehman, N. U. and Uzair, M. "The proper interpretation of analytical sky view factors for isotropic diffuse solar irradiance on tilted planes". In: *Journal of Renewable and Sustainable Energy* 9.5 (2017). DOI: 10.1063/1.4993069 (cited on page 95).

Reis, V., Almeida, R. H., Silva, J. A., and Brito, M. C. "Demand aggregation for photovoltaic self-consumption". In: *Energy Reports* 5 (2019), pp. 54–61. DOI: 10.1016/J.EGYR.2018.11.002 (cited on pages 4, 9).

Rinaldi, A., Soini, M. C., Patel, M. K., and Parra, D. "Optimised allocation of PV and storage capacity among different consumer types and urban settings: A prospective analysis for Switzerland". In: *Journal of Cleaner Production* 259 (2020), p. 120762. DOI: 10.1016/J.JCLEPRO.2020.120762 (cited on page 15).

Ripley, B. "Support Functions and Datasets for Venables and Ripley's MASS [R package MASS version 7.3-58.2]". In: (2023) (cited on page 138).

Roberts, J. J., Mendiburu Zevallos, A. A., and Cassula, A. M. "Assessment of photovoltaic performance models for system simulation". In: *Renewable and Sustainable Energy Reviews* 72 (2017), pp. 1104–1123. DOI: 10.1016/J.RSER.2016.10.022 (cited on page 56).

Roberts, M. B., Bruce, A., and MacGill, I. "A comparison of arrangements for increasing self-consumption and maximising the value of distributed photovoltaics on apartment buildings". In: *Solar Energy* 193 (2019), pp. 372–386. DOI: 10.1016/J.SOLENER.2019.09.067 (cited on pages 6, 9).

Rodríguez-Gómez, F., Campo-Ávila, J. del, Ferrer-Cuesta, M., and Mora-López, L. "Data driven tools to assess the location of photovoltaic facilities in urban areas". In: *Expert Systems with Applications* 203 (2022), p. 117349. DOI: 10.1016/J.ESWA.2022.117349 (cited on page 5).

Rodríguez-Segura, F. J., Osorio-Aravena, J. C., Frolova, M., Terrados-Cepeda, J., and Muñoz-Cerón, E. "Social acceptance of renewable energy development in southern Spain: Exploring tendencies, locations, criteria and situations". In: *Energy Policy* 173 (2023), p. 113356. DOI: 10.1016/J.ENPOL.2022.113356 (cited on page 5).

Roldán Fernández, J. M., Burgos Payán, M., and Riquelme Santos, J. M. "Profitability of household photovoltaic self-consumption in Spain". In: *Journal of Cleaner Production* 279 (2021), p. 123439. DOI: 10.1016/J.JCLEPRO.2020.123439 (cited on page 3).

Roumpakias, E. and Stamatelos, A. "Comparative performance analysis of grid-connected photovoltaic system by use of existing performance models". In: *Energy Conversion and Management* 150 (2017), pp. 14–25. DOI: 10.1016/J.ENCONMAN.2017.08.001 (cited on page 45).

Rövekamp, P., Schöpf, M., Wagon, F., Weibelzahl, M., and Fridgen, G. "Renewable electricity business models in a post feed-in tariff era". In: *Energy* 216 (2021), p. 119228. DOI: 10.1016/J.ENERGY.2020.119228 (cited on page 8).

Sánchez-Aparicio, M., Martín-Jiménez, J., Del Pozo, S., González-González, E., and Lagüela, S. "Ener3DMap-SolarWeb roofs: A geospatial web-based platform to compute photovoltaic potential". In: *Renewable and Sustainable Energy Reviews* 135 (2021), p. 110203. DOI: 10.1016/J.RSER.2020.110203 (cited on pages 5, 21).

Santamouris, M. and Vasilakopoulou, K. "Present and future energy consumption of buildings: Challenges and opportunities towards decarbonisation". In: *e-Prime - Advances in Electrical Engineering, Electronics and Energy* 1 (2021), p. 100002. DOI: 10.1016/J.PRIME.2021.100002 (cited on page 1).

Santiago, I., Trillo-Montero, D., Moreno-Garcia, I. M., Pallarés-López, V., and Luna-Rodríguez, J. J. "Modeling of photovoltaic cell temperature losses: A review and a practice case in South Spain". In: *Renewable and Sustainable Energy Reviews* 90 (2018), pp. 70–89. DOI: 10.1016/J.RSER.2018.03.054 (cited on page 55).

Sark, W. van, Reich, N., Müller, B., and Armbruster, A. "Review of PV performance ratio development". In: *Conference: World Renewable Energy Forum, WREF 2012, Including World Renewable Energy Congress XII and Colorado Renewable Energy Society (CRES) Annual Conference.* Denver, 2012. DOI: 10.13140/2.1.2138.7204 (cited on page 97).

Savvakis, N. and Tsoutsos, T. “Performance assessment of a thin film photovoltaic system under actual Mediterranean climate conditions in the island of Crete”. In: *Energy* 90 (2015), pp. 1435–1455. DOI: 10.1016/J.ENERGY.2015.06.098 (cited on page 65).

Schallenberg-Rodríguez, J. *Photovoltaic techno-economical potential on roofs in regions and islands: The case of the Canary Islands. Methodological review and methodology proposal.* 2013. DOI: 10.1016/j.rser.2012.11.078 (cited on page 89).

Schopfer, S., Tiefenbeck, V., and Staake, T. “Economic assessment of photovoltaic battery systems based on household load profiles”. In: *Applied Energy* 223 (2018), pp. 229–248. DOI: 10.1016/J.APENERGY.2018.03.185 (cited on page 14).

Schreiber-Gregory, D. N., Jackson, H. M., and Bader, K. “Logistic and Linear Regression Assumptions : Violation Recognition and Control”. In: (2018) (cited on page 69).

Seltman, H. J. *Experimental Design and Analysis.* Carnegie Mellon University 2012, 2018 (cited on page 57).

Sheather, S. J. “Diagnostics and Transformations for Multiple Linear Regression”. In: (2009), pp. 151–225. DOI: 10.1007/978-0-387-09608-7_6 (cited on page 137).

Shirazi, A. M., Zomorodian, Z. S., and Tahsildoost, M. “Techno-economic BIPV evaluation method in urban areas”. In: *Renewable Energy* 143 (2019), pp. 1235–1246. DOI: 10.1016/j.renene.2019.05.105 (cited on page 90).

Shiva Kumar, B. and Sudhakar, K. “Performance evaluation of 10 MW grid connected solar photovoltaic power plant in India”. In: *Energy Reports* 1 (2015), pp. 184–192. DOI: 10.1016/J.EGYR.2015.10.001 (cited on page 56).

Simoiu, M. S., Fagarasan, I., Ploix, S., and Calofir, V. “Optimising the self-consumption and self-sufficiency: A novel approach for adequately sizing a photovoltaic plant with application to a metropolitan station”. In: *Journal of Cleaner Production* 327 (2021), p. 129399. DOI: 10.1016/J.JCLEPRO.2021.129399 (cited on pages 6, 10, 135).

SolarPower Europe. *EU Market Outlook For Solar Power 2022-2026.* 2022 (cited on page 128).

Soler-Castillo, Y., Rimada, J. C., Hernández, L., and Martínez-Criado, G. “Modelling of the efficiency of the photovoltaic modules: Grid-connected plants to the Cuban national electrical system”. In: *Solar Energy* 223 (2021), pp. 150–157. DOI: 10.1016/J.SOLENER.2021.05.052 (cited on page 45).

Som Energia. *Histórico de Tarifas de Electricidad* (cited on page 134).

Sredenšek, K., Štumberger, B., Hadžiselimović, M., Mavsar, P., and Seme, S. “Physical, geographical, technical, and economic potential for the optimal configuration of photovoltaic systems using a digital surface model and optimization method”. In: *Energy* 242 (2022), p. 122971. DOI: 10.1016/J.ENERGY.2021.122971 (cited on pages 10, 19, 128, 135).

Strazzera, E. and Statzu, V. “Fostering photovoltaic technologies in Mediterranean cities: Consumers’ demand and social acceptance”. In: *Renewable Energy* 102 (2017), pp. 361–371. DOI: 10.1016/J.RENENE.2016.10.056 (cited on page 5).

Strbac, G., Papadaskalopoulos, D., Chrysanthopoulos, N., Estanqueiro, A., Algarvio, H., Lopes, F., Vries, L. de, Morales-Espana, G., Sijm, J., Hernandez-Serna, R., Kiviluoma, J., and Helisto, N. "Decarbonization of Electricity Systems in Europe: Market Design Challenges". In: *IEEE Power and Energy Magazine* 19.1 (2021), pp. 53–63. DOI: 10.1109/MPE.2020.3033397 (cited on page 1).

Streltsov, A., Malof, J. M., Huang, B., and Bradbury, K. "Estimating residential building energy consumption using overhead imagery". In: *Applied Energy* 280 (2020), p. 116018. DOI: 10.1016/J.APENERGY.2020.116018 (cited on page 1).

Sun, L., Chang, Y., Wu, Y., Sun, Y., and Su, D. "Potential estimation of rooftop photovoltaic with the spatialization of energy self-sufficiency in urban areas". In: *Energy Reports* 8 (2022), pp. 3982–3994. DOI: 10.1016/J.EGYR.2022.03.035 (cited on pages 14, 20, 128).

Sundaram, S. and Babu, J. S. C. "Performance evaluation and validation of 5 MWp grid connected solar photovoltaic plant in South India". In: *Energy Conversion and Management* 100 (2015), pp. 429–439. DOI: 10.1016/J.ENCONMAN.2015.04.069 (cited on page 45).

Tabachnick, B. G. *Experimental Designs Using ANOVA Epidemiology and Neurobehaviour of FASD in South Africa View project CyGaMEs View project.* Tech. rep. 2007 (cited on page 101).

Talavera, D. L., Muñoz-Rodriguez, F. J., Jimenez-Castillo, G., and Rus-Casas, C. "A new approach to sizing the photovoltaic generator in self-consumption systems based on cost–competitiveness, maximizing direct self-consumption". In: *Renewable Energy* 130 (2019), pp. 1021–1035. DOI: 10.1016/J.RENENE.2018.06.088 (cited on pages 9, 128).

Talayero, A. P., Melero, J. J., Llombart, A., and Yürüşen, N. Y. "Machine Learning models for the estimation of the production of large utility-scale photovoltaic plants". In: *Solar Energy* 254 (2023), pp. 88–101. DOI: 10.1016/J.SOLENER.2023.03.007 (cited on pages 137, 138).

Taylor, J., Leloux, J., Hall, L. M. H., Everard, A. M., Briggs, J., and Buckley, A. "Performance of Distributed PV in the UK: A Statistical Analysis of Over 7000 Systems". In: *Conference: 31st European Photovoltaic Solar Energy Conference and Exhibition* (2015). DOI: 10.13140/RG.2.1.2019.6568 (cited on pages 57, 68).

The General Assembly United Nations. *Resolution adopted by the General Assembly on 25 September 2015. Transforming our world: the 2030 Agenda for Sustainable Development.* Tech. rep. 2015 (cited on page 1).

Thebault, M., Desthieux, G., Castello, R., and Berrah, L. "Large-scale evaluation of the suitability of buildings for photovoltaic integration: Case study in Greater Geneva". In: *Applied Energy* 316 (2022), p. 119127. DOI: 10.1016/J.APENERGY.2022.119127 (cited on page 11).

Thebault, M. and Gaillard, L. "Optimization of the integration of photovoltaic systems on buildings for self-consumption – Case study in France". In: *City and Environment Interactions* 10 (2021), p. 100057. DOI: 10.1016/J.CACINT.2021.100057 (cited on page 9).

Thevenard, D. and Pelland, S. "Estimating the uncertainty in long-term photovoltaic yield predictions". In: *Solar Energy* 91 (2013), pp. 432–445. DOI: 10.1016/J.SOLENER.2011.05.006 (cited on page 5).

Tobias Loga, Nikolaus Diefenbach, Britta Stein, Elena Dascalaki, Constantinos A. Balaras, Kalliopi Droutsa, Simon Kontoyiannidis, Marjana Šijanec Zavrl, Andraž Rakuščček, Vincenzo Corrado, Stefano Corgnati, Ilaria Ballarini, Charles Roarty, Michael Hanratty, Bill Sheldrick, Marlies Van Holm, Nele Renders, Małgorzata Popiołek, Jerzy Kwiatkowski, Maria Amtmann, Tomáš Vimmr, Otto Villatoro, Kim B. Wittchen, Jesper Kragh, Hubert Despretz, Zdravko Georgiev, Karin Spets, Leticia Ortega, Begoña Serrano Lanzarote, Milica Jovanovic Popovic, and Dusan Ignjatovic. *Typology Approach for Building Stock Energy Assessment. Main Results of the TABULA project.* Tech. rep. 2012 (cited on page 130).

Torres-Rivas, A., Palumbo, M., Jiménez, L., and Boer, D. “Self-consumption possibilities by rooftop PV and building retrofit requirements for a regional building stock: The case of Catalonia”. In: *Solar Energy* 238 (2022), pp. 150–161. DOI: 10.1016/J.SOLENER.2022.04.036 (cited on page 19).

Tossa, A. K., Soro, Y. M., Coulibaly, Y., Azoumah, Y., Migan-Dubois, A., Thiaw, L., and Lishou, C. “Artificial intelligence technique for estimating PV modules performance ratio under outdoor operating conditions”. In: *Journal of Renewable and Sustainable Energy* 10.5 (2018), p. 053505. DOI: 10.1063/1.5042217 (cited on page 46).

Trela, M. and Dubel, A. “Net-Metering vs. Net-Billing from the Investors Perspective—Impacts of Changes in RES Financing in Poland on the Profitability of a Joint Photovoltaic Panels and Heat Pump System”. In: *Energies 2022, Vol. 15, Page 227* 15.1 (2021), p. 227. DOI: 10.3390/EN15010227 (cited on page 7).

Trigo-Gonzalez, M., Cortés, M., Alonso-Montesinos, J., Martínez-Durbán, M., Ferrada, P., Rabanal, J., Portillo, C., López, G., and Batlles, F. J. “Development and comparison of PV production estimation models for mc-Si technologies in Chile and Spain”. In: *Journal of Cleaner Production* 281 (2021), p. 125360. DOI: 10.1016/J.JCLEPRO.2020.125360 (cited on pages 46, 90).

Trigo-González, M., Batlles, F. J., Alonso-Montesinos, J., Ferrada, P., Sagrado, J. del, Martínez-Durbán, M., Cortés, M., Portillo, C., and Marzo, A. “Hourly PV production estimation by means of an exportable multiple linear regression model”. In: *Renewable Energy* 135 (2019), pp. 303–312. DOI: 10.1016/j.renene.2018.12.014 (cited on pages 90, 96).

Unión Española Fotovoltaica (UNEF). *Informe Anual UNEF - Energía Solar, apuesta segura por la recuperación económica.* Tech. rep. Madrid, 2022 (cited on page 2).

United Nations (Department of Economic and Social Affairs). *World Urbanization Prospects The 2018 Revision.* New york, 2019. DOI: 10.18356/b9e995fe-en (cited on page 1).

United Nations Framework Convention on Climate Change. “The Paris Agreement”. In: Paris, 2015 (cited on page 1).

Valderrama, A., Valle, C., Allende, H., Ibarra, M., and Vásquez, C. “Machine learning applications for urban photovoltaic potential estimation: A survey”. In: *Neurocomputing* 526 (2023), pp. 80–95. DOI: 10.1016/J.NEUCOM.2023.01.006 (cited on page 16).

Vargas-Salgado, C., Aparisi-Cerdá, I., Alfonso-Solar, D., and Gómez-Navarro, T. “Can photovoltaic systems be profitable in urban areas? Analysis of regulation scenarios for four cases in Valencia city (Spain)”. In: *Solar Energy* 233 (2022), pp. 461–477. DOI: 10.1016/J.SOLENER.2022.01.057 (cited on page 128).

Varo-martínez, M., Fernández-ahumada, L. M., López-luque, R., and Ramírez-faz, J. “Simulation of Self-Consumption Photovoltaic Installations: Profitability Thresholds”. In: *Applied Sciences 2021, Vol. 11, Page 6517* 11.14 (2021), p. 6517. DOI: 10.3390/APP11146517 (cited on page 129).

Vergura, S. “A Statistical Tool to Detect and Locate Abnormal Operating Conditions in Photovoltaic Systems”. In: *Sustainability 2018, Vol. 10, Page 608* 10.3 (2018), p. 608. DOI: 10.3390/SU10030608 (cited on page 57).

Vezzoni, R. “Green growth for whom, how and why? The REPowerEU Plan and the inconsistencies of European Union energy policy”. In: *Energy Research & Social Science* 101 (2023), p. 103134. DOI: 10.1016/J.ERSS.2023.103134 (cited on page 4).

Viana-Fons, J. D., Gonzálvez-Maciá, J., and Payá, J. “Development and validation in a 2D-GIS environment of a 3D shadow cast vector-based model on arbitrarily orientated and tilted surfaces”. In: *Energy and Buildings* 224 (2020), p. 110258. DOI: 10.1016/j.enbuild.2020.110258 (cited on pages 95, 98, 132).

Viana-Fons, J. D., Gonzálvez-Maciá, J., and Payá-Herrero, J. *Methodology for the calculation of the shadow factor on roofs and facades of buildings in urban areas.* 2019 (cited on pages 95, 132).

Villar, C. H., Neves, D., and Silva, C. A. “Solar PV self-consumption: An analysis of influencing indicators in the Portuguese context”. In: *Energy Strategy Reviews* 18 (2017), pp. 224–234. DOI: 10.1016/J.ESR.2017.10.001 (cited on page 10).

Walch, A., Castello, R., Mohajeri, N., and Scartezzini, J. L. “Big data mining for the estimation of hourly rooftop photovoltaic potential and its uncertainty”. In: *Applied Energy* 262 (2020), p. 114404. DOI: 10.1016/j.apenergy.2019.114404 (cited on pages 17, 20).

Walch, A., Castello, R., Mohajeri, N., and Scartezzini, J.-L. “A Fast Machine Learning Model for Large-Scale Estimation of Annual Solar Irradiation on Rooftops”. In: *ISES Solar World Congress 2019.* 2019. DOI: 10.18086/swc.2019.45.12 (cited on page 17).

Walker, A., Lockhart, E., Desai, J., Ardani, K., Klise, G., Lavrova, O., Tansy, T., Deot, J., Fox, B., and Pochiraju, A. “Model of Operation-and-Maintenance Costs for Photovoltaic Systems”. In: (2020) (cited on page 66).

Wang, P., Yu, P., Huang, L., and Zhang, Y. “An integrated technical, economic, and environmental framework for evaluating the rooftop photovoltaic potential of old residential buildings”. In: *Journal of Environmental Management* 317 (2022), p. 115296. DOI: 10.1016/J.JENVMAN.2022.115296 (cited on pages 15, 19, 128).

Wang, W., Yang, D., Huang, N., Lyu, C., Zhang, G., and Han, X. “Irradiance-to-power conversion based on physical model chain: An application on the optimal configuration of multi-energy microgrid in cold climate”. In: *Renewable and Sustainable Energy Reviews* 161 (2022), p. 112356. DOI: 10.1016/J.RSER.2022.112356 (cited on page 15).

Weather Similarity (cited on page 130).

Wilcox, R. R. “ONE-WAY ANOVA”. In: *Applying Contemporary Statistical Techniques* (2003), pp. 285–328. DOI: 10.1016/B978-012751541-0/50030-4 (cited on page 68).

Xie, M., Wang, M., Zhong, H., Li, X., Li, B., Mendis, T., and Xu, S. “The impact of urban morphology on the building energy consumption and solar energy generation potential of university dormitory blocks”. In: *Sustainable Cities and Society* 96 (2023), p. 104644. DOI: 10.1016/J.SCS.2023.104644 (cited on page 17).

Xue, Y., Lindkvist, C. M., and Temeljotov-Salaj, A. “Barriers and potential solutions to the diffusion of solar photovoltaics from the public-private-people partnership perspective – Case study of Norway”. In: *Renewable and Sustainable Energy Reviews* 137 (2021), p. 110636. DOI: 10.1016/J.RSER.2020.110636 (cited on page 5).

Yang, J., Mohan Kumar, D. llamathy, Pyrgou, A., Chong, A., Santamouris, M., Kolokotsa, D., and Lee, S. E. “Green and cool roofs’ urban heat island mitigation potential in tropical climate”. In: *Solar Energy* 173 (2018), pp. 597–609. DOI: 10.1016/J.SOLENER.2018.08.006 (cited on page 4).

Zakeri, B., Cross, S., Dodds, P. E., and Gissey, G. C. “Policy options for enhancing economic profitability of residential solar photovoltaic with battery energy storage”. In: *Applied Energy* 290 (2021), p. 116697. DOI: 10.1016/J.APENERGY.2021.116697 (cited on page 6).

Zhou, X., Huang, Z., Scheuer, B., Lu, W., Zhou, G., and Liu, Y. “High-resolution spatial assessment of the zero energy potential of buildings with photovoltaic systems at the city level”. In: *Sustainable Cities and Society* 93 (2023), p. 104526. DOI: 10.1016/J.SCS.2023.104526 (cited on page 12).

Zhu, R., Wong, M. S., Kwan, M. P., Chen, M., Santi, P., and Ratti, C. “An economically feasible optimization of photovoltaic provision using real electricity demand: A case study in New York city”. In: *Sustainable Cities and Society* 78 (2022), p. 103614. DOI: 10.1016/J.SCS.2021.103614 (cited on page 19).